AUTHOR: BELLO, K.O.

TITLE: Modeling multiphase solid transport velocity in long subsea tiebacks - numerical and experimental methods.

YEAR: 2013

This work was submitted to- and approved by Robert Gordon University in partial fulfilment of the following degree: Doctor of Philosophy, School of Engineering

Modeling Multiphase Solid Transport Velocity in Long Subsea Tiebacks – Numerical and Experimental Methods

KELANI OLAFINHAN BELLO

A thesis submitted in partial fulfilment of the requirements of Robert Gordon University for the degree of Doctor of Philosophy

May 2013

Supervisory team and funding organisation

Principal Supervisor: Prof. Babs Oyeneyin

Supervisor's details:

1. Prof. Babs Oyeneyin, School of Engineering Robert Gordon University, Aberdeen, United Kingdom
2. Prof. John A. Steel, School of Engineering, Robert Gordon University, Aberdeen, United Kingdom
3. Dr. Gbenga Oluyemi, School of Engineering, Robert Gordon University, Aberdeen, United Kingdom.

Funding Organization:

Petroleum Technology Development Fund (PTDF), Federal Capital Territory, Abuja, Nigeria

Dedication

This thesis is dedicated to the glory of Almighty Allah, The All-Knowing, and All-Wise

and

my brothers, Prof. A.G.A Bello, Mr. Raheem Bello & Alhaji Yekeen Bello (late)

Acknowledgement

I want to express my deep appreciation to Professor Babs Oyeneyin, my principal supervisor, for his excellent support, guidance, understanding and patience throughout this research work. I have been very fortunate to work under his supervision, he taught me to have self belief and I will remain ever grateful. I cannot thank him enough.

I also like to thank the other members of my supervisory team, Dr. Gbenga Oluyemi and Professor Ian Steel for their guidance, support and encouragement. I am sincerely grateful to Dr. Oluyemi for his valuable comments and criticisms.

Special thanks to the technical team at the school of Engineering, Robert Gordon University, Aberdeen, particularly Alan McLean, Steve Pirie and Bill Walker, for their efforts, support and useful suggestions during the construction and installation of the experimental flow loop used for this work.

My special thanks to Petroleum Technology Development Fund (PTDF) for providing the funding for my doctoral research work; without them it may have been difficult if not impossible. I would also like to express profound gratitude to my employer, University of Benin, Benin City, Nigeria for granting me a study leave to undertake this research work. I also like to thank my colleagues at the Department of Petroleum Engineering, University of Benin for their support and encouragement.

More importantly, I cannot thank my beautiful and beloved wife, Taiwo Funmilola, enough for her love and patience throughout the period of this work. She is a wonderful woman. My children, Kamil Olalekan and Yasmina Oyinkansola have been wonderful even when daddy could not give enough time. The little time we shared has been quite rewarding and they are a constant source of motivation and happiness for me. I know I have not offered the best of support while I was on the program, but I hope they all understand it's for the benefit of all of us.

I thank my research colleagues, Amol Bali, Smail Labed, Patrick Idahosa, Reza Sanaee and Favour Makinde for many useful conversations concerning this research; they are ever willing to help. I thank you all for the great times we shared.

My thanks also go to all my friends, extended family members, well wishers too numerous to mention for their care, prayers and support that has enabled me succeed.

Often the impossible is what has not been attempted. All praise is due to Almighty Allah who has made this possible. This is a fulfilment of a long life ambition and I thank almighty Allah for His guidance, protection abundant grace towards me and my family. I pray for His continued protection and guidance in my future endeavours.

Declarations

I declare that I am the sole author of this thesis and that all verbatim extracts contained in the thesis have been identified as such and sources of information specifically acknowledged in the bibliography.

Parts of the work presented in this thesis have appeared in the following publications. The published papers are attached to this thesis and can be found in Appendix A.

- Bello, K.O., Oyeneyin, M.B and Oluyemi, G.F. 'Minimum Transport Velocity Models for Suspended Particles in Multiphase Flow Revisited' SPE 147045, September, 2011

- Bello, K.O., Oyeneyin, M.B and Oluyemi, G.F. 'A Novel Approach to Subsea Multiphase Solid Transport'. Advanced Materials Research Vol. 367 (2012) pp 413-420

ABSTRACT

Transportation of unprocessed multiphase reservoir fluids from deep/ultra deep offshore through a long subsea tieback/pipeline is inevitable. This form of transportation is complex and requires accurate knowledge of critical transport velocity, flow pattern changes, phase velocity, pressure drop, particle drag & lift forces, sand/liquid/gas holdup, flow rate requirement and tieback sizing etc at the early design phase and during operation for process optimisation.

This research investigated sand transport characteristics in multiphase, water-oil-gas-sand flows in horizontal, inclined and vertical pipes. Two critical factors that influence the solid particle transport in the case of multiphase flow in pipes were identified; these are the transient phenomena of flow patterns and the characteristic drag & lift coefficients (C_D, C_L). Therefore, the equations for velocity profile were developed for key flow patterns such as dispersed bubble flow, stratified flow, slug flow and annular flow using a combination of analytical equations and numerical simulation tool (CFD). The existing correlations for C_D & C_L were modified with data acquired from multiphase experiment in order to account for different flow patterns. Minimum Transport Velocity (MTV) models for suspension and rolling were developed by combining the numerically developed particle velocity profile models with semi-empirical models for solid particle transport. The models took into account the critical parameters that influence particle transport in pipe flow such as flow patterns and particle drag & lift coefficients, thus eliminate inaccuracies currently experienced with similar models in public domain.

The predictions of the proposed MTV models for suspension and rolling in dispersed bubble, slug flow and annular flow show maximum average error margin of 12% when compared with experimental data. The improved models were validated using previously reported experimental data and were shown to have better predictions when compared with existing models in public domain. These models have the potential to solve the problems of pipe and equipment sizing, the risk of sand deposition and bed formation, elimination of costs of sand unloading, downtime and generally improve sand management strategies.

TABLE OF CONTENTS

List of Figures

List of Table

Nomenclatures

Symbol	Description	Unit
A	Pipe cross-sectional area	m^2
C_D	Particle drag coefficient	-
C_L	Particle lift coefficient	-
d_p	Solid particle diameter	m
D	Pipe diameter	m
DH	Hydraulic diameter of pipe	m
f	Friction factor	-
f_{tp}	Two-phase friction factor	-
g	Acceleration due to gravity	m/s^2
H_L	Liquid holdup	-
L	Pipe length	m
N_{fr}	Froude Number	-
r	Distance from pipe wall	m
R	Pipe radius	m
R_{ep}	Particle Reynolds Number	-
t	Time	s
Vc	Critical (slip) velocity	m/s
V_m	Minimum transport velocity	m/s
Vsg	Superficial gas velocity	m/s
Vsl	Superficial liquid velocity	m/s
μ_g	Gas dynamic viscosity	Pa.s
μ_l	Liquid dynamic viscosity	Pa.s
ρ_g	Gas density	kg/m^3
ρ_l	Liquid density	kg/m^3
ρ_m	Mixture density	kg/m^3
ρ_s	Solid density	kg/m^3
ΔP	Pressure drop	Psi
Θ	Pipe inclination angle	degree

Chapter 1

Introduction

1.1 Background

Exploration and production of oil and gas offshore is advancing into deep/ultra deep water environment at a fast pace representing one of the major growth areas of the oil & gas industry today. Offshore fields such as in the Gulf of Mexico, Brazil and West Africa are now developed in deep and ultra deep waters in excess of 2700m (Ronalds 2006). The foray into deeper water is expected to continue with increasing demands for fossil fuel. Many of the new discoveries with potential to bridge the supply gaps are in deep or ultra deep water environment where access is extremely challenging.

The offshore environment is characterised by highly unconsolidated sandstone reservoirs with high pressures and high temperatures which are highly susceptible to sand production. The productive zones tend to be relatively shallow below the mud line with rapid depressurisation and greater chance of gas influx, early water breakthrough and attendant solid production. The production of formation sand into the wellbore and topside facilities is a common problem especially when producing from unconsolidated reservoirs with attendant adverse effect on well productivity and equipment integrity. In such a case, the traditional approach is to minimize the production of sand that enter the production strings by applying downhole sand control techniques, such as gravel packing and screens etc. either at the beginning or at a later date in the production life of the well, aimed at preventing formation sand from entering the production system. In recent times, many oil and gas producers have abandoned the "zero-sand-production-philosophy" by carefully monitoring and regulating sand influx to a tolerable level (Mathis 2003). This change in philosophy is principally driven by production optimization as a result of increasing demands for new oil production (Ball 2006).

In recent years the use of long subsea tiebacks for transportation of unprocessed multiphase reservoir fluid has gained considerable attention and long satellite tiebacks to existing infrastructures either onshore or offshore are now a common scene as can be seen in Figures 1.1 & 1.2.

This requires production from many wells tied to the pipeline/tieback connecting the wells to a processing facility. The multiphase production through the pipeline generally consist of

- Oil, gas bubbles and produced water
- Gas and liquid droplets
- Aquifer water and oil droplets

- Sand, wax, and hydrate

However, the production and transportation of these unprocessed reservoir fluids through the pipeline are most often difficult to predict because of the number of flow patterns and the fact that the velocity of the phases are different. Below are some of the critical issues of concerns for multiphase production through a long pipeline/tieback

1. The sand particle minimum transport velocity necessary to prevent solid deposition especially along the low side of the pipeline/tieback.
2. Possible phase separations as a result of different phase velocity, liquid condensation due to changes in temperature around the pipeline with attendant liquid increase and possible pressure drop.
3. The particles drag & lift forces in multiphase fluids influenced by the effects of changing flow patterns.
4. Sand bed height determination including locating sand bed deposit has continued to be a challenge. The liquid and gas holdup. The sand bed formation depends on the flow rates required to transport the sand either in suspension or rolling. The liquid holdup is the function of flow line geometry and the flow rates.
5. The flow rate requirements including pipeline sizing necessary for process design and optimisation. At low flow rates, liquid may accumulates in the flow line which may increase the pressure drop.
6. The problem of slugging with potential pressure fluctuations which may damage the surface facilities.

These among other issues are the key aspect of flow assurance which over the years have remained critical to the development of long subsea tiebacks in the oil and gas industry. The pertinent questions are how to prevent sand deposition by keeping the solids in suspension or rolling along the bottom of the pipe and track continuous changes in the flow patterns as the multiphase fluids move through the long subsea tiebacks given different pipe dimensions and topographies. The formation of flow patterns from multiphase flow and its continuous changes are a regular occurrence. The key to efficient design and safe operation of pipelines handling multiphase flows is high quality information regarding clear definitions of the flow patterns. The widespread occurrence of transporting unprocessed reservoir fluids in pipes has prompted extensive research in the area of flow patterns characterisation (Mandhane, Gregory and Aziz 1973, Barnea 1987, Acikgoz 1992, Hurlburt and Hanratty 2002). A great deal of effort has gone into investigating and classifying flow regimes occurring under various flow conditions. This will continue to receive great attention from researchers in order to enhance production, recovery and guaranteed flow assurance.

Figure 1.2: A typical long oil and gas onshore pipeline (Sathananthan, 2007)

Figure 1.2: Pictorial impression of long subsea tiebacks (Statoil Exploration and Production 2012)

In ultra deepwater and mature fields, multiphase fluid with entrained sand production is inevitable. Sand transport in multiphase environment is a challenge because of transient flow pattern changes and associated huge pressure drops. Solids are transported in various forms depending on the mean velocity of flow, such as suspension where velocity is high enough, and rolling or saltation where the flow velocity is relatively low as shown in Figure 1.3.

The sand will settle to form beds and may block the pipeline if the fluid velocity is below the minimum transport velocity required for rolling or saltation. The economic implication of any blockage of pipeline is huge given the number of producing wells which may be tied to it.

Therefore understanding the mechanism of sand transport in multiphase flow in pipes taking into account the continuous changes in flow patterns will have direct impact on estimation, design and detail analysis of subsea tiebacks (Bello, Reinicke and Teodorin 2005, Danielson 2007, Bratland 2010).

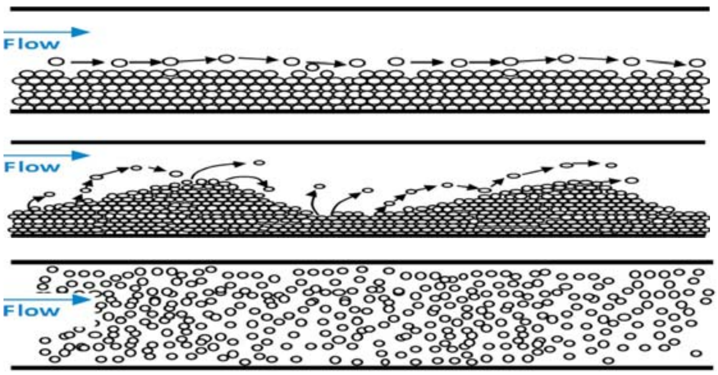

Figure 1.3: Sand flow patterns formation in pipe

Critical review of existing literatures with regards to oil-water-gas-solids reveals limited information on the solid transport in multiphase fluids especially when viewed in the context of flow patterns. Few authors that have dealt with the subject mainly focused on the measurement of pressure drops and sand transport rate which is independent of flow patterns (Bello, Reinicke and Teodorin 2005). In the development of predictive models for solid transport therefore, the objective is to propose models that will apply to all flow patterns at any inclination.

Different multiphase flow patterns will be formed as the fluid travels through the pipeline from dispersed bubble flow to slug flow, annular flow and eventually stratified flow depending on the prevailing fluid mixture properties and pipeline geometry. Investigating the impact of flow patterns on sand transport in multiphase fluids is critical to the sand transport mechanisms. Effective sand transport will require tracking the flow pattern changes as multiphase flow through the pipe. A number of models are reported in the literatures for prediction of sand transport in pipelines. Most are developed to measure sand transport in air/water two phase flows and some extending the existing hydraulic conveying models to multiphase case which cannot accurately predict particle movement in multiphase flow. This is because sand particle input volumetric fraction for most conventional wellbores and oil and gas production pipelines are significantly low, 5 – 40 Ib. per 1,000 barrel of produced crude oil, which is equivalent to 0.014 – 0.11kg sand per cubic meter of produced crude oil (Stevenson et al. 2001).

Accuracy of solid transport models depends on how well the hydrodynamic is described and predicted with sufficient reliability. To establish accurate predictive model(s) for minimum transport velocity in multiphase flow, it is necessary to understand the mechanism of interaction of fluid flow and sand particles movements. The particles are transported differently by different flow patterns because they are subjected to different driving forces such as lift and drag forces.

In this research, developing predictive models for sand transport in multiphase flow either in suspension or rolling is central. A unique concept of fluid velocity profiles combined with minimum transport velocity has been adopted. The velocity profile concept assumes that the fluid point velocity acting on a solid particle on the low side of the pipe wall needs to be greater than the minimum transport velocity for the solid particle to be upwardly mobile. The best way to achieve this was to first determine the carrier fluid velocity profile for each of the common flow patterns. So far, no equation has been developed for predicting velocity profiles for flow patterns in multiphase flow in pipes. Instead of laboratory measurement of velocity profile, the computational fluid dynamics (CFD) was used as virtual laboratory to generate fluid velocity profiles for a combination of fluid mixtures, gas-oil, water-oil, gas-water and water-oil-gas. This led to development of velocity profile models for each of the notable flow patterns by combining analytical equation with point velocity profiles generated numerically. The coupled equation was then used for the development of appropriate minimum transport velocity (MTV) models for suspension and rolling in subsea tiebacks.

The experimental investigations was borne out of the need to explore the hydrodynamic processes governing the water-oil-gas-sand multiphase flow in order to

1. Fully understand the phenomenon between different phases of multiphase fluids flow in pipes. The behaviour of fluid-fluid and fluid-particle interaction in multiphase pipe flow systems giving the associated effects of operating and geometric conditions.
2. Opportunity to define appropriate solid particle C_D & C_L in the context of multiphase flow patterns.
3. The need to have reliable data from controlled experiment for model testing and validation.
4. And an attempt to confirm some of the conclusions made by previous workers regarding solid transport in multiphase and flow pattern characteristics.

The methods adopted in this research will ultimately address solid transport behaviour issues in gas-oil-water-sand multiphase in pipelines/tiebacks which was based on the physics of the multiphase and comprehensive experimental studies. It is believed that any particle transport model must take into account the influence of key parameters such as fluid and particle physical properties, the pipe size and lift & drag coefficients.

1.2 Research objectives

The focus of this research is to

1. Develop velocity profile models for key flow patterns such dispersed bubble flow, slug flow, stratified flow and annular in multiphase fluid flow.
2. Design and construct a fit for purpose multiphase flow loop to experimentally investigate and characterise flow patterns in multiphase fluid flow.
3. Experimentally investigate sand transport phenomenon in multiphase fluid flow in pipes for different flow patterns.
4. Investigate minimum transport velocity for suspension and rolling in three/four phase water-oil-gas-solid multiphase fluid flow in pipelines/tiebacks. This involves acquisition of minimum transport velocity data in different flow patterns.
5. Develop drag and lift coefficient models for solid transport in multiphase fluid flow.
6. Develop precise and accurate sand transport models for suspension & rolling capable of solving multiple challenges associated with long pipeline/tieback in multiphase fluid flow using the concept of multiphase flow velocity profiles.
7. Test and validate the MTV models for suspension & rolling using the acquired experimental data. Compare the models with existing models from the literatures.
8. Develop optimum strategies for sand transport mechanism in multiphase fluid flow in pipes given changes in flow patterns.

1.3 Research methodology

The fundamental objective of this research work was to investigate solid transport phenomenon in three-phase gas-liquid-solid/four-phase gas-oil-water-solid in pipe. The need to understand the physics of multiphase transport phenomenon and relevant transport mechanism controlling particle motion in three-phase/four-phase, gas-oil-water-solid flow systems was the key driver for this project. The particles may be transported differently by different flow patterns because they are subjected to different driving forces. The transient nature of multiphase fluid flow further makes the particle transport driving forces complicated. This understanding formed the basis on which the approaches to this work were developed. The following methods were therefore adopted:

1. Identified the key parameters influencing particle transport in multiphase fluid flow such as flow patterns and drag and lift coefficients.

2. Developed velocity profiles models for key flow patterns such as dispersed bubble flow, slug flow stratified flow and annular flow influencing transport mechanism using combined numerical (computational fluid dynamics) and analytical methods.
3. Developed preliminary minimum transport velocity (MTV) model for suspension and in rolling for multiphase fluid flow in pipes relying on experimental data obtained from literatures.
4. Evaluated the performance of the preliminary models by comparing with existing models from the literatures.
5. Designed and constructed multiphase flow loop for acquisition of pertinent data for flow patterns characterisation and solid minimum transport velocity.
6. Developed the MTV for suspension and rolling in multiphase flow in pipes combined with the velocity profile models obtained for key flow patterns.
7. Tested and validated the models with acquired experimental data. Compared with existing models in public domain.
8. Developed optimisation strategies for solid transport in multiphase fluid flow in pipes.

Chapter 2

Literature review of previous work

2.1 A review of deepwater development strategies

The operators are often faced with multiple challenges of maintaining production output levels in mature fields while seeking better ways of effectively exploiting new discoveries in growth areas, such as, West Africa, US Gulf of Mexico and Brazil. One of the consequences of mature fields is inevitable decline in oil production, high water cut, gas breakthrough and sand influx. And as the finite nature of petroleum resources onshore becomes more apparent, oil and gas operators are now venturing into remote and harsher locations in search of new reserves. The growth areas provide huge opportunities for new discoveries though located in harsher, deep & ultra deep water environments. The pace of technology has been slow in response to industry demand for solution to deepwater field challenges. Globally, deepwater experience and knowledge were limited, so is the technology (Schneider 2001). One of the key technology areas is accommodating large number of small and many large discoveries in remote and difficult environment which can be tied back to an existing facilities and ensuring cost and efficient production. For example, West Africa with significant deepwater oil reserves and favoured by the geographical distribution of its fields, the development will require multiple wells being tied-back to one central processing facility onshore or offshore (Iledare 2009).

However, among many issues to be considered before initiating deepwater development project was suggested by (Abbott, D'Souza, Solberg and Eriksen 1995, Korloo 2007). These include

- Recoverable reserves of oil/gas.
- Number and location of wells.
- Drilling and servicing of wells.
- Required field life.
- Fabrication, transportation, and installation scenario.
- Production and drilling facilities requirements.
- Effects of well fluid properties.
- Means for export of oil and gas.
- Effect of development schedule on economics.
- Contracting issues and market conditions

- Skilled resources requirement
- Environmental conditions and water depth.

The issues here are varied and introduce different complexities from exploration to production. As can be seen, the determination of best development concept is not only technical but can strongly be influenced by non-technical considerations such as market conditions.

Major deepwater developments typically consist of subsea wells tied back to floating surface production facilities such as semi submersibles or Floating Production Storage and Offloading (FPSO) as can be seen in Figure 2.1. Subsea tiebacks to a fixed platform are often considered whenever the distance from the well target back to the platform is beyond the limit of horizontal drilling. The choice of production and transportation options for liquid hydrocarbons and gas is important and is affected by the distance to other infrastructure, the water depths involved, geo-hazards, reservoir fluid characteristics, production rates, and reserves (Hartell and Greenwald 2009). In this kind of scenario, especially in the case of marginal oilfields, the industry faces the challenge of making the exploitation developments technically viable and cost effective to guarantee project success. To make possible the profitable development of such oilfields and increase the project net present value, it is required to keep the capital and operational expenditures within reasonable limits. For capital expenditure reduction for marginal fields, the first suggestion is the elimination of dedicated production platform and adoption of subsea systems which can be tied-in to existing infrastructure (Paulo, et al. 2001).

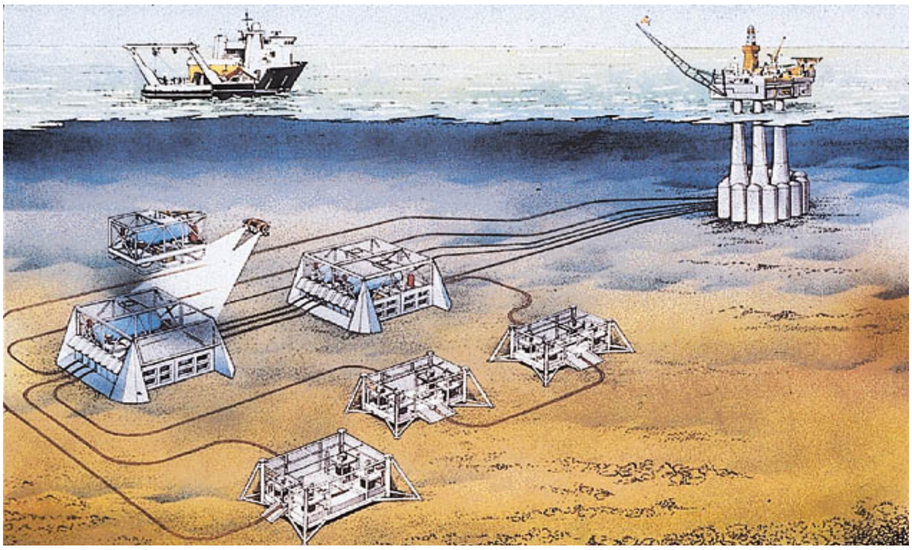

Figure 2.1: Pictorial representation of oil and gas wells tiebacks to FPSO (Universidade Fernando Pessoa 2006)

Deepwater projects presents new transportation challenges, particularly those projects that push the water depth boundaries and those that are remote from existing infrastructure. Some of the major technical difficulties for pipeline transportation in deep and ultra deep water also highlighted by (Schneider 2001, Ewida et al. 2004, Eklund and Paulsen 2007) are

1. The distance from the wellhead to the processing facility either onshore or offshore can sometimes be very long coupled with undulating nature of the sea bed.
2. There is extreme cold sea temperatures at sea bed level coupled with high pressure high temperature fluids from the reservoir flowing through the pipeline with potential for liquid condensation as a result. This constitutes additional liquid mixture with different molecular weight, density and viscosity.
3. The offshore environment is characterised by highly unconsolidated reservoir with productive zones relatively shallow and rapid depressurisation is quite common with greater chance of gas influx, early water breakthrough and attendant solid production. This is a serious problem especially with the surface facilities with sudden pressure drop.
4. Gas cooling forming hydrate which can block the pipeline and could require injecting hydrate inhibitors which introduces additional complexities to the multiphase fluid.

Various strategies have been adopted for different subsea production tiebacks projects in order to meet the challenges identified above. The technical solutions adopted for Ormen Lange have been governed by a subsea development concept where subsea pipeline was tied back to shore over a considerable distance and with a large production capacity. The execution strategy has been heavily influenced by a risk approach both on contract strategy, method and equipment selection. The success of the Ormen Lange Offshore Project has been highly dependant on a strong project management to accommodate and account for various technical issues (Eklund and Paulsen 2007).

The Laggan and Tormore gas condensate fields are situated in 600 meters water depth some 140km north-west of Shetland Islands. The region is served by limited oil and gas infrastructure and the so called "stranded gas" fields have been left undeveloped primarily due to the significant investment required to establish an export route to market in this remote and harsh environment (Cutler 2009). The project represents a significant challenge in terms of its scale and technical difficulty, combined with the harsh and demanding environment of the West of Shetland region. Total and its partners have now adopted development concept which consists of a long distance tieback of subsea wells connected to a new gas processing terminal at Sullom Voe on Shetland.

The incentives for developing deepwater fields are clear. There is increasing demand for oil and is expected to rise. And the declines in resource from mature fields which is no longer meeting the supply gap. But huge development cost and technology have been the key issues of concern for operators in their quest to bring new oil supply to the market from the deepwater resources. They had to deal with the implications of hardware, pipeline and umbilical integrity and functionality at extreme water depths in remote locations. The important issue relates to system integrity and reliability. This is to ensure the system is functioning once it is installed (Abbott et al. 1995).

2.2 A review of deepwater tiebacks technology

There are a number of deepwater fields which are developed with long distance subsea tiebacks either to a host facility or directly to the beach. The first four deepwater oil tiebacks were installed in 1996 in Gulf of Mexico (GOM). Pompano II was the first remote manifold tieback in the deepwater GOM (Heng, Ronalds and Edwards 2000). It is a large oil field, and a tieback to an existing platform fulfilled the project philosophy of reduced initial capital exposure. As can be seen from Figure 2.2, a lot of major reserves finds are located in very challenging operating environments such as deep and ultra deep waters. Subsea tieback systems have evolved over the years as a solution to the challenge of transporting these reservoir fluids in a cost effective manner. The varying challenges are complicated, there are complex seabed topographies and the continuous change in flow patterns, the attendant solids transport phenomenon in multiphase fluids, the quest to track location & height of beds have not in any way hindered interest in the development of tieback projects.

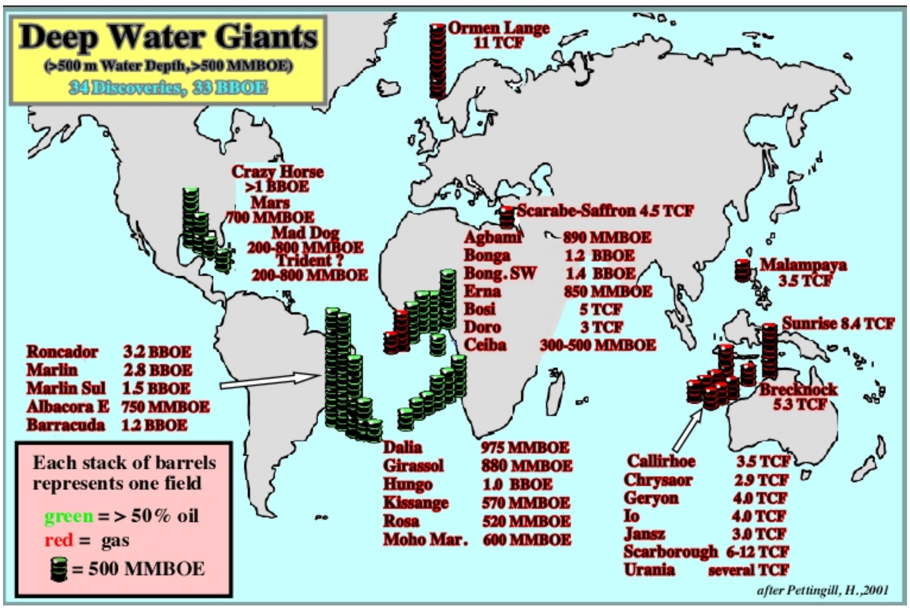

Figure 2.2: World deep water discoveries (Universidade Fernando Pessoa 2006)

The Canyon Express transportation system consists of two 12-inch flow lines running parallel from Camden Hills through Aconcagua and Kings Peak to Canyon Station Platform. The three subsea fields: Camden Hills, Aconcagua, and Kings Peak, are in 1900 to 2210 meters of water. Canyon Express subsea tieback, at 90 kilometers from Camden Hills to Canyon Station Platform, is one of the longest subsea tiebacks in the Gulf of Mexico (Forbord 2007). The tieback was jointly owned and operated by three operators in order to cope with the huge investment outlay (Rijkens, Allen, and Hassold 2003).

The Ormen Lange gas field is located 120 kilometers west northwest of Kristiansund on the Norwegian West Coast. The contract scope of work was laying and commissioning of two 120 kilometers long 6 inches pipelines from the gas processing plant at Nyhamna to the Ormen Lange manifold in water depths ranging from 0 – 850 meters (Eklund and Paulsen 2007). The challenges encountered was the fact that the installations must withstand the exceptional currents that are characteristic of this part of the Norwegian Sea, as well as sub-zero temperatures on the sea bed, and extreme wind and wave conditions. The project execution strategy was challenging to a significant extent, Statoil established collaboration with key sections of the Norwegian research and industrial communities which adopted the concept of tieback as viable means of developing the field.

The first notable oil production subsea tieback in Canada is North Amethyst field offshore Newfoundland & Labrador. The tieback distance is 6 kilometers to the sea of Rose FPSO. This was part of the collaborative efforts to develop 15 other smaller fields located in the Northern Grand Banks, whose resources are insufficient to justify stand-alone production facilities. It will make possible to utilise the spare production capacity of Rose FPSO and exploit the smaller fields via subsea tiebacks technology to help reduce development costs (Hawkins et al 2008).

The ESSO Exploration Angola proposed subsea tieback for the Kizomba Satellites development in Block 15, approximately 145 kilometers west of Soyo at water depths ranging from 1,000 - 1,200 meters (ExxonMobil 2012). Eighteen wells are planned with subsea tiebacks to the existing Kizomba A and B floating, production, storage and offloading (FPSO) vessels. This is to optimize the capabilities of on-block facilities and reduce capital expenditure in order to increase current production levels without requiring an additional FPSO vessel.

The Snohvit project by Statoil represents the longest tieback to land that is entirely subsea. Located 160 kilometers from processing facility represents a milestone for long distance transport of unprocessed well streams (Statoil Exploration and Production 2012). The project also provided facilities for future wells from nearby development to be tied-back. However, some of the challenges are due to the high pressure and the low temperature on the seabed with ice plugs forming in the pipeline. To prevent this occurring, antifreeze was added at the wellheads combined with heating up the pipeline electrically as required. Such technology has been specially developed for the Norwegian continental shelf vital to the operation of offshore oil and gas fields in the far northern regions.

The west of Shetland is thought to contain approximately 17% of the UKs remaining oil and gas reserves; Laggan and Tormore have an estimated 230 mboe. The challenge is to extract the gas and associated condensate from offshore in 600 meters water depth some 140 kilometers North-West of the Shetland Islands. The Laggan-Tormore Project will involve extensive operations to build a new onshore gas terminal plus subsea facilities and pipelines in a demanding offshore environment. The overall development concept consists of a 140 kilometers long distance tie-back of subsea wells connected to a new gas processing terminal at Sullom Voe on Shetland. The project required extensive flow assurance modeling in order to predict the flow regime and liquid hold-up in the pipeline to correctly size the onshore reception facilities (Cutler 2009).

Deep water fields represent a significant part of our future oil and gas projection to bridge the dwindling supply. With advancement in subsea tiebacks and improvement in associated challenges, more fields will become economically recoverable, ensuring the continued growth of the deep and ultra-deepwater sector in the future. Table 2.1 show tieback development projects spread across different regions. Many of the reservoirs to be developed are of reduced sizes that do not justify stand alone surface facilities. And small reservoirs can only be considered as economical provided that we can take advantage of existing facilities for a short to long tieback. Obviously, the longer tieback, the more complex and challenging the flow assurance issues will be.

Table 2.1: Tiebacks developments worldwide (aggregated from various sources by the author)

Year	Project/Location	Water depth [m]	Tieback length [km]	Pipe Size [in]	Field
1996	Malampaya, Philippine	850	30	16	Cond.
1997	Mensa, GoM, USA.	1600	110	12	Gas
1999	Roncador, GoM, USA	1850	2	12	Oil
1999	Tobermory, North Sea UK	1600	175	12	Oil & gas
2000	Mossgas, South Africa	810	60	12	Gas
2002	Canyon express, GoM, USA	2200	90	12	Gas
2003	Na Kika, GoM, USA	2100	39	12/16	Oil & Gas
2003	Scarab Saffron, Egypt	620	90	20	Gas

2004	Coulomb, GoM, USA.	2300	40	12	Gas
2004	Golden Eye, UK	120	105	20	Gas
2004	Thunder Horse, GoM, USA	1860	6	12	Oil
2005	Snohvit, Norway	245	160	27	Gas
2005	Simian & Sienna, Egypt.	90	114	12	Gas
2006	Erha North, Nigeria	1190	10	6/10	Oil
2006	Snow white,NS, Norway	340	161	12	Gas
2007	Ormen Lange, NS, Norway	1100	200	12	Gas
2007	Nuggets, North Sea, UK	120	40	12	Oil & Gas
2009	Burghley, North Sea UK	-	10	10	Oil & Gas
2010	North Amethyst, Canada	-	6	12	Oil
2010	Laggan-Tormore, UK	600	143	18	Oil & Gas
2011	Corrib, Ireland	-	93	20	Gas

Flow assurance has been recognised as one of the main design issues for the development of deepwater fields especially with tiebacks. Effective flow assurance strategy is crucial in the early stages of asset development in order to address the challenges of multiphase flow such as flow patterns, liquid hold-up, sand depositions etc and the resulting effects on operability, deliverability, and system performance (Bello, Falcone, Teodoriu and Udong 2011). The solution is to engage in research and development work to build accurate predictive tools for multiphase flow in pipeline.

2.3 Multiphase flow Patterns

Simultaneous passage of gas and liquid (water and or oil) in a transport or export pipeline / tiebacks often results in a variety of flow patterns as shown in Figure 2.3. Two-phase flow or three-phase flow is simultaneous flow of any two or three of the discrete phases (solid, liquid or gas). These phases are commonly encountered in the petroleum or allied industry. The formation of particular pattern is dependent on flow rates, fluid properties, pipe size and pressure profiles. The critical issue is how to define flow patterns which are somewhat subjective depending on the researchers own interpretation. This is because flow pattern information in multiphase flow is still largely obtained by visual observation (Keskin and Zhang 2007).

The concept of flow patterns in pipes introduces new challenges in the understanding of multiphase fluids principally because of the form in which fluids exist in pipes. The pipe may be horizontal, near horizontal or vertical. For a two-phase gas-liquid system, the flow patterns can be grouped into four main classes where each class can be subdivided into sub-classes for detailed description. The following classes of flow patterns have been documented in literatures for horizontal, high angle and vertical pipes (Hurlburt and Hanratty 2002, Lin and Hanratty 1987, Taitel 1999):

- Stratified flow (Subclasses: stratified smooth, stratified wavy)
- Intermittent flow (Subclasses: elongated bubble, slug, churn)
- Annular flow (Subclass: wispy annular)
- Bubble flow (Subclasses: bubbly, dispersed bubble)

2.3.1. Multiphase flow patterns in horizontal pipes

Pipeline transportation in deep and ultra deep water presents a unique challenge such as extremely uneven seabed and topographies. When oil and gas mixture flows through a long subsea tieback, a number of different patterns can be observed. In a horizontal pipes or slightly inclined pipes different flow patterns are recognisable. For relatively low gas and liquid rates a stratified configuration occurs with the liquid flowing on the bottom and the gas flowing above it. As the liquid rate is increased (at a constant gas rate) waves appear on the interface. At still higher liquid rates the waves can grow to the top of the pipe and, intermittently, form liquid blockages. At low gas velocities this intermittent regime is characterized as a plug pattern, whereby the gas flows as steady elongated bubbles along the top of the pipe. At high gas flows a slug pattern exists whereby slugs of highly aerated liquid move downstream approximately at the gas velocity (Barnea 1987). At low liquid throughputs transitions from stratified-wavy to annular flow occur with increasing gas throughputs. An increase of liquid flow causes a transition to an intermittent slug flow, which is accompanied by large, undesirable pressure pulsations (Chen and Guo 1999).

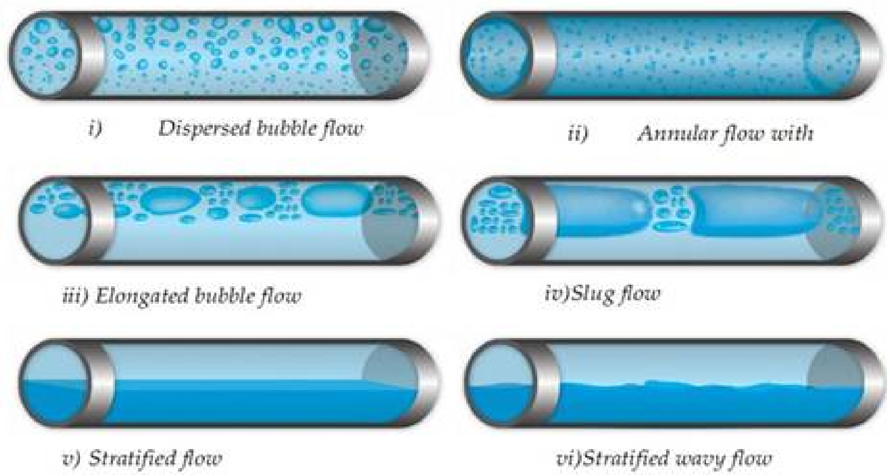

Figure 2.3: Flow patterns in horizontal pipe (Bratland 2010)

For oil dominated systems, the possible flow patterns are dispersed bubble and intermittent flow (Oliemans 1994). Oddie et al. 2003, generated a total of 444 experimental data for water-gas and oil-water-gas flows and observed that bubble, churn, elongated bubble, slug and stratified flow dominate in inclined pipes. While dispersed/homogenous, mixed/semi-mixed and segregated/semi segregated flows were observed for oil water flows.

It is important from the designer's point of view to be able to predict accurately what flow pattern will occur for given input flow rates, pipe size, and fluid properties (Mandhane, Gregory and Aziz 1973). Only then can the proper flow model be selected. Method for the prediction of flow pattern can be classified into two categories, experimental correlations and mechanistic modelling.

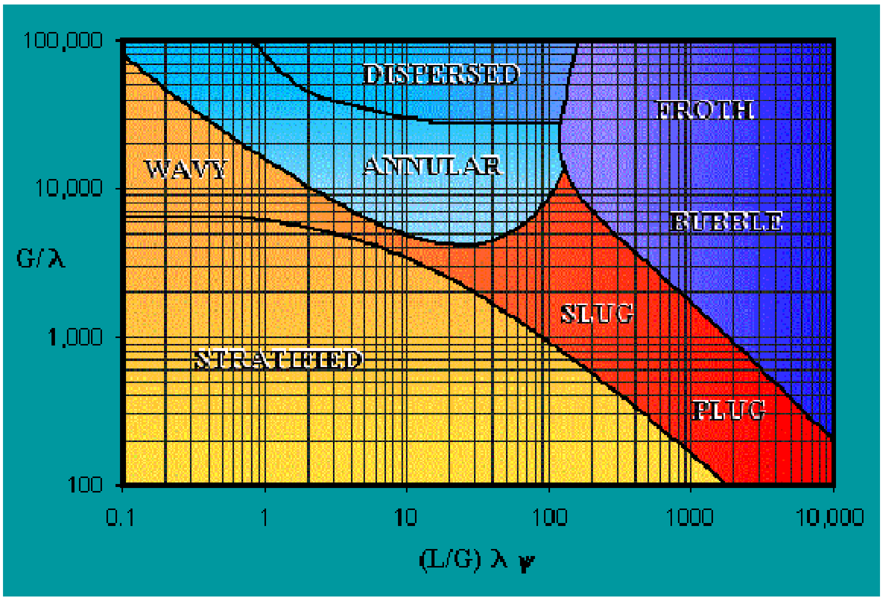

Figure 2.4: Flow pattern maps for horizontal pipes two-phase, air-water (Mandhane, Gregory and Aziz 1973)

The most common correlation used to calculate the conditions for the transition from one flow pattern to another is the Mandhane plot (Lin and Hanratty 1987). However, a number of flow pattern maps exist based on pipe configurations as can be seen in Figure 2.4. Many of these maps result from data covering a rather limited range of fluid properties and pipe diameters. Consequently, large discrepancies are often observed between a predicted flow regime and that actually observed in a subsequent test. The descriptions of various flow patterns in horizontal pipes have been provided in Table 2.2.

Table 2.2: Liquid-gas flow pattern classifications in horizontal pipes

Flow Patterns	Characteristics	Conditions of occurrence
Fluid flow modes		
Annular dispersed flow (ADF)	The liquid travels partly as a continuous film around the perimeter of the pipe and partly as a small droplets distributed in the gas phase.	This occurs at very high gas velocity and low liquid velocity.
Stratified (wavy) flow (SWF)	This is characterised by separation of fluids into different layers, with lighter fluids flowing above the heavier fluids.	For low flow rates of liquid and gas, a smooth or wavy stratified flow will occur. The interface may be smooth or wavy; hence the term wavy stratified flow.
Slug (intermittent)flow	Slugs of liquid are separated by coalesced gas bubbles. The intermittent pattern is evidenced when fluids are subdivided into slugs and elongated bubble patterns.	For intermediate liquid velocities, rolling waves of liquids will be formed. The rolling waves increase to the point of forming a slug flow, sometimes refer to as plug flow.
Dispersed bubble flow	The gas phase is distributed as discrete bubbles in an axially continuous liquid phase. Increased liquid flow rate prevents bubble accumulations and are dispersed more uniformly in the liquid phase.	This occurs at a very high flow rate. For very high liquid velocities and low gas/liquid ratios, the dispersed bubble flow pattern will prevail.

2.3.2. Multiphase flow patterns in vertical pipes

One of the earliest works of Govier and Aziz, 1972 on liquid–liquid two-phase flow through vertical pipes was to study the flow patterns, pressure drop and holdup using three different oils with high-speed photography. Other researchers' have been making efforts at representing the flow patterns observed under different conditions in the form of a flow pattern map, Figure 2.5 shows flow pattern transition description. For the particular case of upwards flow in vertical tubes four main flow patterns may be distinguished (McQuillan and Whalley 1985); these are bubble flow, churn flow, plug flow and annular flow, see Figure 2.6. Similar flow patterns were observed by Zubir and Zainon 2011, which they classified as bubble, bubbly-slug, slug and churn flow. They observed that liquid superficial velocity has great impact on the flow pattern transitions in vertical pipe rather than gas superficial velocity. Churn flow possesses some of the characteristics of plug flow, with the main differences being that the gas plugs become narrower and more irregular; the continuity of the liquid in the slug is repeatedly destroyed by regions of high gas concentration and the thin falling film of liquid surrounding the gas plugs cannot be observed (McQuillan and Whalley 1985). The liquid-liquid, kerosene-water flow experiment carried out by Jana et al 2006, showed that at low flow rates of kerosene, kerosene flows as droplets in the continuous water phase named as bubbly flow pattern. At high flow rates of kerosene, the analysis shows that there may be a separate flow pattern like core annular flow. No slug flow was observed rather there was transition consisting of irregular shaped chunks and bubbles of kerosene in water which they referred to as churn turbulent flow pattern. The descriptions of various flow patterns in vertical pipes have been given in Table 2.3.

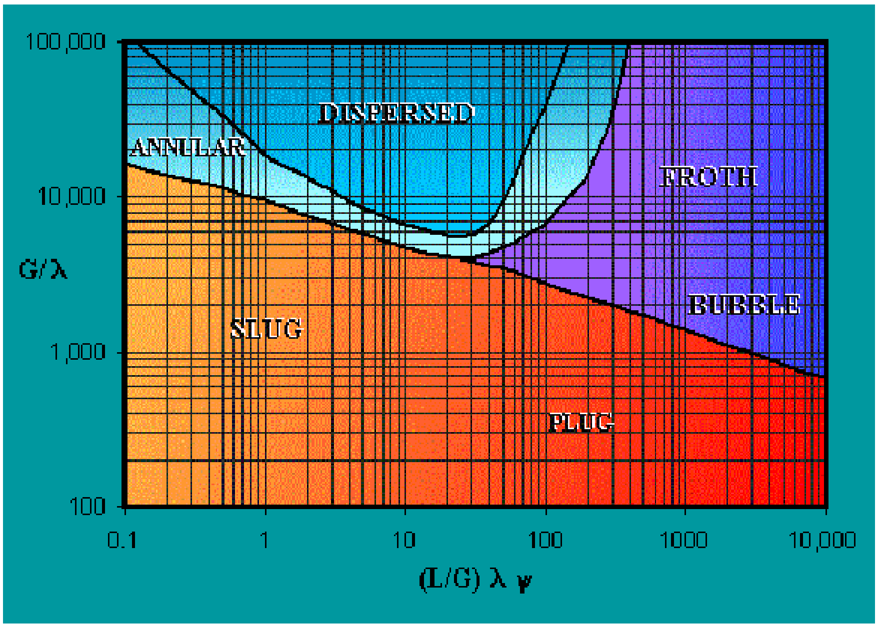

Figure 2.5: Flow pattern maps for vertical pipes two-phase, air-water (Mandhane, Gregory and Aziz 1973)

McQuillan and Whalley, 1985 observed that it is possible to extend the description of flow patterns in vertical pipes. For example, the annular flow regime may be sub-divided into wispy and non wispy annular flow, with wispy annular flow occurring as a result of the agglomeration of the liquid droplets in the gas core into large streaks or wisps. Furthermore, because the transitions between the various flow regimes do not occur suddenly, it is possible to observe a number of transition flow patterns which possess characteristics of more than one of the main flow patterns described above.

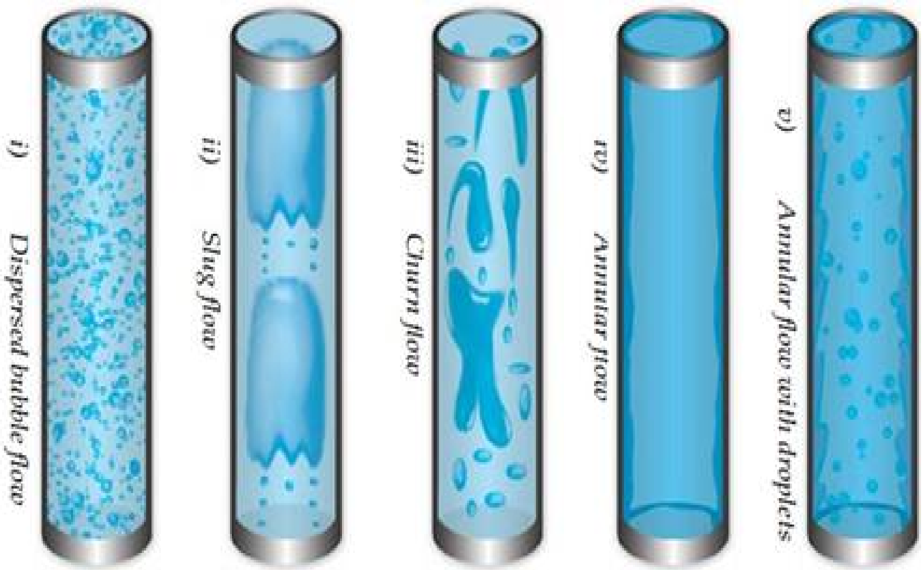

Figure 2.6: Flow patterns in vertical pipe (Bratland 2010)

Table 2.3: Liquid-gas flow pattern classifications in vertical pipes

Flow Patterns	**Characteristics**	**Conditions of occurrence**
	Fluid flow modes	
Annular dispersed flow	The gas flows along the centre of the tube or partially as droplets in the central core. The liquid travels partly in the form of an annulus at the wall.	This occurs at very high gas velocity and low liquid velocity.
Dispersed bubble flow	The gas phase is distributed as discrete bubbles in an axially continuous liquid phase. Increased liquid flow rate prevents bubble accumulations and are dispersed more uniformly in the liquid phase.	This occurs at a very high flow rate. For very high liquid velocities and low gas/liquid ratios, the dispersed bubble flow pattern will prevail.
Slug flow	Slugs of liquid are separated by coalesced gas bubbles. The intermittent pattern is evidenced	For intermediate liquid velocities, rolling waves of liquids will be formed. The

	when fluids are subdivided into slugs and elongated bubble patterns.	rolling waves increase to the point of forming a slug flow, sometimes refer to as plug flow.
Churn flow	This is similar to slug flow pattern but highly disordered in which the vertical motion of the liquid is oscillatory. In this case, the continuity of the liquid in the slug region is destroyed by a high gas concentration.	The liquid and gas rates are intermediate between the annular flow and slug flow for churn flow to occur. Further increase in flow velocity makes the pattern unstable.

2.3.3 Two-phase flow pattern characterisation

A number of authors have made empirical attempts to define the conditions under which the various flow patterns may be expected. This has been done by proposing flow pattern maps of various kinds (Govier and Aziz 1972). It is clear for any given fluid system the major factors in determining the flow pattern are the flow velocities. The fluid densities, viscosities, and interfacial tension and pipe diameter are the other factors though their contributions are still a subject of debate. Predicting flow patterns in multiphase flow in pipes is a rather complex exercise. Experimental data is widely used for the prediction of flow patterns (Taitel 1999). It involves the collection of experimental data followed by mapping of the data in a two-dimensional plot by locating transition boundaries between the flow patterns. Such a plot is termed flow pattern map. This map often serves as the means by which prediction of the flow pattern for design purposes take place.

Another approach is mechanistic modelling. In this approach, the dominant physical phenomena that will cause a specific transition are identified. Then the physical phenomena are formulated mathematically and transition lines are calculated. This can be presented as an algebraic relation or with respect to dimensionless coordinates. Taitel and Dukler, 1976a adopted mechanistic modelling approach for predicting flow pattern transitions. The drawback of their work was that different models were used for horizontal, slightly inclined and for vertical flows. This was improved upon by Barnea 1987, a unified model in which one uses the same models for all inclination angles. However, it is recommended that both approaches are combined (Taitel 1999).

Clearly there exist a number of problems with identifying and defining flow patterns and flow pattern transitions and establishing their range of applicability. Taitel 1999, stated that not less than eleven parameters can be identified as affecting the flow pattern. The parameters are as highlighted below:

- The liquid superficial velocity, U_{LS} , m/s
- The gas superficial velocity, U_{GS} , m/s
- Liquid density, ρ_L , Kg/m3
- Gas density, ρ_G , Kg/m3
- Liquid viscosity, μ_L , Kg/s m
- Gas viscosity, μ_G , Kg/s m
- Pipe diameter, D m
- Acceleration of gravity, g m/s2
- Surface tension, σ Kg/s2
- Pipe roughness, ϵ, m
- Pipe inclination, θ

The complexities associated with flow pattern transitions have given rise to many predictions available in the literatures. Govier and Aziz 1972, reported separate correlations to describe different flow patterns in horizontal pipes.

Beggs and Brill 1973 suggested a number of correlations for the prediction of flow patterns in gas-liquid flow in pipes applicable to both horizontal and vertical pipes. The following are the expressions,

$$N_{Fr} = \frac{u_m^2}{gD} \qquad 2.1$$

$$\lambda_L = \frac{q_L}{q_L + q_G} \qquad 2.2$$

$$L_1 = 316\lambda_L^{0.302} \qquad 2.3$$

$$L_2 = 0.0009252\lambda_L^{-2.4684} \qquad 2.4$$

$$L_3 = 0.10\lambda_L^{-1.4516} \qquad 2.5$$

$$L_4 = 0.50\lambda_L^{-6.738} \qquad 2.6$$

The following relations will determine the flow patterns as suggested by Beggs and Brill 1973

For segregated (stratified) flow will exist if

$$\lambda_L < 0.01 \,\&\, N_{Fr} < L_1 \;\text{ OR }\; \lambda_L \geq 0.01 \,\&\, N_{Fr} < L_2 \qquad 2.7$$

For intermittent (slug) flow will exist if

$$0.01 \leq \lambda_L < 0.4 \,\&\, L_3 < N_{Fr} \leq L_1 \;\text{ OR }\; \lambda_L \geq 0.4 \,\&\, L_3 < N_{Fr} \leq L_4 \qquad 2.8$$

For bubble or dispersed bubble flow will exist if

$$\lambda_L < 0.4 \,\&\, N_{Fr} \geq L_1 \;\text{ OR }\; \lambda_L \geq 0.4 \,\&\, N_{Fr} \;\phi\; L_4 \qquad 2.9$$

Transition flow if

$$\lambda_L \geq 0.01 \,\&\, L_2 < N_{Fr} \leq L_3 \qquad 2.10$$

Taitel and Dukler 1976a, suggested criterion at transition from stratified flow pattern. It was suggested that the flow conditions may generate either stratified smooth or stratified wavy flow. The waves are formed on a smooth liquid interface due to the gas flowing over the liquid or as a result of the action of gravity, even in the absence of gas flow.

Barnea 1987, proposed a general method that will allow the prediction of the flow patterns once the flow rates, the pipe size, fluid properties and angle of inclinations are specified. The models presented transition criteria for different flow patterns.

Taitel, 1999, observed that so far there is no acceptable method to calculate the transition boundaries and the reason why different mechanisms are proposed by different researchers for the same transition boundaries. Taitel 1999, argued that experimental results tend to report different transition boundaries even when the conditions of the experiment are identical. This has gone to show that there is sufficient evidence that current correlations for predicting flow patterns are limited in its applicability. There is the need to develop better and more accurate exact models for flow pattern prediction which are much more amenable to the practical application.

2.3.4 Three-phase flow pattern characterisation

Three-phase flow of two liquids and gas occurs often, especially in the production of hydrocarbons from oil and gas fields when oil, water, and natural gas flow in the transporting pipelines. In such environment, a frequently encountered flow pattern is slug flow (Bonizzi and Issa 2003). Depending on the flow rates of the phases, if sufficient mixing takes place, one liquid may be dispersed in the other; otherwise, the liquids will flow in separate layers. Still within the stratified pattern, mixing layers at the liquid–liquid interface may develop in such a way that even the stratified configurations consist of different phase distributions (Acikgoz 1992).

Stapelberg and Mewes 1994, argued that in horizontal three-phase oil-water-air flow, the same flow patterns are observed as in two-phase flow of a gas and a liquid, as long as the degree of dispersion of the oil and water is not taken into account. While there have been numerous investigations of two-phase flow regimes, however limited efforts have been directed towards investigating three-phase phenomenon. Previous works can be divided into two main categories on the basis of pipe inclination angle. The horizontal and/or slightly inclined case was studied by (Acikgoz 1992, Stapelberg and Mewes 1994, Lee, Sun and Jepson 1993, Chen and Guo 1999, Spedding, Donnelly, and Cole 2005) whilst the vertical case was considered by Chen and Guo 1999.

Taitel, Barnea, and Brill 1995, observed and classified seven flow patterns for three-phase in pipes which are similar to the case of two-phase flow- as stratified smooth flow, stratified wavy flow, rolling wave flow, plug flow, slug flow, pseudo slug flow and annular flow. Acikgoz, 1992 investigated an oil–water–gas system flowing in a horizontal Plexiglas tube of 5.78 meters length and 19 millimeters internal diameter. Different flow pattern maps were constructed for different values of the oil superficial velocity. The authors classified the flow patterns according to the combination of the following flow properties:

- Liquid phase that is predominantly in contact with the pipe walls
- Liquid–liquid flow pattern (either separated or dispersed)
- Relevant flow pattern between the liquid (oil +water) and the gas phases.

For the first part of their three-phase flow pattern determination, they identified either oil based, or water based flows; for the second part dispersed, separated, or separated–dispersed liquid–liquid flow; for the third part they identified six possible patterns: stratified, wavy, plug, slug, annular, and dispersed. Acikgoz 1992, reported similar patterns as outlined in Table 2.4 and Figures 2.7 (a & b) for three-phase horizontal pipe. Keskin and Zhang 2007, in a three-phase oil, water, and gas experiment proposed twelve flow patterns similar to that proposed by Acikgoz and Taitel et al.

Taitel and Dukler 1976a also proposed transition from stratified flow for three phase oil-water-gas especially when the liquid level is unstable. They stated that slug flow will exist for high liquid holdup and annular flow for low liquid holdup.

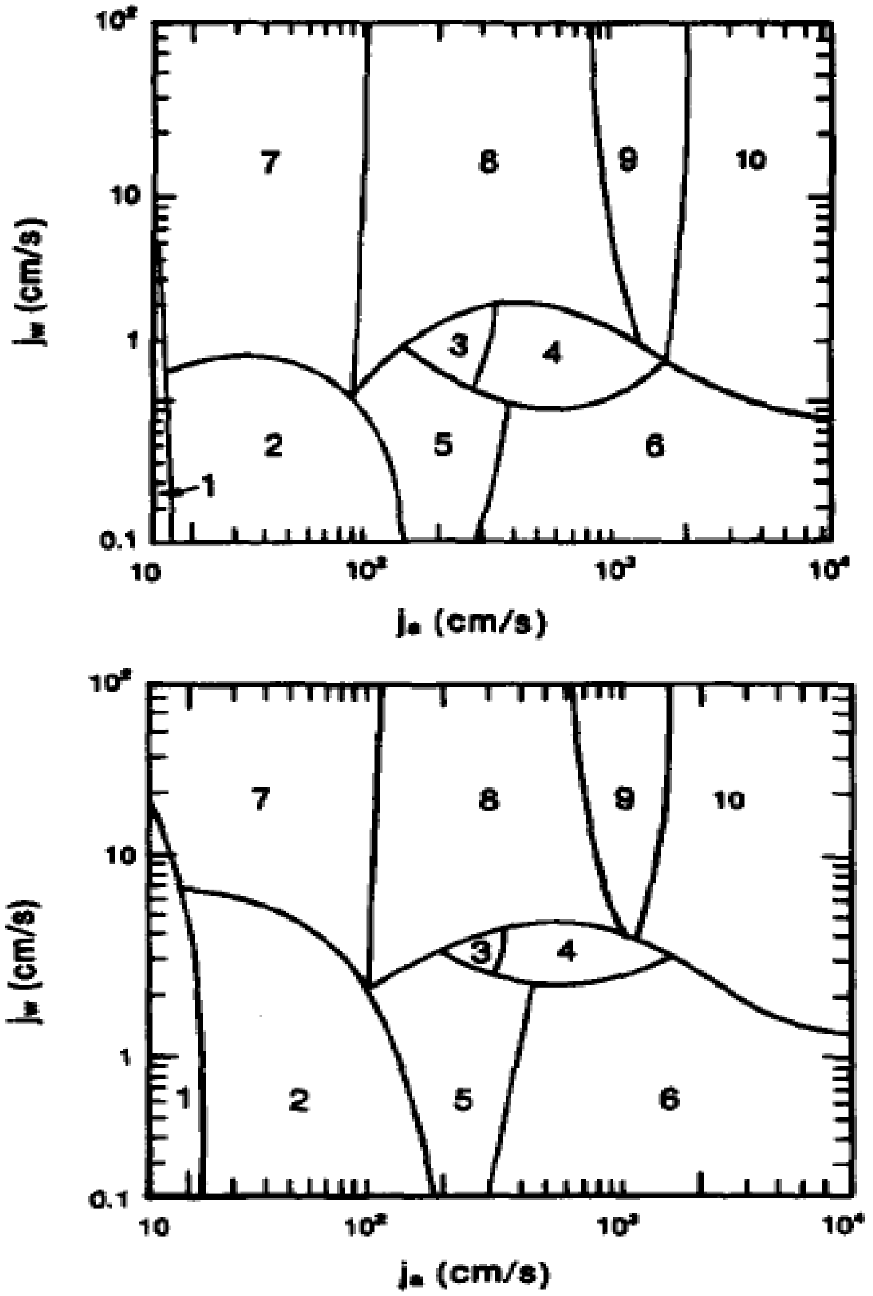

Figure 2.7: (a&b): Flow patterns for three-phase, oil, water and gas in horizontal pipes (Acikgoz et al)

Table 2.4: Three-phase flow pattern classifications

Region	Flow Regime
1	Oil-based dispersed plug flow
2	Oil-based dispersed slug flow
3	Oil-based dispersed stratified/wavy flow
4	Oil-based separated stratified/wavy flow
5	Oil-based separated wavy stratifying-annular flow
6	Oil-based separated/dispersed stratifying-annular flow
7	Water-based dispersed slug flow
8	Water-based dispersed stratified/wavy flow
9	Water-based separated/dispersed incipient stratifying-annular flow
10	Water-based dispersed stratifying-annular flow

2.4 Theory of solid movement through a fluid

The velocity required for effective transport of particles which may settle must be in the turbulent region for horizontal pipes, and for vertical pipes must be greater than the settling velocity of the particles (Brook 1987). In general, the ability of fluid in horizontal motion to be able to suspend solid particles depends on the counterbalance of two actions: gravity, which causes the particles to fall or settle in the fluid, and an upward diffusion of the particles, caused by a concentration gradient of particles, which in turn is created by gravity. However, for large and heavy particles, it may take a strong turbulence in order to suspend the particles in a horizontal pipe. Understanding this mechanism of particle suspension helps comprehend what happens to pipe flows of suspended solids.
The three compelling forces are:

1. Gravity force, F_G acting downward
2. Lift force, F_L acting upward
3. Drag force, F_D acting perpendicular, which appears whenever there is a relative motion between the particle and the fluid.

Where

$$F_G = \frac{\pi d_p^3 \rho_s g}{6} \tag{2.11}$$

$$F_L = 0.5 C_L \rho_f u^2 A_p \quad 2.12$$

$$F_D = C_D u^2 \frac{A_P \rho_f}{2} \quad 2.13$$

m is the mass of particle, g the acceleration due to gravity, ρ is the fluid density, ρ_P is the particle density, A_P is the projected area of the particle, C_D is the drag coefficient and u is the velocity of the particle relative to the fluid.

Therefore, the resultant force will equals the force due to acceleration.

$$m\frac{du}{dt} = mg - \frac{m\rho_f g}{\rho_P} - C_D u^2 \frac{A_P \rho_f}{2} \quad 2.14$$

In many practical use of centrifugal force, $\frac{du}{dt}$ is neglected. For a spherical particle of diameter d_P

$$m = \frac{\pi d_P{}^3 \rho_P}{6} \quad 2.15$$

$$A_P = \frac{\pi d_P{}^2}{4} \quad 2.16$$

Solving equation 2.14 for velocity, u and substituting m *and* A_P from equation 2.15 & 2.16, we can write

$$u_t = \sqrt{\frac{4gD_P(\rho_P - \rho)}{3C_D \rho}} \quad 2.17$$

Generally, the horizontal pipe velocity is the critical criterion of the required velocity in systems with both horizontal and vertical pipes. For a horizontal pipe it can be postulated that the lifting effect of the turbulent fluid should be able to overcome the gravity effect on the particle. The lifting effect depends on the kinetic energy of the fluid, fluid density and on the projected area of the particle (Brook 1987).

The drag coefficient C_D is a function of particle Reynolds number which can be expressed as

$$C_D = \frac{a}{N_{\mathrm{Re}\,p}{}^{b}} \tag{2.18}$$

$$N_{\mathrm{Re}\,p} = \frac{u D_P \rho}{\mu} \tag{2.19}$$

μ the viscosity of the carrier fluid.

The constants a & b are obtained from the sand transport experiments.

The drag coefficient is a function of the particle shape, size, surface roughness, fluid properties and flow parameters. Drag force is present in all types of flow around solids particles and is mostly superior over other forces during particle transportation (Ramadan, Skalle and Saasen 2005).

2.4.1 Solid transport patterns

The conveying of solids by a fluid in a pipe can involve a wide range of flow conditions and phase distributions, depending on the density, viscosity, and velocity of the fluid and the density, size, shape, and concentration of the solid particles (Stevenson et al. 2001, Peden, Ford and Oyeneyin 1990, Darby 2001). In oil & gas multiphase fluid flow, sand is often co-produced with oil especially oil produced from unconsolidated formations. The produced oil with entrained solids can be transported through pipeline to a processing facility nearby or to onshore location. In typical hydrocarbon transportation, pipeline follows the undulating topography of the offshore seafloors and onshore surfaces. This complex geometry thus has effect on how the solids are transported in the pipeline flowing with hydrocarbons.

Liquid-solid-gas flow in pipes can occur in a number of different flow patterns. The classifications of solid transport patterns are fairly consistent with many authors (Danielson 2007, Peden, Ford and Oyeneyin 1990, Oudeman 1993., Salama 2000, Liu 2003) and are grouped as pseudo-homogeneous suspensions, heterogeneous suspensions, heterogeneous suspensions with sliding beds, and stationary beds, as shown in Figures 2.8 & 2.9. The demarcation between the ‘‘homogeneous’’ and ‘‘heterogeneous’’ flow regimes depends in a complex manner on the size and density of the solids, the fluid density and viscosity, the velocity of the mixture, and the volume fraction of solids (Darby 2001).

The sand will settle to form beds along the bottom of the pipe if the fluid velocity is below the minimum transport velocity required for rolling or saltation (Peden, Ford and Oyeneyin 1990, Liu 2003, Bello, Oyeneyin and Oluyemi 2011). These beds can build up and plug the pipe if the velocity is too low, or it can be swept along the pipe bottom if the velocity is near the minimum transport velocity. Table 2.5 presents descriptions of various liquid-gas-solid flow patterns.

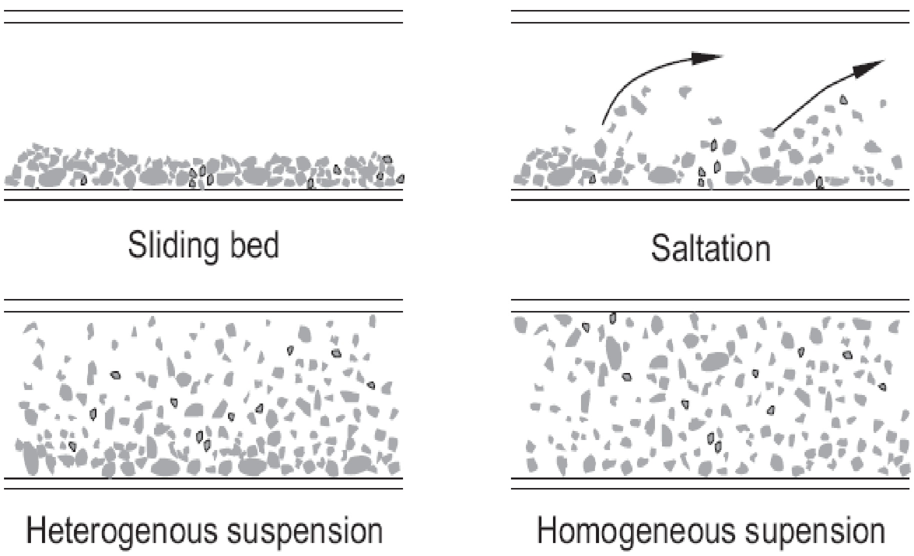

Figure 2.8: Flow Regimes of flow of Settling Slurries in Horizontal Pipe (Doron and Barnea 1996)

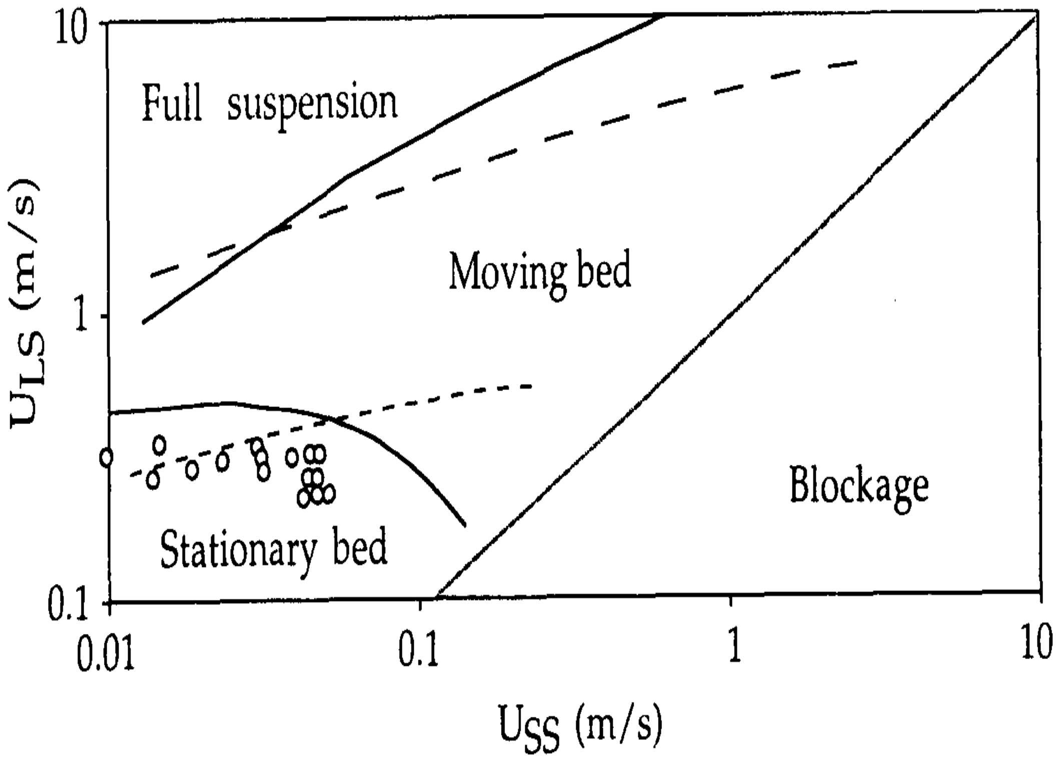

Figure 2.9: A flow pattern map for solid-liquid flow in pipe (Barnea 1987).

Table 2.5: Solid-fluid flow pattern

Sand transport modes		
Stationary bed (SB)	Sand is deposited at the bottom of pipes and become stationary.	This occurs at very low liquid or gas velocities.
Moving bed (MB)	Loosely packed sand deposited at the bottom of the pipe, first in the form of separated dunes and then as continuous moving bed. The sand grains are either rolling or saltating along the bottom of the pipe.	This will occur at increased velocity which keeps the solids moving along the bottom of the pipe.
Suspension flow (SF)	The sand particles are homogeneously suspended within the carrier fluid. This represents ideal dilute phase.	This occurs above the critical velocity. The flow assumes a turbulence condition.

2.5 Multiphase velocity profile models

Not all fluid particles travel at the same velocity within a pipe. The shape of the velocity curve i.e. the velocity profile across any given section of the pipe depends upon whether the flow is laminar or turbulent, single or multiphase. If the flow in a pipe is laminar, the velocity distribution at a cross section will be parabolic in shape with the maximum velocity at the center being about twice the average velocity in the pipe (Govier and Aziz 1972). In turbulent flow, a fairly flat velocity distribution exists across the section of pipe. The velocity of the fluid in contact with the pipe wall is approximately zero and increases the further away from the wall. Figure 2.10 illustrate the above ideas. In multiphase flow, the situation is quite complicated because of transient nature of multiphase fluids. The patterns are irregular and highly unstable depending on the operating conditions.

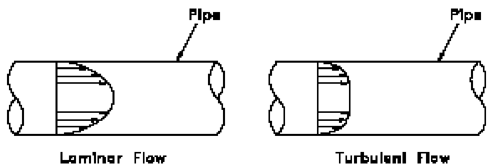

Figure 2.10: Laminar and turbulent flow velocity profiles

The generally accepted criterion for the end of laminar flow and the beginning of turbulent flow in a pipe is when the Reynolds number equal 2100. The fluid Reynolds number can be expressed as:

$$R_e = \frac{Du_f \rho}{\mu} \qquad 2.20$$

Where u_f is the mean velocity. Because of the regularity of the velocity profile in laminar flow, we can define an equation for the local velocity at any point within the flow path given as (Govier and Aziz 1972):

$$u = -\frac{g_c}{4\mu}\left(R^2 - r^2\right)\frac{dP_f}{dx} \qquad 2.21$$

Where,

$-\frac{dP_f}{dx}$ = pressure loss caused by friction

u =point velocity in the x direction
R= D/2= radius of the pipe
By definition of the friction factor, f,

$$-\frac{dP_f}{dx} = \frac{2f\rho V^2}{g_c D} \qquad 2.22$$

Where V, is the average velocity in the x-direction. Equation 2.22 is the well known fanning equation. Combining equations 2.21 and 2.22 to obtain (Govier and Aziz 1972):

$$u = \frac{f}{8} R_e V\left[1 - \left(\frac{r}{R}\right)^2\right] \qquad 2.23$$

In laminar flow, the fanning friction, f is given as:

$$f = \frac{16}{R_e} \qquad 2.24$$

Therefore,

$$u = 2V\left[1 - \left(\frac{r}{R}\right)^2\right] \qquad 2.25$$

Friction factor, f is commonly estimated from standard single phase friction factor relationships; (Taitel and Dukler 1976a) and many others use the standard Blasius equation for turbulent flow as:

$$f = 0.046 R_e^{-0.2} \tag{2.26}$$

For rough pipes, in turbulent flow, Colebrook equation which includes the effect of wall roughness is often used given as:

$$\frac{1}{\sqrt{f}} = -4\log\left[\frac{\varepsilon/D}{3.7} + \frac{1.255}{N_{\mathrm{Re}}\sqrt{f}}\right] \tag{2.27}$$

The term $N_{\mathrm{Re}}\sqrt{f}$ is by definition

$$N_{\mathrm{Re}}\sqrt{f} = \left(\frac{e_f D^3 \rho^2}{2L\mu^2}\right)^{0.5} \tag{2.28}$$

In the fully turbulent region, f is independent of Reynolds number so the Colebrook equation reduces to (Darby 2001):

$$f = \left(\frac{1}{4\log[3.7/(\varepsilon/D)]}\right)^2 \tag{2.29}$$

For multiphase flow, to the author's best knowledge no equation exists for predicting velocity profiles in multiphase flow in pipes. Most recent approaches have focused on finding correlations for the friction terms where two phase flow effects have been incorporated into the model. The lack of appropriate model to predict velocity profiles for different flow patterns in multiphase flow has provided research interest and one of the objectives for this research was to develop appropriate models for important flow patterns in multiphase flow. It was equally recognised that not one single model will be appropriate for predicting varied flow patterns that exist in multiphase flow in pipes (Bello, Oyeneyin and Oluyemi 2011).

2.6 Drag and lift coefficients

Multiphase flows involving suspensions of solid particles are frequently encountered in many industrial processes including oil & gas production. The ability of fluid in horizontal motion to be able to suspend solid particles depends on the counterbalance of two actions: gravity, which causes the particles to fall or settle in the fluid, and an upward diffusion of the particles, caused by a concentration gradient of particles which in turn is created by gravity (Govier and Aziz 1972, Liu 2003). The particle movement thus depends on the properties of the solids: solids density, particle size and particle shape.

The gravitational force causing the particle to rise or fall can be defined as (Govier and Aziz 1972):

$$F_g = \frac{\pi d^3}{6}\left(\rho_p - \rho_f\right)g \qquad 2.30$$

The rise or fall of the particles in the fluid results in a drag force which may be expressed as:

$$F_D = C_D \frac{\rho \upsilon^2}{2}\frac{\pi d^2}{4} \qquad 2.31$$

Where

ρ_p = particle density

ρ_f = fluid density

d = particle diameter

g = gravity

C_D = drag coefficient

υ = rise or fall velocity

The drag force arises from pressure and viscous stresses applied to the particle surface and resist the relative fluid velocity υ (Loth 2008). The magnitude of drag is primarily dictated by the particle Reynolds number (Rep), defined as

$$R_{ep} = \frac{\rho_f \upsilon_f d_p}{\mu_f} \qquad 2.32$$

Where,

R_{ep} = particle Reynolds number

υ_f = fluid velocity, m/s

d_p = particle diameter, m

μ_f = fluid viscosity, cp

The particle drag coefficient is one of the most important hydrodynamic parameters involved in the modelling and design of multiphase processes. Reliable models for forces acting on fluid particles such as drag & lift and virtual mass forces are indispensable in accurate prediction of dispersed multiphase flows using multi-fluid models. Typically, these multiphase operations are carried out under turbulent conditions of varying intensity. In these processes sometimes a uniform dispersion of particles is achieved due to the interaction between turbulent eddies and the dispersed phase (Doroodchi et al. 2008). A better understanding of such interaction is fundamental to the effective design, modelling and operation of multiphase systems. From a hydrodynamic viewpoint, the most important and fundamental aspects of solid-liquid multiphase flow are inter-phase interaction (i.e., interaction between the fluid phase and the particulate phase) and intra-phase interaction (i.e., interaction among solid particles making up the particulate phase). Inter-phase interaction between the fluid phase and the particulate phase is manifested mainly in the drag force exerted on the particles by the fluid stream and the transfer of momentum from one phase to another (Doan and George 1998). Several correlations for drag coefficient have been proposed over a wide range of Reynolds number in the literatures. One of the most widely used was the empirical equation of Schiller and Naumann, which is simple and accurate in the range 0.1 < Re < 800 (Tran-Cong, Gay and Michaelides 2004), expressed as:

$$C_D = \frac{24}{R_e}\left(1 + 0.15R_e^{0.687}\right) \quad 2.33$$

Cheng 2009, proposed a drag coefficient model which has greater applicability when compared with about 15 others that was evaluated. These other models can only be used for limited Reynolds numbers and even those applicable for wider range of Re, may involve tedious application procedure. The proposed model, given below, despite its simple form gives the best approximation of experimental data for Re from stoke regime to about 2×10^5.

$$C_D = \frac{24}{R_e}\left(1 + 0.27R_e\right)^{0.43} + 0.47\left[1 - \exp\left(-0.04R_e^{0.38}\right)\right] \quad 2.34$$

Drag coefficient, C_D in this case is predicted with two terms. The first term on the RHS can be considered as an extended Stokes' law applicable approximately for Re < 100 and the second

term is an exponential function accounting for slight deviations from the Newton's law for high Re. The sum of the two terms is used to predict drag coefficient for any Re over the entire regime.
Similarly, lift force acts in the direction perpendicular to the fluid velocity can be characterised by lift coefficient, defined as:

$$F_L = C_L \frac{\rho \upsilon^2}{2} \frac{\pi d^2}{4} \qquad 2.35$$

Where
F_L = lift force
C_L = lift coefficient.

There are two well known causes for Lift forces on a particle, caused either by a fluid velocity gradient or due to particle rotation imposed from other sources such as particle contact and rebound from a surface (Lataste et al 2000).
Compared to the drag force, significantly less research work has been done to predict the lift force exerted on a particle by the fluid motion. A common assumption for the lift force is that it is proportional to the drag force with the orientation of the particle (Zastawny et al. 2012)
Some of the drawback of available drag and lift correlations in the literature involves smooth spherical particles, or regularly shaped particles like disks or cylinders. This is very convenient due to its simplicity, the fact that the behaviour of spheres is well known, and the availability of a number of models to describe the interaction with fluid flow. But particles encountered in industry usually are not smooth spheres but are irregularly shaped and do not have smooth surfaces (Hottovy and Syvester 1979). In fact there is remarkable difference between spherical and non-spherical particles in the context of the method in which they tend to commence motion, given that spherical particles tend to begin motion via rolling whereas non-spherical particles preferably commence motion via dragging (Laskovski, Stevenson and Galvin 2009). Another drawback is that the correlations are developed from solids transport situations where the solids loading is very high. Typical sand loading in offshore applications is much smaller than most industrial solid-liquid slurry transport, on the order of 5-40 lb of sand per 1000 bbl of produced liquid (Danielson 2007, Stevenson et al. 2001).
The shape factor can therefore be obtained by measuring large numbers of particles in many different orientations to build up a picture of the three-dimensional variability in particle shape. Each particle can be described using a wide range of parameters, such as diameter,

perimeter, surface area, sphericity and shape factor (particle surface smoothness). The combination of several shape factors may be necessary to properly describe the effect of the shape of a particle on the hydrodynamic drag coefficient. After studying the effect of all the shape factors on the drag coefficient, Tran-Cong et al. 2004 found that the particle volume, projected area, flatness and circularity are well-characterized by the nominal diameter, d_n, the surface-equivalent-sphere diameter, d_A the ratio d_n/d_A and the particle circularity, c.

$$d_n = \sqrt[3]{6V/\pi} \qquad 2.36$$

$$d_A = \sqrt{4A_p/\pi} \qquad 2.37$$

$$c = \pi d_A/P_p \qquad 2.38$$

Where,

d_n = nominal diameter

V = particle volume

d_A = surface equivalent sphere diameter

c = particle circularity

P_p = particle perimeter

For the case of flow around a sphere, certain hydraulic analyses require determining the drag coefficient as well as lift coefficient as a function of particle Reynolds number. This is true for this research in the determination of minimum transport velocity models for suspension and rolling. A key parameter is the estimation of the particle settling velocity within the multiphase flow in pipeline. One problem is that the drag coefficient cannot be expressed in an analytical form for a wide range of particle Reynolds numbers, because the flow condition during the process is highly complicated (Almedeij 2008). Even with advent of CFD, performing large scale numerical study of complex multiphase flow requires some assumptions and also empirical data describing the interactions between the fluid and the particles (Zastawny et al. 2012). This relationship can generally be determined experimentally by observing the settling velocities in still fluids (Almedeij 2008, Carmichael 1982).

2.7 Pressure drop in multiphase flow

The pressure difference between two points can be written with the Bernoulli Equation:

$$\mathrm{P}_1 - \mathrm{P}_2 = \lambda \frac{\mathrm{L}}{\mathrm{d}} \frac{\rho v^2}{2} + \sum \zeta \frac{\rho v^2}{2} + \left(\rho_2 \mathrm{gh}_2 - \rho_1 \mathrm{gh}_1\right) + \frac{\left(\rho_2 \mathrm{v}_2{}^2 - \rho_1 \mathrm{v}_1{}^2\right)}{2} \qquad 2.39$$

On the right side of the equation there are four terms which represent friction caused by pipe, local friction, gravity, potential energy difference and kinetic energy difference, respectively.

The complex nature of multiphase flow in pipes resulted in different methods proposed for pressure drop (Beggs and Brill 1973, Hart et al. 1989, Behnia and Llic 1990, Abduvayt, Manabe and Arihara 2003). Although many of these methods were based on empirical correlations, the results were generally satisfactory for the conditions under which they were developed and have provided a good tool for design.

A number of variations of the above equation exist given the results of analysis by different authors. Beggs and Brill 1973 proposed a general pressure gradient correlation for two-phase flow by given by:

$$\frac{dP}{dL} = \frac{2 f_{tp} \rho_{ns} V_m^2}{d_e} \qquad 2.40$$

Where, f_{tp} is two-phase friction factor, ρ_{ns} is no slip density and V_m is mixture velocity

Behnia and Llic 1990 proposed a simple to use multiphase pressure drop correlation that could be applied to design or assessment of pipelines with flow of oil and gas mixtures. The correlation was based on relationship between pressure drop and Froude number.

It is common for some authors to adopt the strategy of dividing the flow conditions into different flow patterns and develop separate correlations for each of the patterns. Abduvayt et al. 2003 proposed pressure drop estimate for dispersed bubble based on experimental data, given by:

$$\frac{dP}{dL} = \frac{2 f_m \rho_m V_m^2}{D} + \rho_m g \sin\theta \qquad 2.41$$

Similarly, Hart et al. 1989 proposed pressure drop correlation for stratified wavy flow pattern in gas-liquid flow through horizontal pipe given by:

$$\frac{dP}{dL} = 4 f_{tp} \frac{L\rho_G V_G^2}{2D} \qquad 2.42$$

2.8 Liquid holdup

Most pressure loss prediction correlations for two-phase flow in horizontal pipes as well as inclined surfaces will require accurate prediction of two key parameters such as liquid holdup and two-phase friction factor. The reliability of these two parameters largely determines the accuracy of pressure drop prediction correlation.

Several correlations have been published for predicting liquid holdup in horizontal pipes and inclined surfaces. Most of these correlations are empirically developed and some from theoretical models with different degrees of complexity. Abdul-Majeed (Abdul-Majeed 1996) developed a simplified model to predict liquid holdup in horizontal pipes based on Taitel and Dukler model.

Beggs and Brill 1973 defined liquid holdup in terms of flow patterns. The expressions for each of the flow patterns are as presented below

For segregated flow:

$$H_L = \frac{0.98\lambda^{0.4846}}{N_{FR}^{0.0868}} \qquad 2.43$$

For intermittent flow:

$$H_L = \frac{0.845\lambda^{0.5351}}{N_{FR}^{0.0173}} \qquad 2.44$$

For distributed flow:

$$H_L = \frac{1.065\lambda^{0.5824}}{N_{FR}^{0.0609}} \qquad 2.45$$

Where the Froude number, input liquid content and mixture velocity are as given below,

$$N_{FR} = \frac{v_m^2}{gd} \quad 2.46$$

$$\lambda = \frac{q_l}{(q_l + q_g)} \quad 2.47$$

$$v_m = \frac{(q_l + q_g)}{A_p} \quad 2.48$$

Abdul-Majeed 2000 also proposed a simple model for liquid holdup in slug flow. It was argued that liquid holdup increases with increase in liquid viscosity. The model accounted for effect of inclination and observed that the liquid holdup is weakly influenced by downward inclination but significantly influenced by upward deviation from horizontal.

Garcia et al. 2005, reported Mattar & Gregory holdup models for slug flow of air-oil flow in horizontal and upward inclined pipes expressed as below:

For upward inclined pipe:

$$H_L = 1 - \frac{U_{sg}}{1.3(U_{sg} + U_{sl}) + 0.7} \quad 2.49$$

For horizontal pipe:

$$H_L = \frac{1}{1 + \left(\frac{U_m}{8.66}\right)^{1.39}} \quad 2.50$$

2.9 Solid transport models

A number of models for predicting solid transport in multiphase fluids exist in the literatures. This section reviewed some of these works especially as they relates to modelling and experimental explorations. The discussions highlighted methods that are adopted, results obtained and challenges encountered in the various studies. This provided opportunity to highlight the knowledge gap and areas for improvement.

A number of published works in multiphase transport have used particle transport in single phase as basis for the development of their models. The reason for this is the fact that many previous works are related to transportation in coal or bauxite industry (Stevenson et al. 2001).

2.9.1 Oroskar and Turian model

Oroskar and Turian 1980 adopted analytical approach for the critical velocity equation and defined a force or energy balance on the particle influenced primarily by the eddy intensity of the turbulent flow and the drag forces. For a case of high particle loading, particles will be subjected to the turbulent core of the fluid and hence will be transported. At low particle loading, similar to what is obtainable in the subsea tieback, the particle will drop to the bottom of the pipe where there is no turbulent eddies and form a stationary bed. Transportation of particle in this case depend on the size of the particle and whether or not is affected by turbulent core. The developed correlation based on turbulent core principle was used for development of critical velocity model as expressed below.

$$V_{OT} = \sqrt{gd(S-1)}\left[1.85C_C^{0.1536}(1-C_C)^{0.3564}\left(\frac{D}{d}\right)^{0.378}\left(\frac{\rho_L D\sqrt{gd(S-1)}}{\mu_L}\right)^{0.09}\chi^{0.3}\right] \quad 2.51$$

Where,

V_{OT} = critical velocity, m/s

g = acceleration due to gravity, m/s^2

D = pipe diameter, m

d = particle diameter, m

S = ratio of coarse solid density to carrier fluid density

C_C = coarse particle volume fraction (particles exceeding 74 microns)

ρ_L = carrier fluid density, kg/m^3

μ_L = carrier fluid dynamic viscosity, Pa-s

χ = hindered settling factor

In recent times, sand transport in multiphase flow in pipelines / tiebacks has received some interest. However, most of the work has been concentrated on measuring sand transport in air / water two phase flows and extending existing hydraulic conveying models to the multiphase case. This has been found to be inadequate for solid transport in multiphase flow.

2.9.2 Oudeman model

Oudeman 1993 approach was to facilitate the design of sand tolerant systems. This led to characterisation of the flow patterns for sand motion as:

- Flow with a stationary bed
- Flow with a moving bed and saltation (with or without suspension)
- Heterogeneous mixture with all solids in suspension

Air-water-sand flow experiment was conducted under varying operating conditions. The conclusions drawn are that, the increased sand transport in multiphase flow can be attributed primarily to the increased turbulent associated with the flow. Sand transport increases strongly with gas fraction. Gas increases sand transport much more than increasing liquid velocity. Oudeman therefore described sediment transport in terms of two dimensionless quantities as below

$$\phi = \frac{S}{\sqrt{d^3 g(F-1)}} \qquad 2.52$$

$$\psi = \frac{v_b^2}{gd(F-1)} \qquad 2.53$$

Where

ϕ = dimensionless sand transport rate

ψ = dimensionless fluid flow rate

S = Transport rate in grain volume per second meter of sand bed width

d = grain diameter

g = acceleration due to gravity

F = Solid – Liquid density ratio

v_b = drag velocity in sand bed

For each gas fraction, a relation between dimensionless transport rate and dimensionless flow rate was expressed in the form of power law as

$$\phi = m\psi^n \qquad 2.54$$

Where m & n depend on the input gas fraction.

The effects of different flow patterns, particle density and concentration profiles on particle transport were not considered and these have direct influence on sand transport.

2.9.3 Turian et al model

Turian and Yuan 1997 developed one of the most widely used solid transport model that correlated a total of 864 experimental critical velocity data, representing a broad variety of solid materials and pertaining to wide ranges of the variables. This was used as the basis for developing a set of critical velocity correlations, established by fitting the data to various forms of standard equations. The expression is as presented below:

$$\frac{v_c}{\sqrt{gD(s-1)}} = 1.7951C^{0.1087}(1-C)^{0.2501}\left(\frac{d}{D}\right)^{0.0662}\left(\frac{D\rho_L\sqrt{gD(s-1)}}{\mu_L}\right)^{0.0017} \qquad 2.55$$

Other researchers such as Oroskar & Turian adopted an analytical approach. The analytical result indicates that v_c depends on pipe diameter and on particle size which was in agreement with the conclusion drawn by (Oroskar and Turian 1980) which gave the best empirical fits to the data.

2.9.4 Gillies et al model

Gillies, Mckibben and Shook 1997 conducted experiments to investigate the ability of gas-liquid mixtures to transport sand in a horizontal pipe or well at low velocities. Both laminar and turbulent liquid flow regimes were investigated. He then extended the Meyer-Peter correlation for hydraulic conveying of slurries to multiphase flow and found that the sand transport rates for sand beds could be roughly predicted. Gillies et al extended Meyer-Peter model by relating dimensionless particle flux to dimensionless shear stress as shown below:

$$\phi = \frac{(q_S/S_S)}{\left[gd^3(S_S-1)\right]^{0.5}} \qquad 2.56$$

$$\psi = \frac{\rho_L g d(S_S-1)}{\tau_O} \qquad 2.57$$

$$\tau_O = \frac{fV^2\rho_M}{2} \qquad 2.58$$

Where,

S_S = Solid – Liquid density ratio

d = Particle diameter

g = Acceleration due to gravity

q_S = Volumetric flow rate of the mixture per unit bed width multiplied by the delivered volume fraction of solids

Ø = dimensionless particle flux

ψ = Dimensionless shear stress

ρ_L = Liquid density

f = friction factor for flow over a bed with a relative roughness (d/D_{eq})

V = mean velocity of the flow above the sand deposit ($V = Q/A_O$)

D_{eq} = hydraulic equivalent diameter

A_O = contact flow area

ρ_M = mean density of the delivered mixture

Meyer-Peter equation links ψ and ϕ by:

$$\phi = \left[\left(\frac{4}{\psi}\right) - 0.188\right]^{1.5} \qquad 2.59$$

This can also be rearranged to provide a prediction of the flow rate. Gillies et al concluded that gas injection has limited influence on the ability of a laminar flow to transport sand at low superficial velocities. They observed that gas injection can increase the solid transport rate if the flow is turbulent. This was similar to conclusion reached by Oudeman on gas increase with sand transport.

2.9.5 King et al model

King, Fairhurst and Hill 2001 extended the model of (Thomas 1962) for hydraulic conveying. The model calculates the minimum pressure gradient for solid transport to occur. It takes into account the viscous sub-layer and particle settling velocity, but the results can only be compared within the viscous sub-layer either with a larger or smaller particle diameter.

For a case where the particle diameter is smaller than the viscous sub-layer thickness, the friction velocity U_O^* at deposition for infinite dilution is given by:

$$U_O^* = \left[100 w_s \left(\frac{\nu}{d}\right)^{2.71}\right]^{0.269} \qquad 2.60$$

For a case where the particle diameter is bigger than the viscous sub-layer thickness, the friction velocity U_O^* at deposition for infinite dilution is given by:

$$U_O^* = \left[0.204 w_s \left(\frac{\nu}{d}\right)\left(\frac{\nu}{D}\right)^{-0.6} \left(\frac{\rho_S - \rho_L}{\rho_L}\right)^{-0.23} \right]^{0.714} \qquad 2.61$$

For a system with a greater particle concentration, the infinite dilution value can be modified to account for the presence of other particles. This correction is only applied if the particle diameter is in excess of the boundary layer thickness and is given by:

$$U_C^* = U_O^* \left[1 + 2.8 \left(\frac{w_s}{U_O^*}\right)^{0.33} \sqrt{\Phi} \right] \qquad 2.62$$

Where,

w_s = Particle settling velocity (ft/s) under quiescent conditions

υ = Kinematic viscosity (ft/s)

d = Particle diameter (ft)

D = Pipe diameter (ft)

ρ_S, ρ_L = Solid and liquid densities (lb/ft3)

Φ = Volume fraction of solids in the slurry

The height of the laminar sub-layer, δ for a smooth pipe and for Reynolds numbers below 10^7 is given by:

$$\delta = 62D \left(\frac{DU_{SL}\rho_L}{\mu_L}\right)^{-7/8} \qquad 2.63$$

Where, U_{SL} is the liquid superficial velocity (ft/s)

The particle velocity under quiescent conditions is dependent on the particle Reynolds number and can be divided into three regimes. The particle Reynolds number is defined as

$$R_{ep} = 1488 \frac{d w_s \rho_L}{\mu_L} \qquad 2.64$$

For R_{ep} <2, Stoke's law region

$$w_s = 1488 \frac{gd^2(\rho_S - \rho_L)}{18\mu_L} \qquad 2.65$$

For 2< R_{ep} <500, intermediate region

$$w_s = \frac{3.54 g^{0.71} d^{1.14} (\rho_S - \rho_L)^{0.71}}{\rho_L^{0.29} \mu_L^{0.43}} \qquad 2.66$$

For R_{ep} >500, Newton's law region

$$w_s = 1.74 \sqrt{\frac{gd(\rho_S - \rho_L)}{\rho_L}} \qquad 2.67$$

Based on above relations the pressure gradient for minimum transport to occur can be estimated as:

$$\frac{\Delta p}{\Delta x} = \frac{4\rho_L (U_C^*)^2}{D} \qquad 2.68$$

If the pressure gradient for minimum transport is lower than the pressure drop predicted by a multiphase flow correlation then the particles would be transported.

The model proffered method for estimating pressure gradient prediction, but they did not treat both minimum velocity required to transport sand particle in pipes.

2.9.6 Stevenson et al model

Stevenson et al. 2001 conducted an experiment to study sand transport at low loading in multiphase flow. This is a typical level of concentration in the transport of sand by oil and gas in subsea pipelines / tiebacks. It stressed the influence of turbulent slug nose and its effect on sand mobility. It highlighted fundamental flaws in extending work from hydraulic conveying where there is no resemblance to transportation of solid in multiphase oil and gas flow. The approach was to obtain dimensionless transport velocity correlations based on experimental observations. The correlations are as given below:

For low viscosities, < 4.1cP

$$V_P = 0.951V_{SL}\left(1+\frac{V_{SG}}{V_{SL}}\right)-\left(1.36\frac{V_{SG}}{V_{SL}}+0.852\sqrt{F_{rL}}\right)\left(R_{eL}\sqrt{F_{rL}}\left(\frac{d}{D}\right)^{1.5}\right)^{-0.181} \quad 2.69$$

For high viscosities, >4.1cP

$$\left(\frac{V_P}{V_{SL}}\right)\left[R_{eL}\sqrt{F_{rL}}\left(\frac{d}{D}\right)^{1.5}\right]^{-1.10} = 0.0167+0.00593\frac{V_{SG}}{V_{SL}}-0.00914\sqrt{F_{rL}} \quad 2.70$$

Where,

$$F_{rL} = \frac{V_{SL}}{\sqrt{gD}} \quad 2.71$$

$$R_{eL} = \frac{\rho_L V_{SL} D}{\mu_L} \quad 2.72$$

2.9.7 Danielson model

Danielson 2007 used SINTEF database to obtain the following relation for the critical velocity:

$$U_c = K\nu^{-n/(2-n)} d^{n/(2-n)}\left(gD(s-1)\right)^{1/(2-n)} \quad 2.73$$

Where d is the sand particle diameter, D is the pipe diameter, g is the acceleration due to gravity, s is the ratio of sand particle to carrier fluid density, and K and n are equal to 0.23 and 0.2 respectively.

The correlation was based on turbulence theory by considering the energy dissipated from turbulent eddies. It equates the strength of turbulence eddies to entrained particles into the fluid against gravity forces, which acts to settle the sand particles out. When the condition of the critical velocity is attained, the energy required for the particles to remain in the suspension must be equal to the fraction of turbulent energy effective in suspending them.

The concept of low loading was adopted similar to Stevenson approach. An essential feature of the model is that the critical slip between the liquid and solid phases is unaffected by the presence of gas.

2.10 Summary

Sand influx from relatively low strength formation is inevitable. The deep and ultra deep offshore environments are prone to sand influx because of the characteristic highly unconsolidated reservoir at shallow depth occasioned by high pressures and high temperatures. The production of formation sand into the wellbore and topside facilities is a common problem with attendant adverse effect on well productivity and equipment. With future projection for high number of offshore production through pipelines / tiebacks, it is desirable to have a robust sand management model in place. The discovery of new and usually massive and even marginal oil and gas reserves offshore is a clear manifestation that more and more companies will rely on the technology of transporting unprocessed reservoir fluid through a long subsea pipelines / tiebacks. The cost of offshore projects is very huge and therefore there is little room for errors. The key issue here is to guaranty unhindered flow of reservoir fluids through the pipeline to the processing facilities.

A major complication in the flow assurance issue is the effective management of complexity associated with the transient nature of multiphase flow and sand transport in pipes. Ineffective management may lead to sand deposition, bed formation, and sand erosion with attendant equipment failure. This explains current interest in the design and performance analysis of liquid-gas-sand multiphase flows in subsea pipelines or tiebacks.

From the literatures reviewed, it can be seen that many of the current works have been largely focused on single and two phase flow. The literatures also highlighted the fundamental flaws in extending hydraulic conveying theory to particle transport in multiphase flow. Many of the models (Oroskar and Turian 1980, Turian and Yuan 1997, Gillies, Mckibben and Shook 1997, Thomas 1962, Thomas 1979) also reflect high sand loading as against typical low sand loading of less than 1 in 1000 by volume, a level of concentration encountered in the transport of sand by oil and gas in subsea pipelines (Stevenson et al. 2001). The influence of flow patterns and flow pattern transitions in multiphase fluids are rarely considered looking at the approach adopted in previous model development for solid transport in pipes. This in the judgement of this author may have been responsible for lack of accuracy of these models. These among others have impeded our understanding of the behaviour and associated problems of three-phase or four-phase (oil, water, gas and solid) in pipes. The result is inappropriate solid transport models for three-phase and four-phase.

In order to bridge these gaps in knowledge, the research adopted an integrated multiphase flow management system supported with comprehensive experimental investigation of solid behaviours in multiphase fluid flow. This involved the simulation of key flow patterns which led to the developments of predictive models for each of the important flow patterns influencing solid transport in pipelines. The multi-fluid modeling and simulation methods coupled with experimental investigation have promising potential and may prove to have the key to unlocking the complexities of solid transport in multiphase fluids in pipeline/tiebacks.

Chapter 3
Velocity profiles model development - numerical methods

3.1 Introduction

A large number of flows encountered in nature and technology are a mixture of phases. The concept of phase in a multiphase flow system is a complex proposition. Therefore the flow of gas-liquid mixture in pipelines results in the manifestation of a number of transient flow pattern changes depending on the fluid properties, flow rates, pressure drop and pipe orientations as discussed in previous chapters. As a result, a number of flow patterns have been identified e.g. stratified wavy, stratified smooth, plug, slug, annular and dispersed bubble flow. Each of these flow patterns exhibits unique flow characteristics. They are very unstable and exhibits constant transition from one flow pattern to another depending on the flow conditions in the pipe. There is always the need to capture and model these changes as the fluids are transported through the pipeline/tieback. The pattern changes will have effect on the solid transport efficiency through the pipeline. A number of solution procedures are available and can be classified into three categories: numerical models, mechanistic models and empirical correlations (Ghorai and Nigam 2006, De Schepper, Heynderickx and Marin 2008, Ekambara et al. 2008). Though all the methods are with some levels of limitations but a combination of two or three approaches may eliminate uncertainties associated with each of the methods significantly. Critical information can be obtained from numerical models such as multi-dimensional distribution of phases, dynamic flow regime transition and turbulent effects. The empirical correlations consider the flow regimes based on physical measurements, this will be discussed in details in subsequent chapters. In this chapter, the focus was on the numerical approach using computational fluid dynamics, CFD.

The CFD has been employed to determine the velocity profiles for different flow pattern because of difficulties with experimental measurement. The CFD therefore served as virtual laboratory to generate fluid velocity profiles for a combination of fluid mixtures, gas-oil, water-oil, gas-water and water-oil-gas. This led to development of velocity profile models for each of the notable flow patterns by combining analytical equation with point velocity profiles generated numerically. On the basis of this, analysis of solid transport mechanism in different flow patterns was carried out and MTV models for suspension and rolling in horizontal, inclined and vertical pipes was determined. Details can be found in chapter 6 of this thesis.

3.2 Approaches to Multiphase Modelling

A number of CFD software is available in the open domain, the Ansys CFX, Fluent and Star-CD. The Ansys Fluent has been used in this study because of its simple adaptation to pipeline flow problems. The Navier stokes equations form the basis of CFD governing equations which includes expressions for the conservation of mass, momentum and pressure. Two well-known methods are available for numerically solving this set of governing equations, the finite volume and the finite element approaches (Ghorai and Nigam 2006). These can be used for analysis of gas-liquid, gas-solid, liquid-solid, and gas-liquid-solid flows. For these types of problems, the use of the volume-of-fluid (VOF), mixture models, and Eulerian models, as well as the discrete phase model (DPM) are recommended (ANSYS Inc 2011). They form the set of coupled partial differential equations which can be solved numerically to obtain the solution for unsteady flow problems, shown in Figure 3.1. Additional transport equations are also solved when the flow is turbulent.

The general form of the mass conservation equation is as expressed below and this is valid for incompressible as well as compressible flows.

$$\frac{\partial \rho}{\partial t} + \nabla(\rho \vec{v}) = S_m \tag{3.1}$$

The source S_m is the mass added to the continuous phase from the dispersed second phase and any user defined sources.

A single momentum equation is solved throughout the domain, and the resulting velocity field is shared among the phases. The momentum equation, shown below, is dependent on the volume fractions of all phases through the properties ρ and μ:

$$\frac{\partial}{\partial t}(\rho \vec{v}) + \nabla.(\rho \vec{v}\vec{v}) = -\nabla p + \nabla.(\bar{\bar{\tau}}) + \rho \vec{g} + \vec{F} \tag{3.2}$$

Where p is the static pressure, $\bar{\bar{\tau}}$ is the stress tensor and $\rho \vec{g}$ & $\vec{F}$ are the gravitational body force and external body forces respectively. The stress tensor is given as:

$$\bar{\bar{\tau}} = \mu\left[\left(\nabla \vec{v} + \nabla \vec{v}^{T}\right) - \frac{2}{3}\nabla.\vec{v}I\right] \tag{3.3}$$

Where μ is the molecular viscosity, I is the unit tensor.

The energy equation, also shared among the phases can be expressed as:

$$\frac{\partial}{\partial t}(\rho \mathrm{E})+\nabla.\left[\vec{v}(\rho \mathrm{E}+p)\right]=\nabla.\left(k_{eff}\nabla \mathrm{T}\right)+S_h \qquad 3.4$$

The VOF model treats energy E, and temperature, T, as mass averaged variables:

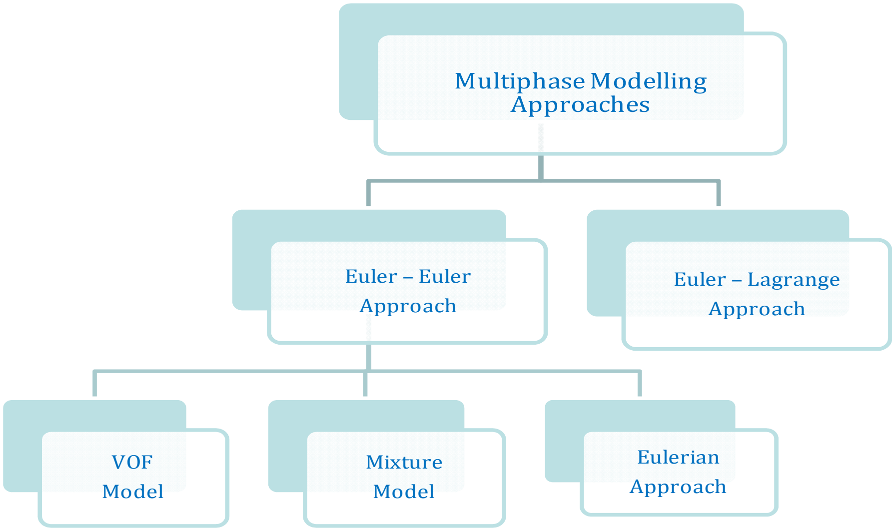

Figure 3.1: Approaches to multiphase modelling

3.2.1 The Euler-Euler Approach

In this approach, the different phases are treated mathematically as interpenetrating continua. Since the volume of a phase cannot be occupied by the other phases, the concept of phasic volume fraction is introduced. These volume fractions are assumed to be continuous functions of space and time and their sum is equal to one. Conservation equations for each phase are derived to obtain a set of equations, which have similar structure for all phases. These equations are closed by providing constitutive relations that are obtained from empirical information, or, in the case of granular flows, by application of kinetic theory. There are three different Euler-Euler multiphase models available in the literature: the volume of fluid (VOF) model, the mixture model, and the Eulerian model.

3.2.2 The VOF Model

The VOF model is a surface-tracking technique applied to a fixed Eulerian mesh. It is designed for two or more immiscible fluids where the position of the interface between the fluids is of interest. In the VOF model, a single set of momentum equations is shared by the fluids, and the volume fraction of each of the fluids in each computational cell is tracked throughout the domain. Applications of the VOF model include stratified flows, free-surface flows, filling, sloshing, the motion of large bubbles in a liquid, the motion of liquid after a dam break, the prediction of jet breakup (surface tension), and the steady or transient tracking of any liquid-gas interface(De Schepper et al. 2008, Al-Yaari and Abu-Sharkh 2011).

3.2.3 The Mixture Model

The mixture model is designed for two or more phases (fluid or particulate). As in the Eulerian model, the phases are treated as interpenetrating continua. The mixture model solves for the mixture momentum equation and prescribes relative velocities to describe the dispersed phases. Applications of the mixture model include particle-laden flows with low loading, bubbly flows, sedimentation, and cyclone separators. The mixture model can also be used without relative velocities for the dispersed phases to model homogeneous multiphase flow.

3.2.4 The Eulerian Model

The Eulerian model is the most complex of the multiphase models. It solves a set of momentum and continuity equations for each phase. Coupling is achieved through the pressure and interphase exchange coefficients. The manner in which this coupling is handled depends upon the type of phases involved; granular (fluid-solid) flows are handled differently than non granular (fluid-fluid) flows. For granular flows, the properties are obtained from application of kinetic theory. Momentum exchange between the phases is also dependent upon the type of mixture being modelled. Eulerian multiphase model has multiple applications e.g. particle suspension.

3.3 Multiphase Model Selection

The process of selection will require identification of the flow patterns that best represent the fluid flow. There are general guidelines for determining appropriate models for each flow pattern as shown in Figure 3.2. Details are provided about how to determine the degree of interphase coupling for flows involving bubbles, droplets, or particles, and the appropriate model for different amounts of coupling. The equations for fluid-fluid and solid-liquid multiphase flows, as coded in Ansys Fluent, are presented here for the general case of an n-phase flow.

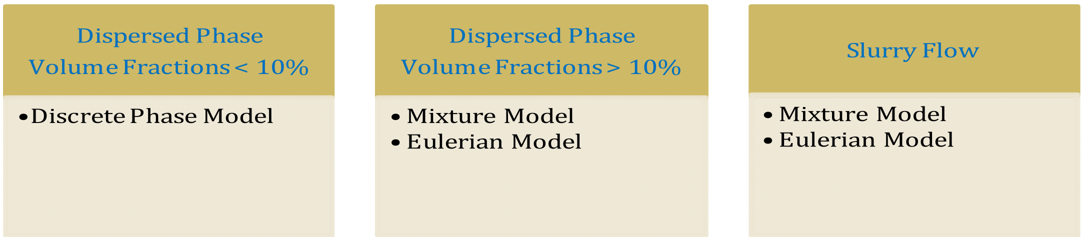

Figure 3.2: Guidelines for choice of multiphase models (ANSYS Inc 2011)

3.3.1 Fluid-Fluid Momentum Equations

The conservation of momentum for a fluid phase q is

$$
\begin{aligned}
&\frac{\partial}{\partial t}\left(\alpha_q \rho_q \vec{v}_q\right) + \nabla.\left(\alpha_q \rho_q \vec{v}_q \vec{v}_q\right) = \\
&\quad - \alpha_q \nabla_q + \nabla.\bar{\bar{\tau}}_q + \alpha_q \rho_q \vec{g} \\
&\quad + \sum_{p=1}^{n}\left[\mathrm{K}_{pq}\left(\vec{v}_p - \vec{v}_q\right) + \dot{m}_{pq}\vec{v}_{pq} - \dot{m}_{qp}\vec{v}_{qp} \right] \\
&\quad + \left(\vec{F}_q + \vec{F}_{lift,q} + \vec{F}_{vm,q}\right)
\end{aligned}
\qquad 3.5
$$

Here $\vec{g}$ is the acceleration due to gravity.

3.3.2 Turbulent Models

The effects of turbulent fluctuations of velocities and scalar quantities in a single phase use various types of closure models. In comparison to single-phase flows, the number of terms to be modelled in the momentum equations in multiphase flows is large, and this makes the modelling of turbulence in multiphase simulations extremely complex.

The mixture turbulence model is the default multiphase turbulence model. It represents the first extension of the single-phase $\kappa - \varepsilon$ model, and it is applicable when phases separate, for stratified (or nearly stratified) multiphase flows, and when the density ratio between phases is close to 1. In these cases, using mixture properties and mixture velocities is sufficient to capture important features of the turbulent flow.

The κ and ε equations describing this model are as follows:

$$
\frac{\partial}{\partial t}\left(\rho_m \kappa\right) + \nabla * \left(\rho_m \vec{v}_m \kappa\right) = \nabla * \left(\frac{\mu_{t,m}}{\sigma_k}\nabla \kappa\right) + G_{k,m} - \rho_m \varepsilon \qquad 3.6
$$

and

$$\frac{\partial}{\partial t}(\rho_m \varepsilon) + \nabla * (\rho_m \vec{v}_m \varepsilon) = \nabla * \left(\frac{\mu_{t,m}}{\sigma\varepsilon} \nabla \varepsilon \right) + \frac{\varepsilon}{\kappa}(C_1 \varepsilon G_{\kappa,m} - C_2 \varepsilon \rho_m \varepsilon) \qquad 3.7$$

Where the mixture density and velocity ρ_m and $\vec{v}_m$ are computed from

$$\rho_m = \sum_{i=1}^{N} \alpha_i \rho_i \qquad 3.8$$

and

$$\vec{v}_m = \frac{\sum_{i=1}^{N} \alpha_i \rho_i \vec{v}_i}{\sum_{i=1}^{N} \alpha_i \rho_i} \qquad 3.9$$

The turbulent viscosity, $\mu_{t,m}$ is computed from

$$\mu_{t,m} = \rho_m C_\mu \frac{\kappa^2}{\varepsilon} \qquad 3.10$$

And the production of turbulence kinetic energy $G_{k,m}$ is computed from

$$G_{k,m} = \mu_{t,m} \left(\nabla \vec{v}_m + (\nabla \vec{v}_m)^T \right) : \nabla \vec{v}_m \qquad 3.11$$

3.4 General approach to CFD

The ANSYS Fluent software package included a pre-processor, a solver and a post processor. Pre-processing includes geometry and mesh generation, flow specification, and setting solver control parameters. Once the geometry has been created and meshed, the fluid properties, flow models and solver control parameters are then specified. The boundary and initial conditions are also specified.

Generally, all the data defined in the pre-processing step are fed into the solver programme in the form of a data file. The solver is a specialised programme that solves the numerical equations based on the data specified in the data file. The results obtained by the solver are written to a results file for examination using the post-processor software. Thereafter, the data obtained by the solver can be visualised and displayed using a variety of graphical methods such as contour, plane, vector and line plots. Calculations can also be made to obtain the values of scalar and vector variables, such as pressure and velocity, at different locations.

3.4.1 Geometry

The geometry of the flow domain can be created using workbench. In this case, a 2 meter length pipe was created on x-y axis with the face along the x-z plane. There was provision for angle variation on x-y plane to account for the inclined surface. The pipe shape was generated with 3-D tools and then exported for meshing generation.

3.4.2 Mesh generation

Mesh generation must be well designed to resolve important flow features which are dependent upon flow conditions as shown in Figure 3.3. The flow domain is divided into sufficiently small discrete cells, the distribution of which determines the positions where the flow variables are to be calculated and stored. The grid refinements inside the wall boundary layer are desirable to enhance accuracy of the simulation. A fine mesh is particularly important in regions where large changes in the flow variables are expected. The Mesh can be generated from the workbench or by any other means. The mesh, together with the boundary conditions needs to be exported from the workbench directly into fluent software.

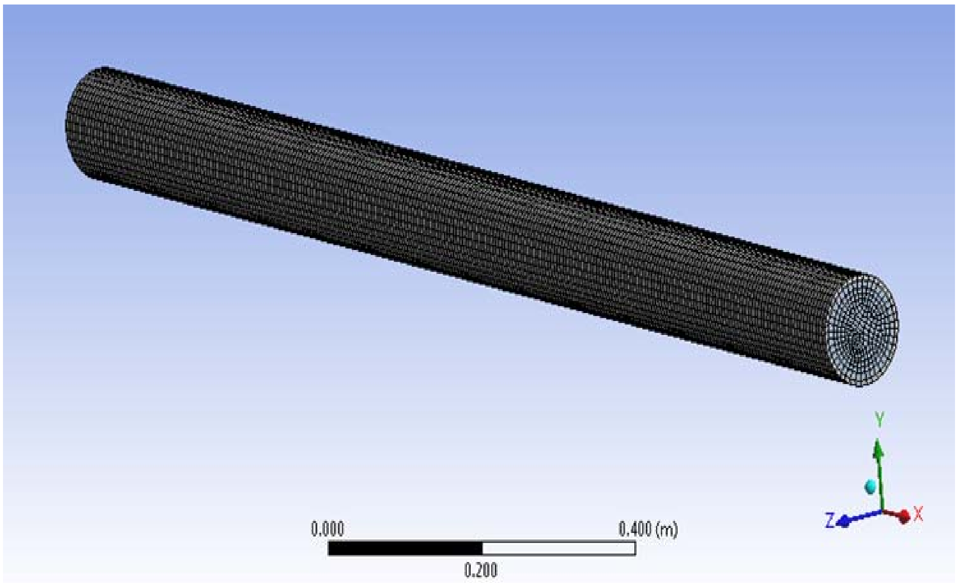

Figure 3.3: 3D geometry creation and mesh generation for horizontal pipe

3.4.3 Numerical simulation

The flow conditions and fluid properties are specified, inviscid, viscous, laminar, or turbulent flow. The fluid properties such as density, viscosity, and thermal conductivity among other properties are equally specified. The appropriate model for the simulation is also selected. Initial boundary conditions and flow conditions are also specified prior to simulation. When all the information required for the simulation has been specified, the CFD software performs iterative calculations to arrive at a solution to the numerical equations representing the flow. The user needs also to provide the information that will control the numerical solution process such as the convergence criteria.

3.4.4 Results

When the simulation is completed, the report generated will include the integral quantities such as total pressure drop and velocity vector lines as can be seen in Figure 3.4. From the XY plots, one can obtain the centerline velocity/pressure distribution and friction factor distribution. The results analysis can be carried out in order to check that the solution is satisfactory. If the results obtained are unsatisfactory, the possible source of error needs to be identified, which can be an incorrect flow specification, a poor mesh quality, or a conceptual mistake in the formulation of the problem (De Schepper et al 2008). The data from the XY plots can be exported to excel spreadsheet for further analysis.

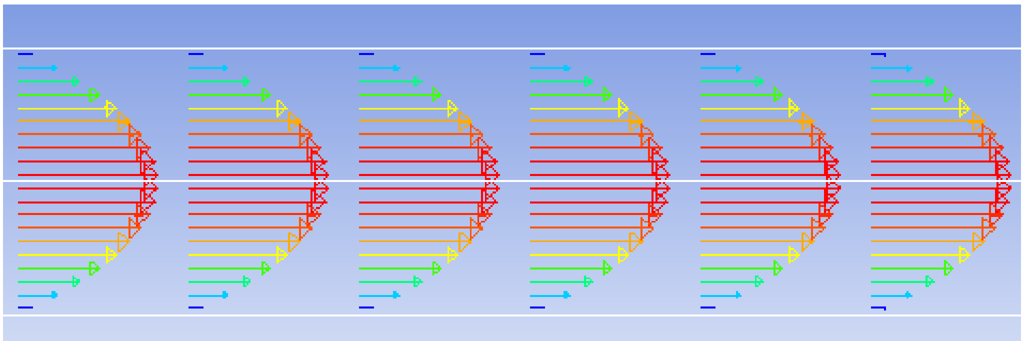

Figure 3.4: Velocity vector plot obtained for laminar flow in horizontal pipe

3.5 Flow modelling using CFD

The thrust of this work was to develop the velocity profiles models for important flow patterns for multiphase fluid flow in pipes. It also established the operating windows for experimental phase for different flow patterns in the laboratory. For gas–liquid two-phase or three phase flow in horizontal pipes, there is a number of possible flow patterns discussed in previous sections. A detailed classifications of all possible flow patterns relevant to operating conditions such as superficial gas and liquid velocities (water and or oil). Water or oil was considered as the continuous phase, and air considered as the dispersed phase.

Determination of the flow patterns is a central problem in two/three/four phase flow analysis. For the specific case of oil–water systems, oil properties can be quite diverse, and the oil–water viscosity ratio can vary from more than a million to less than one, and its rheological behaviour can be Newtonian or non-Newtonian, so it is quite difficult to determine oil–water flow patterns (Xu 2007).

A CFD package was used to model the liquid-gas (water, oil & gas) velocity profiles. In the development of velocity profile models, a combination of analytical and numerical methods was adopted. Equation 3.12 was used as the basis for analytical computation to generate appropriate velocity profile models for different flow patterns. A detail of this equation was discussed in chapter 2, Equations 2.29 – 2.32.

$$V_R = \frac{f}{8} * R_e * V * \left[1 - \left(\frac{r}{R} \right)^2 \right] \qquad 3.12$$

Where,

V_R- Velocity of fluid particle at a particular point in the pipe cross-section,

V – Average velocity of the fluid in the pipeline,

r – Distance from the pipeline centre to any point in the flow field

R - Radius of the pipeline.

R_e- Fluid Reynolds number which defines the fluid flow regime whether laminar or turbulent flow

f = Fluid flow friction factor which is a function of the pipe roughness, fluid flow regime and type of fluid.

Equation 3.12 is dependent on friction factor and fluid Reynolds number. For single phase flow, the friction factor can generally be estimated by any well known friction factor equations such as Blasius equation. For multiphase flow, the complexity associated with flow patterns makes the basic friction factor equations unsuitable. Among the numerous empirical correlations proposed in the literature for multiphase friction factor, one that was adopted for this study was the correlation based on the work of (Garcıa et al. 2003). The correlation was a pseudo average friction factors for different flow patterns in multiphase flow. They have developed different models for each of the flow patterns rather than using a-model-fits-all approach as seen from many authors. Full details of model developments can be found in (Garcıa et al. 2003) and they proposed the following friction factor models:

For slug flow:

$$fm = 0.1067R_e^{-0.2629} + \frac{13.98R_e^{-0.9501} - 0.1067R_e^{-0.2629}}{\left[1+\left(\frac{R_e}{293}\right)^{3.577}\right]^{0.2029}} \qquad 3.13$$

For dispersed bubble flow:

$$fm = 0.1067R_e^{-0.2629} + \frac{13.98R_e^{-0.9501} - 0.1067R_e^{-0.2629}}{\left[1+\left(\frac{R_e}{304}\right)^{2.948}\right]^{0.2236}} \qquad 3.14$$

For stratified flow:

$$fm = 0.0445R_e^{-0.1874} + \frac{13.98R_e^{-0.9501} - 0.0445R_e^{-0.1874}}{\left[1+\left(\frac{R_e}{300}\right)^{9.275}\right]^{0.0324}} \qquad 3.15$$

The velocity profiles models for single phase in pipe flow was extended for multiphase in pipes. But the flow of multiphase fluids must be treated differently and with caution as it introduces different complexities. There are issues of changing flow patterns as multiphase fluids moves through the pipelines/tiebacks. The knowledge of flow pattern and flow pattern transitions is essential to the development of reliable predictive tools in multiphase solids transport. As the pattern changes so the pressure variations and transport velocity may vary. In order to track the patterns, velocity profile models have been developed for each of the possible flow patterns in multiphase fluid flow in pipe.

The flow pattern signatures from the CFD are well defined and are presented below. The flow velocity profiles obtained from CFD for multiphase fluids, water and gas with varying superficial velocities are shown in Figure 3.5. The observed changing patterns (dispersed bubble flow and stratified flow) at different points along the pipe length are indication of continuous changes in flow patterns as the fluids move through the pipes. What is obvious here is that not one model is adequate for the description of multiple patterns encountered in multiphase flow in pipelines.

These observations therefore informed the development of velocity profile models for each of the important flow patterns encountered in pipes such as dispersed bubble flow, annular flow, slug flow and stratified flow.

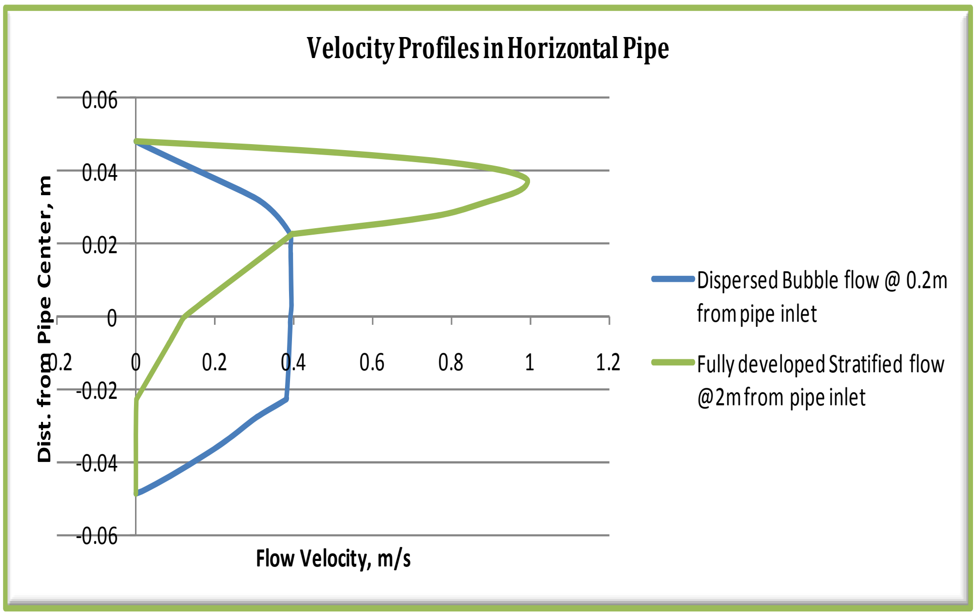

Figure 3.5: Velocity Profile Distributions in Multiphase Flow in Horizontal Pipe

3.6 Velocity profiles for laminar and turbulent Flow

Many fluids travel at different velocity within a pipe. The shape of the velocity profile across any given section of the pipe depends upon whether the flow is laminar or turbulent. Generally, if the flow in a pipe is laminar, the velocity distribution at a cross section will be parabolic in shape with the maximum velocity at the center of pipe. In turbulent flow, a fairly flat velocity distribution exists across the section of pipe. Figures 3.6 helps illustrate the above ideas. The velocity of the fluid in contact with the pipe wall is essentially zero and increases the further away from the wall.

The velocity profile for turbulent flow is different from the parabolic distribution for laminar flow. The fluid velocity near the wall of the pipe changes rapidly from approximately zero at the wall to nearly uniform velocity distribution throughout the bulk of the cross section.

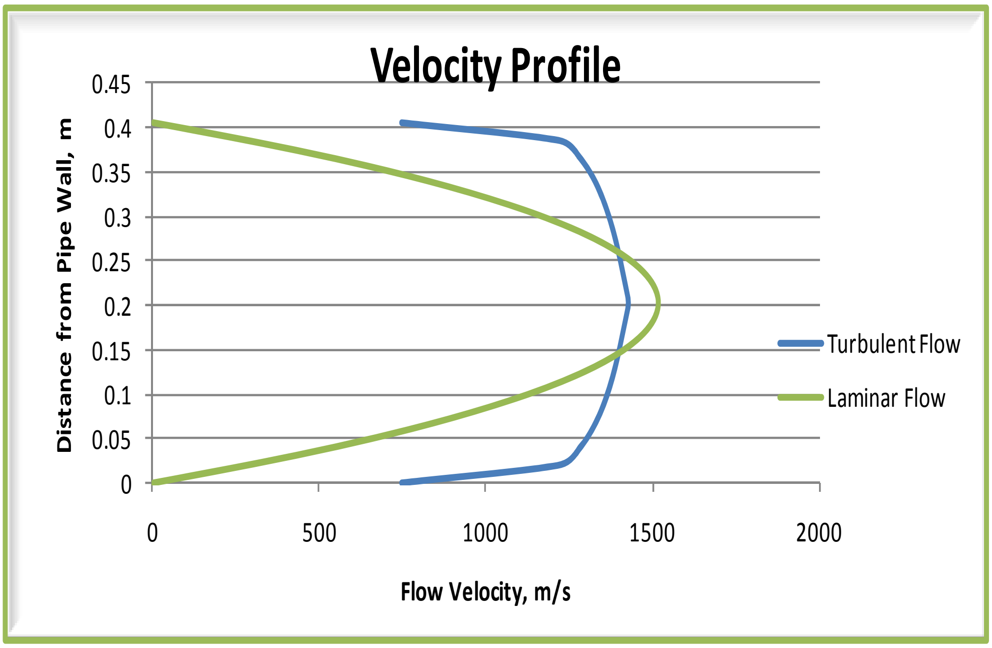

Figures 3.6: Velocity profiles for laminar and turbulent flow.

3.7 Velocity profile for multiphase flow

A multiphase flow in pipe may exhibit several different flow patterns depending on the operating conditions. In general, three steps need to be considered when modelling multiphase flow (Ghorai and Nigam 2006). The first step is the definition of the number of phases and possible flow patterns to enhance selection of the modelling approach. The second step is the choice of the governing equations which describe the multiphase flow. Numerical simulation of any flow problem is based on solving the basic flow equations describing the conservation of mass, momentum and energy in the control volume. And finally, the solution of these governing equations is critical in obtaining appropriate results.

The simulations were carried out as a three dimensional transient flow in a horizontal pipe. In all cases, liquid (water or oil) was considered as the continuous phase, and air was considered as the dispersed phase. The k–ε model was used to treat turbulence phenomena in both phases with adoption of Renormalisation Group (RNG) method. Compared to other turbulence models, RNG k–ε was observed to deliver the best performance in terms of accuracy, computing efficiency, and robustness for modelling in multiphase fluids (De-Schepper et al. 2008).

The VOF model was used for the numerical calculation of the multiphase flow patterns in horizontal pipe. The existing code in the software was made use of. For the simulations, an Eulerian–Eulerian approach is chosen, in which the grid is fixed and the fluids are assumed to behave as continuous media. This model solves one single set of conservation equations for both phases and tracks the volume fraction of each of the phases throughout the computational domain. For all simulations, a no-slip condition is imposed at the tube wall. The influence of the gravitational force on the flow has been taken into account as well. At the inlet of the tube, uniform profiles for all the variables have been employed. A pressure outlet boundary is imposed to avoid difficulties with backflow at the outlet of the tube.

The transient behaviour of the multiphase flow requires simulation with a time step of 0.001 seconds to be adopted though it does varies depending on the scaled residual value. Both phases are introduced at the inlet and the transient simulation is initiated. The superficial velocities of the liquid (water or oil) and gas phase, corresponding to a given flow patterns are set as inlet conditions. After a time step as indicated on calculation window, the flow of both phases is observed and flow pattern established.

The physical properties of the fluids are given in Table 3.1 and the superficial velocities of fluid used including the boundary conditions for the simulation are presented in Table 3.2. Water or oil and air entered the horizontal pipe perpendicular to its inlet plane. They have an inlet temperature of 298 K. The fluid pressure at the tube inlet is set to 101,325 Pa.

Table 3.1: Physical properties of water, vegetable oil and air

Sample	**Fluid density, ρ (kg/m3)**	**Fluid viscosity, μ (Pas)**
Tap water	998.8	0.001003
Vegetable oil	940	0.001001
Air	1.225	0.0000183

Table 3.2: Summary of model parameters

Flow conditions		
Type	Multiphase with turbulence	VOF, Eulerian model and k-ε model
Scenario	2 and 3 phase flow	Secondary phases volume fractions
Phase	water, oil and gas	Phase properties
Pipeline		
Pipeline sizes	0.07, 0.08, 0.1 m	3-D geometry
Inclination	0, +15, +25	3-D geometry
Boundary condition		
Inlet	Mixture velocity	Velocity inlet
Outlet	Pressure outlet	Pressure outlet
Pipe wall	Roughness 0.0001 m	Non-slip wall
Operating conditions at inlet		
Pressure	Constant	
Temperature	Constant	

3.8 Results and discussion

3.8.1 Multiphase flow simulation

The simulations was carried out to obtain results for dispersed bubble flow, slug flow and stratified flow conditions in the 0.07, 0.08 and 0.1 meters for pipe diameters and 2 meters long horizontal pipelines using Ansys Fluent for air-liquid (water & oil) system. The liquid and gas superficial velocities are varied in the range from 0.02 to 2.1 m/s, and 2 to 15 m/s respectively. The simulation results were modelled to obtain representative models for all the common flow patterns. Details of the simulation boundary conditions can be found in the table below.

3.8.2 Contour plots

The velocity contours for dispersed bubble flow, slug flow and stratified wavy are presented in Figures 3.7 to 3.11. Figures 3.7 & 3.8 showed high intensity at the centre, an indication of maximum velocity attainable at the pipe centre and low velocity at the pipe wall for dispersed bubble flow. Generally the fluid experience low velocity at the pipe wall and tend to increase toward the centre of the pipe. Figures 3.9 & 3.10 show a slug flow contour consists of liquid regions moving rapidly in plug separated by gas bubbles. These depict existence of front nose of the slug which is very turbulent as the transport forces are concentrated in this region. A typical lumping movement as the mixture flow through the pipe. Slug flow pattern is very common and most likely to be encountered in a typical subsea pipeline / tieback. Figure 3.11 showed two phases flowing in parallel plane with wavy interface clearly depicting stratified wavy flow. Barnea, Shoham, Taitel and Dukler, 1980 stated that at low liquid and gas velocities and under normal gravity conditions, a flow condition is calculated in which the heavy liquid flows over the bottom of the tube and the gas flows over the liquid. Both phases are separated by a smooth or wavy liquid–gas interface.

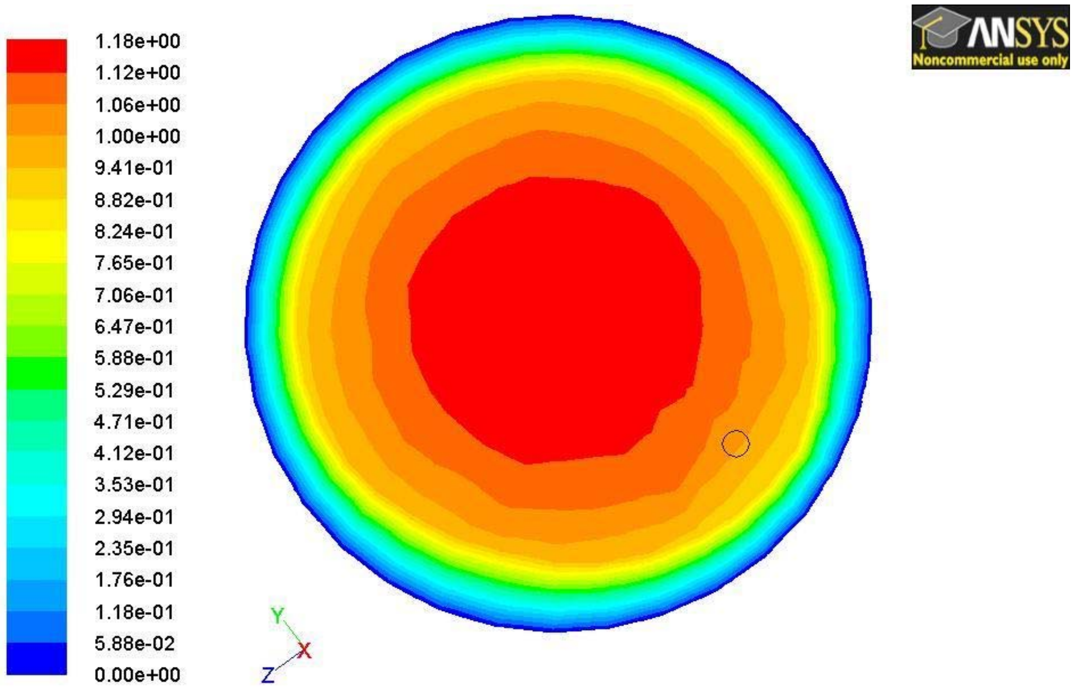

Figure 3.7: Contours of mixture velocity for water–air flow for dispersed bubble flow in 0.08m pipe.

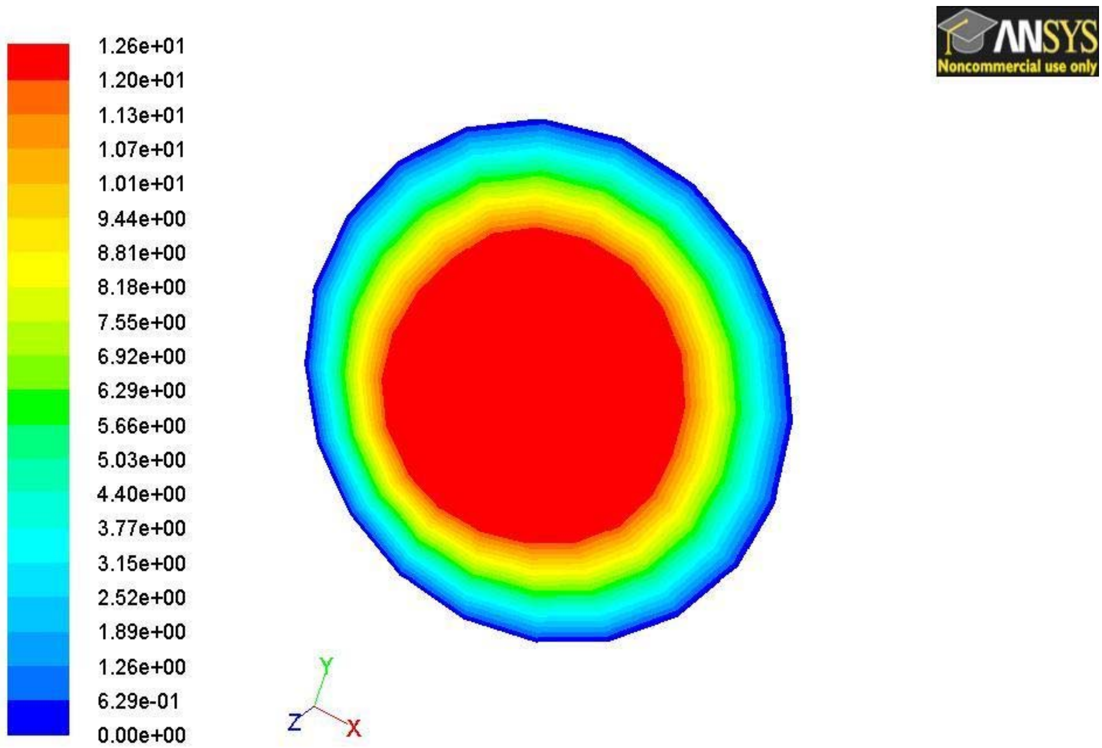

Figure 3.8: Contours of mixture velocity for water–air flow for dispersed bubble flow in 0.07m pipe.

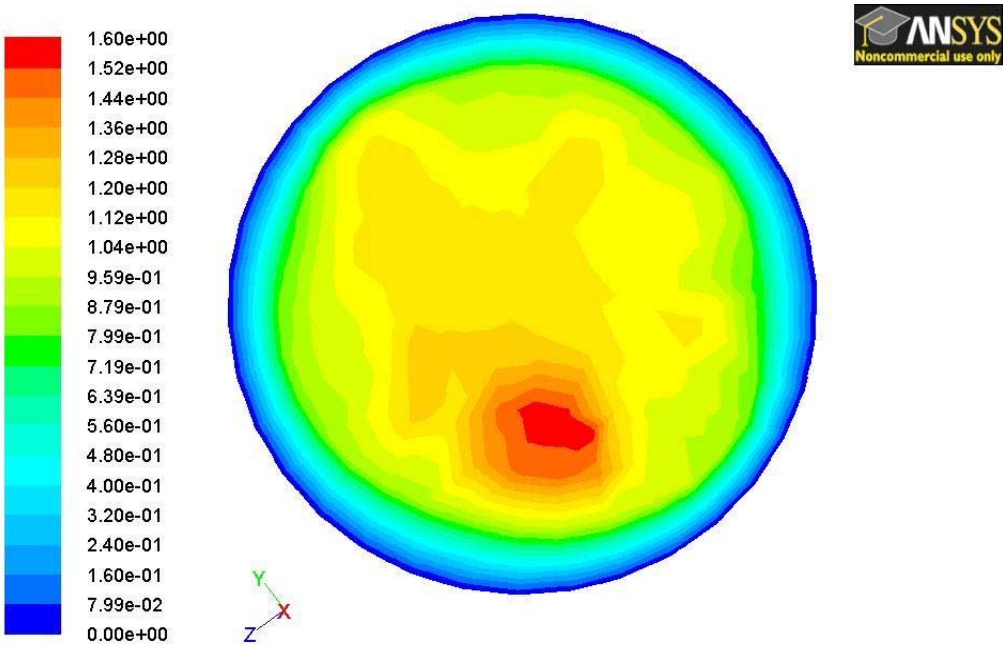

Figure 3.9: Contours of mixture velocity for water–air flow for slug flow in 0.1m pipe inclined at 15^{o}

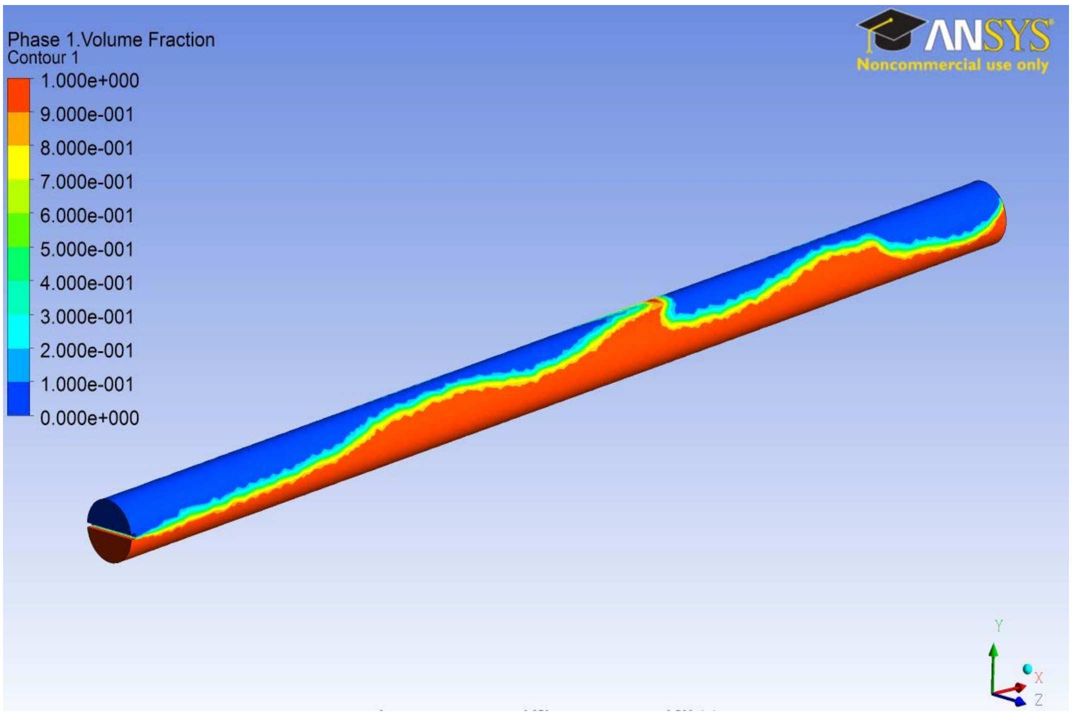

Figure 3.10: Contours of mixture velocity for water–air flow for slug flow in 0.1m pipe inclined at 15^{o}

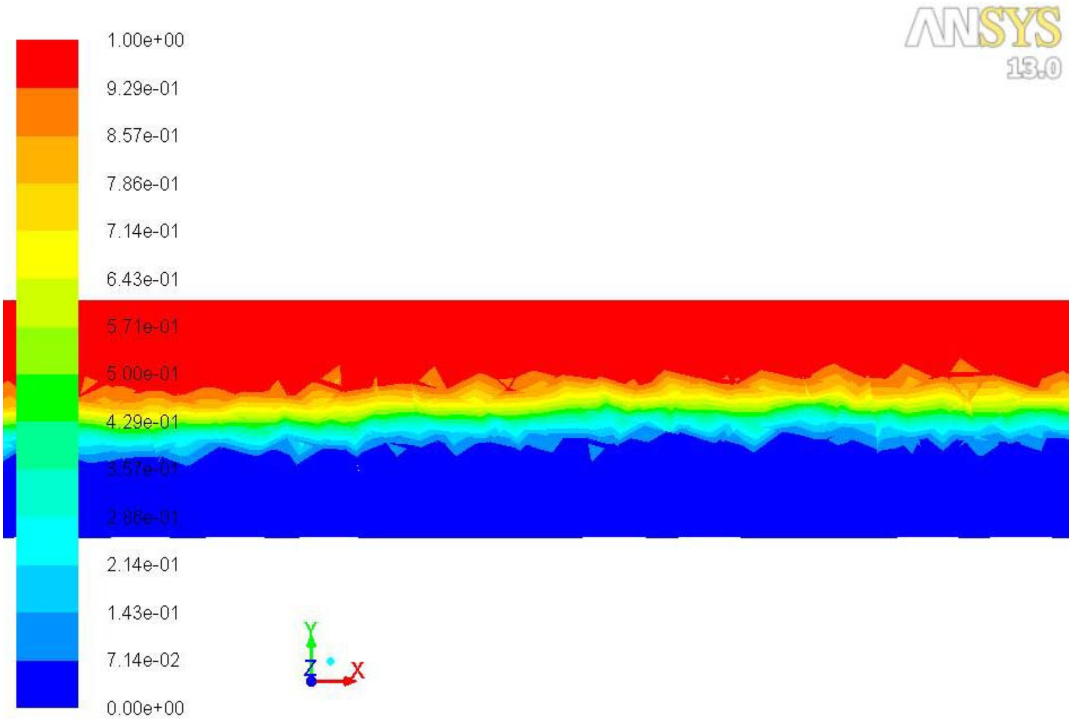

Figure 3.11: Contours of mixture velocity for water–air flow for stratified wavy flow in 0.07m horizontal pipe

3.9 Velocity profile models

There is obvious need to improve our understanding of the transient nature of flow patterns in pipeline. Many approaches have been presented in the literatures especially with the use of CFD to model flow of multiphase in pipelines / tiebacks. What has not been done is the use of CFD to model velocity profiles for different flow patterns. This work explored and demonstrated the capability of CFD to generate fluid point velocity profile data and when combined with analytical equation able to build velocity profile models for important flow patterns in pipeline.

Due to the complexity of multiphase flow systems, it is not possible to obtain one model that will be suitable to predict multiple flow patterns that exist. This was demonstrated in previous section, Figure 3.6. The starting point was to identify a base equation stemmed from analytical model for a single phase turbulent flow. Equation 3.12 was used in this case and as presented below with modification to include underlying constants,

$$V_R = a\frac{f}{8} * R_e^b * V * \left[1 - \left(\frac{r}{R}\right)^2\right]^c \qquad 3.12b$$

The equation is a function of friction factor and the Reynolds number. The friction factor for a gas-liquid mixture can be defined as,

$$f_m = \frac{(\Delta P/L)D}{2\rho_m U_m^2} \qquad 3.16$$

Where the pressure drop per unit length $(\Delta P/L)$ is related to the wall shear stress, D is the pipe diameter, U_m is the mixture velocity and ρ_m is the mixture density

The mixture Reynolds number can be defined as,

$$R_e = \frac{U_m D}{\upsilon_L} \qquad 3.17$$

Where, $\upsilon_L = \mu_L / \rho_L$ is the kinematic viscosity of the liquid.

The mixture friction factor of Garcıa et al 2003 for different flow patterns have been adopted in this research, equations 3.13 to 3.15. This was because the empirical models were developed based on large body of data sourced from different reputable researchers. The mixture Reynolds number appropriate for multiphase flow in horizontal pipes is based on the mixture velocity and the liquid kinematic viscosity. Both parameters are greatly important in the development of an appropriate model for velocity profiles.

In order to obtain constants a, b and c in equation 3.12b, simulations of different flow patterns was conducted with CFD software. A simulation run for varying input superficial velocity for liquid and for gas flow generated a number of point velocity data across the plane of pipe diameter from the pipe wall where the fluid velocity is generally zero to the pipe centre. The input superficial velocities are experimental data for different flow patterns. For example, the data generated in a 0.08 meters pipe for superficial oil velocity of 0.006m/s and superficial gas velocity of 0.344 m/s from the simulation is presented in Table 3.3 below. More simulations data for multiphase flow are presented in Appendix B.

Table 3.3: Simulation output for stratified flow pattern in 0.07m horizontal pipe

Fluid velocity, m/s	Dist. from pipe centre, m
0.230673	0.002421
0.245736	0.006991
0.275742	0.016093
0.280419	0.018222
0.295159	0.022644
0.285392	0.027453
0.268324	0.031461
0.241549	0.034802
0.204055	0.037587
0.165571	0.039909
0.130101	0.041844
0.09873	0.043456
0.071766	0.044801
0.048653	0.045921
0.029316	0.046854
0.013342	0.047632
0	0.048281

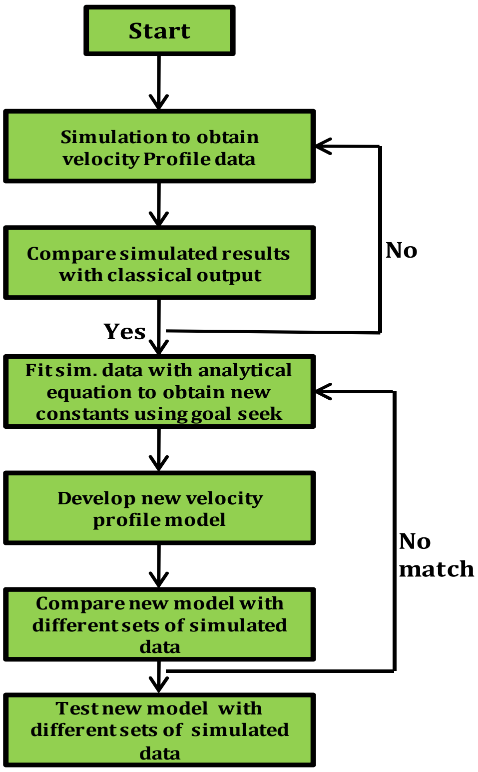

Figure 3.12: Schematic of the method for velocity profile model development

Next was fitting the simulated data with the analytical equation defined by 3.12b using the multiple constant optimisation method (MCOM) of Microsoft excel solver based on goal seek approach. It involved a process of changing the values in a cell to see how those changes affect the outcome of the formulas on the worksheet. The method requires definition of the relationship between two or more parameters by initially guessing a constant and adjusting the value (s) of the other parameters. Excel varies the value in a cell that you specify until a formula that's dependent on that cell returns a result that closely match other parameters otherwise the process is repeated. The schematic of the method is as presented in Figure 3.12 above.

The analysis involved combining analytical equation with profiles generated numerically from simulations. This led to the development of velocity profiles for multiphase flow in pipe. The model equations for each of the flow patterns are as presented below.

For annular flow pattern,

$$V_r = 1.863 * f * R_e^{0.4} * V_m \left[1 - \left(\frac{r}{R} \right)^2 \right]^{0.11} \qquad 3.18$$

For dispersed bubble flow pattern,

$$V_r = 3.7 * f * R_e^{0.366} * V_m \left[1 - \left(\frac{r}{R} \right)^2 \right]^{0.15} \qquad 3.19$$

For slug flow pattern,

$$V_r = 3.3 * f * R_e^{0.347} * V_m \left[1 - \left(\frac{r}{R} \right)^2 \right]^{1.11} \qquad 3.20$$

The simulation results for the different flow patterns in horizontal and inclined pipes can be found in Figures 3.13 to 3.17. The figures represent the calculated velocity profiles of mixture two-phase fluids for different flow patterns. The numerically obtained velocity profiles are compared; the agreement between the analytical results and CFD is excellent in all cases and are within reasonable error margin, see Table 3.4 below and Figures 3.18 & 3.19.

Table 3.4: Statistical Parameters for the Velocity Profile Models

	Velocity Profile Models			
	Slug Flow	**Dispersed Bubble Flow**	**Annular Flow**	**Stratified Flow**
Average Percent Error (APE)	3.48	1.56	2.75	4.97
R – Square Value (R^2)	0.9611	0.9289	0.9707	0.7544
RSQ & Correlation Coefficient, %	98.84	86.92	97.14	70.52

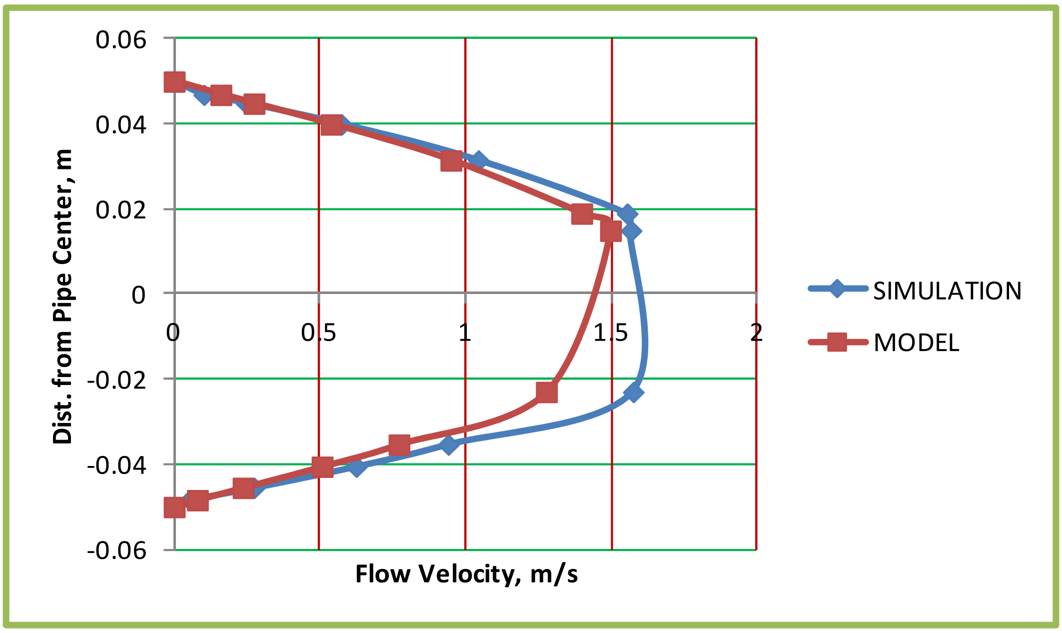

Figure 3.13: Calculated velocity profile compared with simulation for slug flow pattern, Vsl = 0.982m/s, Vsg = 0.751m/s, Inclination angle =15°

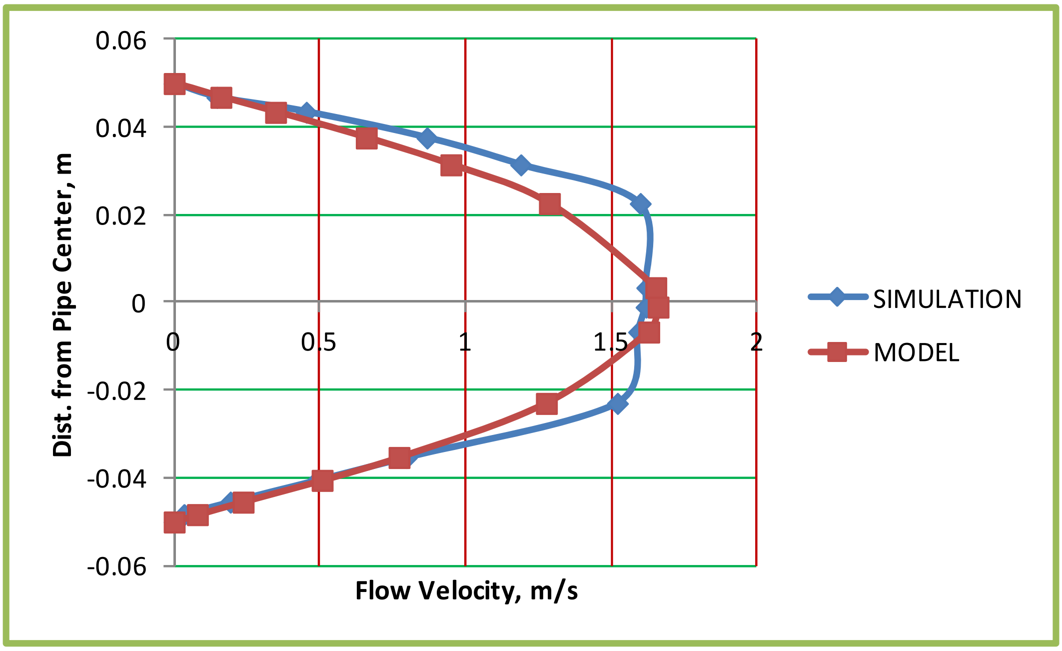

Figure 3.14: Calculated velocity profile compared with simulation for slug flow pattern, Vsl = 0.982m/s, Vsg = 0.751m/s, pipe inclination = 20°

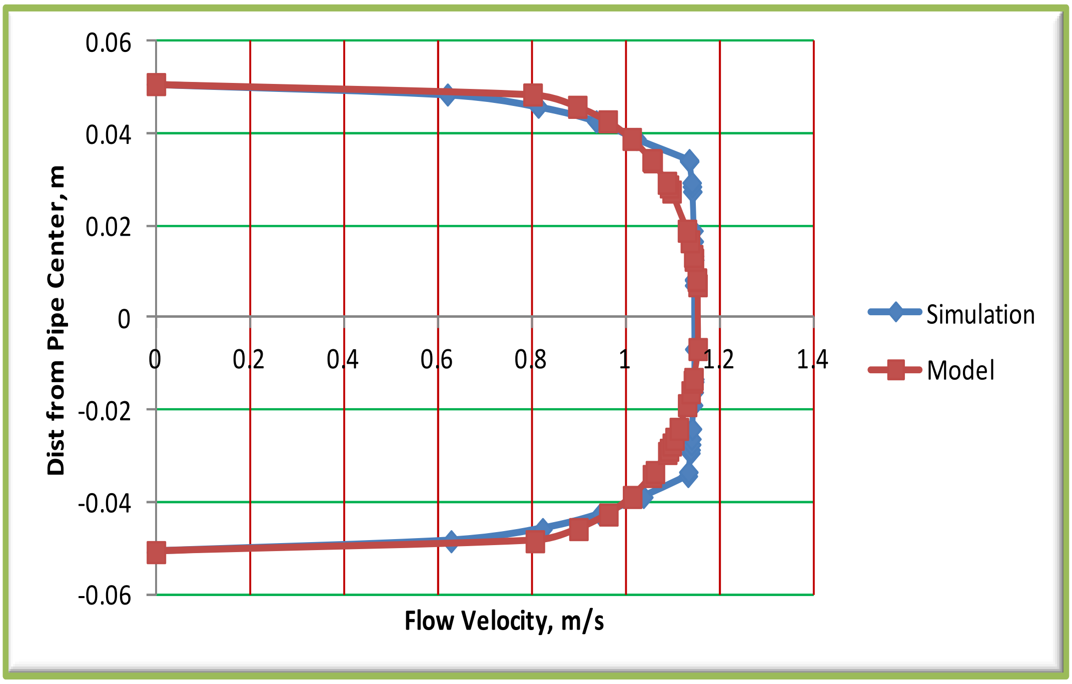

Figure 3.15: Calculated velocity profile compared with simulation for dispersed bubble flow pattern, Vsl = 0.8m/s, Vsg = 0.2m/s, horizontal pipe

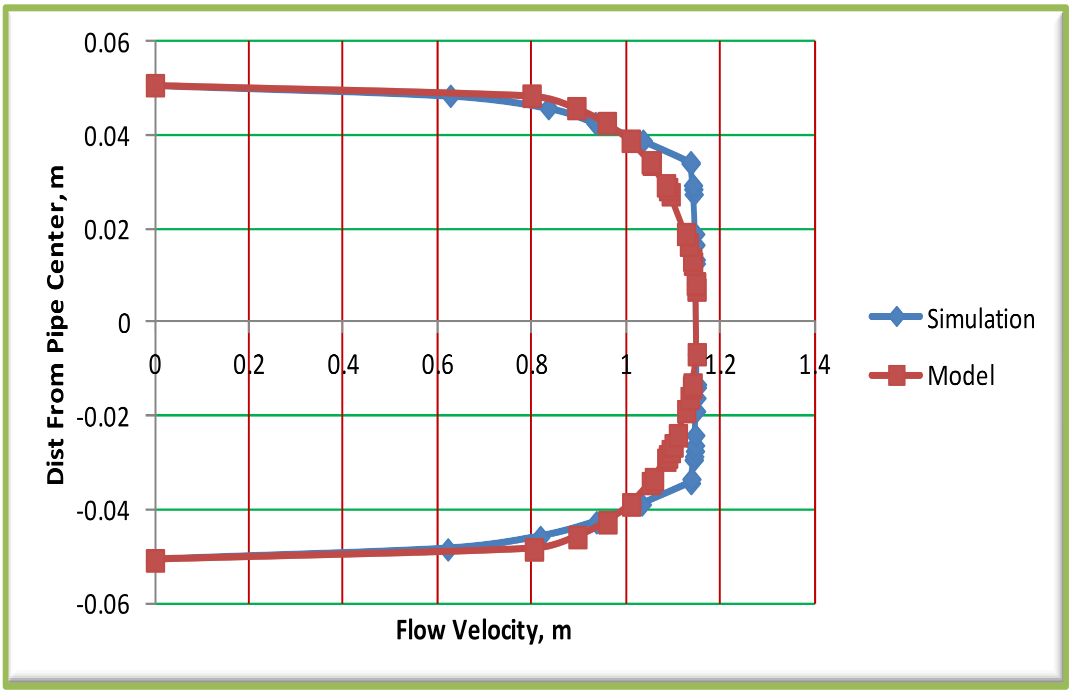

Figure 3.16: Calculated velocity profile compared with simulation for dispersed bubble flow pattern, Vsl = 0.65m/s, Vsg = 0.35m/s, horizontal pipe

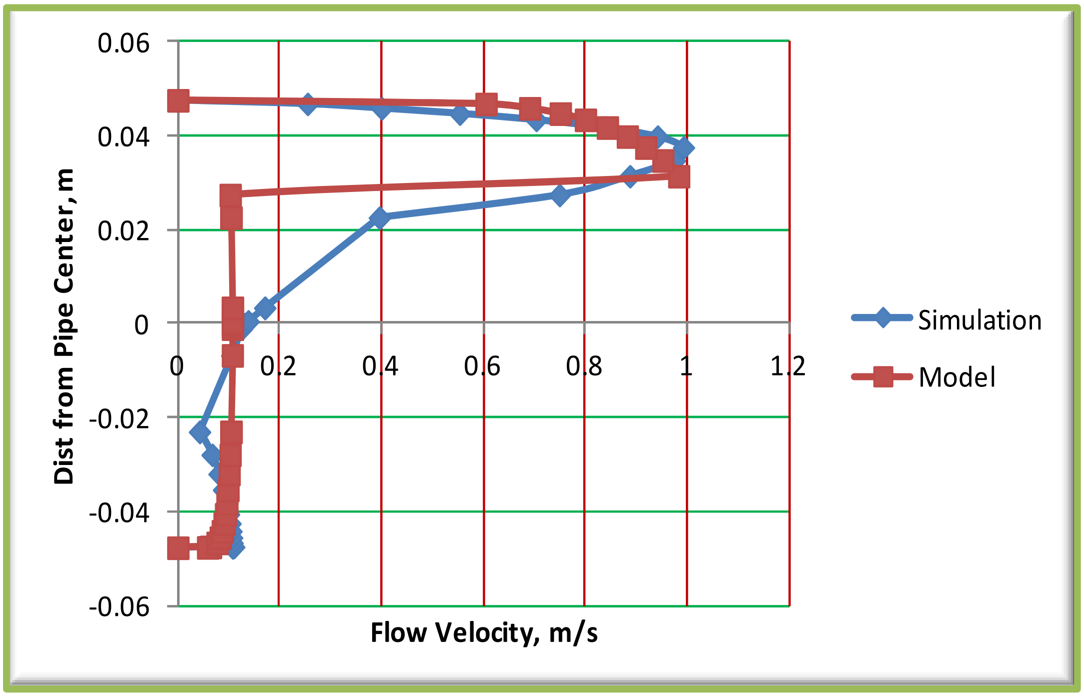

Figure 3.17: Calculated velocity profile compared with simulation for stratified flow pattern, Vsl = 0.006m/s, Vsg = 0.344m/s, horizontal pipe

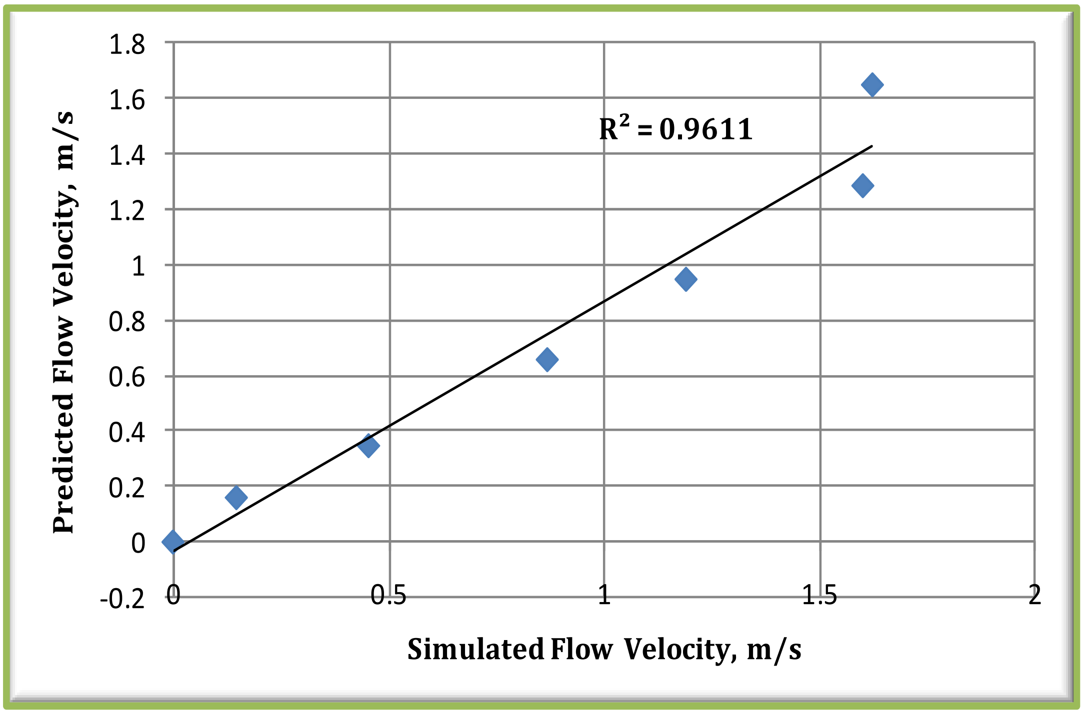

Figure 3.18: Comparison of simulated results with analytical prediction model for velocity profile in slug flow.

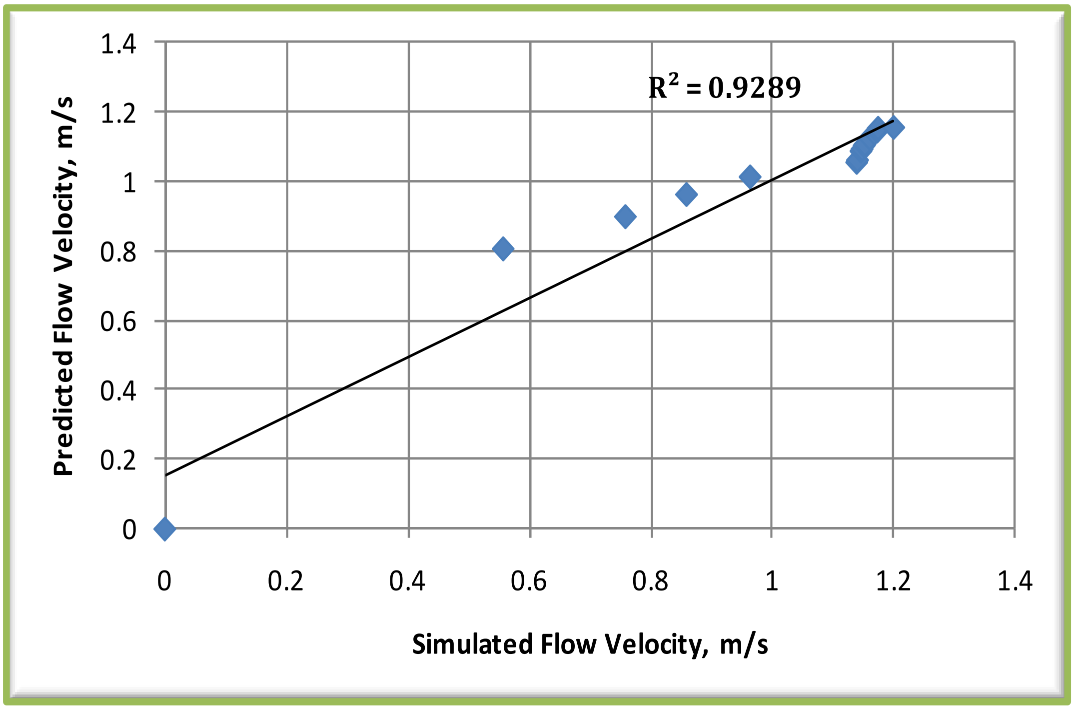

Figure 3.19: Comparison of simulated results with analytical prediction model for velocity profile in dispersed bubble flow.

3.9.1 Velocity profile model for stratified flow regime

Depending on the phase velocities, stratified flow patterns will form at low gas-liquid velocities which were observed from numerical simulations as shown in Figure 3.20. The phases are completely separated and create stratification under the effect of gravity as can be seen in Figure 3.20. It may either be stratified smooth or stratified wavy flow. This often occurs in the horizontal and in downwardly inclined section of a long pipeline.

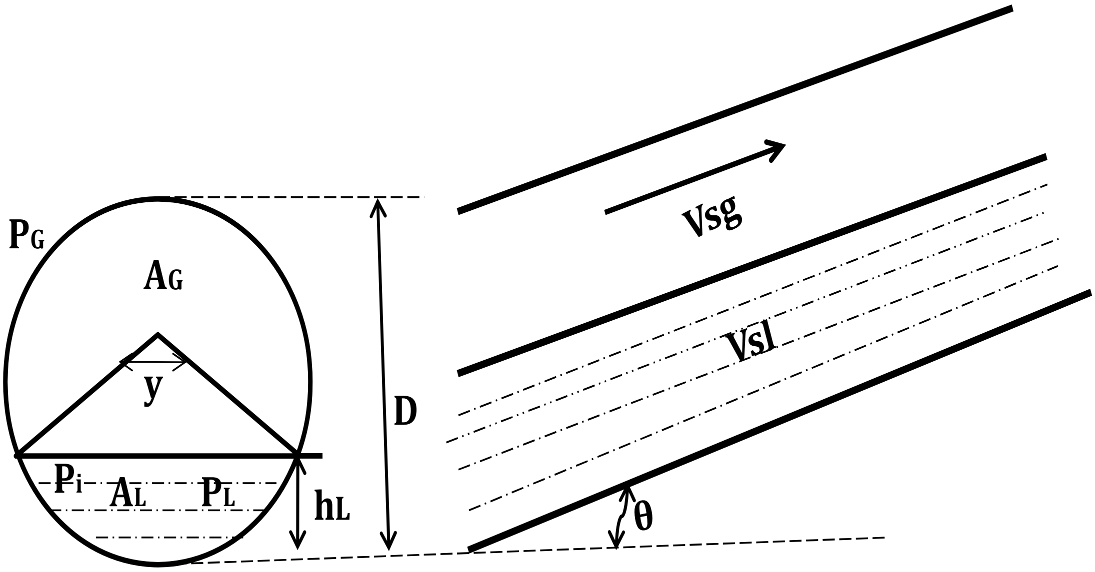

Figure 3.20: Schematic of stratified flow pattern in pipe adapted from (Oliemans and Pots 2006)

The method of determining the velocity profile for different flow patterns especially for stratified flow pattern defers among various authors. In this work, the combination of numerical and analytical methods has been adopted which provided for definition of various flow patterns and thus helps modeling of flow velocity profiles for each of the important flow patterns in multiphase flow. This makes for greater understanding of the carrying capacity of the stratified flow pattern as well as other flow patterns encountered in oil and gas production pipelines/tiebacks.

Therefore, in the development of velocity profile model for stratified flow as was done previously for other flow patterns, it was critical to determine the liquid hold-up, the liquid phase velocity and the liquid height. Some authors adopted iterative solution to determine liquid hold-up based on two-phase momentum balance. The model developed by (Taitel and Dukler 1976a) assumed smooth interface and interfacial friction factor equal to the gas-wall friction factor. They evaluated the gas interfacial shear stress with the same equation as the gas wall shear stress. The phases are treated as two parallel plates with distinct separation between the gas and the liquid phase especially for stratified smooth flow. This method of analysis was adopted by some authors (Kuru, Leighton and McCready 1995, Levy and Mason 2000, Wilson, Clift and Sellgren 2002). In a separate article, Taitel and Dukler 1976b showed that the hold up and the dimensionless pressure drop for stratified flow are unique functions under the assumption that $f_G / f_i \cong const$.

The liquid hold-up, α_L can be related to the angle extended by the gas interface as shown in Figure 3.20.

Therefore,

$$\alpha_L = \frac{y - \sin y}{2\pi} \tag{3.21}$$

$$h_L = 0.5[1 - \cos(y/2)]D \tag{3.22}$$

If the liquid height, h_L is considered as an input parameter, then

$$y = 2\cos^{-1}\left(1 - \frac{2h_L}{D}\right) \tag{3.23}$$

$$\alpha_L = 1 - \alpha_G \tag{3.24}$$

Therefore, the velocity profiles for both gas & liquid phase can be determined using

$$V_{rl} = U_{SL}\left[1-\left(\frac{r}{R}\right)^{2}\right]^{0.32} \qquad 3.25$$

Where,

$$R = \frac{\alpha_L * D}{2} \qquad 3.26$$

$$V_{rg} = U_{SG}\left[1-\left(\frac{r}{R}\right)^{2}\right]^{0.7} \qquad 3.27$$

Where,

$$R = \frac{(1-\alpha_G)D}{2} \qquad 3.28$$

3.10 Summary

The main objective of this chapter was to explore the potential of CFD tools to model multiphase fluid in horizontal or inclined pipe under different flow conditions. Initially, the single phase validation was conducted and a good match was achieved with the well known analytical equation for single phase in horizontal pipe. Multiphase fluids flow in pipes was then considered and all simulations gave good agreement with the different flow patterns. It can thus be concluded that all horizontal or inclined pipe flow patterns can be simulated using existing CFD codes.

Based on the simulation results, it was possible to develop an appropriate model for different flow patterns by using the numerical results obtained from simulations combined with analytical equations. Four velocity profile models was developed, there was a good match between the model predictions and simulation results as can be seen in Figures 3.13 to 3.17. Therefore, multiphase fluids flowing through horizontal or inclined pipe can be sufficiently modelled using CFD. The definitions and predictions of flow patterns using CFD contributed hugely to the development of minimum transport velocity models for suspension and rolling in a pipeline. It has does eliminated uncertainties in the flow patterns prediction in multiphase flow.

Chapter 4

Experiment set-up for multiphase solid transport and flow pattern characterisations

4.1 Introduction

Multiphase flow of oil, water, gas and solid frequently occur in the production process of oil and gas industry. Multiphase-flow systems can be complex because of the simultaneous presence of different phases such as liquid, gas and solid in the same flow stream. Thus, the development of adequate models especially for sand transport in multiphase presents a formidable challenge. The phenomenon are well understood but the models have limited applicability especially velocity profile and solid transport models. To develop and validate an integrated solution for this type of flows, laboratory experiments are required to mimic these conditions (Falcone, Teodoriu, Reinicke and Bello 2007). The combination of experimental investigations and numerical modelling as adopted in this study provided opportunity to enhance the understanding of multiphase fluid flow. In the light of this, a multiphase flow loop was designed and constructed to achieve these objectives.

This chapter discussed the design and construction of the multiphase process flow loop used for the experimental phase of this research. The experimental facility was to create a replica of actual field production processes under different system, operating and geometric conditions in a laboratory setting. The experimental work was focussed on the following objectives:

- Determine the physical properties of the materials to be used such as water, vegetable oil, gas and sand.
- Characterise flow patterns for water-gas and water-oil & gas multiphase flow in horizontal and inclined pipes at various flow rates.
- Determine the minimum transport velocity for suspension and for rolling in water-gas-solid, water-oil-solid and water-oil-gas-solid for three pipe sizes and inclinations. The data acquired was then used for testing and validation of the models developed.
- Characterised solid flow patterns in slurry flow for both horizontal and inclined pipes.

This chapter presents the methods and underlying principles adopted to achieve these objectives. The details of the results from the experiments conducted with the flow loop are discussed in the next chapter.

4.2 Multiphase flow loop

The proper design of oil and gas production pipeline systems requires a thorough understanding of the behaviour of multiphase flow. Therefore, a new test facility was designed and built to replicate real time multiphase oil-water-gas transport in pipeline with topographical conditions in order to generate appropriate data for multiphase particle Reynolds number, C_D, C_L and for MTV models validation in multiphase flow. It was designed for gas, liquid and solids multiphase flows with pressures up to 10bar and temperature up to 60°C. Various design layouts was considered based on the experiment objectives and space allocated within the laboratory environment before deciding on the final layout that met the set objectives.

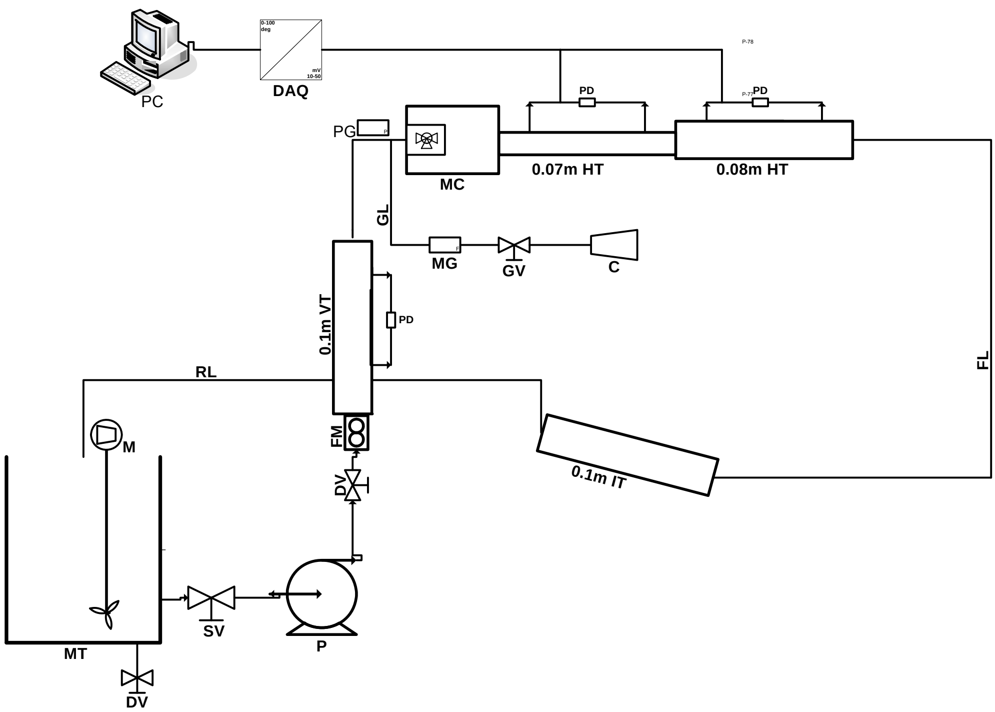

Figure 4.1: Sketch of multiphase flow loop

Legend

MT	Slurry mixing tank
M	Mixer
DV	Drain valve
SV	Suction valve
P	Pump
DV	Discharge valve
FM	Doppler flow meter
PG	Line pressure gauge

PD	Differential pressure transducer
MG	Gas flow meter
MC	Mixing compartment
C	Compressor
FL	Flow line
RT	Fluid return line
GV	Gas control valve
HT	Test pipe

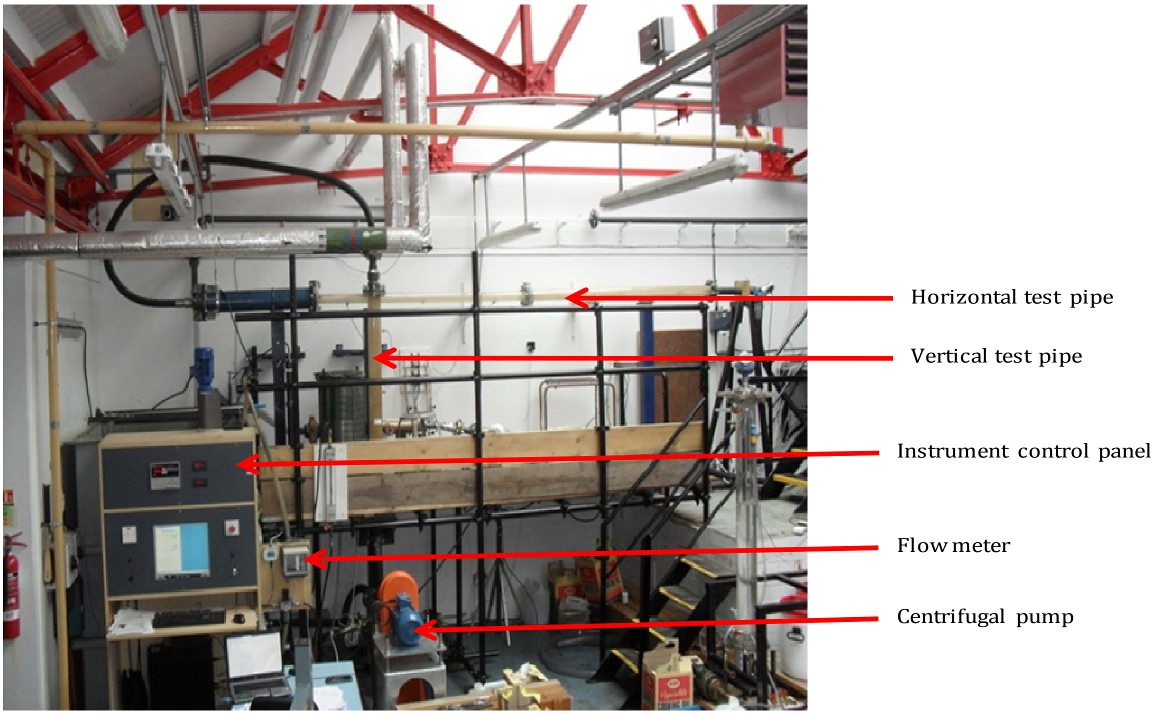

Figure 4.2: Digital picture of the multiphase flow loop

A schematic diagram and pictorial view of the multiphase flow loop for flow visualization and particle transport in three-phase or four-phase water-oil-gas-sand flow in a pipe are shown in Figures 4.1 & 4.2. There are four test sections made up of one vertical test pipe, two horizontal test pipes and one test pipe inclined at variable angles provided for the visualisation of various fluid flow patterns and minimum sand transport velocity measurements. The vertical test section consists of transparent 0.1 meters internal diameter straight acrylic pipe. The horizontal test sections consist of transparent 0.07 & 0.08 meters internal diameter straight acrylic pipe. The inclined test section consists of transparent 0.1 meters acrylic pipe equipped with angle adjustment fulcrum varying from 15° to 25°. The test pipes are of 2 meters length each. The entire pipe structures were placed on a platform about 1.5 meters above the laboratory floor plan. The circulating system was equipped with IBC mixers, E-400 folding impellers mounted on top of the tank and fitted through a standard 150mm screw cap opening. This allow for quick and uniform suspension of slurry. The mixer impeller diameter is 400mm and located one diameter off bottom. The electric motor was the standard IE2 energy efficient fixed speed. It came with 240 volts and 3-phase 50Hz frequency included a starter with overload protection, safety switch and 16 amperes appliance plugs. The loop was equipped with a LabView data acquisition connected directly to a desktop computer on a central control console where all processes are manipulated.

Table 4.1: Major specifications for the multiphase flow test facility

S/No.	Property	Range
1	Number of phases	Four-phase, water, oil, gas and solid
2	Liquid rate, m^3/s	0.001 – 0.009
3	Gas rate, m^3/s	0.001 – 0.2
4	Flowing phase	Water, oil and gas
5	Test pipe diameters, meters	0.07, 0.08 and 0.1
6	Test pipe material	Perspex tubes
7	Test sections geometry	Horizontal, inclined and vertical
8	Inclination angle	15^0, 20^0 & 25^0
9	Liquid phase	Water and oil
10	Gas phase	Compressed air
11	Solid phase	White fine-coarse particles
12	Particle size, microns	50 - 600
13	Design pressure, bar	1.5
14	Design temperature, ^0C	25

The major technical specifications of the facility are given in Table 4.1. The specified superficial velocities enabled for identification of major flow patterns in oil and gas production pipelines/tiebacks. This was based on the initial simulation work carried to establish various flow patterns in multiphase pipe flow given a combination of liquid-gas mixture superficial velocities.

The main components of the multiphase flow test facility can be found in Table 4.2. The design methodology involved a careful understanding of the basic principles of operation of major equipment in order to minimise the total cost and optimise flow loop performance.

Table 4.2: The main components of the multiphase flow loop

S/No.	Parameters	Components
1	Liquid supply system	• Doppler flow meter • Centrifugal pumps with variable speed controller • Flow lines
2	Gas supply system	• Compressors • Flow lines • Flow meter
3	Solid mixing system	• Mixing tank • Mixer • Bypass valves
4	Multiphase system	• Gas injection • Liquid mixing tank • Mixing chamber • Flow control valves
5	Control and instrumentation system	• Differential pressure transducers • Pressure gauges • Liquid level indicator • Flow control valves • Flow meters • Pressure tap and temperature indicator
6	Data acquisition system	• Desktop computer • RS-232 • LabView software installed on computer
7	Visualisation system	• Transparent test sections • Digital camera

4.2.1 Review of similar multiphase flow loop

Other notable designs of multiphase flow loop both for characterisation of multiphase flow patterns and sand transport patterns that exist in literatures are briefly discussed here. Doron et al. 1987 conducted experiment on slurry flow in horizontal pipes. The set up consisted of a test section which has a transparent Plexiglas pipe. The slurry flow rate was controlled by a butterfly control valve and a bypass line, and was measured by slurry magnetic flow meter. The pressure drop in the test section was measured using two Validyne differential pressure transducers with direct connection to a digital computer for data acquisition and reduction. The flow patterns were determined by visual observation. Similarly, Takahashi, Masuyama and Noda 1989, used a transparent acrylic pipe to allow for visual observation of the particle behaviour by a video camera. It consisted of a water tank, a pump with a variable-speed drive, an electromagnetic flow meter and pressure transducers for pressure data acquisition.

Gilles et al. 1997 flow loop was approximately 30 m in length and employed a centrifugal pump to circulate water and water-sand mixtures. The velocity of the water or slurry was controlled by the pump speed and was measured with the magnetic flux flow meter. Transparent plastic piping was used extensively in the loop construction so that the flow conditions could be observed. Gas was injected into the loop at a point just downstream of the flow meter after passing through a rotameter. The pressure drop test section and the weighed section were constructed from 52 mm transparent pipe. A progressive cavity pump with an oversized rotor-stator combination was used to circulate the oil. With the oversized rotor, the relationship between pump speed and flow rate is constant as the discharge pressure increases so that the liquid flow rate can be determined from the pump speed.

Marcano, Chen, Sarica and Brill 1998 designed a flow loop consisted of a long horizontal flow line, a two-stage air compressor, a centrifugal pump, and a data acquisition system utilizing LabView. The flow loop was designed primarily to collect data during the multiphase experimental tests which consisted of continuous readings of pressures, temperatures, flow rates, and liquid holdup.

Falcone, Teodoriu, Reinicke and Bello 2007 carried out a comprehensive review of existing multiphase flow loop worldwide. They reiterated the need for experimental measurements in order to develop and validate multiphase flow models under controlled conditions and access range of applicability. It was suggested that a multiphase flow experiment should includes the following factors; loop geometry, operating pressure and temperature, range of phase flow rate, equipment and instrumentation, piping dimension and material, fluid properties, data acquisition and information processing systems. Falcone et al. 2007 identified two niche areas of research that still lack dedicated test facilities for multiphase flow model. Two of these niche areas are sand transport in single phase and multiphase flows and the investigation of the dynamic interaction between flow in porous media and flow in pipes under transient flow conditions.

It was obvious that the multiphase test facilities are limited more so for solid transport in multiphase. For improved solid transport models, there is need to acquire useful experimental data for model testing and validation. In this research work, relevant data for solid transport was acquired with the aid of the multiphase loop.

4.3 Laboratory equipment and sensors

4.3.1 Pump selection

A pump is a device used to move fluids. There are two classes of pumps that were considered, the kinetic and positive displacement pumps. Figure 4.3 gives an overview of the pump types. Making a choice of pump could be a challenge, especially choosing a pump that will meet all requirements. The operational requirements and available budget dictated the choice of the pump in this case. The centrifugal pump was finally selected as this met both requirements. The self priming centrifugal pump was mechanical, self lubricated carbon rotating face. It was 76 mm x 76 mm NPT with maximum operating pressure of 87 psi and maximum liquid temperature of 71 ^{0}C.

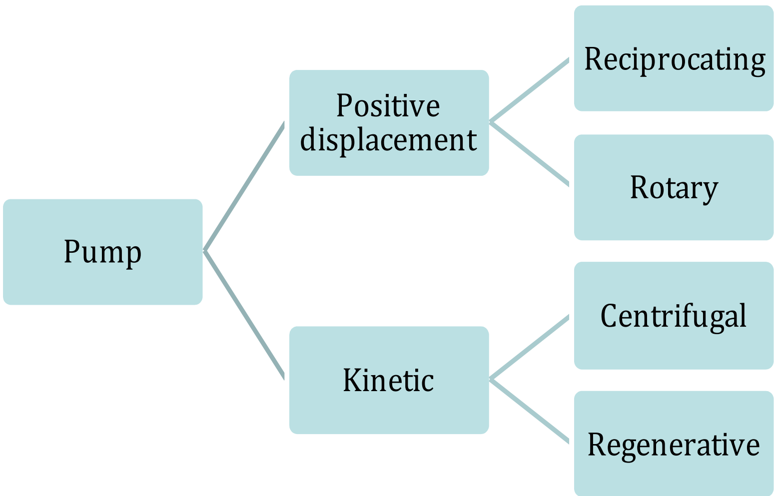

Figure 4.3: Types of pumps

4.3.2 Data acquisition

LABVIEW software was used for acquisition and display of data from key equipment and sensors such as pump, differential pressure transducers, gas flow meter and liquid flow meter as shown in Figure 4.4. It converted the output voltage to physical values based on the results of calibrations for each of the equipment and sensors. The data acquisition rate was set to record and save every 0.01 seconds during each experimental run.

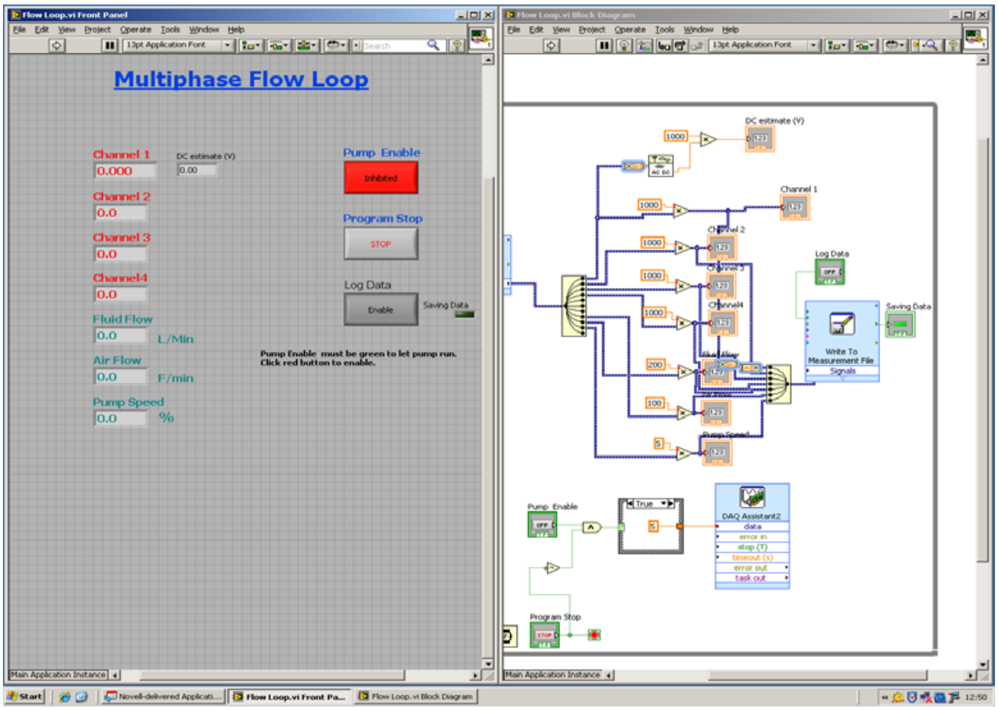

Figure 4.4: Block diagram for data acquisition on LABVIEW

4.3.3 Calibrations and safety checks

Part of the requirement for this kind of large scale experiment was to carry out pre-test, calibrations of equipment, sensors and equipment safety checks prior to commissioning. This was to ensure the safety of personnel and equipment.

The pump was function tested by discharging flow of water into the loop starting from low to maximum pump deliverable speed. The pipe connections were checked for any leakage while water flowed through it. During this phase the pump was observed for vibration and any undue noise from bearings or couplings. The valves were checked to ensure it opens and closes as required. The gas flow line was checked, allowed flow of gas into the loop and checked for any leakage.

The sensors comprised of flow meter, gas meter and differential pressure transducer were all function tested and calibrated in turns to ensure their functionality and accuracy.

4.4 Material preparations

4.4.1 Sieve Analysis – Sand grain distributions

The sand size distribution among other physical properties is of critical importance to the way the material performs when put into use. A number of classifications exist in literature; (Govier and Aziz 1972) proposed the following in terms of average particle size, *dp*:

- Ultrafine particles, *dp* < 10 microns, where gravitational forces are negligible.

- Fine particles, 10 microns < dp < 100 microns, usually carried fully suspended but subject to concentration gradients and gravitational forces.
- Medium sized particles, 100 microns < dp < 1000 microns, will move with a deposit at the bottom of the pipe and with a concentration gradient.
- Coarse particles, 1000 microns < dp < 10,000 microns. These are seldom fully suspended and form deposits on the bottom of the pipe.
- Ultra coarse particles are larger than 10mm. These particles are transported as a moving bed on the bottom of the pipe.

For the purpose of this research, dry clean sand samples are sourced and are put through series of sieves to determine the grain size distributions. See Figures 4.5 & 4.6 for the sand sample and the vibratory sieve shaker used for the experiment. This defined the relative amounts of particle sizes present, sorted according to size. Two different particle sizes with corresponding densities were considered. The average sizes, d_p or d_{50} in this case fall within the medium size category as defined above for different sand samples. The results of the sieve analysis are as presented in Figures 4.7 & 4.8.

Figure 4.5: Sand sample

Figure 4.6: Vibratory sieve shaker

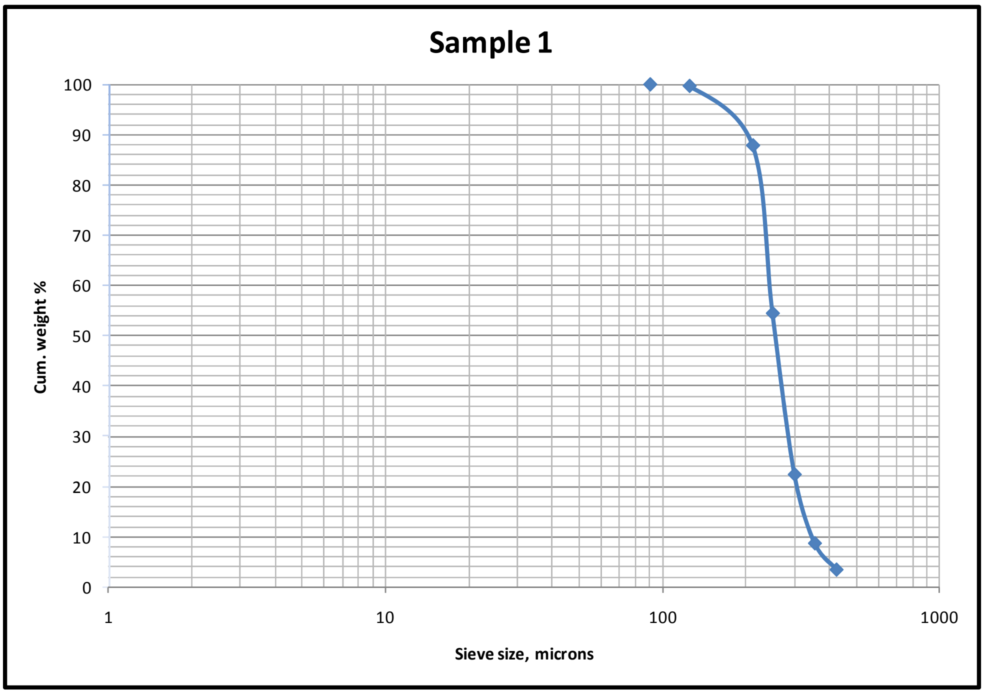

Figure 4.7: Sand grain size distribution for sample 1

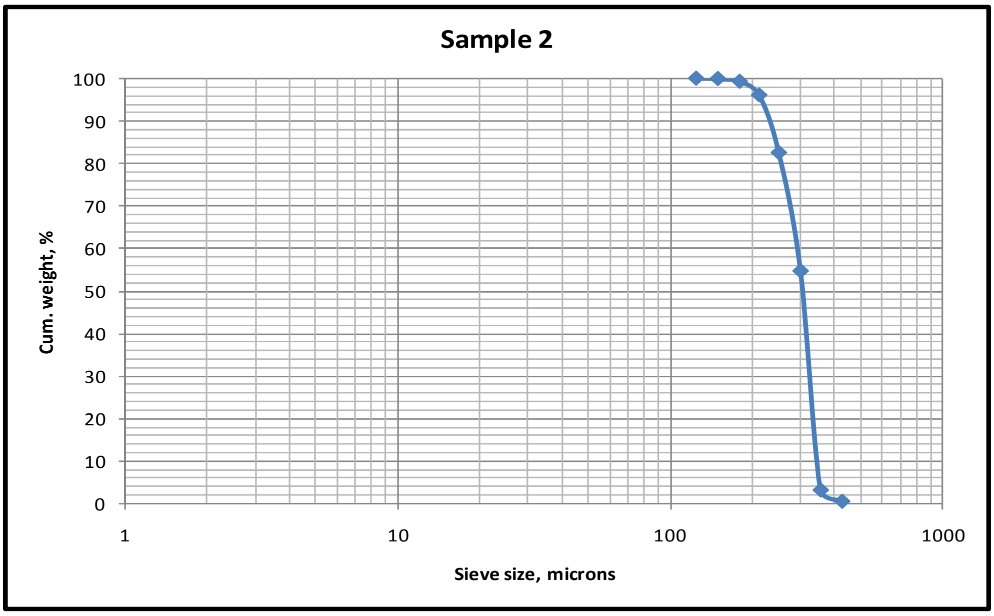

Figure 4.8: Sand grain size distribution for sample 2

4.4.2 Fluids density and viscosity

The density of a material is defined as its mass per unit volume. The term is applicable to solids, liquids and gases. These are materials used in this research and its accurate determination is very critical to the results. The densities of the liquids were obtained with the aid of conventional mud balance and or by weighing known volume of liquid to estimate the density. Samples of water and vegetable oil were measured at room temperatures to obtain the densities using the above two methods and results obtained in both instances are consistent. The values are reported in kilogram per cubic meter as presented in Table 4.3 below.

Viscosity is the resistance to flow experienced as the internal layers of liquid move over each other. Any kind of fluid, liquid or gas has resistance to flow. This is caused at the molecular level by the drag between adjacent molecules. Viscosity becomes important in all cases where a material flows especially for multiphase fluids. The fluids viscosities obtained with the aid of Brookfield viscometer which measures viscosity by measuring the force required to rotate a spindle in a fluid. On the DV-II, the viscosity was read directly as shown in Figure 4.9 below.

Table 4.3: Properties of material used

Sample	Density, ρ (kg/m3)	Viscosity, μ (Pas)
Water	998.8	0.001003
Vegetable oil	940	0.001
Sand	2150	-
Air	1.225	0.0000183

Figure 4.9: Brookfield viscometer

4.4.3 System volume

The total volume of the system is made up of two components which are pipe volume and mixing tank volume. The tank used volume is approximately 0.561 m^3. The pipe volume can be estimated as:

$$V_{pipe} = A * L \tag{4.1}$$

The volume for different pipe sections was calculated, summed up and added to the tank's volume to arrive at the total volume of the whole system. This is shown in Table 4.4 above.

Table 4.4: System volume

Pipe section	**Length (m)**	**Diameter (m)**	**Area (m^2)**	**Volume (m^3)**
Test pipe 1	1.5	0.1	0.007855	0.0118
Test pipe 2	2	0.08	0.003849	0.0077
Test pipe 3	2	0.07	0.005027	0.0101
Test pipe 4	2	0.1	0.007855	0.0118
Other pipes	7	0.0508	0.00203	0.0142
Tank volume				0.561
Total volume of the system				0.6166

4.5 General Experiment Procedures

4.5.1 Flow patterns experiment

In order to develop various multiphase flow patterns by controlling the flow rates of gas, liquid (water and or oil) and slurry. The water and the oil were mixed in the large tank and the mixture pumped through the flow loop. The oil-free pressurized air supplied from central air compressor was fed into a mixing chamber through a flexible hose. The mixing chamber was made of perforated stainless tube inserted into a cast iron pipe. This section served as flow stabilisation region before fluids exits into the horizontal test section. The flow patterns are observed in the test sections as the fluids move through it. The flow rates of the mixture are controlled by the pump variable speed controller and measured with the aid of Doppler flow meter. The compressed air flow rates are measured by a gas flow meter mounted on the line just before air entered into the mixing chamber. As the mixture of liquid (water & or oil) and gas moves through each of the test sections, the flow patterns are observed and recorded. The observed flow pattern changes are captured using a powerful digital camera including video recording.

Samples are collected during the experiment at regular interval to ensure the actual flow matched the input compositions especially for oil-water mixture as specified for each experiment.

4.5.2 Sand transport experiment

In carrying out sand transport experiment, a known quantity of sand was added to a known volume of liquid, water and or oil in the mixing tank. The mixture was well agitated by a mixer mounted on top of the tank. The mixture was then pumped through the loop and rate measured with the aid of flow meter. The measured values can also be captured and recorded on the LabView. At each run of the experiments, the minimum transport velocities (MTV) for suspension was determined visually and recorded as the particle just begin to drop off of the flowing slurry. The MTV for rolling was also determined similarly just as the settled sand began to move or slide. At the end of an experimental run, the sand was separated from the liquid by means of a sand screen filter placed inside the tank below the discharge pipe as the slurry exits the loop. The sand was recovered with the aid of the screen, the water re-circulated back into the loop continuously until all sand particles are recovered.

Data are acquired for sand MTV in suspension and in rolling modes. To achieve minimum transport velocity for a particular sand size, the fluid flow rate was set such that all particles are initially in suspension. Gradually, the rates are reduced at regular interval and observed when the particle started to drop out of body of fluid or remain in suspension.

Similarly, MTV for rolling, the liquid flow rates was increased gradually to exerts impart force on the particles already in settled mode. At the point the particles began to move, the fluid flow rate was noted and recorded.

After a set of experiment has been concluded, to ascertain level of attrition of the sand, a quick check of the sand distribution was carried out and compared with d_{50} obtained at the start of the experiment. The initial slurry concentration was checked against the slurry samples collected at the end of the experiment to ascertain consistencies in concentrations.

4.5.3 Flow pattern visualization and characterisation

A number of different methods have been proposed for the recognition of flow patterns ranging form visual observation to characteristic fluctuations in holdup. Barnea et al. 1980 observed that the designation of flow pattern has been based largely on individual interpretation of visual observation. While some instrumental methods of analysis have been proposed by some workers, these are not simple to use and did not find widespread application (Mishima, Hibiki and Nishihara 1997, Heindel, Gray and Jensen 2008). Spedding and Spence 1993 conducted a two phase flow experiment in a horizontal pipe. The flow regimes were identified by a combination of visual/video observations. They observed that the existing regime maps and theories for the prediction of phase boundary transitions did not satisfactorily predict observed flow pattern regimes, particularly when the geometrical parameters and physical properties of the phases were varied. Oddie et al. 2003 conducted transient experiments of water–gas; oil–water and oil–water–gas multiphase flows in a transparent inclinable pipe using kerosene, tap water and nitrogen. The flow pattern data were obtained and recorded by visual observations and photographic evidence. Rodriguez and Oliemans 2006 conducted experiment with oil–water two-phase flow in an inclinable steel pipe using mineral oil brine. The characterization of flow patterns and identification of their boundaries were achieved via the observation of recorded movies and by the analysis of relative deviation from the homogeneous behaviour.

The flow pattern experiments in this work adopted visual, photographic and video recording methods for identification and classification of different flow patterns. As it has been mentioned in previous chapters, many authors have proposed different descriptions of the flow patterns. In describing flow patterns in this case, Barnea et al. 1980 descriptions of the location of gas and liquid phases in pipe are adopted with some modifications to account for peculiar patterns encountered. The stratified flow is said to exist when liquid flows at the bottom of the pipe with gas at the top. The interface can either be smooth or wavy. The intermittent flow; in this flow pattern the inventory of liquid in the pipe is non-uniformly distributed axially. Slugs of liquid which fill the pipe are separated by gas zones which contain a stratified liquid layer flowing along the bottom of the pipe. The liquid may be aerated by small bubbles which are concentrated toward the front of the liquid slug and the top of the pipe. The intermittent pattern is usually subdivided into slug and elongated bubble flow patterns. In dispersed bubble, the gas phase is distributed as discrete bubbles within a continuous liquid phase. This is defined by the condition where bubbles are first suspended in the liquid or elongated bubbles which when in contact with the top of the pipe are destroyed. At higher liquid rates these bubbles are dispersed more uniformly.

4.5.4 Sand transport patterns and characterisation

Sand flow patterns classifications in horizontal pipes are similar with many authors generally identified three key sand transport patterns such as stationary bed, suspension (heterogeneous or homogeneous) and rolling or saltation (Darby 2001, Oudeman 1993., Doron and Barnea 1996, Takahashi, H., Masuyama, T. and Noda, K. 1989). The characterisation are often achieved by direct visual observation, video recording or with the aid of acoustic sand detection (Oudeman 1993, Salama 2000, Doron, Granica and Barnea 1987, Takahashi, Masuyama and Noda 1989, Gilles, McKibben and Shook 1997).

For the purpose of this work, the definition of Govier and Aziz 1972 and (Peden, Ford and Oyeneyin 1990) will suffice with variation to meet the requirement of this experiment. The average mixture velocities at which, in any given system, the transition takes place from one flow pattern to another. The minimum transport velocity, MTV for suspension is the velocity at and above which the mixture flows in asymmetric suspension pattern; the velocity below which solids form a deposit on the bottom of the pipe. The minimum transport velocity, MTV for rolling is the velocity at and above which a moving bed of particle exists on the bottom of the pipe and some particles move by saltation; the velocity below which the part of the bed in contact with the pipe wall becomes stationary.

4.6 Deposit velocity

The deposit velocity for solid-liquid mixture is the velocity below which solid particles will settle out of slurry to form a moving bed or a stationary bed. This is an important parameter in order to determine minimum transport velocity, MTV in pipeline/tieback. A key component of this parameter is the drag and lift coefficients. The deposit velocity was determined experimentally both at static and dynamic conditions in order to evaluate the drag and lift coefficients. An experimental set-up was designed and constructed; see the schematic and pictorial vertical test column in Figures 4.10 & 4.11.

In order to determine deposit velocity in static condition, the vertical pipe column was filled with required fluid. The particle sample was dropped from the top of the vertical tube and observed as it travelled through the liquid column. On the side of the column are marked different points. The time taken for the particle to travel from the top to different level or distant from the top was noted and recorded with the aid of stop watch. This procedure was repeated three times for each sample particle for single phase water, oil and two-phase oil-water, oil-gas, water-gas and for three phase oil-water-gas. In each case gas flow rates was varied and settling velocity observed at different gas rates.

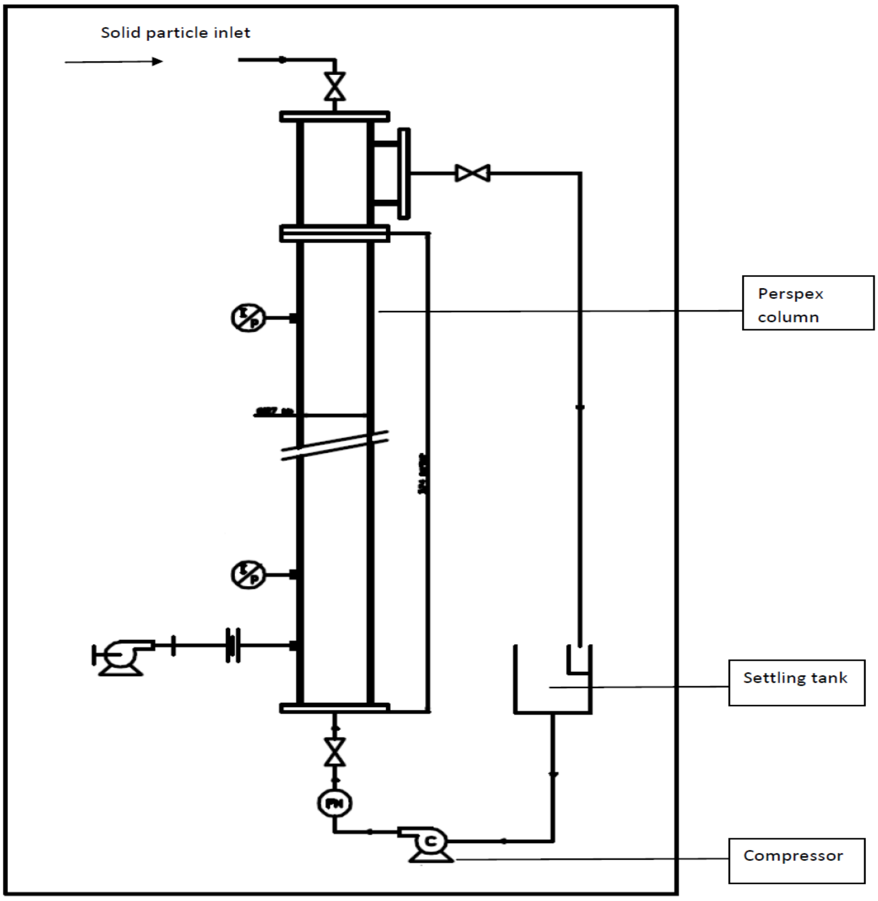

Figure 4.10: Schematic of the vertical test column

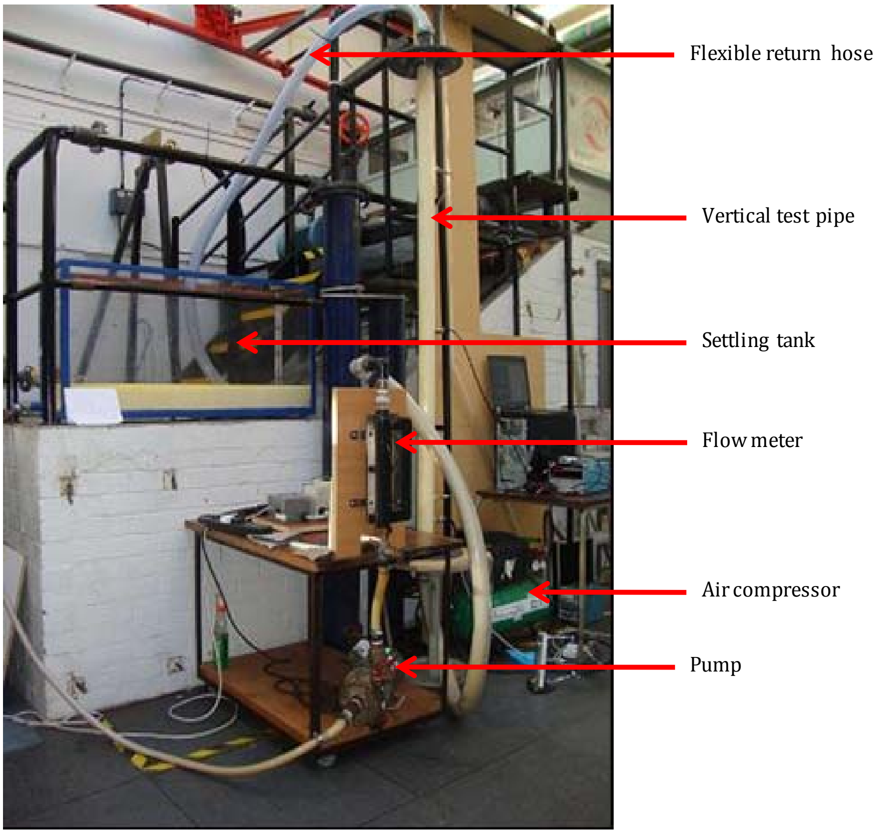

Figure 4.11: Digital picture of the vertical test column

In a horizontal pipeline, transportation velocity should be larger than the deposit velocity to prevent sand settling at the bottom of the pipeline. Solid particles will be transported horizontally without deposition if the transport condition for horizontal flow is satisfied, which is true when fluid velocity exceeds the critical deposition velocity i.e. $U_f > U_{crit}$. In general, transportation velocity is expected to be approximately 1.2 times the deposit velocity (Tian, Li, Jiang and Han 2005). The dynamic condition experiment involved circulating the fluid and particle with a pump and noted the particle travel time between two marked levels on the vertical column. This procedure was repeated for water, oil, oil-water and oil-water-air systems.

4.7 Summary

In this chapter the experimental facility and instrumentation used to carry out the critical measurements relating to flow pattern characterisations and solid particle transport in multiphase flow in pipes have been presented. This includes the methods proposed for measurement of different multiphase flow patterns, sand minimum transport velocity in multiphase flow and pressure drop. The experimental design has taken into account multiphase mixture compositions and equipment capacities for required measurements given the experiment operating window and the limitations identified here and by previous researchers. Some of the existing multiphase flow loops were reviewed in a view to improve on the existing methods and identified opportunities for improvements. The possible risks and hazards have been identified and mitigation methods have been accessed. The areas for possible errors in the measurement have also been identified and methods to be adopted to minimise the errors have been highlighted.

Chapter 5

Experiment Data Acquisitions and Analysis

5.1 Introduction

The transportation of unprocessed multiphase reservoir fluid through long subsea tiebacks has generated significant research interest in recent times. The reservoir fluid comes along with entrained solids which may drop off and form bed in the low side of the pipeline as the flow pressure declines. In order to continuously transport this unprocessed multiphase fluids through a long subsea tiebacks without solid depositions, there is the need for proper understanding of the various multiphase flow patterns and how it affect solid transport. This among other factors will enable for the development of appropriate predictive models for solid transport either in suspension or rolling modes.

Two approaches are generally recognised for development of solid transport models in pipelines, the analytical and empirical methods. Because of the complexities of multiphase flow, the analytical approach will often require some assumptions and inputs from empirical measurement particularly when describing the interactions between fluids and particles. The combination of these approaches is believed to have better predictive tendency. A combination of analytical equation and experimentally determined parameters has been used to develop semi-empirical models for sand minimum transport velocity in suspension and rolling. It is pertinent to say that during the course of this study, the dearth of experimental data for model testing and validation was apparent. Clearly, this is the missing link that has contributed to the inconsistent results from existing models.

In this chapter, the results of the experiments carried out for flow patterns and sand transport velocity are presented, analysed and discussed. The experimental facilities and measurement techniques adopted are as described in Chapter 4. There were essentially three fluids used in this experiment, water, oil and gas in different combinations such as air-water, air-water-oil, water-sand, water-oil-sand, water-air-sand and water-oil-air-sand. The observed flow patterns for different input flow rates for liquid (water or oil) and gas both in two-phase and three-phase flow are presented. The results of minimum transport velocity for suspension and rolling at various input flow rates for liquid and gas are also presented. The representative flow rates for different flow pattern maps and sand minimum transport velocities are presented using the concept of superficial velocities for liquid and gas.

The use of transparent acrylic pipe for test sections allows for visual observation of flow patterns and sand deposition as shown in Figure 5.1. The large pipe size used in this case was necessary to adequately capture the flow patterns in relation to solid transport either in suspension and or rolling. The effect of pipe sizes on the development of flow patterns was evident in the various flow patterns observed. The design of the multiphase flow loop was to replicate different pipe sizes and topography of the sea floor in order to get as close as possible to the actual field scenario to improve on the quality and reliability of the results. Table 5.1 are examples of pipe sizes from selected multiphase flow loop.

Table 5.1: Examples of pipe diameters for different flow loop

S/no	Pipe ID, meter	Reference
1	0.07, 0.08 & 0.1	Present study
2	0.0195 & 0.0255	(Barnea, Shoham, Taitel and Dukler 1980)
3	0.05	(Andreussi and Persen 1987)
4	0.051	(Doron, Granica and Barnea 1987)
5	0.038 & 0.054	(Lovick and Angeli 2004)
6	0.15	(Oddie et al. 2003) (Large pipe size)

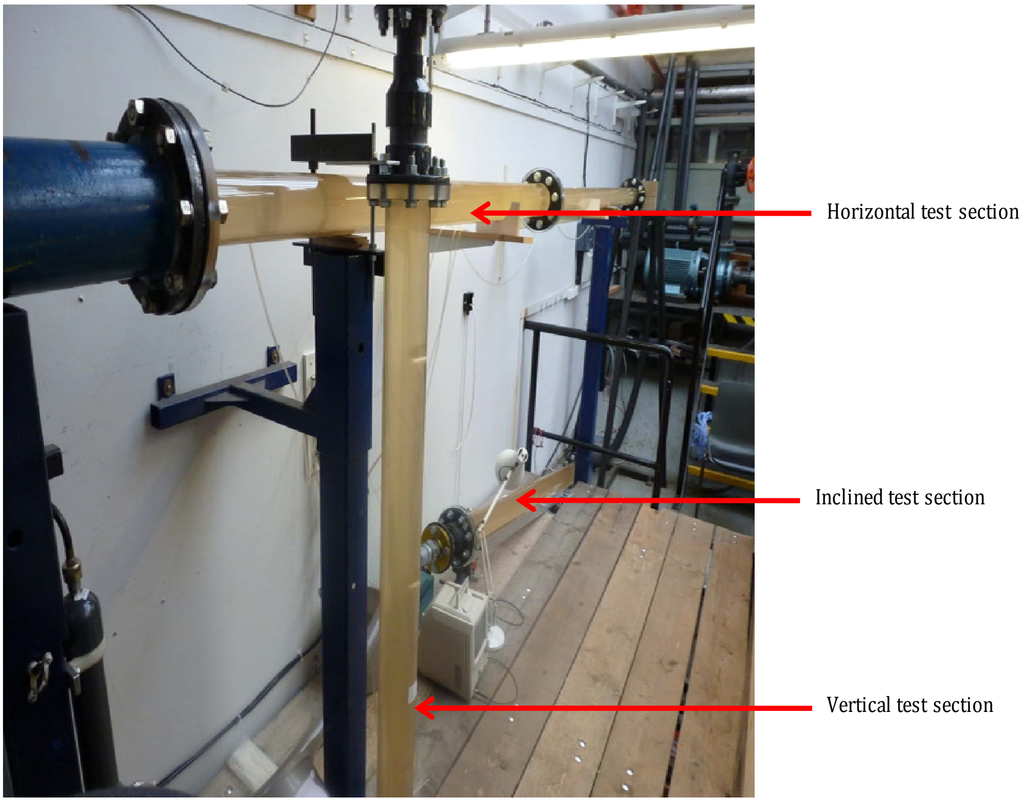

Figure 5.1: Picture of flow loop showing the acrylic test sections

5.1.1 Superficial flow velocity and mixture velocity

The superficial velocity as a form of analysis of the results was adopted in this experimental study. Average fluid velocity is often used in a case of single phase flow, where the volumetric flow rate Q, (m^3/s) is divided by the cross sectional area of the pipe A, (m^2).

$$V_{avg} = \frac{Q}{A} \quad 5.1$$

In multiphase flow, the part of the area occupied by one particular phase varies in space and time, so the flow is no longer proportional to the velocity at a given point. Therefore, a hypothetical fluid velocity is calculated as if the given phase or fluid was the only one flowing or present in a given cross sectional area (Bratland 2010). This served as convenient parameters for analysis in this case and can be expressed as below.

$$V_{sl} = \frac{Q_w}{A} \quad 5.2$$

$$V_{sg} = \frac{Q_g}{A} \quad 5.3$$

Where:

V_{sw}, V_{sg} are superficial velocities of water and gas phase, m/s.

Q - Volumetric flow rate of the phase, m^3/s

A - Cross sectional area, m^2

The liquid – gas mixture velocity can therefore be estimated by

$$V_m = V_{sl} + V_{sg} \quad 5.4$$

Where V_{sl} is the liquid velocity

5.1.2 Experiment measurement error

It is appropriate to state that spurious data may be recorded especially for this kind of large scale experiment. There were data that seems to be out of range and could be attributed to anything ranging from equipment malfunctioning or human errors. However, care was taken in the operation of the equipment and sensors. The measurement error was reduced by repeating measurement three times and then averaging for every recorded flow patterns and MTV data in all given experimental activities. The multiple data collection techniques enhanced the accuracy of the data collected and each data set compared to reduce the error margin.

5.2 Flow pattern maps

Five different flow patterns were observed in gas-liquid flow experiments. The observed flow patterns are stratified smooth flow, stratified wavy flow, dispersed bubble flow, elongated bubble flow and slug flow. In horizontal pipes the common flow patterns observed are stratified smooth, stratified wavy, dispersed bubble flow and elongated bubble flow. The elongated bubble flow featured prominently in 0.08 meter horizontal test pipe and as well as 0.1 meter inclined test pipe. For the inclined test pipe section, three flow patterns are prevalent, the slug flow, elongated bubble flow and dispersed bubble flow for different pipe inclinations and for various liquid and gas superficial velocities.

5.2.1 Two-phase flow patterns

The experimental flow-pattern map with superficial velocity coordinates is presented in Figure 5.2 and 5.3 for water–gas flow in 0.07 meter & 0.08 meter horizontal test pipe respectively. For two-phase water-gas flow, the patterns observed are stratified smooth and stratified wavy in 0.07 meter pipe while stratified smooth flow, stratified wavy flow and elongated bubble flow were observed in 0.08 meter test pipe. It can be seen from the figures that at relatively low gas and water flow rates, a stratified smooth flow was observed. At higher gas rates, the interface becomes wavy, and stratified wavy flow was observed distinctly. With further increase in gas rates, elongated bubble flow was observed. The large gas bubbles flow along the top of the pipe; it has a striking resemblance with a slug flow.

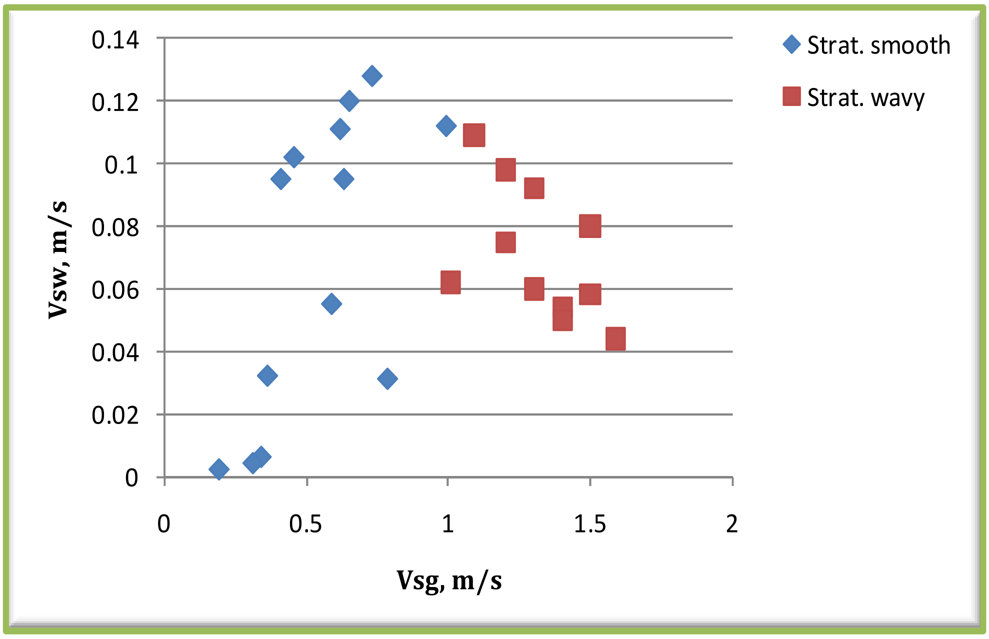

Figure 5.2: Two-phase water-gas flow in 0.07m horizontal pipe at various superficial water and gas velocities.

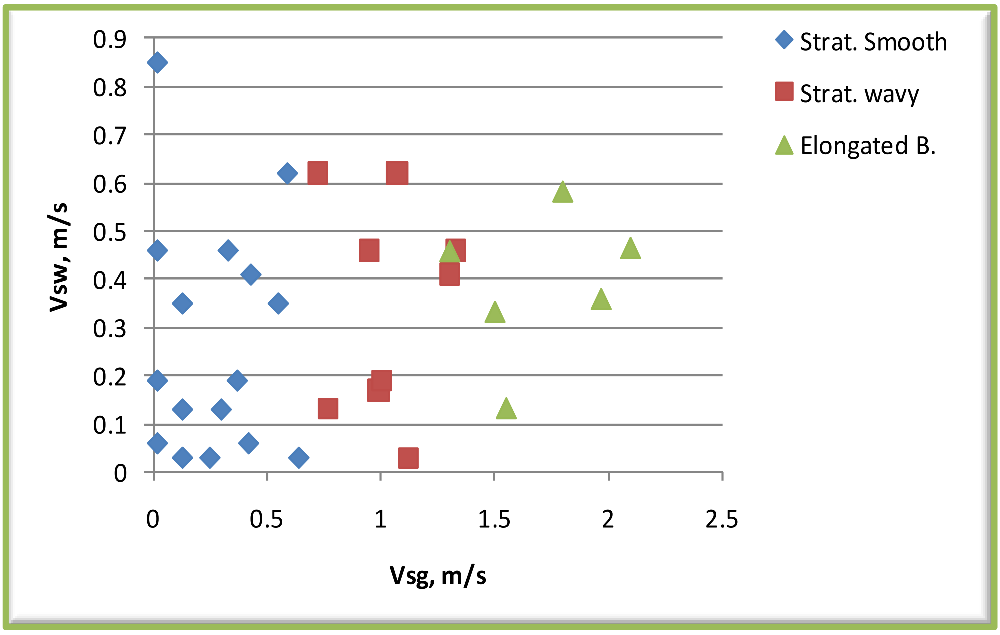

Figure 5.3: Two-phase water-gas flow in 0.08m horizontal pipe at various superficial water and gas velocities.

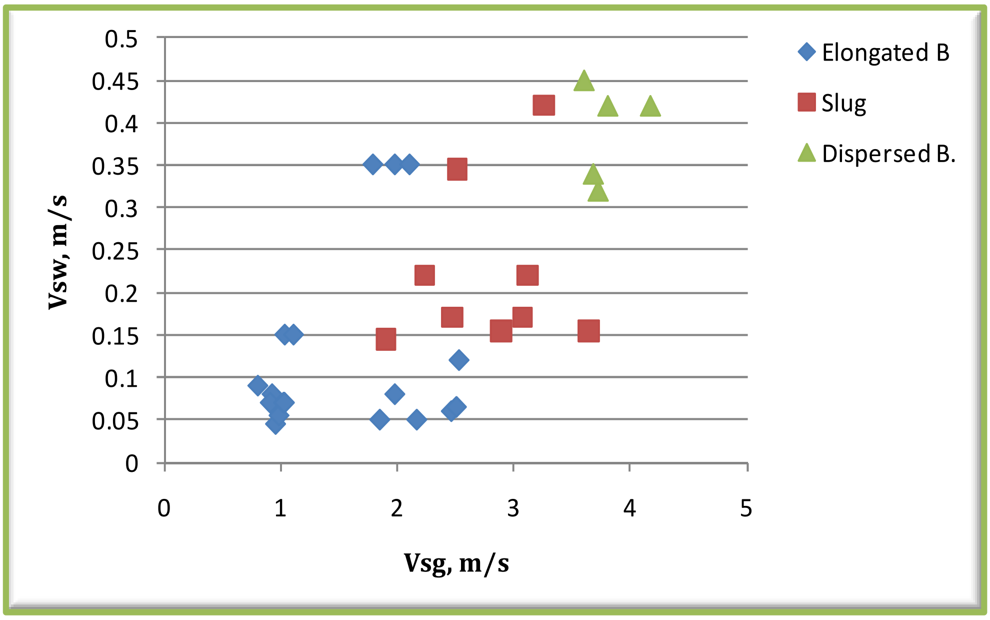

Figure 5.4: Two-phase water-gas flow in 0.1m inclined test pipe at various superficial water and gas velocities.

In inclined pipe section, the dominant flow patterns are slug flow; elongated bubble flow and dispersed bubble flow see Figures 5.4. The change in angle orientation for inclined test pipe section aggravated formation of slug flow and rapid transition from dispersed bubble to elongated bubble flow. This was similar observation reported by (Oliemans 1994, Oddie et al. 2003). At 25 degree inclined surface, most of the experiments conducted revealed elongated bubble flow and slug flow. In few cases where dispersed bubble flow was observed, it was mostly at the entrance and accompanied by high turbulence. This may be attributed to the pipe geometry as the fluids exits into inclined pipe section.

Figures 5.5 to 5.7 show the pictures captured for observed flow patterns during the experiments. The green marking was to trace the clear demarcation for the stratified smooth flow surfaces captured during the water-gas experiment in horizontal pipes.

Figure 5.5: Intermittent slug for water-gas in 0.1m test pipe inclined at 15^{0}.

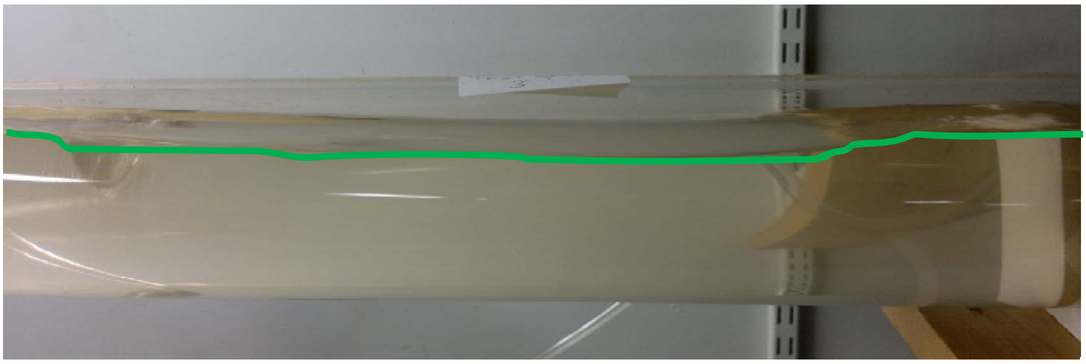

Figure 5.6: Stratified wavy (gentle undulating) flow in 0.08m horizontal pipe.

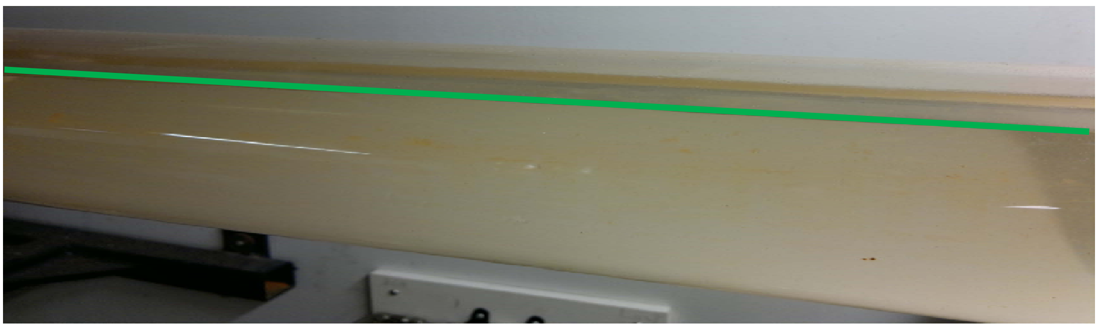

Figure 5.7: Stratified smooth flow in 0.1m horizontal pipe.

5.2.2 Three-phase flow patterns

For three-phase water-oil-gas, identification of the flow pattern was a bit challenging especially at high flow rates. The water dominated water-oil mixture appeared creamy and clear identification of the phases became very difficult as seen in Figure 5.8. Each of the experimental run was repeated three times for a clear identification of the patterns and each data compared. Therefore, after careful observation it was apparent that the dominant flow patterns for oil in water flow in horizontal test pipes with different oil concentrations are stratified smooth flow, stratified wavy flow and elongated bubble flow with varying superficial velocities for liquid mixture and gas. The patterns are as presented in Figures 5.9 & 5.10.

Figure 5.8: Two-phase water-oil mixture in horizontal pipe, Vm=2.25 m/s.

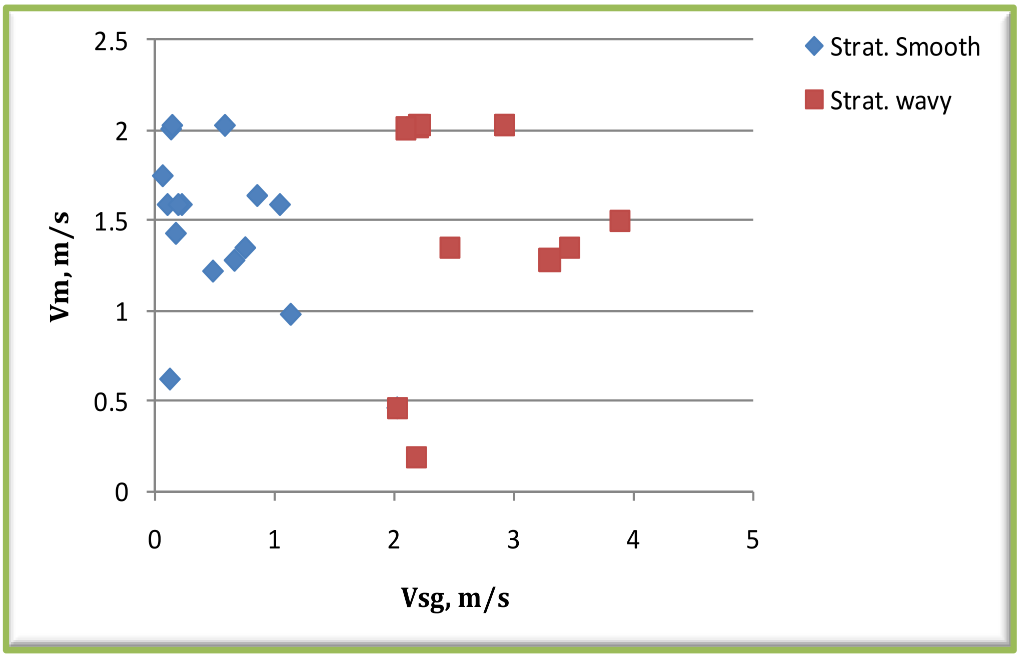

Figure 5.9: Three-phase water-oil-gas with 10% oil flowing in 0.07m horizontal test pipe at various superficial liquid (water & oil) and gas velocities.

For relatively low mixture velocity of water-oil mixture, the flow is gravity dominated and the phases are totally segregated which represents the stratified smooth flow and stratified wavy flow. These patterns were also observed for two-phase water-gas flow in horizontal pipes. The flow patterns observed for three-phase stratified flow closely resembles a two phase stratified flow except that the liquid phase is a non-transparent dispersion. This striking resemblance may have informed the suggestion by (Oddie et al. 2003) that three phase flow can probably be modelled as a two phase flow, though the properties of the phases may differ from the properties of the pure components. It was also observed that no appreciable change in the flow patterns with change in the angle of inclinations. The elongated bubble flow observed at 15^0 and 20^0 to the vertical were similar as can be seen in Figure 5.11.

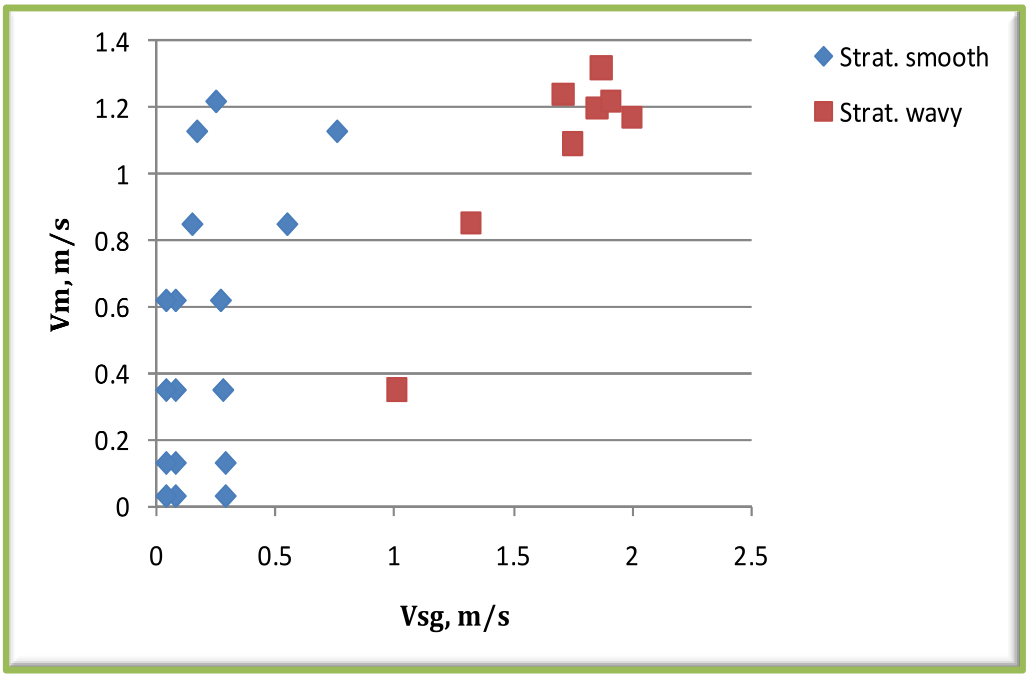

Figure 5.10: Three-phase water-oil-gas with 5% oil flowing in 0.07m horizontal test pipe at various superficial liquid (water & oil) and gas velocities.

With increase in flow velocity in a water dominated mixture, the continuity of the oil layer is disrupted and a dispersion of oil in water is formed thus created complete creamy colour which made visibility difficult. Similar observations were reported by (Oddie et al. 2003, Vielma et al. 2008). In this case, it may be due to the vegetable oil used which has foaming tendencies when subjected to turbulent as result of high flow rates.

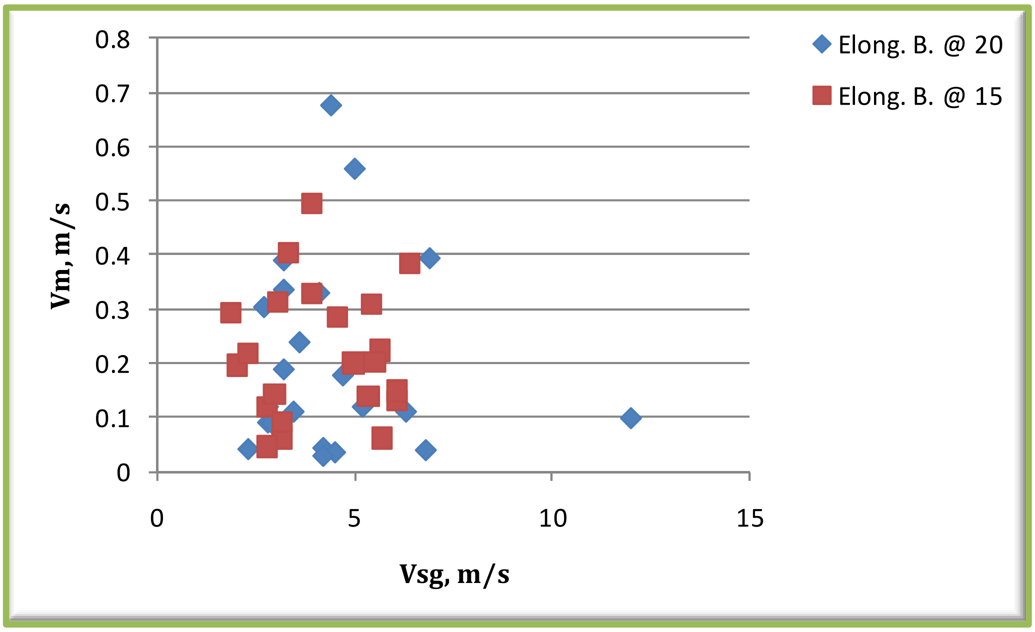

Figure 5.11: Three-phase water-oil-gas in 0.1m inclined test pipe at various superficial liquid (water & oil) and gas velocities.

5.2.2.1 Effect of angle

It was noted that when the pipeline was inclined from horizontal, the flow pattern behaviour is very similar to that seen in a horizontal line. The major change however was that stratified flow disappears immediately at inclined angle. The reason for this is that with upward inclination greater velocity will be required to transport the fluid as compared to the relatively low velocity characterised by stratified flow. At 15^0 up to 25^0 of pipe inclinations considered in these experiments, the observed flow patterns are slug flow and elongated bubble flow though dispersed bubble was also observed on few occasions. At high gas superficial gas velocities, the predominant pattern observed was slug flow as shown in Figure 5.12. At 25^0 only slug and elongated bubble flows were observed. For horizontal flow, the flow patterns were stratified or stratified wavy for all water and gas superficial velocities investigated.

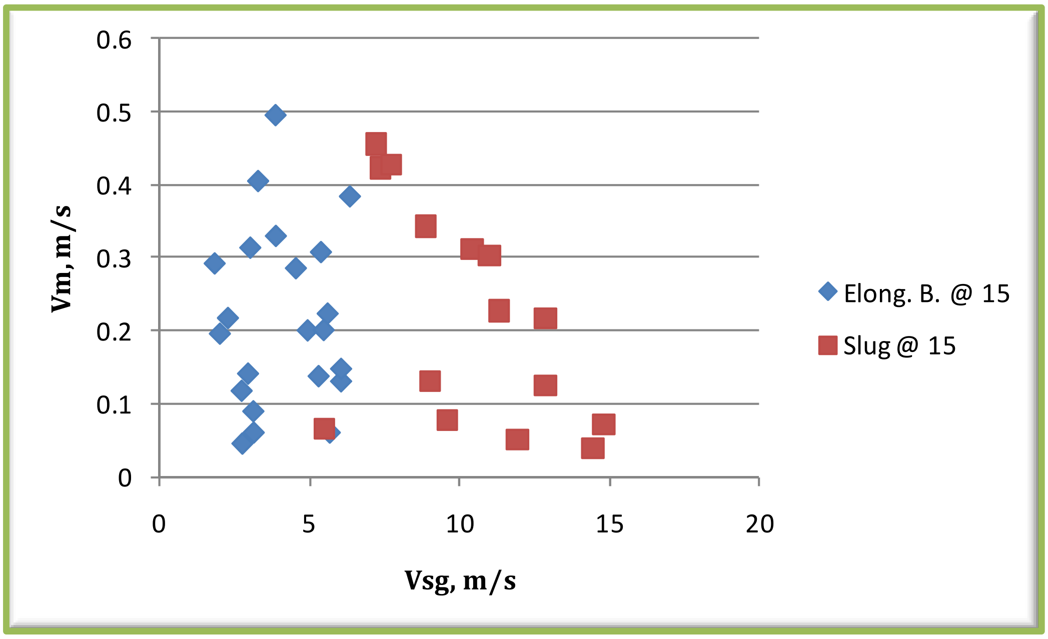

Figure 5.12: Three-phase water-oil-gas in 0.1m inclined test pipe at various superficial liquid (water & oil) and gas velocities.

5.3 Flow pattern prediction

Table 5.2 below compares the results of the different flow patterns for three-phase, water-oil-gas obtained from the experiments with Beggs and Brill flow pattern prediction models which is applicable to horizontal and slightly inclined pipes. The results showed more than 90% of the data were predicted with the models. This generally enforces the choice of flow pattern prediction model used for solid transport modelling. Some of the flow pattern data are presented here and details can be found in Appendix C.

Table 5.2: Comparison of observed flow patterns with Beggs & Brill model predictions

Experimental data		Flow pattern	
Vsl	**Vsg**	**Observed pattern**	**Model prediction**
0.001	15.18	Dispersed bubble flow	Dispersed bubble flow
0.002	15.02	Dispersed bubble flow	Dispersed bubble flow
0.005	15.37	Dispersed bubble flow	Dispersed bubble flow
0.01	15.09	Dispersed bubble flow	Dispersed bubble flow
0.032	0.366	Stratified flow	Stratified flow
0.006	0.344	Stratified flow	Stratified flow
0.031	0.787	Stratified flow	Stratified flow
0.128	0.733	Stratified flow	Transition flow
0.004	0.315	Stratified flow	Stratified flow
0.102	0.459	Stratified flow	Transition flow

0.0705	14.818	Slug flow	Dispersed bubble flow
0.13	15.037	Slug flow	Slug flow
0.2165	12.881	Slug flow	Slug flow
0.3125	10.43	Slug flow	Slug flow
0.0385	14.446	Slug flow	Dispersed bubble flow
0.0765	17.577	Slug flow	Slug flow

5.4 Pressure drop

Figures 5.13 to 5.17 present the measured pressure drops versus superficial liquid velocity at different superficial gas velocities for horizontal and inclined test sections. The results obtained suggested that at high flow rate, the flow experienced higher pressure loss. Also observed that pressure drop strongly depends on flow patterns and consequently on variations of liquid and gas superficial velocities. The flows with oil mixtures tend to have higher pressure drops. This was greatly influenced by formation of elongated bubble and slug flows especially in the inclined pipe section. No significant different was observed in pressure drops with change in gas superficial velocity in 0.08 meters horizontal pipe because the flow pattern observed was consistently in dispersed bubble tending to elongated bubble flow as can be seen in Figure 5.14. At relatively low gas and liquid flow where flow pattern are generally stratified smooth or stratified wavy flow in water-gas flow, the pressure drop recorded are quite low when compared with elongated bubble flow observed with water-oil flow shown in Figure 5.17. Detailed pressure drop data can be found in Appendix D.

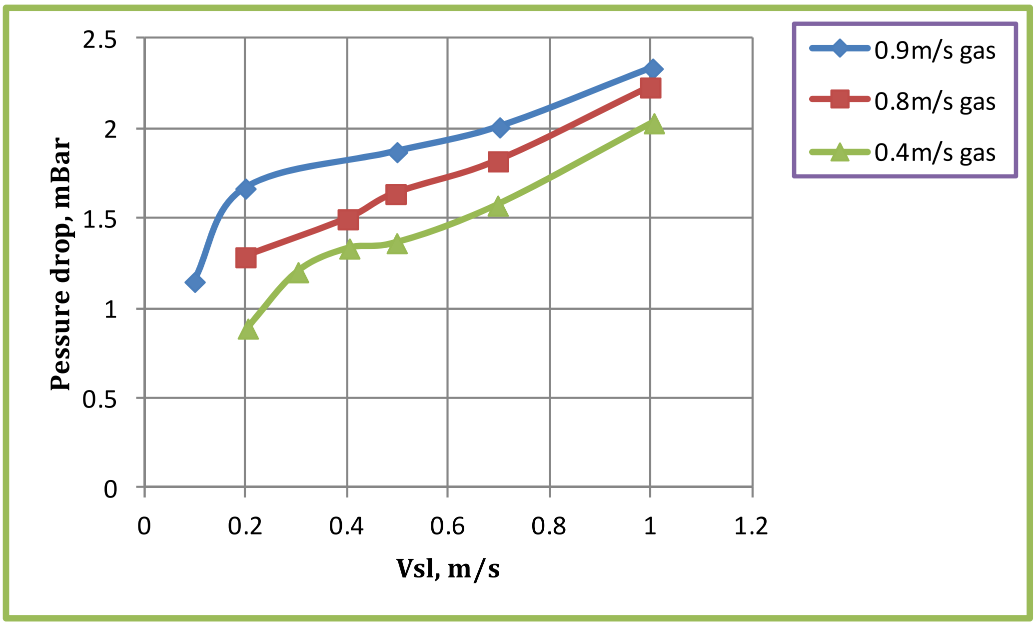

Figure 5.13: Pressure drop in water-oil mixture for 0.1m test pipe inclined @15°

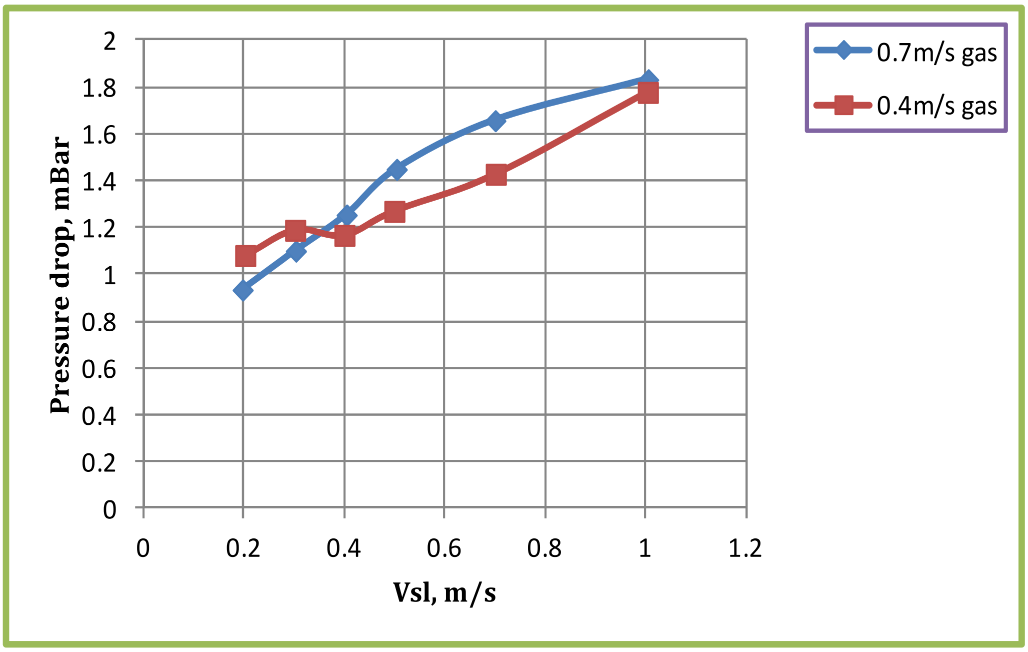

Figure 5.14: Pressure drop in water-oil mixture for 0.08m horizontal test pipe

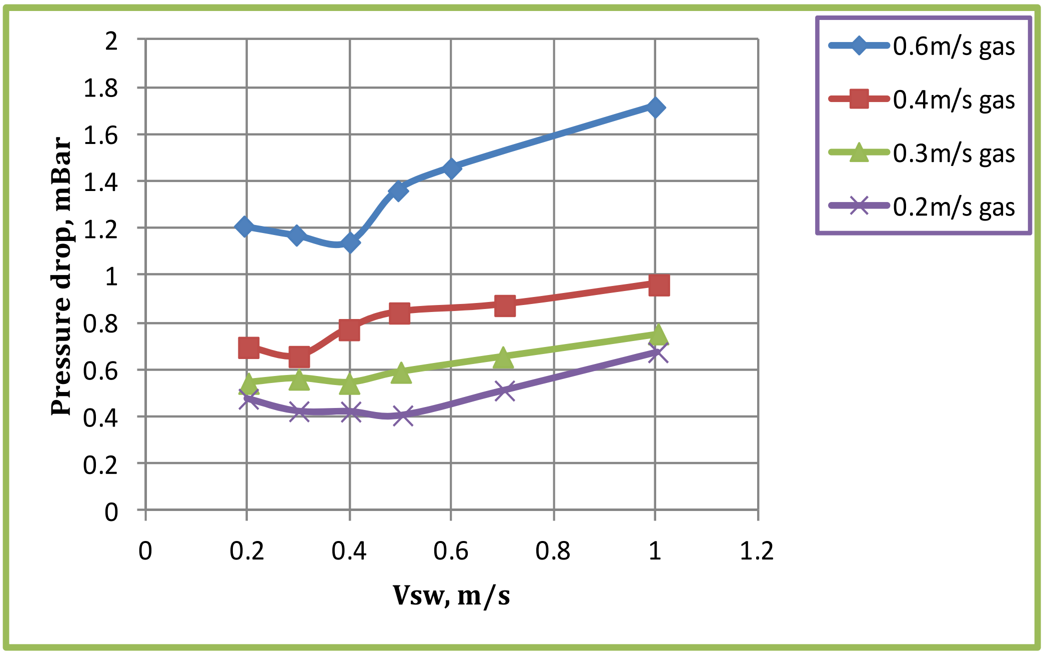

Figure 5.15: Pressure drop in 0.07m horizontal test pipe with water & gas flow

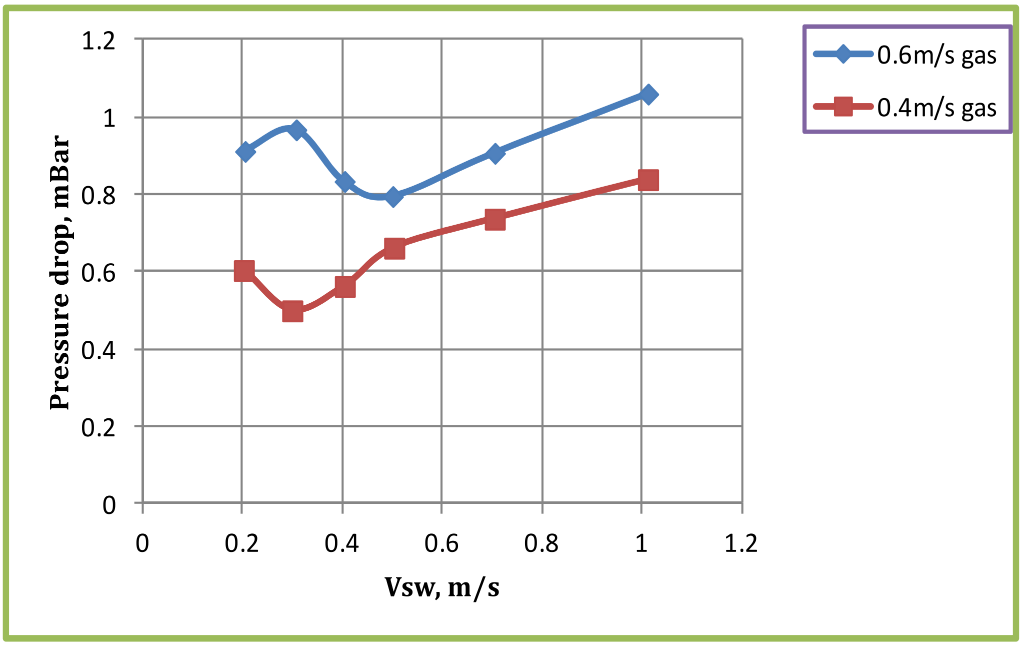

Figure 5.16: Pressure drop in 0.08m horizontal test pipe with water & gas flow

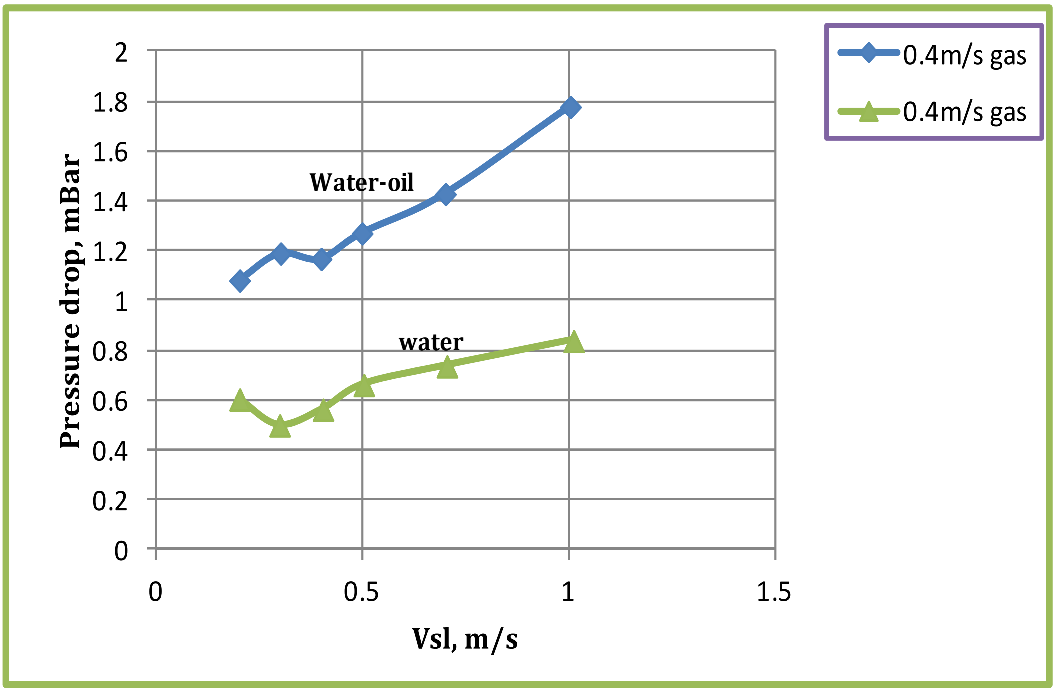

Figure 5.17: Effect of viscosity on pressure drop in water & oil and water flow in 0.08m horizontal test pipe

5.5 Sand transport Experiments

In this section the results of the experimental investigation for minimum transport velocity in suspension and rolling are presented. The theories underlying the observed phenomenon are analysed and discussed. The sand transport experiments conducted used three different fluid systems and two sand sample sizes. The concentrations of the sand samples including the fluid systems were varied for each experimental run. The flow rates were varied to determine the MTV for either suspension or rolling and for each of the pipe sizes. A combination of the fluid systems, water-oil-gas mixtures was used to create multiphase fluids. Different pipe orientations were used; the horizontal test sections and inclined test section. The horizontal pipes consist of the 0.07 & 0.08 meters while the inclined test section with pipe size of 0.1 meter which can be varied at three different angles; 15^0, 20^0 and 25^0. The results for each of the pipe sizes and orientations are presented for each of the fluid systems. Detailed experimental results for sand transport velocity are presented in Appendix E.

The sand flow patterns identified in the conducted sand transport experiments have similarly been observed by other researcher and can be distinctly classified as follows, (Ford, Peden, Oyeneyin, Gao and Zarrough, 1990) and (Danielson 2007)

- Homogeneous suspension: Sand is transported in suspension and distributed uniformly over the inside of the pipe.
- Suspension/Saltation: Sand is still transported in suspension but it is densely populated near the low-side wall so that it is virtually transported by jumping forward or saltating on the surface of the low-side pipe wall.
- Continuous Moving Bed: A thin, continuous sand bed is formed on the low-side wall of the pipe with the sand near the low-side wall rolling or sliding forward at a lower velocity than that above the bed.
- Stationary Bed: A continuous sand bed is formed on the low-side wall of the pipe with the sand on the surface of the bed rolling or sliding forward whilst the sand inside the bed is stationary.

5.5.1 Minimum transport velocity (MTV) in single-phase water

The flow visualisation method was used to determine the minimum transport velocity for each of the experimental run. This relies upon identifying the exact flow rate at which the solid begin to drop out of the flowing fluid when initially in suspension, that is MTV for suspension. Or exact flow rate when the solid begin to move when initially at rest for MTV rolling. By measuring the flow rates at which the particles begin to drop off or move from stationary position, the minimum transport velocity was then estimated either for suspension or for rolling in each of the test pipes. Prior to each experimental run, sand particle suspension was achieved at maximum flow rate of 2.04 m/s. The water-sand mixture was then allowed to flow continuously through the test sections for about 10 minutes to ensure suspension homogeneity as shown in Figure 5.18.

Figure 5.18: Suspended sand particles in single-phase water flow

The MTV results for water-sand flow experiments are as presented in Figures 5.19 to 5.21. The sand was run with water alone in three different pipe sizes; the measured velocities are remarkably different for suspension and rolling as shown in Figure 5.19. It can be seen that, the velocity required to initiate sand rolling is less than that to maintain solid particle in suspension. The pipe diameter also affects MTV to a reasonable extent. Figures 5.20 and 5.21 are results for MTV suspension and rolling given different sand concentration profiles. For MTV rolling, no significant change was observed when the sand concentration was changed from 1.9% to 2.5%. However, there was significant change in measured MTV for suspension when sand concentration was increased.

For lower sand concentrations, transportation mechanism will be enhanced and will require less energy. The two sand concentrations investigated for the same particle size both in horizontal and inclined test sections clearly showed the significant effects of sand loading with respect to flow rates on sand transportation patterns in water-gas flow. The d_{50} used in this experiment, 250-300 microns is a representative of the particle size commonly found in oil and gas production pipelines (Stevenson et al. 2001).

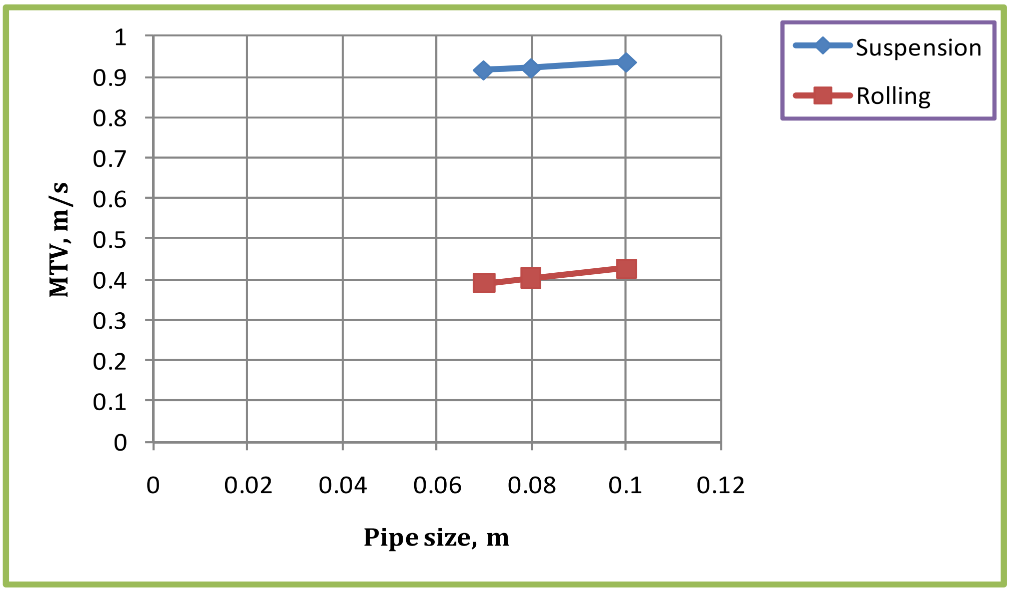

Figure 5.19: MTV for suspension and rolling in water-sand flow, 0.07m, 0.08 and 0.1m pipe sizes. The 0.07m & 0.08m are horizontal and 0.1m pipe at 15^0

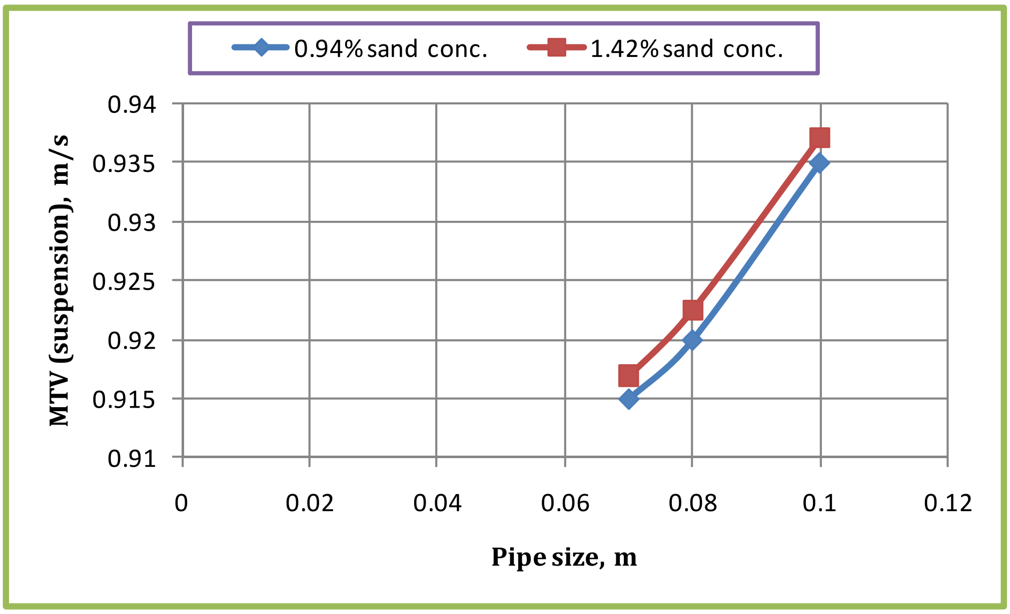

Figure 5.20: MTV for suspension in water-sand flow with different pipe sizes and sand concentrations. The 0.07m & 0.08m are horizontal and 0.1m pipe at 15^0

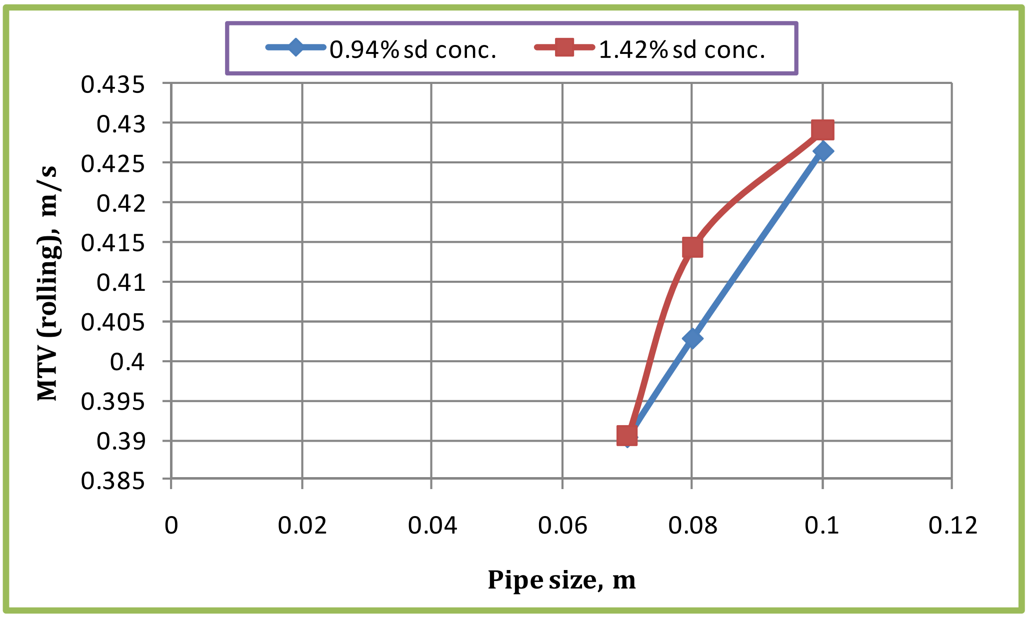

Figure 5.21: MTV for rolling in water-sand flow with different pipe sizes and sand concentrations. The 0.07m & 0.08m are horizontal and 0.1m pipe at 25^0

5.5.2 Minimum transport velocity (MTV) in multiphase

5.4.2.1 Effect of gas injection on MTV

The injection of gas into water-sand slurry introduced different propositions. The effect of superficial gas velocity, Vsg on the fluid capacity to transport sand particle has been studied. Figures 5.22 & 5.23 illustrate significant influence of superficial gas velocity on sand particle movement. The observed MTV may have been influenced by characteristics of the changes in flow patterns. The gradual increase in gas flow rates led to formation of dispersed bubbles which initiated strong turbulence and vortex formation in the pipe flow. This was a common scene in the 0.1m inclined pipe as was discussed earlier. With further increase in gas flow rates; there was transition to stratified wavy and stratified smooth in 0.07 meter & 0.08 meter horizontal pipes. There it was observed that the fluid mixture has less capacity to transport the solid and increasingly the sand bed begin to form. In contrast, for 0.1 meter inclined pipe where slug flow developed there was enhanced solid transportation in the pipe which resulted in lower sand hold up. This phenomenon was also observed by previous investigators such as (Oudeman 1993.) and (Danielson 2007)

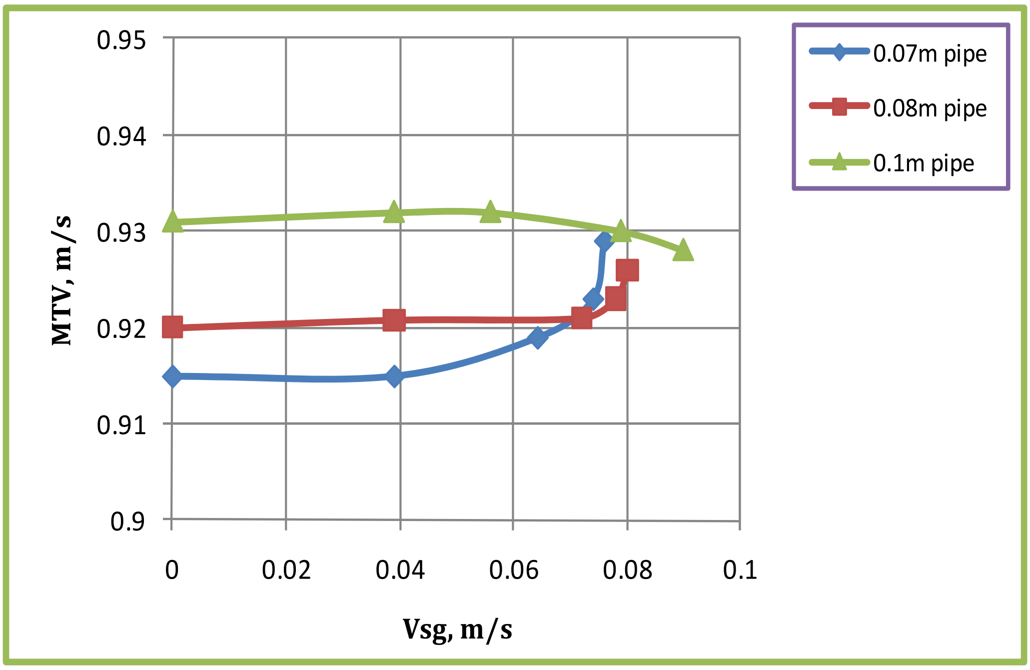

Figure 5.22: MTV suspension in water-gas-sand flow for different pipe sizes. The 0.07m & 0.08m are horizontal and 0.1m pipe at 15^0

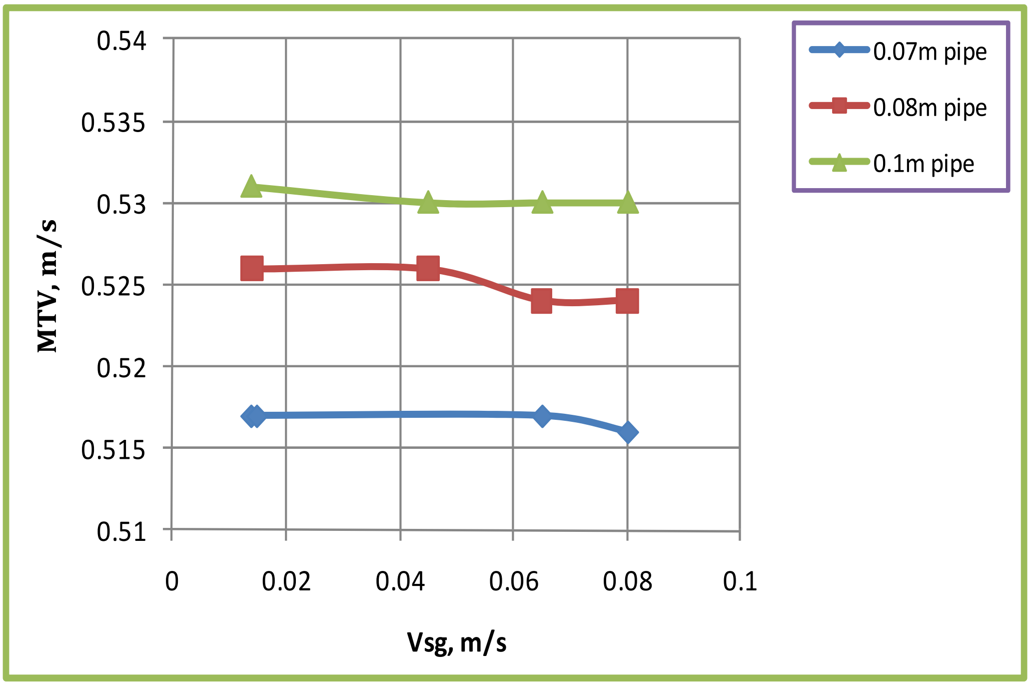

Figure 5.23: MTV rolling in water-gas-sand flow for different pipe sizes. The 0.07m & 0.08m are horizontal and 0.1m pipe at 15^{0}

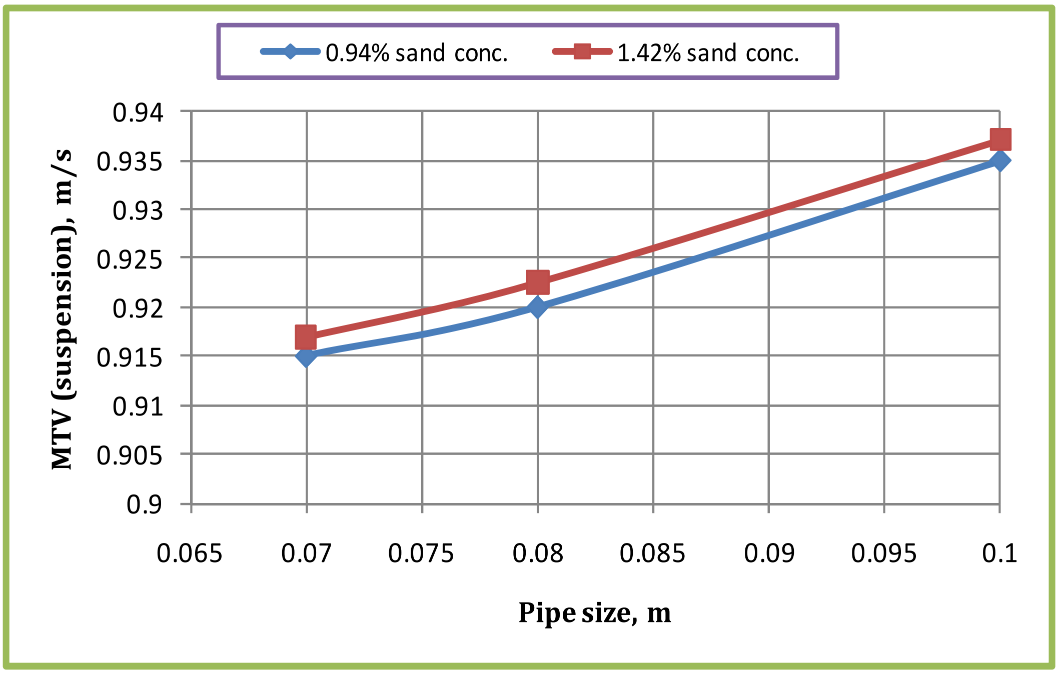

Figure 5.24: MTV for suspension in water-oil-sand flow with different pipe sizes sand concentrations

5.5.2.2 Effect of sand concentration on MTV

Figures 5.24 to 5.28 reveal the increase in MTV with increase in sand particle concentration for each of the pipe sizes. The increase in sand concentration resulted in increased sand loading in each of the pipe sizes considered. The associated decrease in carrier fluid velocity had direct consequence on MTV and resulted in sand hold up. The effect increases with increase in sand particle loading which can be attributed to the reduction in particle-particle, particle-wall interactions and liquid phase turbulence intensity.

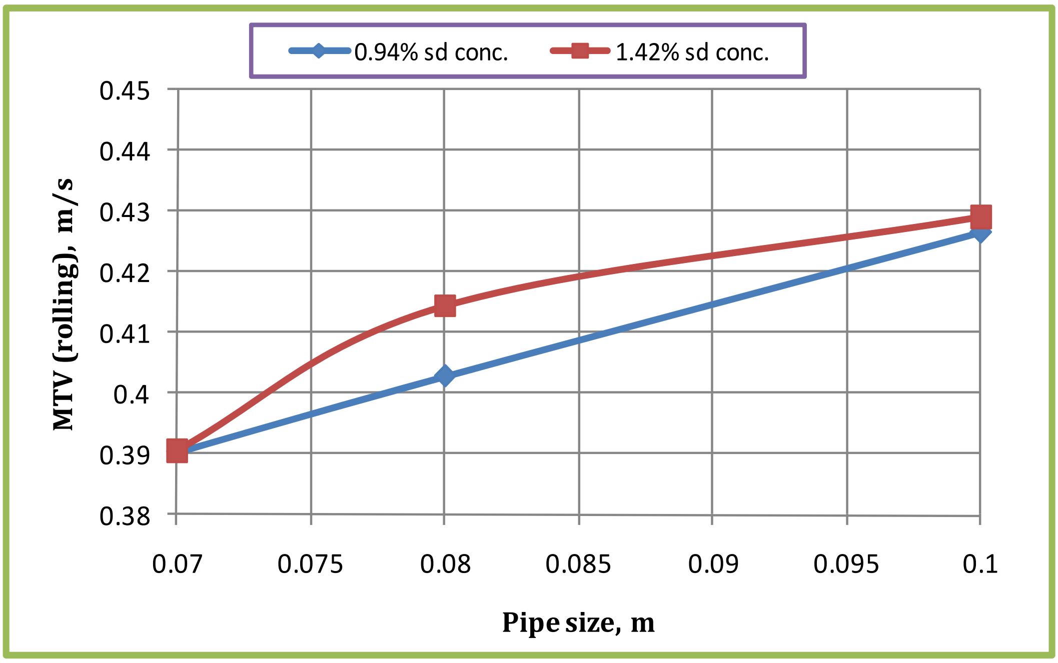

Figure 5.25: MTV for rolling in water-oil-sand flow with different pipe sizes sand concentrations. The 0.07m & 0.08m are horizontal and 0.1m pipe at 15^0

Figures 5.26 & 5.27 introduced additional complexities because of the slug patterns formed in 0.1m inclined pipe section.

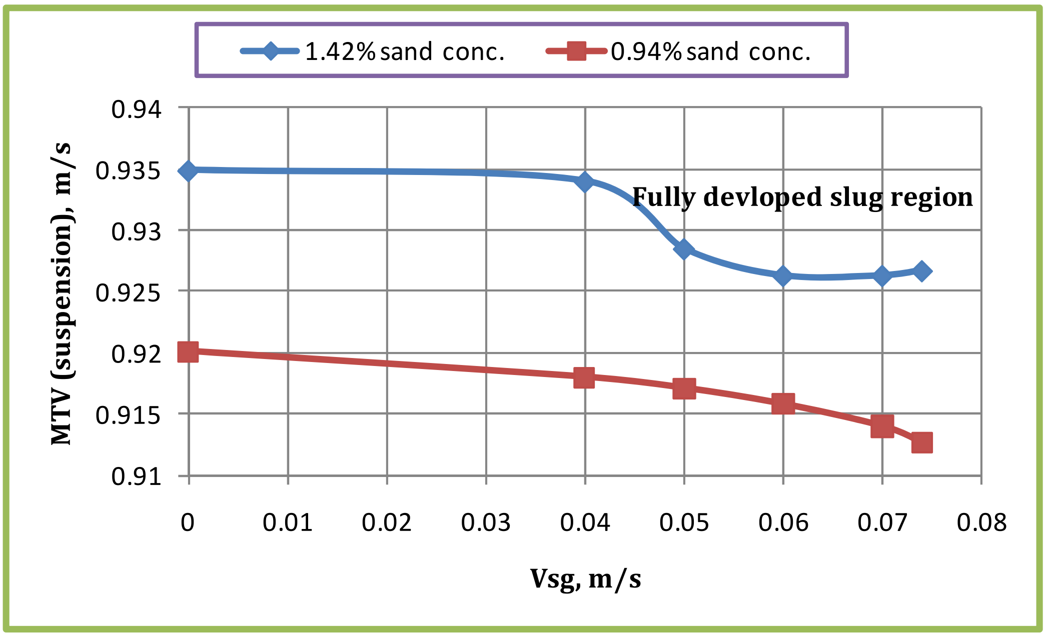

Figure 5.26: Effects of sand concentration on MTV in water-oil-gas-sand flow in 0.1m pipe size inclined at 15^0

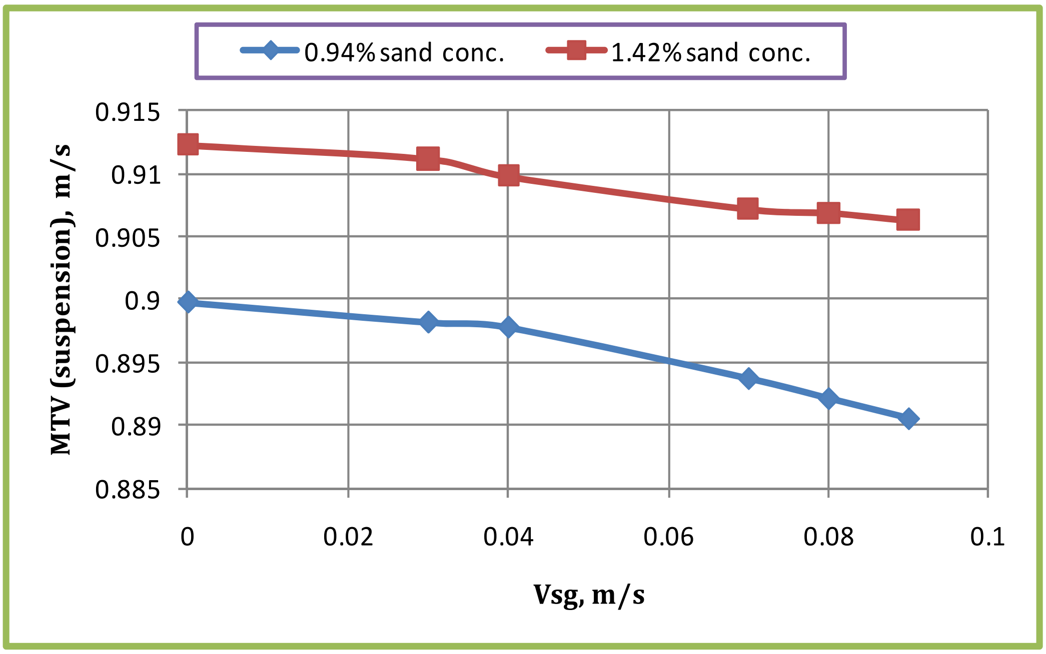

Figure 5.27: MTV suspension in water-oil-gas-sand flow with different sand concentrations in 0.1m pipe size inclined at 25^0

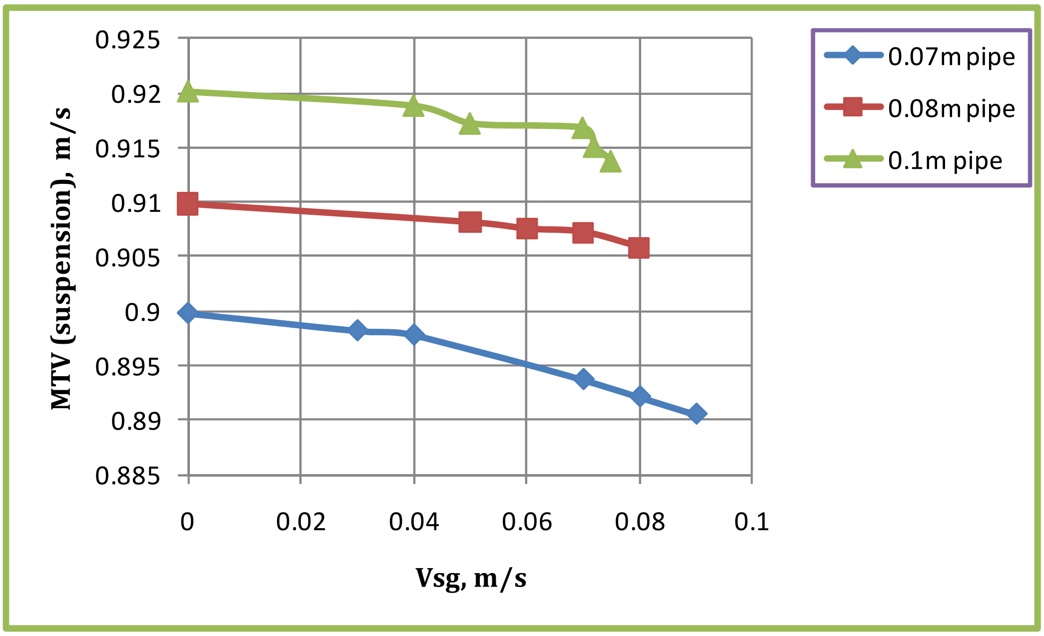

Figure 5.28: Effect of flow patterns on MTV in water-oil-gas-sand flow with 10% oil concentration. The 0.07m & 0.08m pipe sizes are horizontal and 0.1m pipe size inclined at 15^0

5.5.2.3 Effect of flow patterns on MTV

Figures 5.28 & 5.29 shows the results of the experiments on the effects of flow patterns on sand particle transport velocity profiles in horizontal & inclined test pipe sections for water-oil-gas-sand flow systems. The flow pattern in 0.1 meter pipe section was predominantly slug flow as compared to the stratified and elongated bubble flow patterns in 0.07 meter & 0.08 meter pipe sections respectively. Generally, there was decrease in sand deposition for all the three flow patterns. The greatest observable reduction in sand deposition was in slug flow, followed by elongated bubble flow and stratified flow patterns. The particle transport enhancement in slug flow can be attributed to the significant turbulent nature of the slug nose (King, Fairhurst and Hill, 2001).

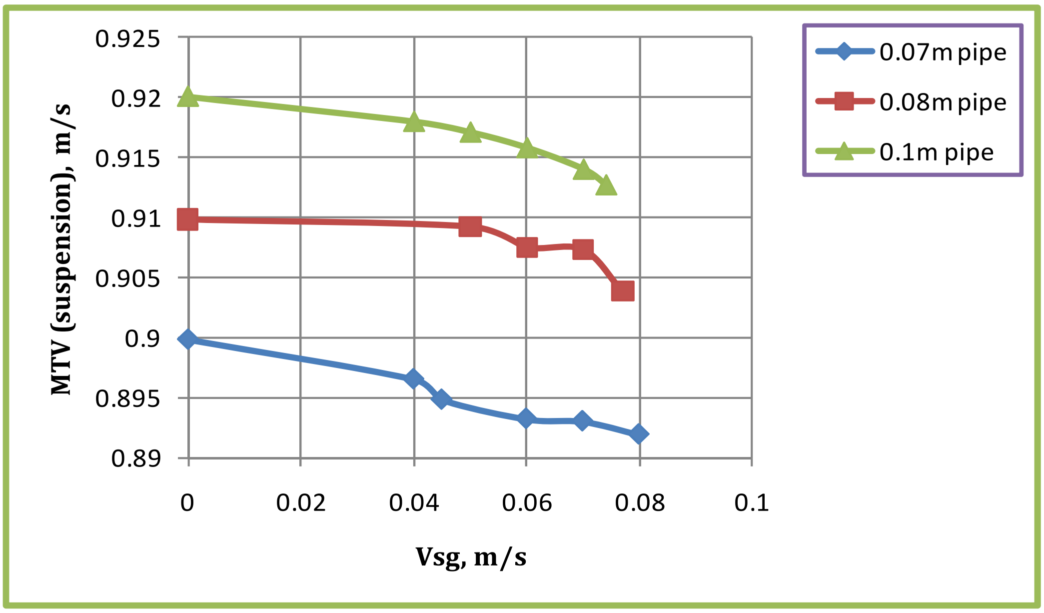

Figure 5.29: Effect of flow patterns on MTV in water-oil-gas-sand flow with 5% oil concentration. The 0.07m & 0.08m pipe sizes are horizontal and 0.1m pipe size inclined at 15^0

5.5.2.4 Effect of pipe angle/inclination on MTV

The effect of angle of inclination on MTV can be shown in Figures 5.30 – 5.32. Generally, the expectation will be that increasing angle of inclination upwardly will require higher MTV. Because increasing the angle of inclination upwardly requires a higher driving force for the solid particles. Coupled with the additional effect of the gravitational force should result in a normally result in high MTV as angle of inclination increases. However, reduction in MTV was observed which in this can be attributed to formation of slug flow. At higher upward inclinations, around 20°-40°, depending on the operational conditions the limit deposit velocity passes through a maximum and then decreases at a moderate rate (Doron, Simkhis and Barnea, 1997).

At various superficial velocities, it was observed that improved sand transport occurred primarily in the slug flow region as a result of upward inclination as can be seen in Figures 5.30 – 5.32. When compared to horizontal pipe, upward pipe inclinations contributed to formation of slug flow patterns for various superficial velocities used in this experiment. As the pipe angle was adjusted to 15^0 & 20^0, there was apparent transition from disperse bubble flow to slug and this pattern is often characterised by lower MTV. Beyond 20^0, minimal changes in MTV for suspension was observed, that is when pipe angle was adjusted to 25^0, as shown in Figures 5.30 – 5.32. This indicated that the change in pipe inclinations affects the flow patterns and consequently the MTV required for sand particle transport. Stevenson (Stevenson et al. 2001) argued that the impact of slug flow on solid particle transport is better appreciated on arrival of the turbulent core of the slug. It was obvious from the experiment that the slug flow played significant role in the transportation of solid particles in pipes caused by change in pipe angles. It was also noted that as the inclination increases, the slug flow transited to elongated bubble flow which resulted in increased MTV and the effect of angle diminished.

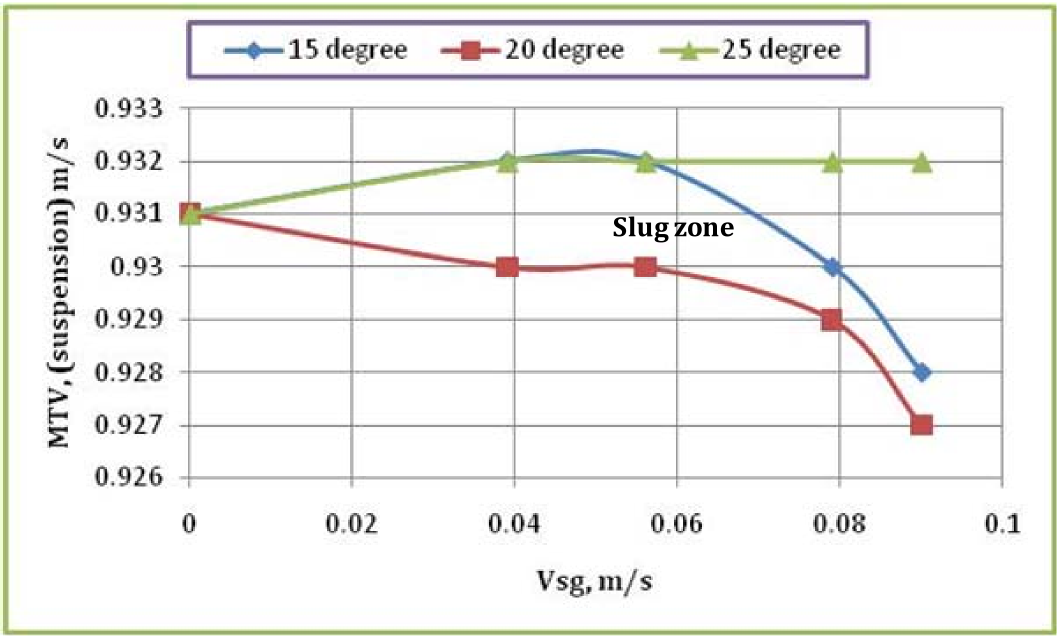

Figure 5.30: Effect of pipe angle and flow patterns on MTV for water-gas-sand flow in 0.1m pipe size.

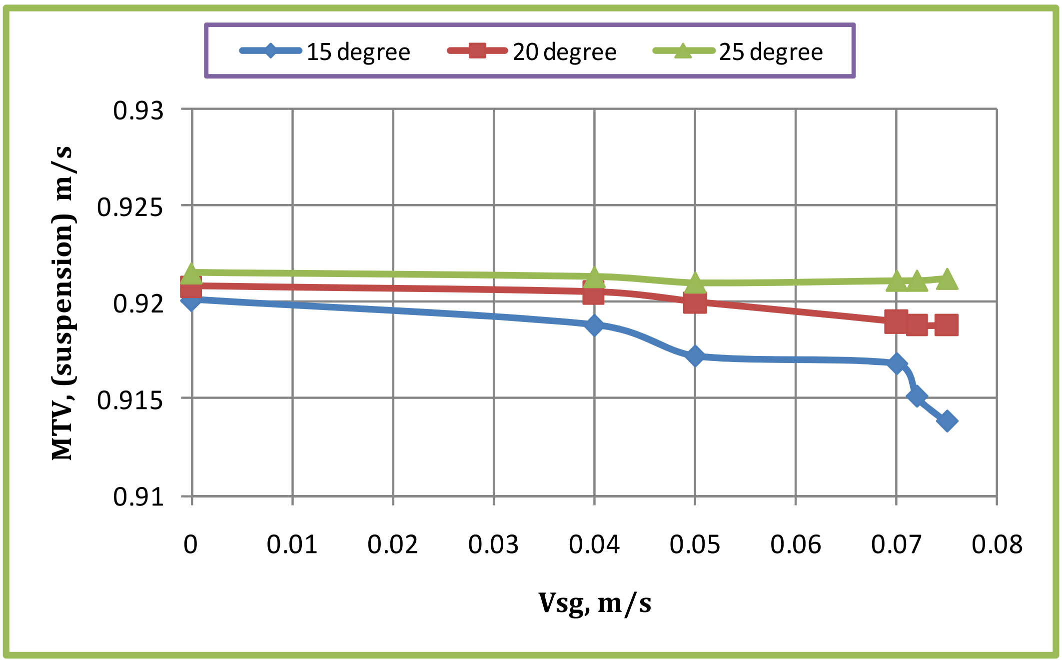

Figure 5.31: Effect of pipe angle and flow patterns on MTV for water-oil-gas-sand flow (10% oil by volume, 0.1m pipe)

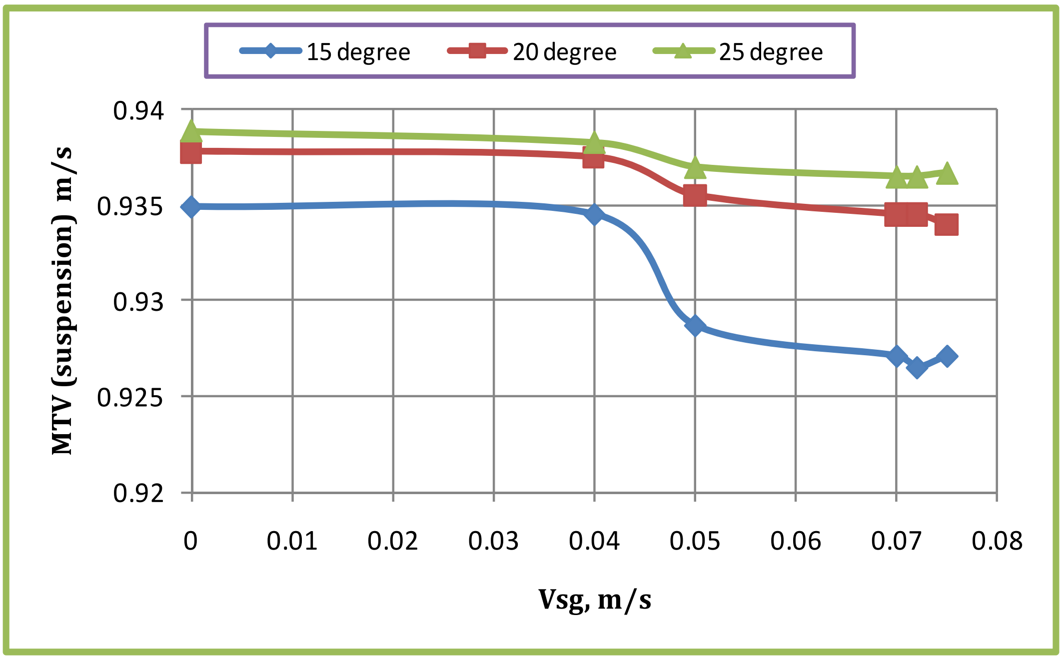

Figure 5.32: Effect of pipe angle and flow patterns on MTV for water-oil-gas-sand flow (5% oil by volume, 0.1m pipe)

5.6 Pressure drop in water-oil-sand flow

The mixture of water-oil-sand for different superficial mixture velocities was carried out. The pressure differential in each case was recorded including different flow patterns in the pipes of different diameters. It was observed that the pressure drop in 0.1 meters pipe inclined at 15^0 was quite high and appeared to be relatively constant from the beginning of slug to fully developed slug flow as shown in Figure 5.33. The sand concentration was maintained at 1.9% by volume of the mixture. The pressure drops were measured at various velocities, initially at suspension velocity where the pipes are free of solid depositions. Transportation of fluids entrained with solids particles in pipes is usually accompanied by increase in pressure drop. The pressure drop increase was as a result of increased frictional losses given the change in the forces on individual solid particles as a result of change in pipe angle.

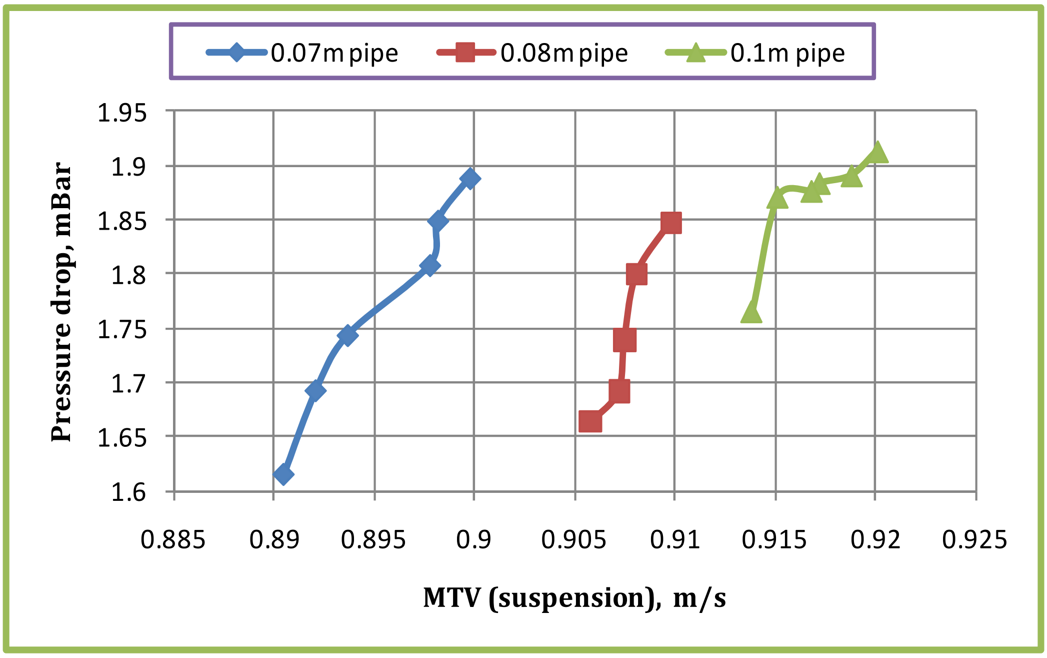

Figure 5.33: MTV suspension and Pressure drops in water-oil-sand flow with 1.9% by volume of sand concentrations

5.7 Summary

The key observations from the experiments carried out were the following

- The minimum transport velocity is greatly influenced by the flow patterns. It was observed that the slug provided better solid carrying capacity in pipes. For large pipe size, especially 0.1 meter pipe, there was tendency for flow patterns transiting directly from disperse bubble flow into slug flow or elongated bubble flow with slight change in flow conditions.
- The MTV required for transporting solid particle either in suspension or rolling is greatly influenced by pipe inclination of up to 20^0 upward and the influence of angle appears to be diminishing beyond that.

- The change in fluid viscosity was found to reduce MTV required to transport solid particle in suspension and rolling. This was apparent when oil was added to water at incremental volume.
- It was found that the solid particle concentration influence deposition either with water flowing or water-oil-gas flow.
- Expectedly, it was found that solid particle suspension is strongly dependent on the intensity of fluid velocity in pipes irrespective of angle of inclination.
- The pressure drop was found to be higher in slug and elongated flow patterns when compared with dispersed bubble flow and stratified flow in that order.

Most importantly, the comprehensive experimental work has provided data base in multiphase sand transport flow in pipeline. This was a valuable measured data which served as input parameters in the development and validation of a new model for minimum transport velocity, MTV. This was quite significant in the development of true and accurate models.

Many of the existing models relied on simulated data for development of sand transport models. These have not worked well because of the inaccuracies experienced with such models. The painstaking efforts required in the acquisition of experimental data may have discouraged a number of researchers in pursuing this method. However, there is never a substitute for measured experimental data if the objective was to develop accurate models.

Though the primary focus of this experimental work was on fluid velocity required for sand transport, but as it has been highlighted in the previous sections the importance of flow patterns in the transport phenomenon cannot be underestimated. As we have seen flow patterns definitions contributed significantly in the sand transport modes in multiphase flow. For water-oil-gas-sand flow given different superficial velocities, it was noted that greater sand particle transport occurred in slug flow pattern. With arrival of slug flow, the sand particle experienced pick-up and drop form of movement from the pipe bottom into the turbulent core of the fluids. The pressure drop observed in this phase was relatively high though with greater sweep of the pipe bottom. In the stratified smooth and stratified wavy flows, most of the sand particles were transported in the liquid phase. But due to low liquid phase velocity, the sand particle tends to settle at the pipe bottom more quickly. However, with stratified wavy flow, the existence of turbulent liquid-gas interface slightly improved the transport capacity of the flowing fluids.

Chapter 6

Drag and lift coefficient models in multiphase flow

6.1: Forces acting on a solid in horizontal, high angle and vertical pipe

Several solids transport models have been proposed in the literature for prediction of solid transport in pipeline. Some of these models have been discussed in chapter 2 and their limitations have been highlighted. It is important to understand the forces influencing different interactions such as fluid-particle, particle-particle and particle-wall and for any pipe orientations.

The major forces acting on a solid particle flowing in any pipe orientations can be shown in Figure 6.1. The dominant forces are lift (C_L), drag (C_D), gravity (F_G) and buoyancy (F_B) forces. The gravity and buoyancy forces referred to as static forces and can be expressed as

$$F_G = \frac{\pi d_p^3}{6} \rho_p g \qquad 6.1$$

$$F_B = \frac{\pi d_p^3}{6} \rho_f g \qquad 6.2$$

The lift and drag forces referred to as hydrodynamic forces and can be expressed as below,

$$F_L = 0.5 C_L \rho_f V^2 A \qquad 6.3$$

$$F_D = 0.5 C_D \rho_f V^2 A \qquad 6.4$$

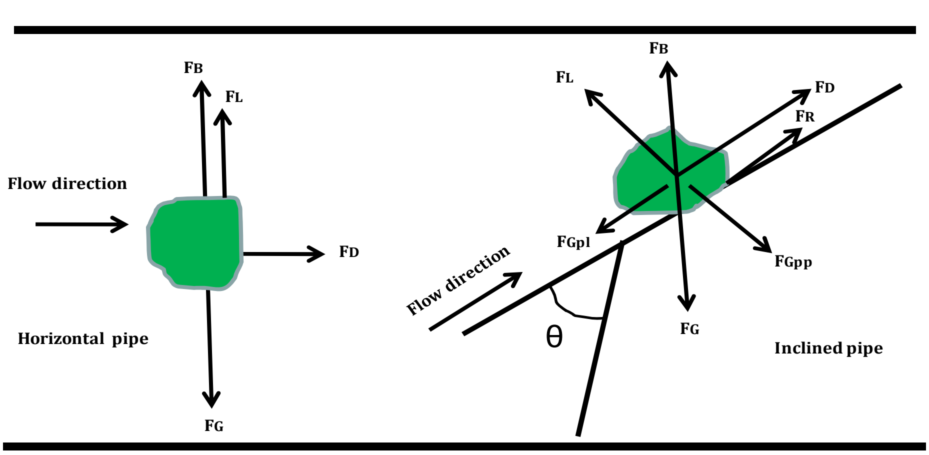

Figure 6.1: Forces acting on a solid particle in horizontal and inclined pipe surfaces

Zhou et al. 2004, stated that moments acting on the particle due to the lift force, drag force and buoyancy force tend to initiate rolling while the moment created by gravity tends to prevent the particle from rolling. To initiate rolling of the particle, the moments of forces (F_B + F_L + F_D) tending to initiate rolling must exceed the moments of the force (F_G) that tend to prevent it. At the same time, the bed particle can also be lifted up if the sum of the forces in the upward direction is greater than the one in downward direction. These can be expressed as

$$F_B + F_L + F_D > F_G \qquad 6.5$$

$$F_B + F_L > F_G - F_D \text{, for rolling} \qquad 6.6$$

$$F_B + F_L > F_G \text{, for suspension} \qquad 6.7$$

Assuming friction forces are zero at the beginning of particle movement.
Obviously, particle rolling occurs at lower flow velocities than suspension as can be seen from Equations 6.7 & 6.8, since F_D is considered to be always greater than zero. Zhou et al. 2004, suggested that Equation 6.6 can be taken as the main criterion for particle movement initiation in horizontal pipe.
In an inclined pipe surface, the forces acting on a particle being transported upward are predominantly lift force (F_L), drag force (F_D), gravity force (F_G) and friction force (F_R) as can be seen in Figure 6.1. Peden et al. 1990 proposed that the gravity force should be resolved into two components, namely:

$$F_{Gpl} = F_G \cos(\theta) \text{, parallel to the pipe axis} \qquad 6.8$$

$$F_{Gpp} = F_G \sin(\theta) \text{, perpendicular to the pipe axis} \qquad 6.9$$

The friction force can therefore be expressed as,

$$F_R = [F_G \sin(\theta) - F_L] f_s \qquad 6.10$$

$$F_R = \lfloor F_{Gpp} - F_L \rfloor \qquad 6.11$$

Where, F_{Gpl} is the resolved gravitational force parallel to pipe axis, FGpp is the resolved gravitational force perpendicular to the pipe axis, f_s is the friction coefficient between the sand particle and the pipe wall.

In general, the forces controlling solid particle movements in multiphase flow in horizontal, high angle or vertical pipes are drag forces, lift forces, friction forces and gravitational forces (Peden, Ford and Oyeneyin, 1990) and (Zastawny, Mallouppas, Zhao and Wachem, 2012). For solid particles to be in suspension and or rolling mode, two conditions must be fulfilled, Peden et al. 1990,

1. The drag force must be greater than gravitational forces, i.e. solid particle in rolling mode.
2. The lift force must be greater than gravitational forces, i.e. solid particle in suspension mode.

The coupled equations for MTV rolling and suspension in horizontal and inclined pipes can be expressed as (Well Engineering Research Group 2007):

For solid particle rolling,

$$V_m = \left[\frac{a * gd_p \left(\frac{\rho_p}{\rho_f} - 1 \right) (\cos\theta + f_s \sin\theta)}{(C_D + f_s C_L)} \right]^b \qquad 6.12$$

Where f_s can be expressed as

$$f_s = \frac{\sin\theta_c^{/}}{\cos\theta_c^{/}} \qquad 6.13$$

$$\theta_c^{/} = 55 * \frac{\pi}{180} \qquad 6.14$$

For solid particle in suspension,

$$V_m = a * \left[\frac{gd_p}{C_L \rho_f} * (\rho_p - \rho_f) \sin\theta \right]^b \left[\frac{D\rho_f}{\mu_l} \right]^c \qquad 6.15$$

Where C_D & C_L are hydraulic drag and lift coefficients determined from deposit velocity and MTV rolling experiments respectively, ρ_P & ρ_f are solid particle density and fluid density, d_P is the particle diameter, a, b & c are empirical constants which was determined from the experimental data.

$$V_m = a * \left[\frac{gd_p(\rho_p - \rho_f)}{C_D \rho_f} \right]^b \tag{6.16}$$

The magnitude of drag and lift coefficients are primarily dictated by the particle Reynolds number (Rep), defined as

$$R_{ep} = \frac{\rho_f V_f d_p}{\mu_f} \tag{6.17}$$

Where,

R_{ep} = particle Reynolds number

V_f = fluid velocity, m/s

d_p = particle diameter, m

μ_f = fluid viscosity, cp

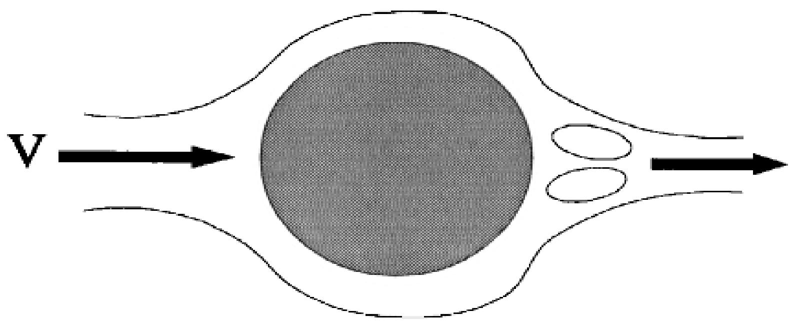

Figure 6.2: Drag on a solid particle.

6.2: Development of drag coefficient (C_D) correlation

The definition of the drag force on a particle in a fluid flow generally involve understanding the relationship between the drag coefficient C_D and particle Reynolds number, Rep. The drag coefficient represents the fraction of the kinetic energy of the settling velocity that is used to overcome the drag force on the particle, while the Reynolds number is a ratio between the inertial and viscous forces of a fluid (Chien 1994). As the particle size or flow velocity increases for a given kinematic viscosity, so does the Reynolds number, and the character of flow changes as expressed in Equation 6.17.

For very small Reynolds numbers, Stokes proposed an analytical solution of drag coefficient by solving the general differential equation of Navier–Stokes.

$$C_D = \frac{24}{\mathrm{Re}} \tag{6.18}$$

An analytical attempt to extend the range of approximation for the drag coefficient beyond Stokes flow has been proposed by some authors by including the inertia terms in the solution of Navier–Stokes as reported by (Almedeij 2008).

$$C_D = \frac{24}{\mathrm{Re}}\left(1 + \frac{3}{36}\mathrm{Re}\right) \tag{6.19}$$

A number of C_D–Re formulas, empirical or semi empirical can be found in the literature, some examples are reported by (Loth 2008) and (Almedeij 2008). Four of the C_D correlations were selected here for comparisons because they were generally considered to be of high accuracy and with wide range of applicability, see Equations 6.20 through to 6.23.

$$C_D = \left[\left(\frac{24}{\mathrm{Re}}\right)\left(1 + \left(0.173\mathrm{Re}^{0.657}\right)\right) + \left(\frac{0.413}{1 + 16300\mathrm{Re}^{-1.09}}\right)\right], \text{(Turton \& Levenspiel, 1986)} \tag{6.20}$$

$$C_D = \left[0.5\left(\frac{24}{\mathrm{Re}}\right)^{1.6} + \left(\left(\frac{130}{\mathrm{Re}}\right)^{0.72}\right)^{2.5} + \left(\left(\left(\frac{40000}{\mathrm{Re}}\right)^{2} + 1\right)^{-0.25}\right)^{0.25}\right], \text{(Swamee and Ojha, 1991)} \tag{6.21}$$

$$C_D = \left[\left(\frac{24}{\mathrm{Re}}\right)(1 + 0.27\,\mathrm{Re})^{0.43} + 0.47\left(1 - \exp\left(-0.04\,\mathrm{Re}^{0.38}\right)\right)\right], \text{(Cheng, 2009)} \tag{6.22}$$

$$C_D = \left[\left(\frac{24}{\mathrm{Re}} \right) \left(1 + \left(0.15\,\mathrm{Re}^{0.687} \right) \right) \right], \text{ (Schiller Naumann, 1933)} \tag{6.23}$$

An experimental determination of the drag coefficient is often based on measurement of the terminal settling velocity of a sand particle in fluid medium. In this case, the data from experiment conducted for particle settling velocity has been used to determine the Rep and C_D. The full data are presented in Appendix F.

The above Equation 6.23 formed the basis for the development of new C_D correlation model. The Schiller Naumann C_D correlation is commonly used as drag correction expression in multiphase flows since many particles are constrained to Reynolds number values in this range. However, it was observed that the main limitation of the model was its limited capability for predicting the laminar flow region. The model was then modified especially to improve on this limitation. This led to the development of a new C_D correlation based on the experimental data for multiphase, water-oil-gas flow. The development of the new C_D correlation that is a function of Reynolds number was based on fitting the experimental data to the base equation using MS-Excel goal-seek program. The generic form of the equation was described as:

$$C_D = \left[\left(\frac{24}{\mathrm{Re}} \right) \left(1 + \left(0.15\,\mathrm{Re}^{0.687} \right) \right) + \left(\frac{a}{\left(b + c\,\mathrm{Re}^{d} \right)} \right) \right] \tag{6.24}$$

Where Re is the particle Reynolds number and a, b, c and d are constants dependent on experimental data. Solving for these unknowns, the equation that best fits the experimental data was determined and can be expressed as:

$$C_D = \left[\left(\frac{24}{\mathrm{Re}} \right) \left(1 + \left(0.15\,\mathrm{Re}^{0.687} \right) \right) + \left(\frac{3.5}{\left(1 + 42500\,\mathrm{Re}^{-1.17} \right)} \right) \right] \tag{6.25}$$

The experimental data was divided into three parts; one part was used mainly for model development, the second sets of data were used for model testing and the third sets of data were dedicated to model validation. In total, seven different glass bead samples were used during the experiments. The predictions with the model match the measurements quite well.

Only a minor deviation was observed as can be seen in Figure 6.3 with oil-gas experiment. The RSQ correlation coefficient was 79%.

The developed C_D model was an improvement on Schiller Naumann model as shown in Figure 6.4. It incorporated an extended Stokes law and the deviations from the Newton's law. This can be applied to both the turbulent and laminar flow regions and reasonably predict C_D over a wide range of Reynolds number in multiphase fluid flow.

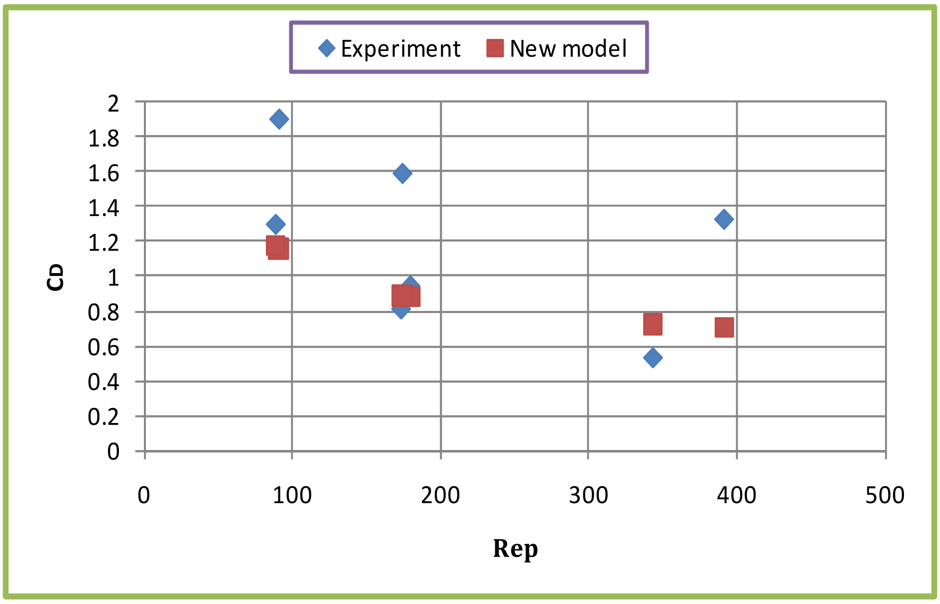

Figure 6.3: C_D **- Rep for two phase oil-gas flow**

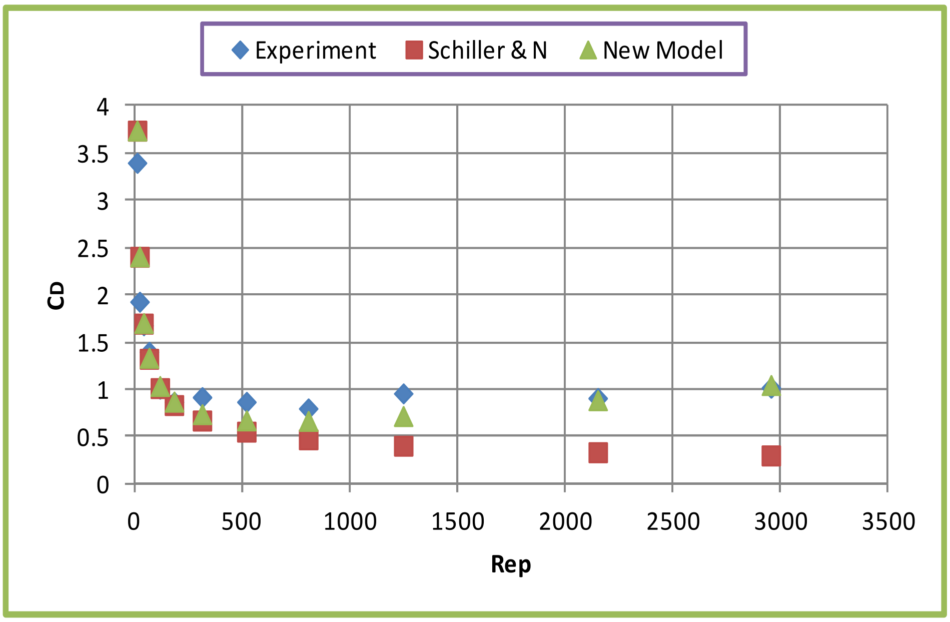

Figure 6.4: C_D **- Rep for single phase water showing improved correlation with new model**

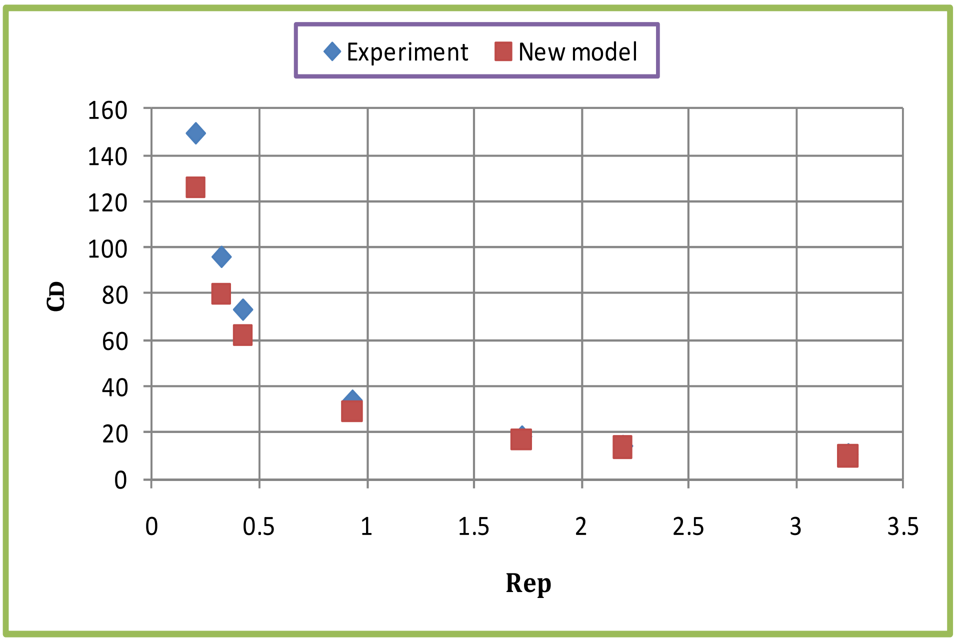

Figure 6.5: CD-Rep for two phase oil-water flow

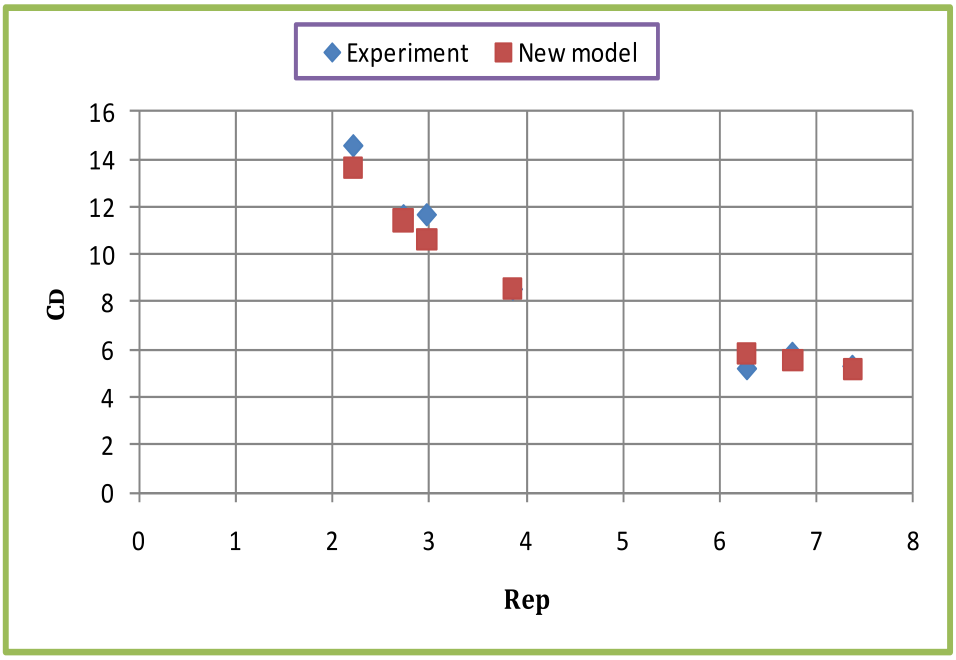

Figure 6.6: CD-Rep for three phase oil-water-gas flow

6.2.1 Drag coefficient (C_D) Model testing, validation and comparison

In order to establish the reliability and accuracy of the model, it was tested with other sets of data. The results for two-phase oil-water flow and three-phase oil-water-gas flow are as presented in Figures 6.5 & 6.6. The new drag coefficient model performed well with the experimental data given high RSQ correlation coefficient which was 98% & 99% respectively. When the viscosity is relatively high, such as in single phase oil flow, the regime is usually laminar and the Reynolds number tends to be very small as can be seen in Figure 6.7. The particle in this case experiences a higher drag coefficient and low particle settling rate. The flowing fluid properties around the solid particle are an important factor in determining the drag coefficient (Almedeij 2008). The RSQ correlation coefficient was 99%.

Independent C_D - Re data (Hottovy and Syvester 1979) from literature was used to validate the model, shown in Figure 6.8. There was excellent agreement between the experimental data and model prediction including published data. The RSQ correlation coefficient was 97%.

The new model was equally compared with the selected drag coefficient from the literature, see Figure 6.9. It shows better correlation with the experimental data. In general, comparison of the experimental results and that of the C_D model predictions are found to be largely in agreement as can be seen in Figures 6.5 – 6.9 and Figures 6.10 – 6.12 with Table 6.1 showing the statistical parameter between the two measured drag coefficient and drag coefficient predicted with the new model.

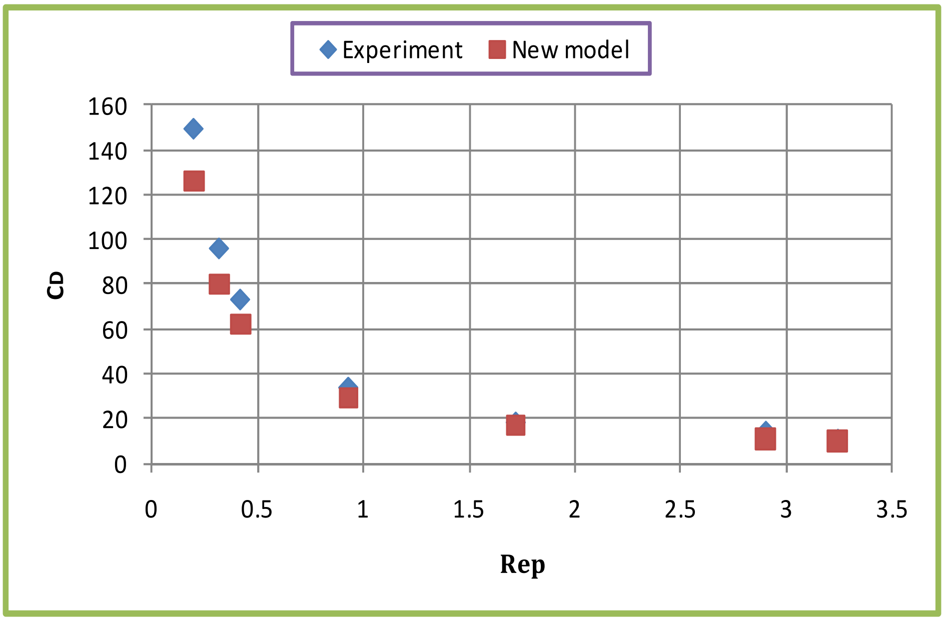

Figure 6.7: C_D - Rep for single phase oil flow

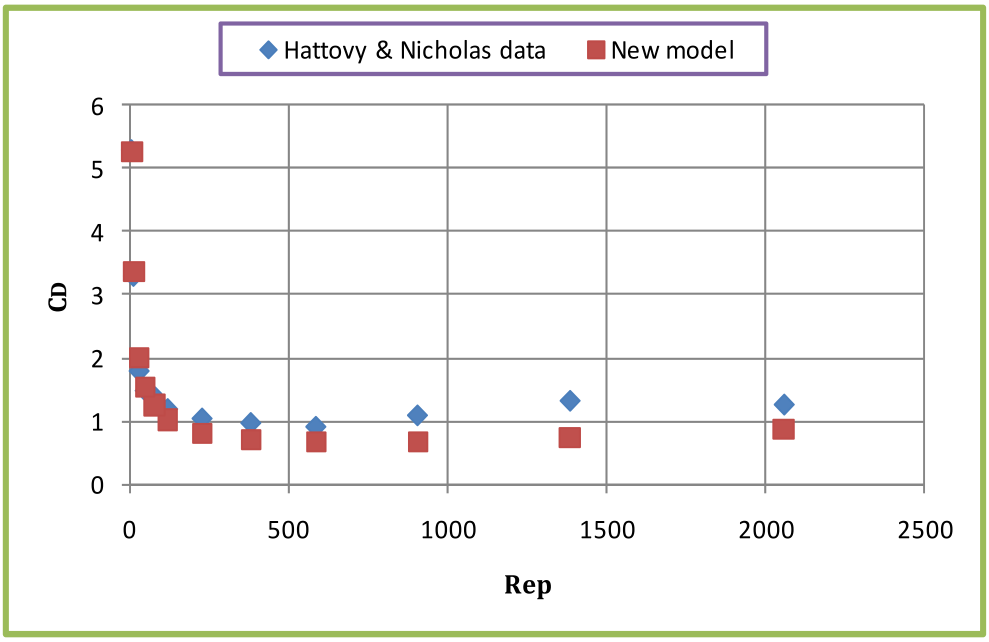

Figure 6.8: New C_D model prediction with literature data

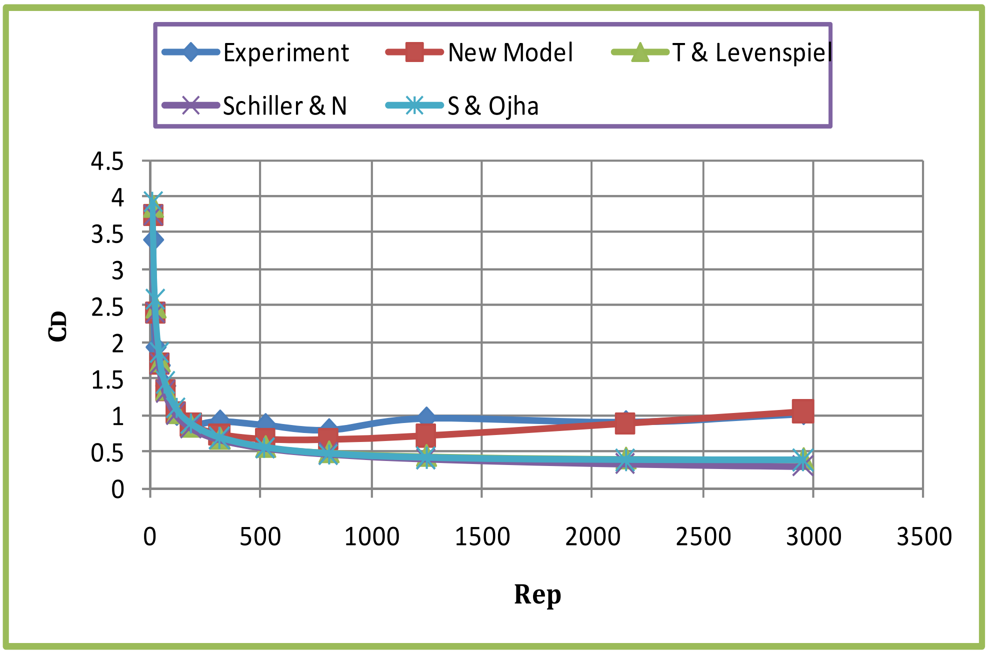

Figure 6.9: New C_D model compared with selected models from literature

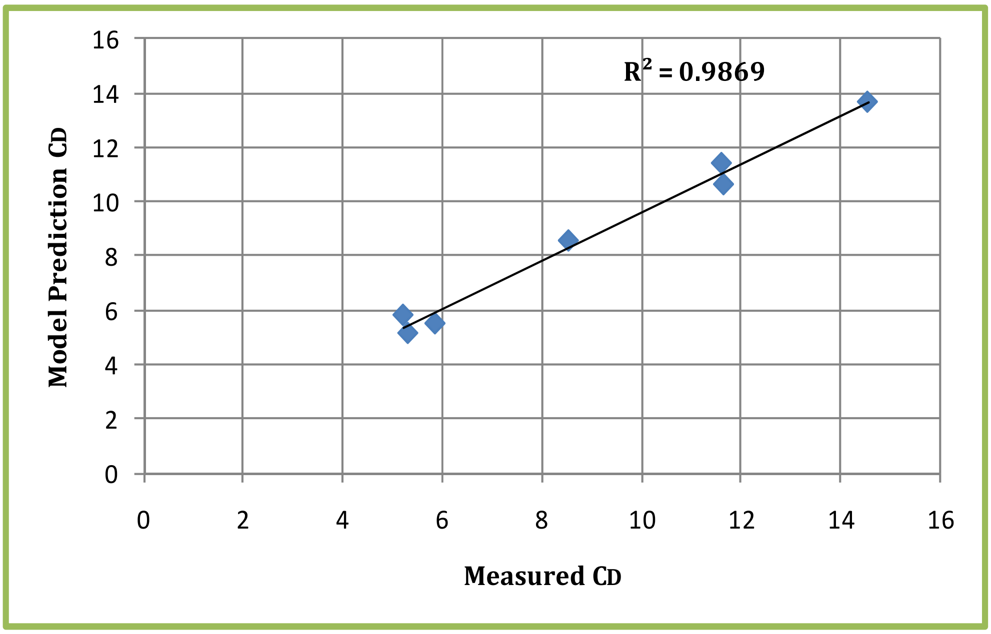

Figure 6.10: Comparison of measured and model prediction C_D for water-oil-air flow

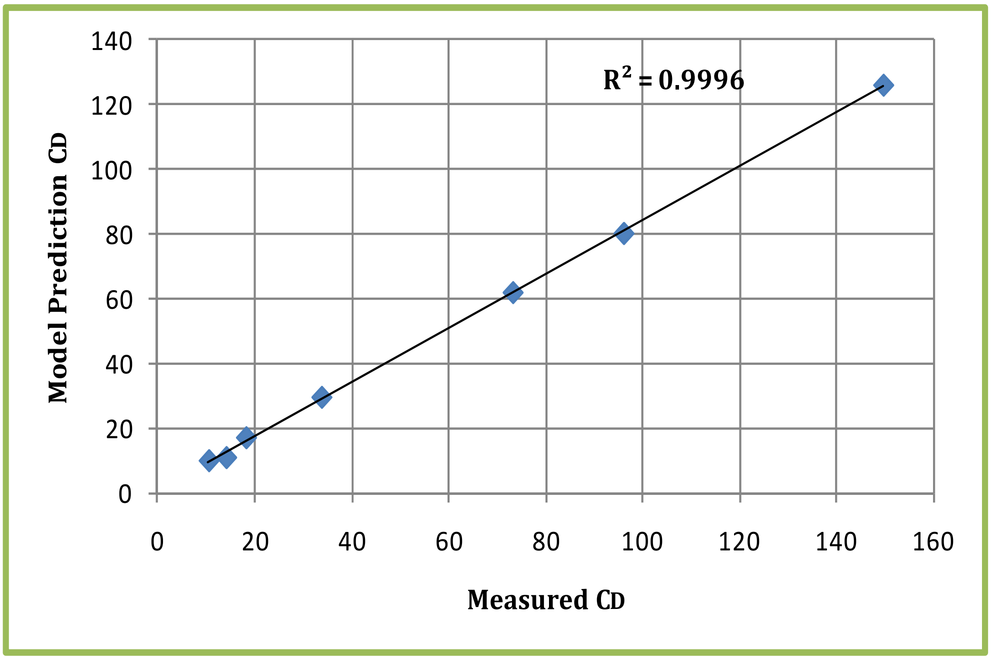

Figure 6.11: Comparison of measured and model prediction C_D for single-phase oil flow

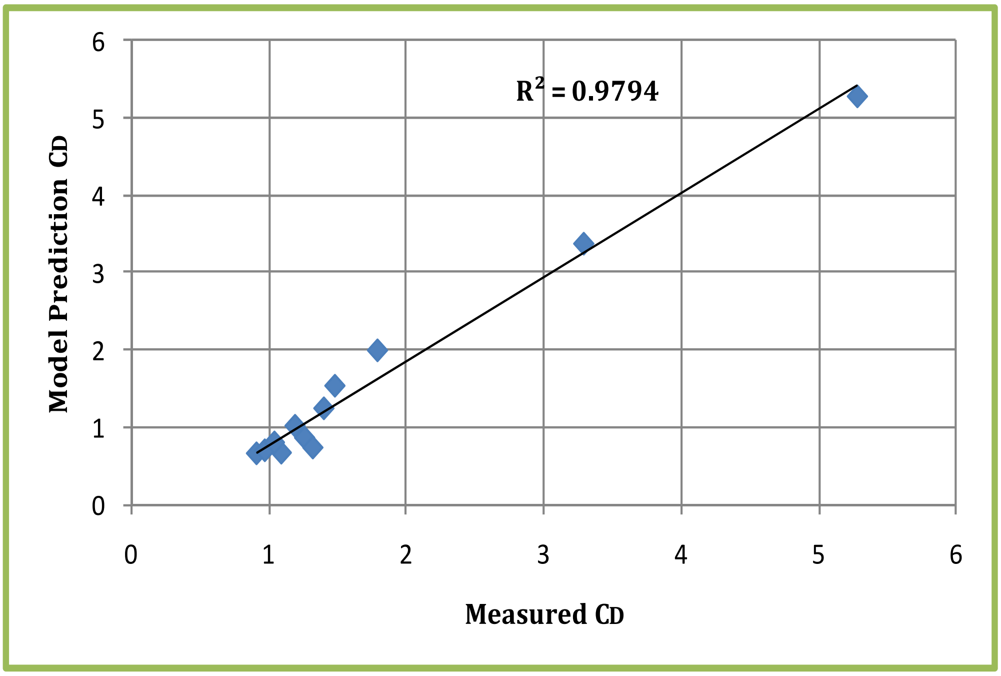

Figure 6.12: Comparison of measured and model prediction C_D for single-phase water flow

Table 6.1: Statistical Parameters for the Drag Coefficient Model

	Drag Coefficient Model Predictions			
Error margin	**Single-phase oil**	**Single-phase water**	**Two-phase oil-water**	**Three-phase water-oil-air**
Average percent error (APE)	13.81	16.30	10.86	1.71
R-Square value (R^2)	0.9996	0.9794	0.9996	0.9869

6.3 Development of lift coefficient (C_L) correlation

Lift force acts in the direction perpendicular to the fluid velocity characterised by lift coefficient, defined previously as:

$$F_L = 0.5 C_L \rho_f V^2 A \qquad 6.3$$

Where F_L is lift force, C_L is lift coefficient, ρ_f is the fluid density, A is the projected area of the particle and V is the fluid velocity relative to the particle.

The rolling or saltating motion of particles on a surface of pipe wall when in contact with flow occurs in multiphase fluids transport situations. In order to describe the particle motion in these situations it is important to accurately know the hydrodynamic forces exerted on the particle by the surrounding fluid. The particle motion will then be dictated by a balance between the hydrodynamic forces, gravitational effect, contact friction with the wall and other influences such as electrostatic forces.

The hydrodynamic lift force is based on Bernoulli's Principle, which relates the total fluid pressure on a body to the sum of static and dynamic pressure. The Lift is the sum of two component forces of pressure and wall shear in the direction normal to the flowing fluid tending to move the body in its direction. The hydrodynamic forces experienced by a solid particle in a pipe govern the particle movement in multiphase flow. Here, the lift coefficient was defined as the minimum lift force required initiating the hydraulic movement of solid particle at rest.

In an attempt to develop a representative model for the lift coefficient, it was observed that compared to the drag force, significantly few research work has been done to predict the lift force exerted on a particle by the fluid motion (Zastawny, Mallouppas, Zhao and Wachem, 2012). One was proposed by (Bagchi and Balachandar 2002) to estimate lift coefficient in turbulent and laminar flow and can be expressed as,

$$C_L = 0.375\left(\frac{24}{R_{ep}}\right)\left(1 + 0.597 R_{ep}^{0.593}\right) \qquad 6.26$$

Clearly, both the lift and drag coefficients exhibit strong dependence on the flow velocity and particle Reynolds number.

$$C_L = \frac{a}{\left(R_{ep}^{b} + c\right)^{d}} \qquad 6.27$$

Where constants a, b, c & d are constants derived from experimental data.

In developing C_L correlation, the data from experiment conducted for particle minimum transport velocity in rolling/saltation mode was used to determine the particle Reynolds number, R_{ep} and lift coefficient, C_L. Though this method was not error proof but measures were taken to prevent sudden turbulent disturbances arising from fluid velocity. The full data are presented in Appendix B.

Similarly, the C_L model was developed by obtaining constants a, b, c & d in Equation 6.27 using the data from multiphase experiment for water-oil-sand flow in pipe. The constants for

the new C_L correlation were obtained as a function of Reynolds number by fitting the experimental data to the base equation using MS-Excel goal-seek program.
Solving for these empirical constants, the equation that best fits the experimental data was determined and can be expressed as:

$$C_L = \frac{2.975}{\left(R_{ep}^2 + 1.2\right)^{0.165}} \qquad 6.28$$

The predictions with the model match the measurements quite well. Only a minor deviation was observed as can be seen in Figure 6.13 with water-oil experiment. The RSQ correlation coefficient was 98%. Though this was a laminar flow scenario but can reasonably predict C_L over a wide range of Rep in multiphase fluid flow.

6.3.1 Lift coefficient (C_L) Model testing, validation and comparison

The reliability and accuracy of the model was tested with (Feng and Michaelide 2002) data. The result presented in Figure 6.14 showed a close match except for very low Reynolds number. The RSQ correlation coefficient was 70%.

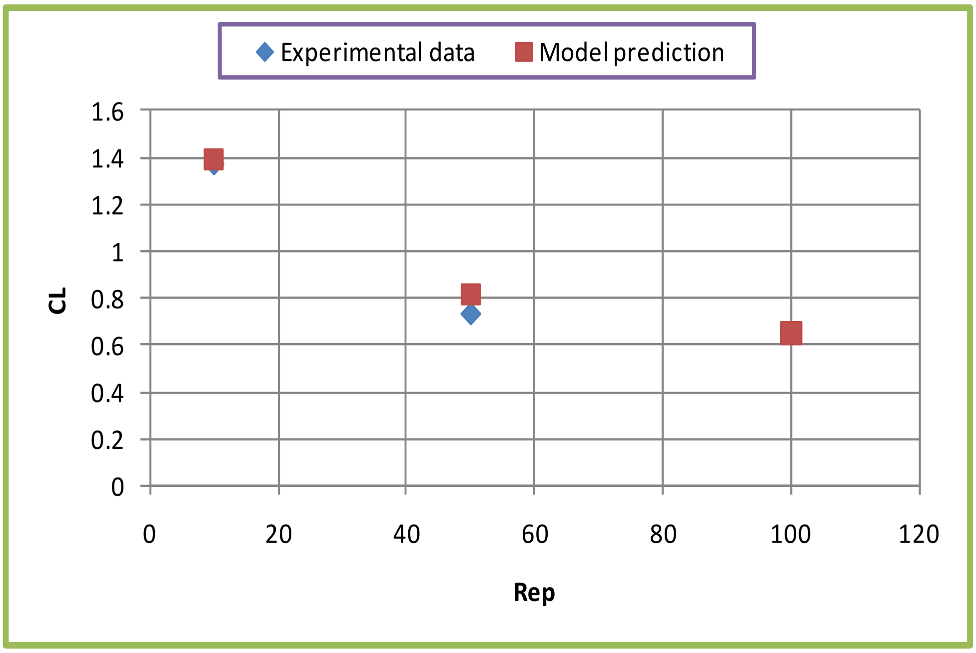

Figure 6.13: C_L - Rep for two phase water-oil flow

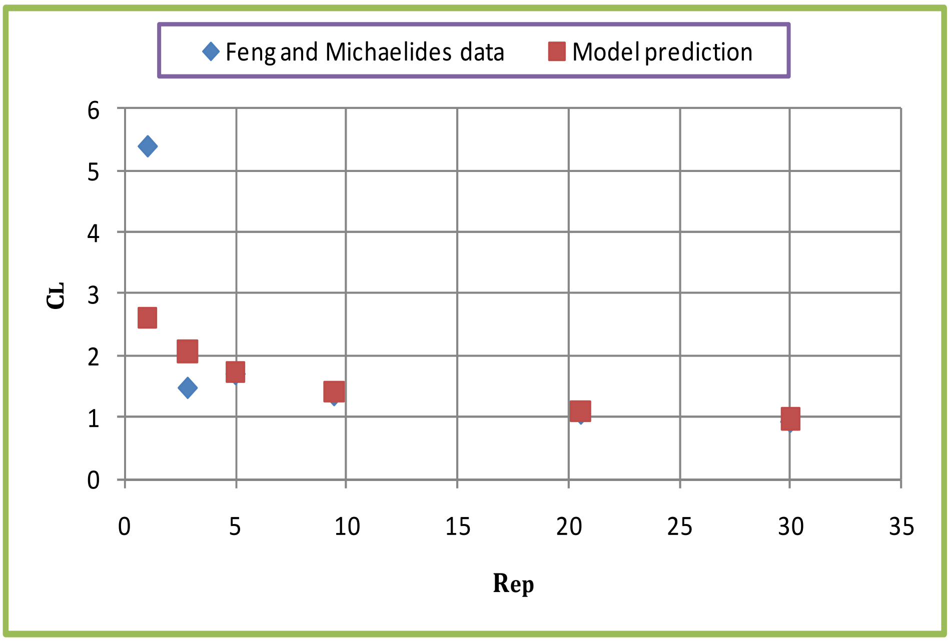

Figure 6.14: C_L **- Rep using** (Feng and Michaelide 2002)

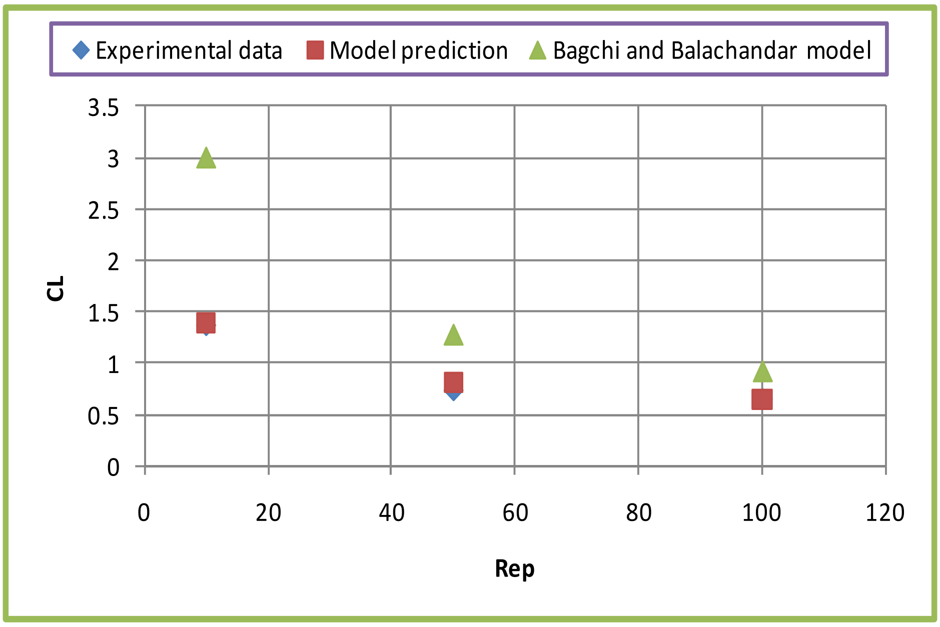

Figure 6.15: Comparison of new C_L **model with that of** (Bagchi and Balachandar 2002)

The new model was compared with (Bagchi and Balachandar 2002) lift coefficient model as shown in Figure 6.15.

6.4: Summary

The predictions with the proposed drag and lift coefficient correlations gave the best representation of the multiphase experimental data and data obtained from the literatures. These models accounts for the changing flow patterns in multiphase flow (water-oil-gas) while the existing drag and lift coefficients models were based on single phase or at best two-phase, water-gas flow which was found to be inadequate for multiphase prediction as it has been shown previously. The methods adopted were responsible for the improvement recorded with the MTV prediction for sand transport models in multiphase flow.

Chapter 7

Sand Minimum Transport Velocity Models in Multiphase

7.1 Introduction

The solid transport mechanism in multiphase flow in pipelines is dependent on several parameters of which the most important are the carrier flow velocity and solid particle size. These two parameters also determine the flow regime which exists when transportation of solid particles takes place. The key objective however is to keep the solid particles in suspension and/or rolling along the bottom of the pipe to prevent sand bed formation. In transporting unprocessed oil and gas reservoir fluids, it is important to avoid the solids entrained in the body of multiphase fluids to settle. This can be done by keeping the multiphase reservoir fluid velocity in the pipe lines above certain levels referred to as minimum transport velocity (MTV) in this case. The MTV depend primarily on the type and size of the entrained solid. If solids settle, the area of the pipe available to flow will be reduced and the fluid velocity may tend to increase initially until such a stage where settled solids completely block the flow part.

There are systems of governing equations that have been developed for solid transport velocity based upon behaviour of water-sand and water-oil-gas-sand multiphase flow in pipes. The mathematical model involves balance equations deduced from mass and momentum conservation laws, constitutive models and forces due to drag force, gravitation force, buoyancy force, friction force, particle-liquid turbulent interaction force, particle-particle interaction force and particle-pipe wall interaction force.

In addition to the conservation laws for mass, energy and momentum, there are additional laws that govern the rate at which these quantities are transported from one region to another in a continuous medium (Darby 2001). These are called phenomenological laws because they are based upon observable phenomena and logic but they cannot be derived from more fundamental principles. These rate or transport models can be written for all conserved quantities (mass, energy, momentum, electric charge, etc.) and can be expressed in the general form as (Darby 2001)

$$\text{Rate of transport} = \text{Driving force} / \text{Resistance} \qquad 7.1$$

The ability to predict the behaviour of solid-liquid-gas flows is vital for the successful design and determination of optimum operating conditions of the production pipelines. The dynamics of these types of systems can be investigated through experiments or through numerical simulations. The experimental method coupled with numerical method was adopted in this research for the formulation of appropriate MTV models for suspension and rolling in pipeline/tieback.

Generally, whenever there is relative motion between solid particle and a flowing fluid, the solid particle will experience drag and lift forces from the surrounding fluid. Accurate predictions of these forces are crucial to MTV models and served as input parameters.

7.2 Concept of minimum transport velocity (MTV)

The sand particle transport driving forces are somewhat complicated in a transient multiphase flow environment. Multiphase fluid flow in pipeline/tieback is a transient phenomenon. The flow of multiphase oil and gas production in the long tieback is accompanied by pressure drop with the multiphase pattern generally changing as a result, from dispersed bubble through to slug, plug, annular and stratified flow patterns depending on liquid-liquid-gas flow velocities, pipe angle among other factors. Solids entrainment is subjected to different driving forces given different flow patterns as they are transported through the pipeline. For practical purposes and to simplify the complex phenomena, the concept of Minimum Transport Velocity (MTV) mechanism has been adopted. The underlying principle of the MTV concept is that solids in subsea tiebacks/pipelines will be transported as long as they are upwardly mobile whether by rolling/sliding along the low side wall of a pipeline or in heterogeneous suspension. The concept assumes that the fluid point velocity acting on a solid particle on the low side wall of the pipe needs to be greater than the minimum transport velocity for the solid particle to be upwardly mobile (Peden, Ford and Oyeneyin, 1990), (Larsen, Pilehvari and Azar 1997) and (Bello, Oyeneyin and Oluyemi, 2011). Thus for average fluid velocity below the MTV for rolling, stationery bed will result. When the velocity is below the MTV for suspension, will result in solids sliding along the pipe wall which may result in stationary bed as the pressure drops along the pipeline causing further reduction in the particle drag forces. However, the key issue here was to integrate the velocity profile models for different flow patterns in the overall development of the solid transport models. This formed the basis for MTV predictive models for suspension and rolling. The velocity profiles models developed for different flow patterns have been discussed in chapter 3 of this thesis.

7.3 Development of MTV models

The primary objective was to determine the minimum transport velocity for sand particle movement in multiphase fluid either in suspension or rolling using a semi-empirical method. Equations 6.12 & 6.15 for rolling and suspension respectively and Equation 6.16 for

suspension in a vertical were successfully fitted to the experimental data to obtain the empirical constants a, b & c in all the models. This involved using hybrid models which combined empirical and analytical solutions. This is commonly used where model is not only based on analytical principle or derived from first principle. The model relates to physical properties, but the value of that property is determined by fitting it as a parameter to experimental data (Bian, S. and Henson, M.A. 2006). The use of a base analytical model coupled with physical parameters obtained experimentally was adopted.
The frames of the hybrid models as presented earlier are,

For rolling,

$$V_m = \left[\frac{a * gd_p \left(\frac{\rho_p}{\rho_f} - 1 \right)(\cos\theta + f_s \sin\theta)}{(C_D + f_s C_L)} \right]^b \tag{6.12}$$

For suspension,

$$V_m = a * \left[\frac{gd_p}{C_L \rho_f} * (\rho_p - \rho_f) \sin\theta \right]^b \left[\frac{D\rho_f}{\mu_l} \right]^c \tag{6.15}$$

For suspension in vertical pipe,

$$V_m = a * \left[\frac{gd_p (\rho_p - \rho_f)}{C_D \rho_f} \right]^b \tag{6.16}$$

The key parameters in Equations 6.12, 6.15 & 6.16 are the particle drag, C_D and lift C_L coefficients which can be determined from Equations 6.25 & 6.28 respectively previously developed. The experimental data for MTV suspension and rolling were presented and discussed earlier.
In the development of MTV for suspension and rolling, the adoption of velocity profile estimates for key flow patterns coupled with semi empirical model was used. These involved iterative procedures and computer codes were developed. The visual basic (VB) code was written into excel and presented in appendix D. The MTV predictions are presented in Figures 7.1 to 7.9. The results presented here illustrated the minimum transport velocity required for solid transport in suspension or rolling for multiphase in tieback/pipeline. Table

7.1 presents the parameters used as input data into the proposed MTV models for suspension and rolling.

7.3.1 MTV Calculation Procedures

The schematic of the calculation module is provided in Appendix D and the input parameters are as shown in Table 7.1. The calculation procedure is given below:

1. Specify input parameters such as mixture flow rates, particle properties and fluid properties.

2. Determine the liquid holdup and flow patterns from equations 2.2 – 2.6 & 2.7 – 2.10 ((Beggs and Brill 1973).

3. Calculate velocity profiles for prevailing flow pattern from equations 3.18 – 3.20 and 3.36 & 3.38.

4. Assume a value for average flow velocity.

5. Determine particle Reynolds number Re, drag & lift coefficients C_D, C_L from equations 6.25 & 6.28 respectively.

6. Calculate particle point velocity in suspension & or in rolling mode either for horizontal pipe or vertical pipe from equation 6.12, 6.15 & 6.16.

7. Carry out iterative trial and error calculations starting from step 4 until absolute value of particle point velocity and the assumed average flow velocity is less than 0.001.

8. Determine the minimum transport velocity.

7.3.2: Summary of equations

1. $\lambda_L = \dfrac{q_L}{q_L + q_G}$ (equation 2.2)

2. $L_1 = 316\lambda_L^{0.302}$ (equation 2.3)

3. $L_2 = 0.0009252\lambda_L^{-2.4684}$ (equation 2.4)

4. $L_3 = 0.10\lambda_L^{-1.4516}$ (equation 2.5)

5. $L_4 = 0.50\lambda_L^{-6.738}$ (equation 2.6)

6. $\lambda_L < 0.01 \,\&\, N_{Fr} < L_1$ OR $\lambda_L \geq 0.01 \,\&\, N_{Fr} < L_2$ (equation 2.7)

7. $0.01 \leq \lambda_L < 0.4 \,\&\, L_3 < N_{Fr} \leq L_1$ OR $\lambda_L \geq 0.4 \,\&\, L_3 < N_{Fr} \leq L_4$ (equation 2.8)

8. $\lambda_L < 0.4 \,\&\, N_{Fr} \geq L_1$ OR $\lambda_L \geq 0.4 \,\&\, N_{Fr} \phi L_4$ (equation 2.9)

9. $\lambda_L \geq 0.01 \,\&\, L_2 < N_{Fr} \leq L_3$ (equation 2.10)

10. $V_r = 1.863 * f * R_e^{0.4} * V_m \left[1 - \left(\frac{r}{R}\right)^2\right]^{0.11}$ (equation 3.18)

11. $V_r = 3.7 * f * R_e^{0.366} * V_m \left[1 - \left(\frac{r}{R}\right)^2\right]^{0.15}$ (equation 3.19)

12. $V_r = 3.3 * f * R_e^{0.347} * V_m \left[1 - \left(\frac{r}{R}\right)^2\right]^{1.11}$ (equation 3.20)

13. $V_{rl} = U_{SL} \left[1 - \left(\frac{r}{R}\right)^2\right]^{0.32}$ (equation 3.25)

14. $V_{rg} = U_{SG} \left[1 - \left(\frac{r}{R}\right)^2\right]^{0.7}$ (equation 3.27)

15. $C_D = \left[\left(\frac{24}{\mathrm{Re}}\right)\left(1 + \left(0.15\,\mathrm{Re}^{0.687}\right)\right) + \left(\frac{3.5}{\left(1 + 42500\,\mathrm{Re}^{-1.17}\right)}\right)\right]$ (equation 6.25)

16. $C_L = \dfrac{2.975}{\left(R_{ep}^2 + 1.2\right)^{0.165}}$ (equation 6.28)

17. $V_m = \left[\dfrac{a * gd_p\left(\dfrac{\rho_p}{\rho_f} - 1\right)(\cos\theta + f_s \sin\theta)}{(C_D + f_s C_L)}\right]^b$ (equation 6.12)

18. $V_m = a * \left[\dfrac{gd_p}{C_L \rho_f} * \left(\rho_p - \rho_f\right)\sin\theta\right]^b \left[\dfrac{D\rho_f}{\mu_l}\right]^c$ (equation 6.15)

19. $V_m = a * \left[\dfrac{gd_p\left(\rho_p - \rho_f\right)}{C_D \rho_f}\right]^b$ (equation 6.16)

Table 7.1: Computational data for the model predictions

S/N	Variables	Value
1	Maximum liquid flow rate, m^3/s	0.008333333
2	Maximum gas rate, m^3/s	0.01
3	Pipe diameters, m	0.07, 0.08 & 0.1
4	Oil density, kg/m^3	940
5	Oil viscosity, Pa.s	0.001001
6	Angle of inclination, degrees	15, 20, 25
7	Sand particle density, kg/m^3	2150
8	Sand particle size, m	0.00027, 0.0003
9	Sand grain size distribution, %	20% coarse, 70% medium and 10% fine
10	Coarse grain size, m	0.00035
11	Medium grain size, m	0.00027
12	Fine grain size, m	0.0002

7.3.3 Model validation and comparison

Several correlations have been advanced to predict sand settling conditions. In this study, semi-empirical models to determine minimum transport velocity (MTV) for suspension and rolling both in horizontal and inclined pipe sections under different flow conditions have been developed. The development, testing and validation of the proposed models required acquisition of reliable experimental data. A multiphase flow loop was designed and constructed for this purpose as discussed in chapter 4. The acquired data for sand particle transport in multiphase fluids are presented in appendix E.

Figures 7.1 through 7.7 give the results of the comparison between the proposed model prediction and measured experimental data of sand particles velocity in three-phase / four-phase pipe flow systems. The measured experimental data and predicted MTV results using velocity profile concept show good agreement. The margin of errors recorded between the MTV predicted and measured results was 12% maximum both in horizontal and inclined pipe sections. The agreement between the prediction and experimental data was due to the fact that the proposed model was based on the fundamental principle underlying physics guiding the behaviour of the particle-particle and fluid-fluid interaction in the three-phase flow and therefore it is more reliable under any operating system.

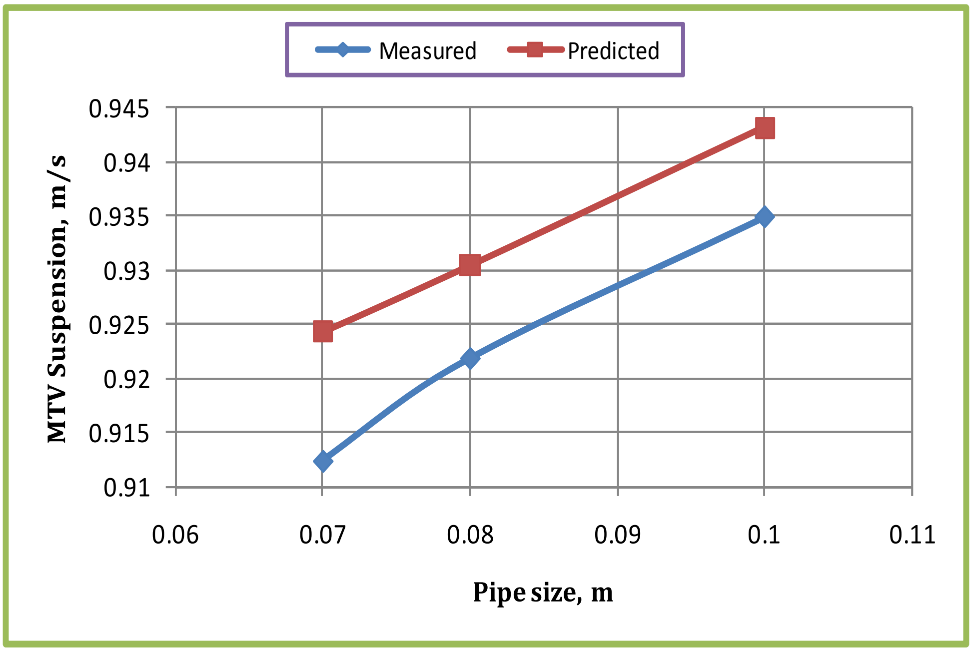

Figure 7.1: Comparison of measured & predicted MTV suspension in slug flow. ρ_S **= 2150 kg/m³,** ρ_M **= 930kg/m³, dp= 270μm, Cs=2.05%.**

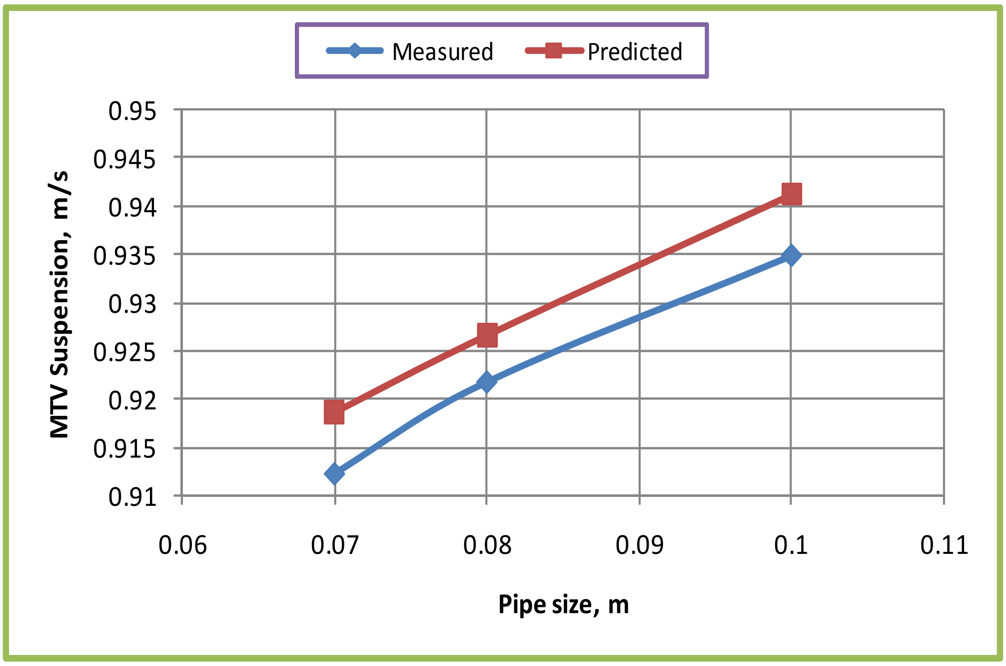

Figure 7.2: Comparison of measured & predicted MTV suspension in dispersed bubble flow. ρ_S = 2150 kg/m^3, ρ_M = 930kg/m^3, dp= 270μm, Cs=2.05%.

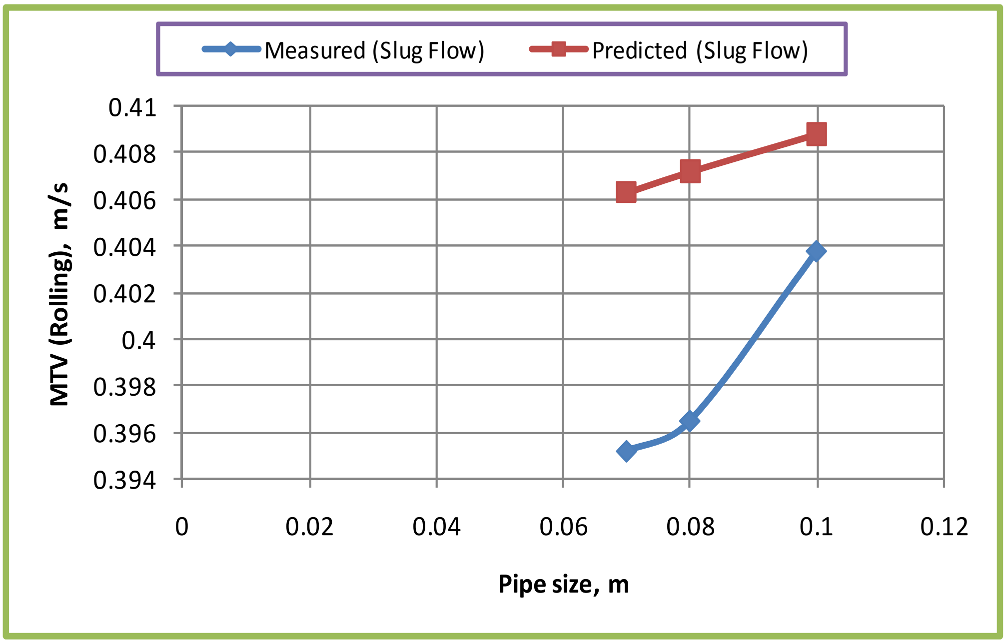

Figure 7.3: Comparison of measured & predicted MTV rolling in slug flow. ρ_S = 2150 kg/m^3, ρ_M = 930kg/m^3, dp= 270μm.

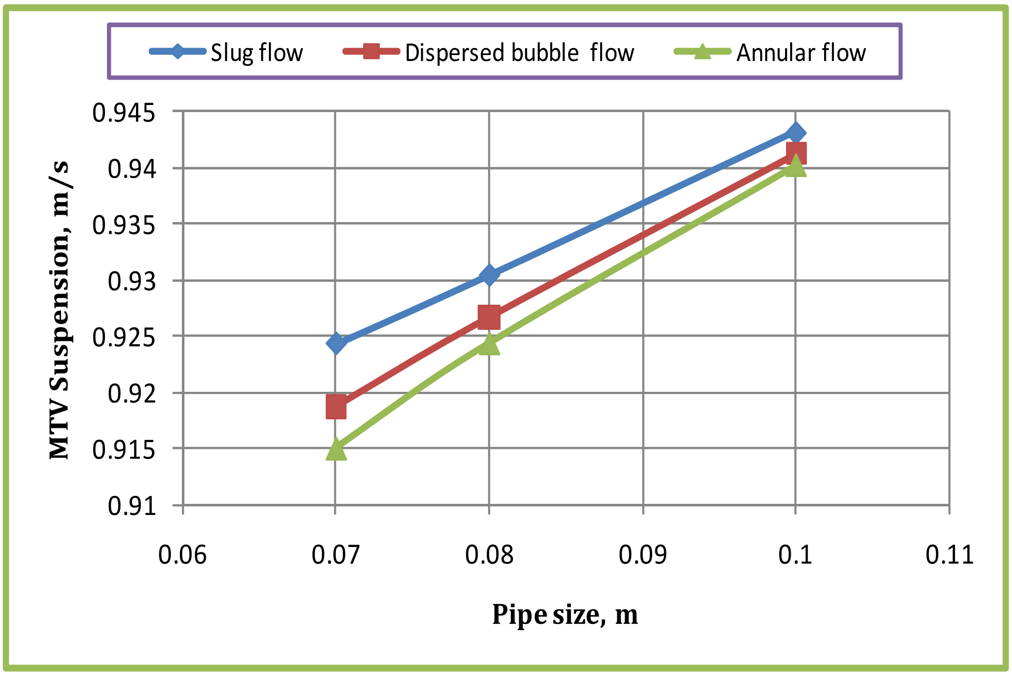

Figure 7.4: Comparison of MTV Suspension for Slug, Dispersed Bubble & Annular flow. ρ_S = 2150 kg/m³, ρ_M = 930kg/m³, dp= 270μm, Cs=2.05%.

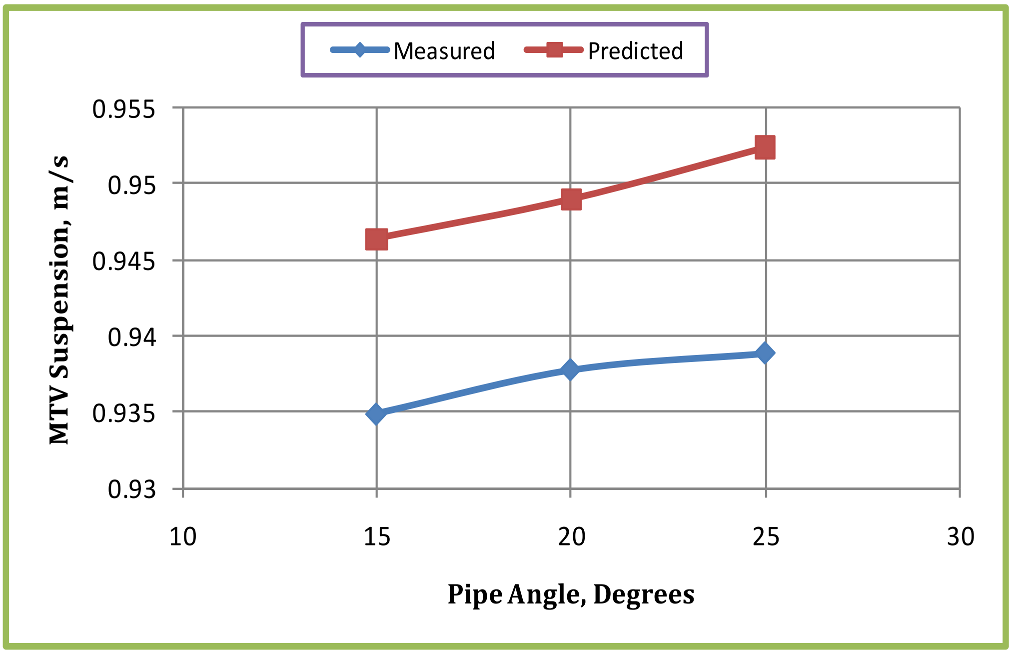

Figure 7.5: Comparison of measured and predicted MTV Suspension in Slug flow. ρ_S = 2150 kg/m³, ρ_M = 930kg/m³, dp= 270μm, Cs=2.05%.

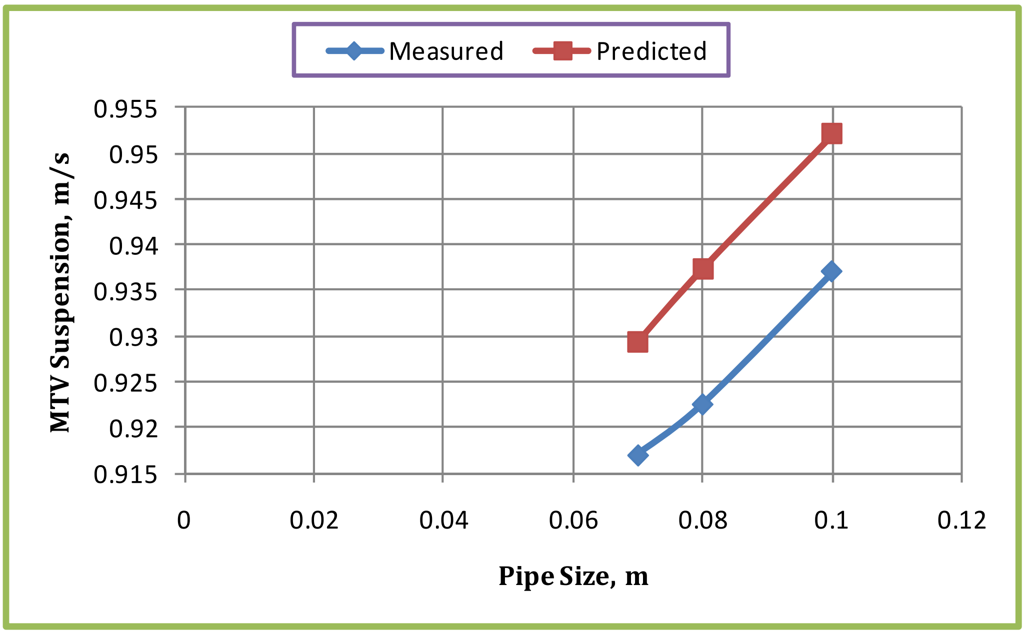

Figure 7.6: Comparison of measured and predicted MTV Suspension in water-sand flow. ρ_S = 2150 kg/m^3, ρ_M = 930kg/m^3, dp= 270μm, Cs=2.05%.

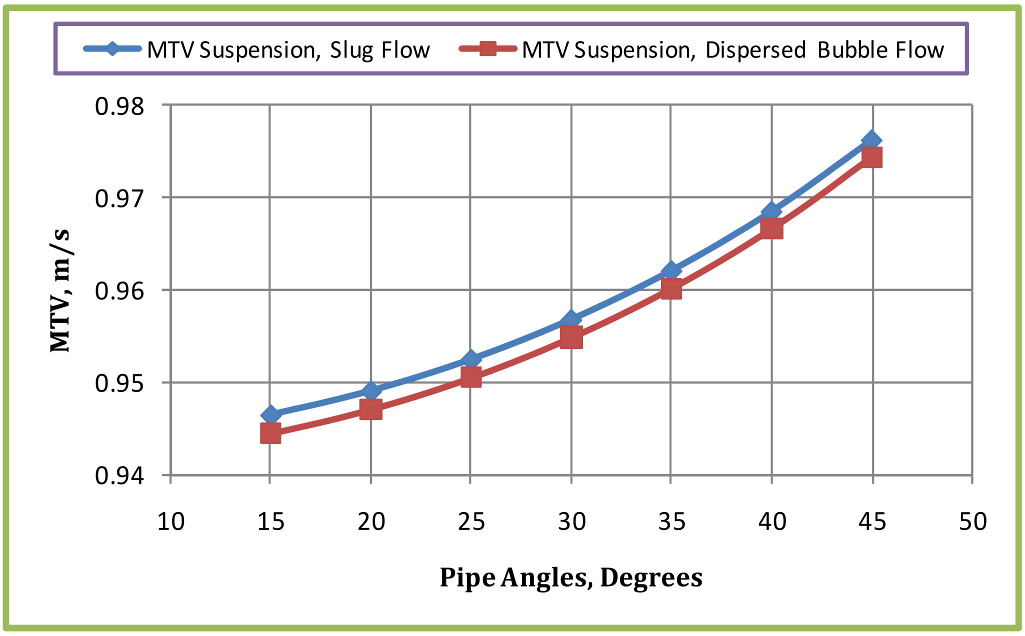

Figure 7.7: Comparison of MTV Suspension for Slug & Dispersed Bubble flow. ρ_S = 2150 kg/m^3, ρ_M = 930kg/m^3, dp= 270μm, Cs=2.05%.

The model predictions were tested against the data of (Thomas 1979) and (Ramadan, Skalle and Saasen 2005) and found to predict reasonably accurate. It was also compared with some selected models from the literatures and showed better correlations than any of the selected models as can be seen Figures 7.8 & 7.9. The comparisons of the experimental results with that of model predictions are found to be largely satisfactory as shown in Figures 7.10 – 7.12.

Table 7.2 & 7.3 presents the statistical parameter for measured MTV and the MTV predicted with the new model.

The comparisons evaluated the capability of the various models in public domain. This was to show the capabilities of these models to effectively predict the solid particle transport in tieback / pipeline. The independent experimental data provided a yardstick for assessment which was to quantify the difference between the predictions of the various models in comparison with proposed MTV models. The same input parameters have been used for all the models thereby a fair assessment can be reached.

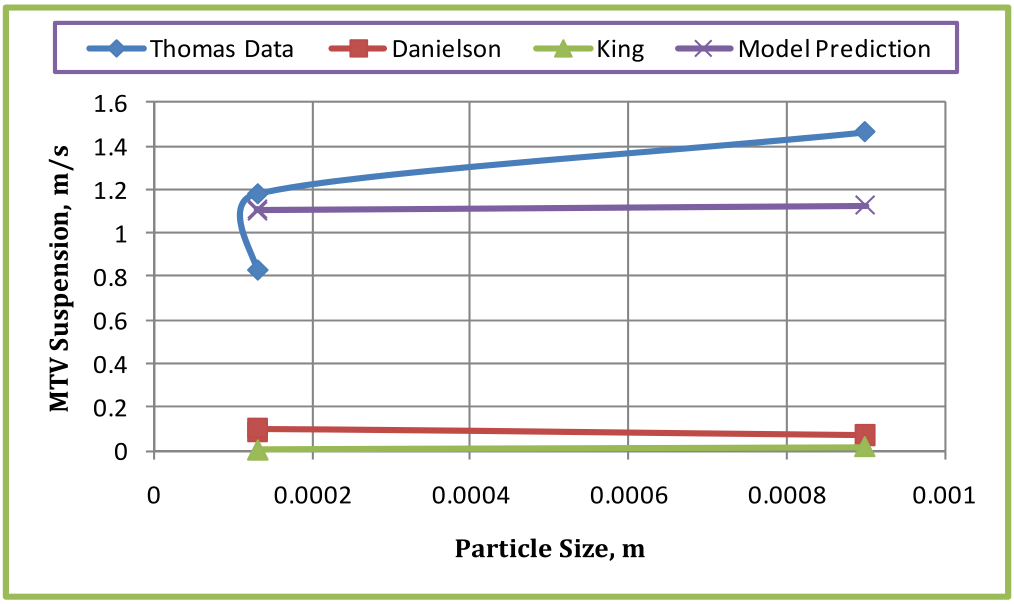

Figure 7.8: Comparison of prediction of proposed model and literature models with Thomas data (Thomas 1979)**.**

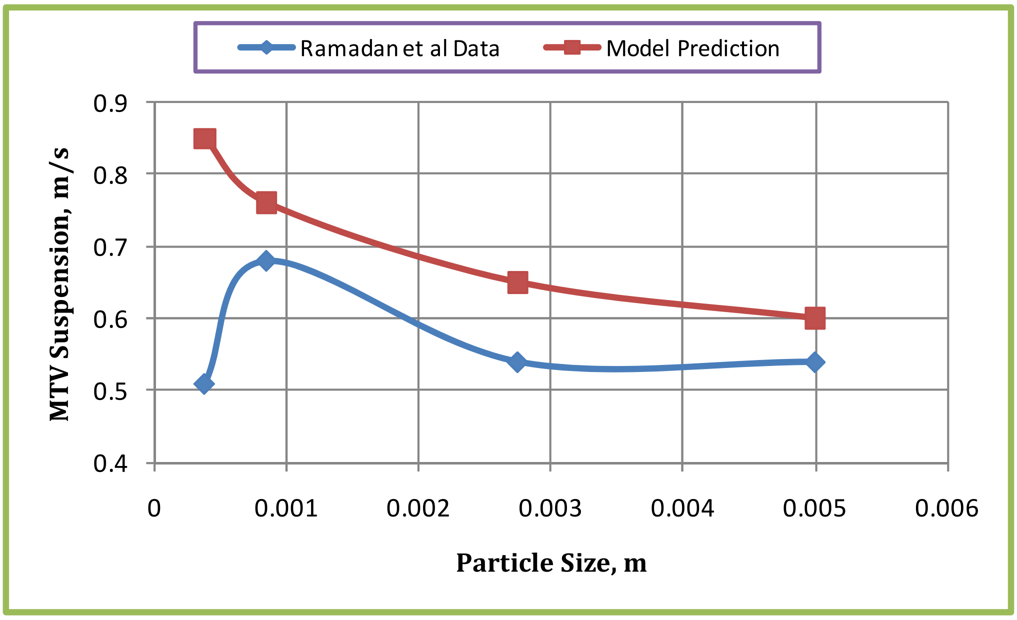

Figure 7.9: Comparison of prediction of proposed model with Ramadan et al data (Ramadan, Skalle and Saasen 2005)**.**

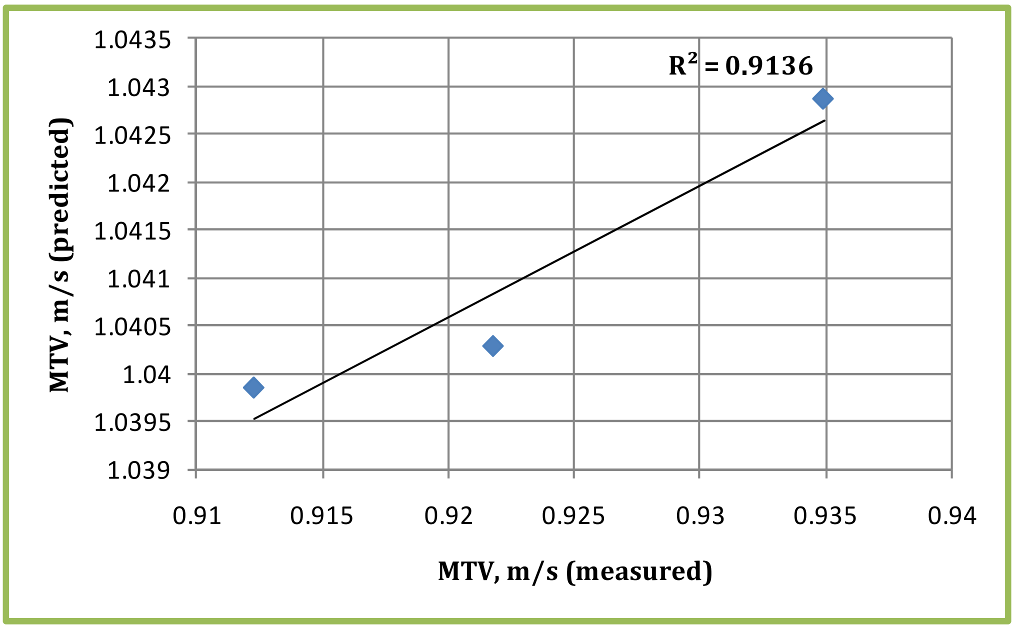

Figure 7.10: Comparison of measured and model prediction for MTV suspension in multiphase flow

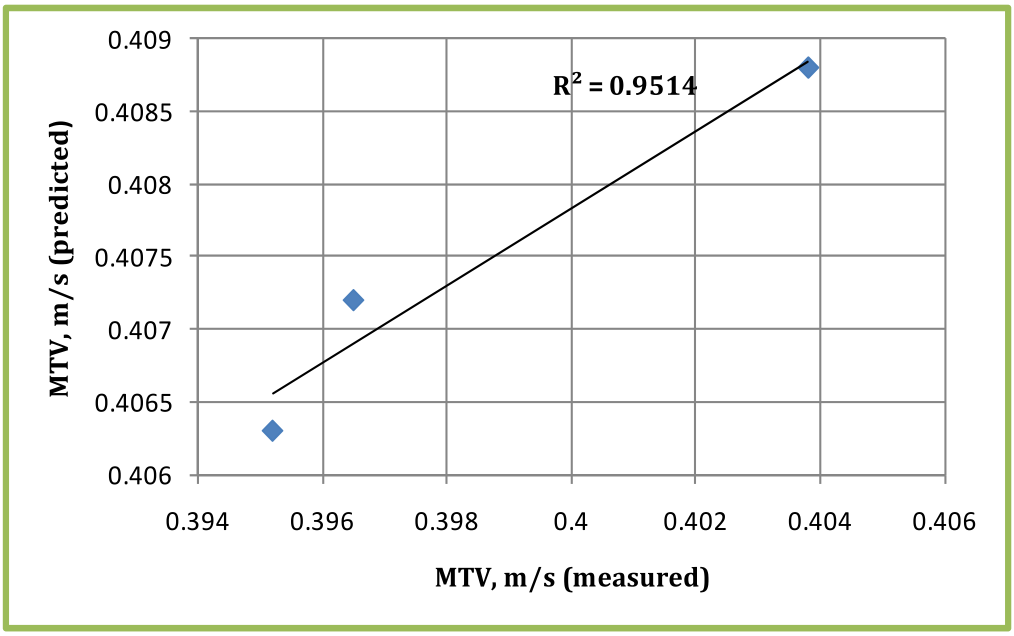

Figure 7.11: Comparison of measured and model prediction for MTV rolling in multiphase flow

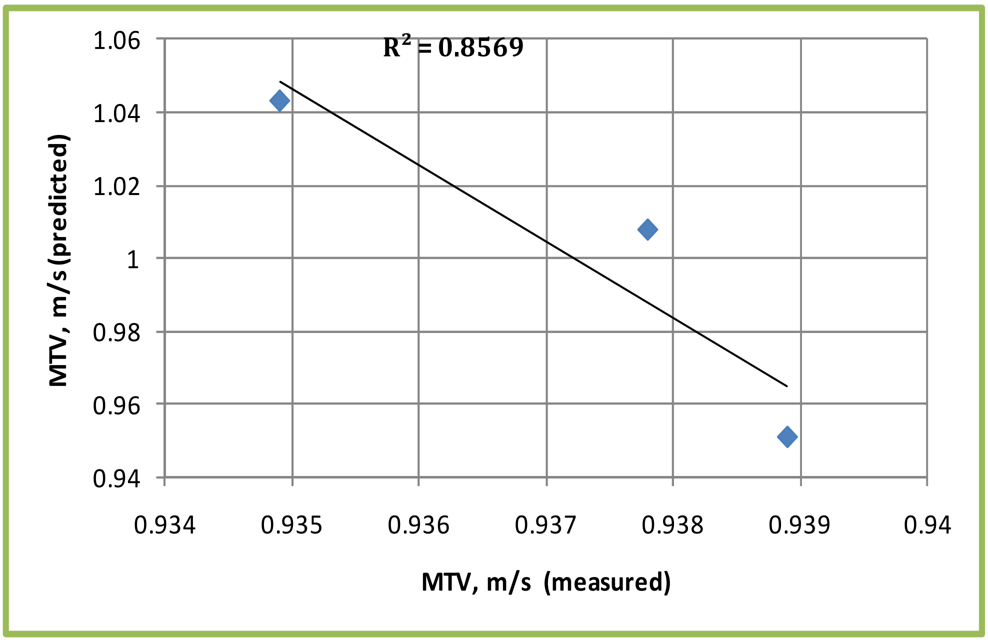

Figure 7.12: Comparison of measured and model prediction for MTV suspension in multiphase flow.

Table 7.2: Statistical Parameters for the MTV Model predictions in horizontal pipes

	MTV Model Predictions			
	Horizontal pipes, suspension		**Horizontal pipes, rolling**	
Average percent error	12.27 (0.07m)	11.39 (0.08m)	2.73 (0.07m)	2.63 (0.08m)
R-Square value (R^2)	0.9136	0.9136	0.9514	0.9514

Table 7.3: Statistical Parameters for the MTV Model predictions in 0.1m inclined pipe

	MTV Model Predictions		
	15^0	**20^0**	**25^0**
Average percent error	1.21	1.18	1.42
R-Square value (R^2)	0.8569	0.8569	0.8569

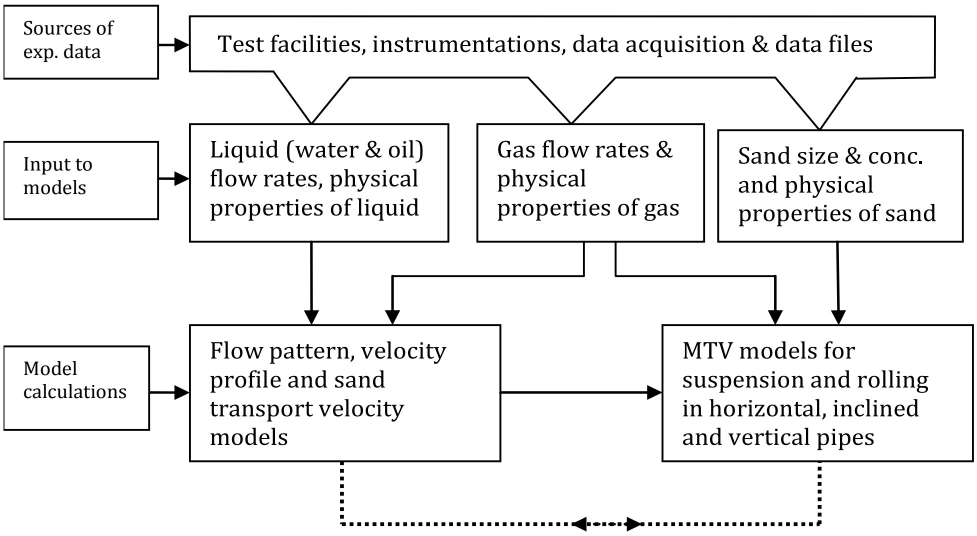

Figure 7.13: Solution strategy for the integrated model to determine the minimum transport velocity for three-phase flow

The accuracy recorded with the present model was as a result of the method adopted for MTV prediction as presented in Figure 7.13 for the solution strategy adopted. It can be seen in Figure 7.8 that the predictions of other models are not satisfactory when they are compared with an independent experimental data from the literature. The reason for better predictive potential of the proposed model is based on a method which is derived from the fundamental law of physics of various interactions phenomena in a multiphase pipeline flow.

7.4: Sand Transport Optimisation strategies

For effective design and operation of long subsea pipeline/tiebacks, there are critical issues bothering on flow assurance which must be considered. These issues have been highlighted and discussed in detail in previous chapters and it includes flow pattern characterisations and sand particle minimum transport velocity necessary to prevent solid deposition among others. The sand transport modelling is therefore an important component to ensure flow assurance in multiphase transport in pipeline.

The multiphase solid transport experimental results indicates fluid velocity, flow patterns, fluid viscosity, pipe inclinations, pipe size and sand concentration have profound effects on solid particle transport in multiphase flow, details have been presented and discussed in Chapter 5. In order to prevent solid bed formation by keeping the solid in suspension and if settled, to keep the solid moving at the bottom of the pipe require careful design and optimisation of the critical parameters. In this chapter, analysis procedures that have been developed to determine effective operating window in horizontal, high angle and vertical pipeline to prevent solid deposition is presented.

7.5: Sand transport system optimisation

Optimization is a suite of methods and strategies to design engineering systems in order to make it as perfectly as possible with respect to decision parameters. In this research, an optimisation strategy was designed to solve sand minimum transport velocity in single-phase and multiphase flow in pipes. The strategy employed a combination of velocity profile models and analytical models to optimise minimum transport velocity in pipeline based on the system and multiphase fluids characteristics. The optimisation schematic is presented in Appendix G.

The strategy requires

1. Determination of prevalent flow patterns which was achieved by using Beggs and Brill models for flow pattern predictions applicable to all pipe geometry (Beggs and Brill 1973). There is continuous change in flow pattern as the fluids enter the pipeline from dispersed bubble flow, to stratified flow, slug flow and annular flow depending on multiphase flow characteristics, pipe size and pipe inclinations.
2. Determination of the velocity profile for the identified pattern by calling on the appropriate model(s) matching the prevailing flow pattern. The flow velocity profiles developed are for dispersed bubble flow, slug flow, annular flow and stratified flow.
3. Assume a flow velocity necessary to transport sand particle and determine if the assumed flow velocity is sufficient to achieve suspension or rolling in horizontal, high angle and vertical pipe.
4. If not, an iterative procedure is carried out using the MS Excel VB program developed, see Appendix H by comparing the particle velocity with assumed flow velocity to estimate appropriate minimum transport velocity sufficient to transport solid particles either in suspension or in a rolling mode in horizontal, high angle and vertical pipes.
5. The parameters used were as presented earlier in Table 7.1. Some of the entry data for flow pattern characterisation are presented in Table 7.4. Details of this data can be found in Appendix B. The main descriptions of the parameters are presented in Table 7.5.

7.6: Modeling multiphase solid transport

The VB on Excel code developed was for optimisation of Minimum Transport Velocity (MTV) in single-phase and multiphase (water-oil-gas) flow in horizontal, high angle and vertical pipes. A typical production system schematic is as shown in Figure 7.14. The producing system includes the oil and gas reservoir, the production tubing in the well, the surface flow line, the processing equipment and the storage facility which are interrelated and thus affect each other. The system optimisation must allow for efficient and safe operation of every component of the production system. The focus in this project was on the transport of solids in multiphase through the surface flow line to prevent sand bed formation.

Different parameters are optimised depending the phase of operation, either at the design phase or during the operation of the multiphase pipeline/tieback. The problem has been represented with the developed semi-empirical models and decision parameters can therefore be optimised. The models for MTV suspension and rolling in horizontal, high angle and vertical pipes have been presented in Chapter 6 while the velocity profile models for different flow patterns are presented in Chapter 3. The key parameters used in these models and its effects on solid transport in multiphase optimisation either at design phase or operation phase are as presented in Table 7.1.

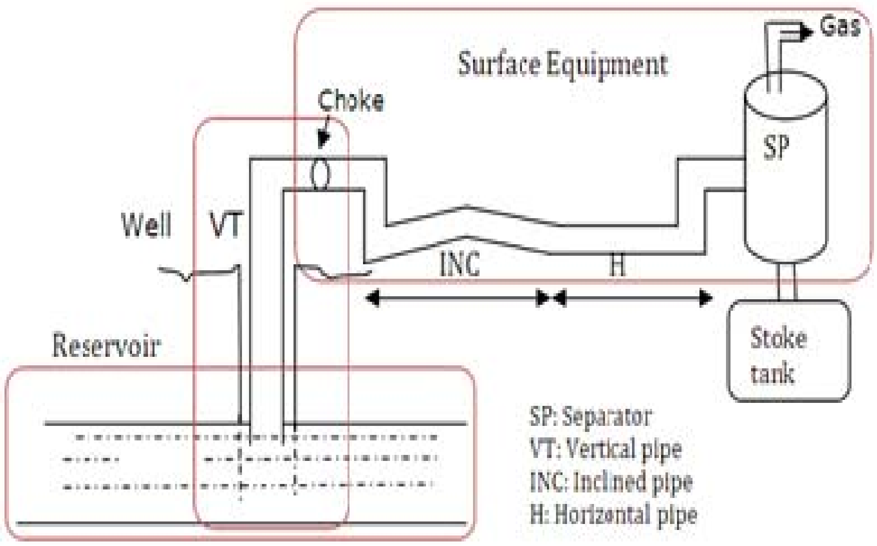

Figure 7.14: Schematic of production system from reservoir to processing facility

Table 7.4: Flow pattern data used for MTV optimisation program

Disp. bubble flow		Slug flow		Stratified flow		Annular flow*	
Vsl, m/s	Vsg, m/s	Vsl, m/s	Vsg, m/s	Vsl, m/s	Vsg, m/s	Vsl, m/s	Vsg, m/s
0.001	15.18	0.42	6.26	0.032	0.366	5.8	20
0.002	15.02	0.345	5.52	0.006	0.344	3.1	20
0.005	15.37	0.155	6.64	0.12	0.653	1	15
0.01	15.09	0.17	5.47	0.095	0.413	1.5	14.4
0.015	15.01	0.22	4.23	0.031	0.787	1.5	14.6

Annular flow* data obtained from (Abdul-Majeed 2000)

Table 7.5: Parameters for MTV optimisation program

Parameters	Process design	Process optimisation
Flow rate	Yes, to prevent solid deposition and bed formation. This depends on the well deliverability which can be varied for optimum flow to prevent sand influx. The rate of return on investment may also drive the flow rate requirement.	Yes, to prevent solid deposition and bed formation. The flow rate can be adjusted in order to minimise solid deposition and initiate formation of particular flow pattern.
Fluid density	Possible, depending oil/gas ratio. The fluid mixture will change as the flow velocity and pressure drop decline with length of and possible gas expansion.	Possible, depending oil/gas ratio.
Fluid viscosity	Possible, depending oil/gas ratio.	Possible, depending oil/gas ratio
Pipe size	Yes, depending on require flow rate. Optimum pipe size is desirable.	No, this is already in place and will not change.
Pipe angle, θ	Yes, during pipeline construction and installation. Can pre-determine the part of the pipeline ways.	No, the terrain is fixed.
Particle density	No, the reservoir particle sand may be known and cannot be changed.	No, this is a known value.
Particle size	No, the reservoir particle size can be obtained the sand grain distribution.	No, this will not change. The underlying assumption was that the sand particle is insoluble.
Particle conc.	Yes, can model optimum flow rate to prevent sand influx into the well bore and consequently into the surface facility.	Yes, can adjust the choke for a desired flow rates.

7.7: Sensitivity results

It was observed that variation of pipe angle in 0.1m pipeline transport sand particles better as a result slug formation but a steep increase was observed in dispersed bubble flow as shown in Figure 7.15. Two key factors may be responsible for this; the viscosity of the carrier fluid and the turbulence slug nose. However, with change in particle sizes, the effect of flow patterns is not very obvious with small particle sizes as shown in Figure 7.16. That was also replicated in the rolling mode, Figure 7.17. The preferred scenario in this case however, is to have dispersed bubble flow.

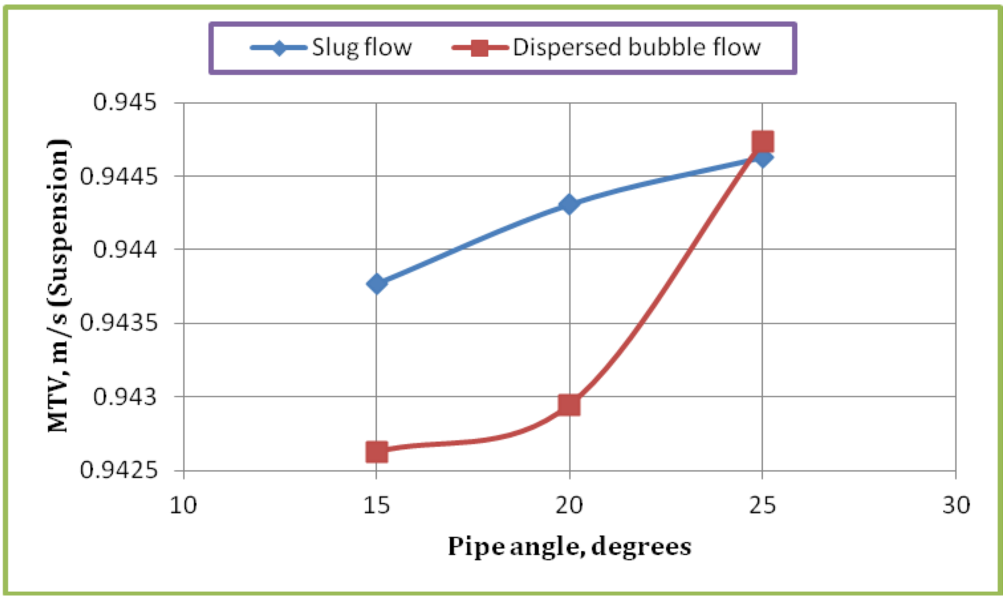

Figure 7.15: Comparison of effect of pipe inclination on sand transport with different flow patterns; pipe size = 0.1m, particle size = 0.00027m, mixture density = 930kg/m^3

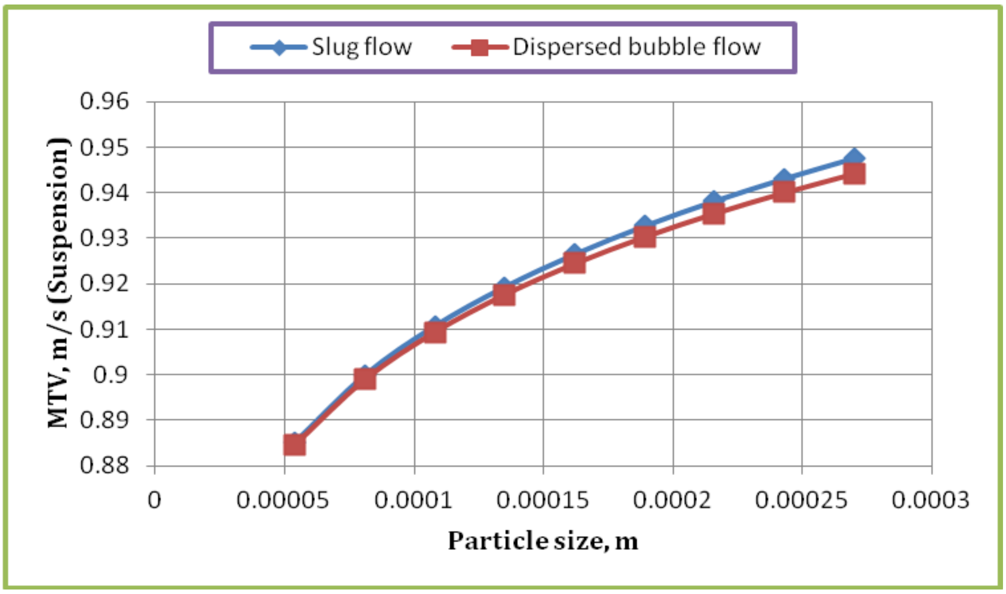

Figure 7.16: Comparison of transport efficiency (suspension) of flow patterns with different particle sizes, particle density = 2150kg/m^3, mixture density = 930kg/m^3

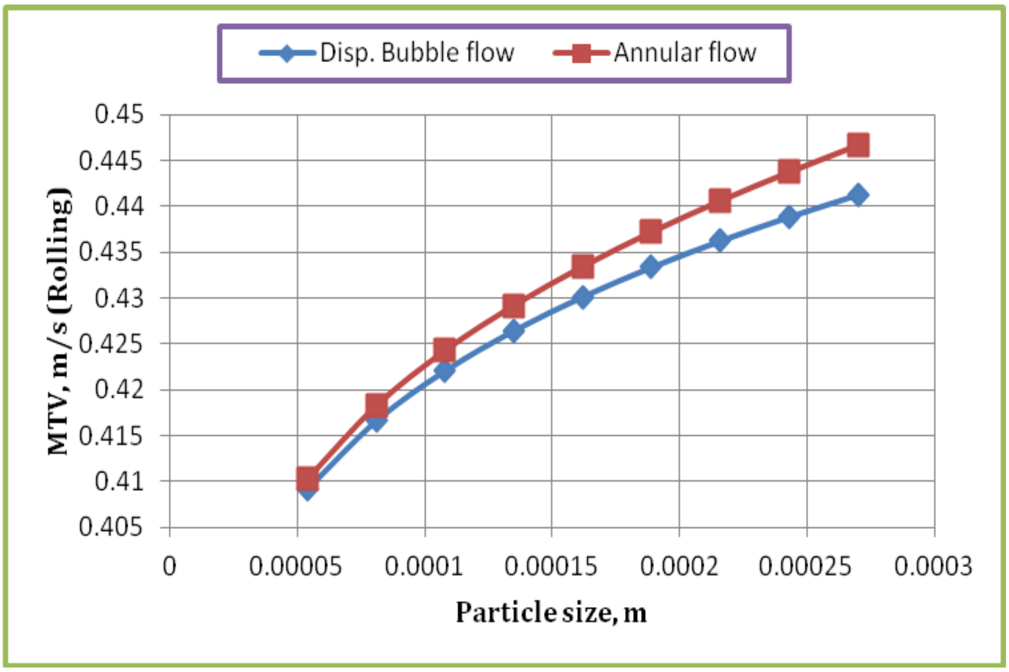

Figure 7.17: Comparison of transport efficiency (rolling) of flow patterns with different particle sizes, particle density = 2150kg/m^3, mixture density = 930kg/m^3

7.8 Summary

It is fair to say that it was rather difficult finding published research papers that present reliable experimental data for sand particle transport in multiphase fluid flow. Most of the data in the public domain are mainly those generated from hydraulic conveying experiment. The trend within hydraulic transport research was to predict deposit velocity or critical velocity of liquid that will cause solid to drop out of suspension. Such models are unable to predict solid particle movement either in suspension or rolling in multiphase production and multiple fluid flows in subsea tiebacks given the multiple complexities associated with it. Merely extending the hydraulic transport concept to solid particle transport in multiphase fluid flow will not serve any useful purpose.

In the light of this, the solid particle Minimum Transport Velocity (MTV) in multiphase flow measurements was conducted in three phase flow loop. The impacts of key parameters influencing solid particle transport in multiphase flow in pipes, such as pipe inclinations and size, flow patterns transitions and solid particle concentrations were considered. It was shown that for any meaningful result to be obtained from predictive solid particle transport models, these factors must be considered. The impact of pipe inclinations and flow patterns on solid transport was significant as well as the solid particle concentration profiles and pipe sizes. Considerations of these factors contributed immensely to the significant improvement in results obtained with the proposed MTV models when compared with those in public domain.

It is also clear from the results obtained that a single model cannot be used to predict the MTV for all the flow patterns. There was significant difference both in terms of MTV for suspension and rolling for dispersed bubble, slug as well as single phase. The adoption of minimum transport velocity using the velocity profiles concept has thrown more light on solid transport mechanism in multiphase flow.

The optimisation strategy employed provided insight on the influence of key parameters on solid transport efficiency in multiphase transport pipelines. The strategy employed a combination of velocity profile models and analytical models to optimise minimum transport velocity in pipeline based on the system and multiphase fluids characteristics.

The proposed models have taken into account various factors affecting solid transport in multiphase production which were lacking in the literature models considered. The key differences between these models and the present model are given in Table 7.6 below. Some of the predictions carried out with the current models with error margin above 12%, the error could be attributed to the accuracy of the datasets in view of measurement errors associated with visual observations. Improved data collection methods have been suggested in the recommendations.

Table 7.6: Comparison of the features of proposed MTV models with selected models

S/N	Model	Features / Characteristics
1	Ramadan (Ramadan, Skalle and Saasen 2005)	• Mechanistic model, three layer concept • Consider two-phase, water & PAC solution • Suitable for horizontal and inclined pipes • Assumed stratified flow pattern • Consider only suspension velocity • Considered particle size distributions
2	Salama (Salama 2000)	• Semi-empirical model • Considered two-phase flow • Does not account for flow patterns • Particle size distribution not considered • Suitable for horizontal pipe
3	Danielson (Danielson 2007)	• Drift flux model • Two-phase, water-gas flow • Suitable for horizontal pipe

4	Thomas (Thomas 1979)	• Mechanistic model using sliding bed concept • Hydraulic conveying • Single-phase, water-sand flow • High solid loading • Suitable for horizontal pipe
5	Stevenson (Stevenson et al. 2001)	• Semi-empirical model • Considered two-phase, gas-water • Particle-particle interaction not considered • Only considered intermittent slug flow • Considered only suspension velocity • Small pipe sizes used, max 0.07m • Suitable for horizontal pipe • Sand particle concentration less than 0.1%
6	**Proposed MTV model**	• Semi-empirical model combined with numerically derived particle velocity profiles. • Three-phase, water-oil-gas flow • Considered solid particle distributions and effects of particle-particle interactions • Four flow patterns considered, dispersed bubble, slug, stratified and annular flow patterns • Predicts MTV suspension and rolling • Applicable to horizontal and inclined pipes • Used typical sand particle concentration profile in oil & gas production, up to 2.05% by volume • Large pipe sizes, maximum 0.1m in diameter.

Chapter 8

Conclusions and Recommendations

8.1 Conclusions

The huge oil and gas reserves in the deep/ultra deep offshore are enough incentive for oil and gas companies to increase capital expenditures in exploration and production from these difficult terrains. One of the major concerns is the transportation of unprocessed reservoir fluid with potential risk of entrained solid particle deposition and bed formation thereby blocking the tieback / pipeline. The concerns are genuine and the requirements are quite simple. The available procedure or predictive models must guaranty uninterrupted flow of oil and gas with sufficient reliability.

The transportation of sand particle in multiphase fluid, oil-water-gas flow in pipes has been studied using numerical and experimental methods. Solid particle minimum transport velocity (MTV) for suspension and rolling in multiphase fluid flow in horizontal, slightly inclined and vertical pipes system have been developed. Experiment was performed in order to acquire critical data to improve and validate the MTV models. Fundamental understanding of the mechanism of solid transport in multiphase flow in pipes has been established for achieving an accurate solid particle transport model. The following are key conclusions drawn from this study and are presented below:

1. The use of computational fluid dynamic (CFD) as a substitute for determining velocity profiles experimentally proved to be sufficiently reliable. The virtual laboratory was used to generate fluid velocity profiles for a combination of fluid mixtures, gas-oil, water-oil, gas-water and water-oil-gas. This led to development of velocity profile models for each of the notable flow patterns. This is a novel approach which can be adopted for a range of multiphase processes. Detailed velocity profile model development can be found in Chapter 3.
2. The design and construction of automated multiphase flow loop provided opportunity to acquire critical data such as solid transport velocity, flow patterns and pressure drops in different combination of oil-water-gas-sand flow in order to develop and improve on the accuracy of solid particle MTV for suspension and rolling in multiphase flow. It thus eliminates the problems encountered when sourcing for experimental data for model testing and validation. The detailed design, equipment requirements and construction processes can be found in Chapter 4 and the data acquired are presented and discussed in Chapter 5.
3. The comprehensive experimental investigations of fluid-fluid and particle-fluid interactions in multiphase fluids were carried out. The direct observation of three-

phase water-oil-gas flow experiment shed more lights on the flow mechanism in two-phase and three-phase thereby corroborating the simulation results that single-phase solid particle transport model cannot be used to predict solid particle transport in multiphase flow. The results obtained in the experiment clearly demonstrated this fact and detailed discussions are presented in Chapter 5. It also showed that variation of flow parameters and pipe inclination has profound effects on transport mechanism. This can be very valuable in the operation of oil and gas production pipeline.

4. The experimental results clearly showed that the solid particle MTV for suspension and rolling are very sensitive to variations in pipe inclination and fluid viscosity. The implications of various parameters to transport efficiency were discussed in Chapter 5. In reality, no pipeline is completely horizontal due to undulating nature of the sea bed or onshore terrain, therefore effects of pipe inclination on sand particle transport presented in Chapter 5 was significant. There was also a decrease in MTV for suspension and rolling with increase in fluid viscosity. One striking phenomenon was formation of slug flow at inclined surfaces for large diameter pipe which generally aided sweeping/transport of the settled solid particle prior to arrival of turbulent slug nose.
5. The experimental results clearly showed that the capacity of multiphase fluid to transport solid particle was found to be dependent on the constituents of the carrier fluid and pipe inclinations. In water-sand flow, there was no appreciable change in MTV even with changes in pipe angles. However, with water-oil-gas flow, there was significant change in MTV with change in pipe inclinations. Therefore, in a multiphase flow where there is continuous change in flow patterns, it was observed that different flow patterns exhibits different transport capability. Stratified flow pattern exhibited the least carrying capacity with various combination of water-oil-gas flow, see Chapter 5. And the sand particles are better transported in slug flow regime. Therefore, for accurate solid particle transport model, flow patterns characterisation must be considered. The proposed MTV models were defined based on the prevailing flow patterns.
6. The adoption of minimum transport velocity using the velocity profiles concept has thrown more light on solid transport mechanism in multiphase flow. The analysis clearly showed that single-phase model is inadequate for multiphase flow prediction or merely extending hydraulic transport model to sand transport in oil & gas production system is quite misleading, detailed discussions in Chapter 3 & 6. The developed models have taken on board these concerns. It has been shown to adequately predict for both single-phase and multiphase flow when compared with

experimental data. This was evident in the analysis of the results presented in Chapter 6. This can also be extended to cutting transport in drilling fluids in wells. It has the potential to solve the problem of sand depositions.

7. The prediction of MTV for suspension and rolling in horizontal and vertical pipes rely on accurate determination of the particle drag and lift coefficients. The generalised C_D & C_L models were found to be inadequate for accurate prediction of MTV in multiphase flow. Many of the existing models were developed based on single phase flow. In this research, drag and lift coefficient models have been developed that accurately account for the complexities associated with multiphase flow in pipes. The models developed were found to have better prediction when compared with existing models from the literatures and within tolerable margin of error, see Table 6.1
8. The predictions of the proposed MTV models for suspension and rolling in slug and dispersed bubble flow show satisfactory agreement when compared with experimental data as well as independent data from previous studies see Chapter 6 and Table 6.3 – 6.4 for error margin of the model. The improved model also showed better prediction over a range of operating systems and geometric conditions when compared with other similar models in the public domain.
9. The proposed MTV models for suspension and rolling combined the numerically developed particle velocity profile models with semi-empirical models for solid particle transport. It took into account the key parameters that influences particle transport in pipe flow and thus eliminates inaccuracies currently experience with similar models in public domain. The combined models were implemented on Microsoft Excel (VB) program for optimisation of MTV models in multiphase flow.
10. The proposed models can be used to predict sand bed formation in subsea tieback/pipeline. It can be applied in typical field scenarios by up scaling the operating parameters. It has the potential to solve problems of pipe and equipment sizing, risk of sand deposition and bed formation, elimination of costs of sand unloading, downtime and generally improve sand management strategies.

8.2 Contributions to knowledge

This research contributes to five key aspects of the flow assurance;

1. The development of minimum transport velocity models for suspension and rolling based on the concept of particle velocity profiles is a significant breakthrough in particle transport in multiphase flow. This has the potential to solve problems of pipe & equipment sizing, risk of sand deposition & bed formation, elimination of costs of sand unloading, downtime and generally improve sand management strategies.
2. The prediction of MTV for suspension and rolling in horizontal, high angle and vertical pipes rely on accurate determination of the particle drag and lift coefficients. The generalised C_D & C_L models were found to be inadequate for accurate prediction of MTV in multiphase flow. Many of the existing models were developed based on single phase flow. In this research, drag and lift coefficient models have been developed that accurately account for the complexities associated with multiphase flow in pipes. The models developed were found to have better prediction within tolerable margin of error when compared with existing models from the literatures.
3. The research presents a unique concept of velocity profile for the development of appropriate minimum transport velocity (MTV) models for solid transport in subsea tiebacks. Clear definitions and prediction of flow patterns contributed hugely to the development of MTV for suspension and rolling in subsea tiebacks, therefore eliminating the uncertainties in flow pattern prediction and characterisation in multiphase flow. This was novel as the concept has never been used in the study of solid transport in multiphase flow.
4. Part of the deliverable for this research was the design and construction of multi-purpose multiphase flow loop. The new test facility was designed and built to replicate real time multiphase oil-water-gas transport in pipeline with varied pipe dimensions and inclination in order to replicate true field scenarios and generate appropriate data for multiphase particle Reynolds number, C_D, C_L and for MTV models validation in multiphase flow.
5. The research presents new experimental data on solid transport behaviour in multiphase pipe flow systems and the associated effects of system, operating and geometric parameters. This information about the effects of system, design and operating conditions on solids transport characteristics is valuable and useful. There was obvious lack of experimental data for multiphase flow and this over the years has impeded our understanding of the behaviour and associated problems of multiphase flow in pipes.

8.3 Recommendations

In academic research such as this, there is always the need to improve on existing methods or prediction models. However, the research work was plagued with some challenges which can be highlighted here.

1. The research involved experimental work that investigates different flow phenomenon associated with multiphase sand transport in pipes. The influence of flow patterns on the carrying capacity of the fluid was well documented in Chapter 5. Sand transport velocity data in different flow patterns was acquired in order to develop particle drag and lift coefficients in multiphase. This was critical in the development of appropriate minimum transport velocity models either for particle suspension or rolling in pipeline/tieback. However, the flow patterns observed are constantly changing and the observer needed to keep pace with these changes in real time. There were obvious difficulties experienced with visual observation and video capturing of changing flow patterns through the transparent test section during the experiment. Though the method met the objectives but the limitations of the method cannot be ignored. It is sometimes difficult to recognise the flow pattern and results may therefore be subjective. Some area for further improvement could be use of instrument such as Neutron radiography and X-radiography for flow pattern measurement and analysis which have been proposed by some workers but have not found serious application.
2. The research work involved development of appropriate solid transport velocity models in multiphase flow in pipes. The principal method adopted was the concept of particle minimum transport velocity. It required CFD simulation of multiphase fluid flow in pipes in order to develop velocity profiles models for different flow pattern predictions, discussed in Chapter 3. The developed velocity profile models served as basis upon which solid minimum transport velocity models in multiphase flow were developed. The alternative approach could be laboratory measurement of particle velocity profiles in multiphase which could potentially improve the overall accuracy of the MTV models with sophisticated tools such as Particle Image Velocimetry (PIV).
3. The sand transport models took into consideration the effects and changing flow patterns in multiphase flow. However, there is the need to track the changes as the multiphase flow through the length of pipe. It will be useful to determine where the solid particle will settle and the height of the settled bed in order to know the appropriate pig and at what location to deploy it.
4. The model developed in this case assumed isothermal system. A possible new area of research for solid transport in multiphase flow in subsea tieback could be to look at an

adiabatic system. The investigation of the impact of temperature on the sand transport mechanism in multiphase can be achieved either by experiment or numerical method. It may be possible to install heating system as part of the experimental set up in order to increase the flowing temperate above room temperate and generate valuable data for modelling.

References

1. ABBOTT, P.A., D'SOUZA, R.B., SOLBERG, I.C. AND ERIKSEN, K., 1995. Evaluating Deepwater Development Concepts. *Journal of Petroleum Technology,*
2. ABDUL-MAJEED, G.H., 1996. Liquid holdup in horizontal two-phase gas-liquid flow. *Journal of Petroleum Science and Engineering,* 15, pp. 271-280
3. ABDUL-MAJEED, G.H., 2000. Liquid slug holdup in horizontal and slightly inclined two-phase slug flow. *Journal of Petroleum Science and Engineering,* 27, pp. 27-32
4. ABDUVAYT, P., MANABE, R. AND ARIHARA, N., 2003. Effects of Pressure and Pipe Diameter on Gas-Liquid Two-Phase Flow Behaviour in Pipelines. In: SPE, ed. *Annual Technical Conference and Exhibition.* October, 2003. Denver, USA: SPE.
5. ACIKGOZ, M., 1992. An Experimental Study of Three Phase Regimes. *International Journal of Multiphase Flow,* 18, pp. 327-336
6. ALMEDEIJ, J., 2008. Drag coefficient of flow around a sphere: Matching asymptotically the wide trend. *Powder Technology,* 186, pp. 218-223
7. AL-YAARI, M.A. AND ABU-SHARKH, B.F., 2011. CFD Prediction of Stratified Oil-Water Flow in a Horizontal Pipe. *Asian Transactions on Engineering,* 01(05), pp. 68-75
8. ANDREUSSI, P. AND PERSEN, L.N., 1987. Stratified Gas-Liquid Flow in Downwardly Inclined Pipes. *International Journal of Multiphase Flow,* 13(4), pp. 565-575
9. ANSYS INC, 2011. *ANSYS FLUENT Theory Guide.* 2011th ed. USA: ANSYS Inc.
10. BAGCHI, P. AND BALACHANDAR, S., 2002. Shear Versus Vortex-Induced Lift Force on a Rigid Sphere at Moderate Re. *Journal of Fluid Mechanics,* 473, pp. 379-388
11. BALL, I.G., 2006. Challenges of Long Satellite Tiebacks. *Offshore Technology Conference,*
12. BARNEA, D., 1987. A Unified Model for Predicting Flow Pattern Transitions for the Whole Range of Pipe Inclinations. *International Journal of Multiphase Flow,* 13, pp. 1-12
13. BARNEA, D., SHOHAM, O., TAITEL, Y. AND DUKLER, A.E., 1980. Flow Pattern Transition for Gas - Liquid Flow in Horizontal and Inclined Pipes - Comparison of Experimental Data with Theory. *International Journal of Multiphase Flow,* 6, pp. 217-225
14. BEGGS, H.D. AND BRILL, J.P., 1973. A Study of Two-Phase in Inclined Pipes. *SPE/JPT,* , pp. 607-617
15. BEHNIA, M. AND LLIC, V., 1990. A Simple Correlation for Estimation of Multiphase Pressure Drop in an Oil Pipeline. *SPE Production Engineering,* , pp. 370-372

16. BELLO, K.O., OYENEYIN, M.B. AND OLUYEMI, G.F., 2011. Minimum Transport Velocity Models for Suspended Particles in Multiphase Flow Revisited. In: SPE, ed. *Annual Technical Conference & Exhibition.* October, 2011. Denver, USA: SPE.
17. BELLO, O., FALCONE, G., TEODORIU, C. AND UDONG, I, 2011. A Mechanistic Model for Predicting and Optimising Oil-Sand Flow in Horizontal Wells. *Oil & Gas Science and Technology*
18. BELLO, O.O., REINICKE, K.M. and TEODORIN, C., 2005. Particle Holdup Profiles in Horizontal Gas-liquid-solid Multiphase Flow Pipeline. *Chemical Engineering Technology,* Vol. 28 PT 12, pp. 1546-1553
19. BIAN, S. AND HENSON, M.A., 2006. Measurement selection for on-line estimation of nonlinearwave models for high purity Distillation columns. *Chemical Engineering Science,* 61, pp. 3210-3222
20. BONIZZI, M. AND ISSA, R.I., 2003. On the Simulation of Three-Phase Slug Flow in Nearly Horizontal Pipes Using the Multi-fluid Model. *International Journal of Multiphase Flow,* 29, pp. 1719-1747
21. BRATLAND, O., 2010. *Pipe Flow 2 - Multiphase Flow Assurance.* First ed. Ovi Bratland.
22. BROOK, N., 1987. Fluid Transport of Coarse Solids. *Mining Science and Technology,* 5, pp. 197-217
23. CARMICHAEL, G.R., 1982. Estimation of the Drag Coefficient of Regularly Shaped Particles in Slow Flows from Morphological Descriptors. *American Chemical Society,* 21, pp. 401-403
24. CHEN, X. AND GUO, L., 1999. Flow Patterns and Pressure Drop in Oil-Air-Water Three Phase Flow Through Helically Coiled Tubes. *International Journal of Multiphase Flow,* 25, pp. 1053-1072
25. CHEN, X. and GUO, L., 1999. Flow Patterns and Pressure Drop in Oil-Air-Water Three Phase Flow Through Helically Coiled Tubes. *International Journal of Multiphase Flow,* 25, pp. 1053-1072
26. CHENG, N., 2009. Comparison of formulas for drag coefficient and settling velocity of spherical particles. *Powder Technology,* 189, pp. 395-398
27. CHIEN, S., 1994. Settling Velocity of Irregularly Shaped Particles. *SPE Drilling and Completion,* , pp. 281-289
28. CUTLER, J., 2009. Laggan & Tormore - Development of Two New Deepwater Gas Condensate Fields and Associated Gas Export Infrastructure. In: SPE, ed. *Offshore Europe Oil & Gas Conference & Exhibition.* September, 2009. Aberdeen, UK.: SPE.
29. DANIELSON, T.J., 2007. Sand Transport Modeling in Multiphase Pipelines. *Offshore Technology Conference.* May. Houston, USA: SPE.

30. DARBY, R., 2001. *Chemical Engineering Fluid Mechanics.* Second ed. New York, USA: Marcel Dekker, Inc.
31. DE SCHEPPER, S.C.K., HEYNDERICKX, G.J. AND MARIN, G.B., 2008. CFD modeling of all gas–liquid and vapor–liquid flow regimes predicted by the Baker chart. *Chemical Engineering Journal,* 138, pp. 349-357
32. DOAN, Q. AND GEORGE, A.E., 1998. Flow of Oil and Sand in a Horizontal Well. *Journal of Petroleum Technology,* 37(10), pp. 39-45
33. DORON, P., GRANICA, D AND BARNEA, D., 1987. Slurry Flow in Horizontal Pipes - Experimental and Modelling. *International Journal of Multiphase Flow,* 13(4), pp. 535-547
34. DORON, P., SIMKHIS, M. AND BARNEA, D., 1997. Flow of Solid-Liquid Mixtures in Inclined Pipes. *International Journal of Multiphase Flow,* 23(2), pp. 313-323
35. DORON, P. and BARNEA, D., 1996. Flow Patterns Maps for Solid-Liquid Flow in Pipes. *International Journal of Multiphase Flow,* 22, pp. 273-283
36. DOROODCHI, E., EVANS, G.M., SCHWARZ, M.P., LANE, G.L., SHAH, N. AND NGUYENA, A., 2008. Influence of turbulence intensity on particle drag coefficients. *Chemical Engineering Journal,* 135, pp. 129-134
37. EKAMBARA, K., SANDERS, R.S., NANDAKUMAR, K., MASLIYAH, J.H., 2008. CFD simulation of bubbly two-phase flow in horizontal pipes. *Chemical Engineering Journal,* 144, pp. 277-288
38. EKLUND, T AND PAULSEN, G., 2007. Ormen Lange Offshore Project Subsea Development Strategy and Execution. In: THE INTERNATIONAL SOCIETY OF OFFSHORE AND POLAR ENGINEERS, ed. *Proceedings of the Sixteenth International Offshore and Polar Engineering Conference.* July, 2007. Lisbon, Portugal: The International Society of Offshore and Polar Engineers.
39. EWIDA, A.A., HURLEY, S.J., EDISON, S.H. AND TEH, C.E., 2004. Shallow to Deepwater Facilities and Flow Assurance Challenges in Offshore Newfoundland. In: THE INTERNATIONAL SOCIETY OF OFFSHORE AND POLAR ENGINEERS, ed. *The Fourteenthe International Offshore and Polar Engineering Conference.* May, 2004. Toulon, France: The International Society of Offshore and Polar Engineers.
40. EXXONMOBIL, 2012. *ExxonMobil starts production from the kizomba satellites project in angola.* [online] Irvin Texas: ExxonMobil Producing. Available from: http://news.exxonmobil.com/press-release/exxonmobil-starts-production-kizomba-satellites-project-angola
41. FALCONE, G., TEODORIU, C., REINICKE, K.M. AND BELLO, O.O., 2007. Multiphase Flow Modelling Based on Experimental Testing: An Overview of Research Facilities

Worldwide and the Need for Future Development. In: SPE, ed. *Annual Technical Conference and Exhibition.* November, 2007. California, USA: SPE.

42. FENG, Z-G. AND MICHAELIDE, E., 2002. Interparticle forces and lift on a particle attached to a solid boundary in suspension flow. *Physics of Fluids,* 14(1), pp. 49-60
43. FORBORD, P.E.A., 2007. The Challenges Associated with the Installation of Long Distance Tiebacks. *OTC 18672,*
44. FORD, J.T., PEDEN, J.M., OYENEYIN, M.B., GAO, E. AND ZARROUGH, R, 1990. Experimental Investigation of Drilled Cuttings Transport in Inclined Boreholes. In: SPE, ed. *Annual Technical Conference and Exhibition of the Society of Petroleum Engineers.* September, 1990. New Orleans, USA: SPE. pp. 197-206
45. GARCIA, F., GARCIA, R. AND JOSEPH, D.D., 2005. Composite power law holdup correlations in horizontal pipes. *International Journal of Multiphase Flow,* 31, pp. 1276-1303
46. GARCIA, F., GARCIA, R., PADRINO, J.C., MATA, C., TRALLERO, J.L. AND JOSEPH, D.D., 2003. Power law and composite power law friction factor correlations for laminar and turbulent gas– liquid flow in horizontal pipelines. *International Journal of Multiphase Flow,* 29, pp. 1605-1624
47. GHORAI, S. AND NIGAM, K.D.P., 2006. CFD modeling of flow profiles and interfacial phenomena in two-phase flow in pipes. *Chemical Engineering and Processing 45 (2006) 55–65,* 45, pp. 55-65
48. GILLES, R.G., MCKIBBEN, M.J. AND SHOOK, C.A., 1997. Pipeline Flow of Gas, Liquid and Sand Mixtures at Low Velocities. *The Journal of Canadian Petroleum Technology,* 36(9),
49. GILLIES, R. G., MCKIBBEN, M. J. AND SHOOK, C., 1997. Pipeline flow of gas, liquid and sand mixture at low velocity. *Journal of Canadian Petroleum Technology,* , pp. 36-42
50. GOVIER, G.W. AND AZIZ, K., 1972. *The Flow of Complex Mixtures in Pipes.* 4th ed. Malabar Florida: Robert E. Krieger Publishing Company.
51. HART, J., HAMERSMA, P.J. AND FORTUIN, J.M.H., 1989. Correlations Predicting Frictional Pressure Drop and Liquid Holdup During Horizontal Gas-Liquid Pipe Flow with a Small Liquid Holdup. *International Journal of Multiphase Flow,* 15(6), pp. 947-964
52. HARTELL, W.D. AND GREENWALD, J.R., 2009. Deepwater Development Production and Export Options. In: SPE, ed. *SPE Asia Pacific Oil and Gas Conference and Exhibition.* August, 2009. Jakarta, Indonesia: SPE.

53. HAWKINS, D., DILLABOUGH, G., RUELOKKE, M. AND WAY, F., 2008. Small Field Development—Offshore Newfoundland and Labrador, Canada. In: SPE, ed. *Offshore Technology Conference.* May, 2008. Houston, USA: SPE.
54. HEINDEL, T.J., GRAY, J.N. AND JENSEN, T.C., 2008. An X-ray System for Visualizing Fluid Flows. *Flow Measurement and Instrumentation,* 19, pp. 67-78
55. HENG, E.I., RONALDS, B.F. and EDWARDS, T.J., 2000. The Deepwater Subsea Tieback Options for Future Oil and Gas Production in Australia. *SPE 64485,*
56. HOTTOVY, J.D. AND SYVESTER, N.D., 1979. Drag Coefficients for Irregularly Shaped Particles. *American Chemical Society,* 18(3), pp. 433-436
57. HURLBURT, E.T. and HANRATTY, T.J., 2002. Prediction of the transition from stratified to slug and plug flow for long pipes. *International Journal of Multiphase Flow,* 28, pp. 707-729
58. ILEDARE, O.O., 2009. Worldwide Deepwater Petroleum Exploration and Development Prospectivity: Comparative Analysis of Efforts and Outcomes. *SPE Annual Technical Conference and Exhibition.* 4-7, October. New Orleans, USA: SPE.
59. JANA, A.K., DAS, G. AND DAS, P.K., 2006. Flow Regime Identification of Two-Phase Liquid-Liquid Upflow through Vertical Pipe. *Chemical Engineering Science,* 61, pp. 1500-1515
60. KESKIN, C. and ZHANG, H., 2007. Identification and Classification of New Three-Phase Gas/Oil/Water Flow Patterns. *SPE 110221,*
61. KING, M.J.S., FAIRHURST, C.P. AND HILL, T.J., 2001. Solid Transport in Multiphase Flows - Application to High Viscosity Systems. *Transaction of ASME,* 123, pp. 200-204
62. KORLOO, J., 2007. Indonesia Deepwater Field Development Technical, Contracting and Execution Challenges. In: SPE, ed. *Asia Pacific Oil & Gas Conference and Exhibition.* November, 2007. Jakarta, Indonesia: SPE.
63. KURU, W.C., LEIGHTON, D.T. AND MCCREADY, M.J., 1995. Formation of Waves on a Horizontal Erodible Bed of Particles. *International Journal of Multiphase Flow,* 21(6), pp. 1123-1140
64. LARSEN, T.I., PILEHVARI, A.A. AND AZAR, J.J., 1997. Development of a New Cuttings Transport Model for High Angle Wellbores Including Horizontal Wells. *SPE Drilling & Completion,* , pp. 129-135
65. LASKOVSKI, D., STEVENSON, P. AND GALVIN, K.P., 2009. Lift and drag forces on an isolated cubic particle in pipe flow. *Chemical Engineering Research and Design,* 87, pp. 1573-1581

66. LATASTE, J., HUILIER, D., BURNAGE, H. AND BEDNAR, J., 2000. On the shear lift force acting on heavy particles in a turbulent boundary layer. *Atmospheric Emvironment,* 34, pp. 3963-3971

67. LEE, A.H., SUN, J.Y., JEPSON, W.P., 1993. Study of Flow Regime Transitions of Oil-Water-Gas Mixtures in Horizontal Pipelines. *The International Society of Offshore and Polar Engineers.* June, 1993. Singapore:

68. LEVY, A AND MASON, D.J., 2000. Two-Layer Model for Non-Suspension Gas - Solids Flow in Pipes. *Powder Technology,* 112, pp. 256-262

69. LIN, P.Y. and HANRATTY, T.J., 1987. Effect of Pipe Diameter on Flow Patterns for Air-Water Flow in Horizontal Pipes. *International Journal of Multiphase Flow,* 13(4), pp. 549-563

70. LIU, H., 2003. *Pipeline Engineering.* Lewis Publisher, A CRC Press Company.

71. LOTH, E., 2008. Drag of non-spherical solid particles of regular and irregular shape. *Powder Technology,* 182, pp. 342-353

72. LOVICK, J. AND ANGELI, P., 2004. Experimental studies on the dual continuous flow pattern in oil–water flows. *International Journal of Multiphase Flow,* 30, pp. 139-157

73. MANDHANE, J.M., GREGORY, G.A. and AZIZ, K., 1973. A Flow Pattern Map for Gas-Liquid Flow in Horizontal Pipes. *International Journal of Multiphase Flow,* 1, pp. 537-553

74. MARCANO, R., CHEN, X.T., SARICA, C. AND BRILL, J.P., 1998. A Study of Slug Characteristics for Two-Phase Horizontal Flow. In: SPE, ed. *International Petroleum Conference and Exhibition.* March, 1998. Villarhermosa, Mexico: SPE.

75. MATHIS, S.P., 2003. Sand Management: A Review of Approaches and Concerns. In: SPE, ed. SPE European Formation Damage Conference. The Hague, The Netherlands: SPE.

76. MCQUILLAN, K.W. and WHALLEY, P.B., 1985. Flow Patterns in Vertical Two-Phase Flow. *International Journal of Multiphase flow,* 11, pp. 161-175

77. MISHIMA, K., HIBIKI, T AND NISHIHARA, H., 1997. Visualisation and Measurement of Two-Phase Flow by Using Neutron Radiography. *Nuclear Engineering and Design,* 175, pp. 25-35

78. ODDIE, G. et al., 2003. Experimental Study of Two and Three Phase Flows in Large Diameter Inclined Pipes. *International Journal of Multiphase Flow,* 29, pp. 527-558

79. OLIEMANS, R.V.A., 1994. Multiphase Science and Technology for Oil/Gas Production and Transport. *SPE 27958*

80. OLIEMANS, R.V.A AND POTS, B.F.M., 2006. Gas-Liquid Transport in Ducts. In: C.T. CROWE, ed. *Multiphase Flow Handbook.* Boca Raton, USA: Taylor & Francis. pp. 1-40

81. OROSKAR, A. R., AND TURIAN, R. M, 1980. The Critical Velocity in Pipeline Flow of Slurries. *Journal of American Institute of Chemical Engineers,* 26(4), pp. 550-558
82. OUDEMAN, P., 1993. Sand Transport and Deposition in Horizontal Multiphase Trunk lines of Subsea Satellite Developments. *SPE Production & Facilities,*
83. PAULO, C.A., EUPHEMIO, M., NAGLE, F.J.M., OLIVEIRA, P.S. AND MENDONCA, J.E, 2001. Deepwater Field Development - Combination of Mature and Non-conventional Technologies. In: SPE, ed. *Offshore Technology Conference.* May, 2001. Houston Texas, USA: SPE.
84. PEDEN, J.M., FORD, J.T. AND OYENEYIN, M.B., 1990. Comprehensive Experimental Investigation of Drilled Cuttings Transport In Inclined Wells Including the Effects of Rotation and Eccentricity. In: SPE, ed. *SPE Europe 90.* October, 1990. The Hague, Netherlands: SPE. pp. 393-404
85. RAMADAN, A., SKALLE, P. and SAASEN, A., 2005. Application of a Three-Layer Modeling Approach for Solids Transport in Horizontal and Inclined Channels. *Chemical Engineering Science,* 60, pp. 2557-2570
86. RATNAM SATHANANTHAN, March, 2007. *Process Engineering and Flow Assurance Management, for Now & Future.* Cape Town, South Africa: Subsea 7.
87. RIJKENS, F., ALLEN, M. AND HASSOLD, T., 2003. Overview of the Canyon Express project, business challenges and “industry firsts”. In: SPE, ed. *Offshore Technology Conference.* May, 2003. Houston, USA: SPE.
88. RODRIGUEZ, O.M.H. AND OLIEMANS, R.V.A., 2006. Experimental study on oil–water flow in horizontal and slightly inclined pipes. *International Journal of Multiphase Flow,* 32, pp. 323-343
89. RONALDS, B.F., 2006. Features, challenges and opportunities in Australian gas and oil technology. *Journal of Constructional Steel Research,* 62, pp. 1184-1191
90. SALAMA, M.M., 2000. Sand Production Management. *Journal of Energy Resources,* 122, pp. 29-33
91. SCHNEIDER, D.R., 2001. A History of a Gulf of Mexico Deepwater Subsea Production System Development Strategy. *Offshore Technology Conference.* May, 2001.
92. SPEDDING, P.L. AND SPENCE, D.R., 1993. Flow Regimes in Two - Phase Gas - Liquid Flow. *International Journal of Multiphase Flow,* 19(2), pp. 245-280
93. SPEDDING, P.L., DONNELLY, G.F., COLE, J.S., 2005. THREE PHASE OIL–WATER–GAS HORIZONTAL CO-CURRENT FLOW - Experimental and Regime Map. *Chemical Engineering Research and Design,* , pp. 401-411

94. STAPELBERG, H.H., MEWES, D., 1994. The Pressure Loss and Slug Frequency of Liquid-Liquid-Gas Slug Flow in Horizontal Pipes. *International Journal of Multiphase Flow,* 20(2), pp. 285-303

95. STATOIL EXPLORATION AND PRODUCTION, 2012. *The development of ormen lange field.* [online] Norway: Statoil Exploration and Production. Available from: http://www.statoil.com/en/ouroperations/explorationprod/partneroperatedfields/ormenlange/pages/default.aspx [Accessed March, 2007 2007]

96. STEVENSON, P. et al., 2001. The Transport of Particles at Low Loading in Near-Horizontal Pipes by Intermittent Flow. *Chemical Engineering Science,* 56, pp. 2149-2159

97. TAITEL, Y., 1999. Flow Pattern Transition in Two Phase Flow. *Annual Meeting of the Institute of Multifluid Science and Technology,* 2

98. TAITEL, Y. AND DUKLER, A.E., 1976a. A Model for Predicting Flow Regime Transition in Horizontal and Near Horizontal Gas-Liquid Flow. *Journal of American Institute of Chemical Engineers,* 22, pp. 47-55

99. TAITEL, Y. AND DUKLER, A.E., 1976b. A theoretical Approach to the Lockhart-Martinelli Correlation for Stratified Flow. *International Journal of Multiphase Flow,* 2, pp. 591-595

100. TAITEL, Y., BARNEA, D AND BRILL, J.P., 1995. STRATIFIED THREE PHASE FLOW IN PIPES. *International Journal of Multiphase Flow,* 21, pp. 53-60

101. TAKAHASHI, H., MASUYAMA, T. AND NODA, K., 1989. Unstable Flow of a Solid - Liquid Mixture in a Horizontal Pipe. *International Journal of Multiphase Flow,* 15(5), pp. 831-841

102. THOMAS, A.D., 1962. Transport Characteristics of Suspension Part IV. *Journal of American Institute of Chemical Engineers,* 8, pp. 373-378

103. THOMAS, A.D., 1979. Predicting the Deposit Velocity for Horizontal Turbulent Pipe Flow of Slurries. *International Journal of Multiphase Flow,* 5, pp. 113-129

104. TIAN, L., LI, P., JIANG, L. AND HAN, W, 2005. Experimental Study on Critical Velocity in Vertical Pipes for Hydraulic Lifting. In: ISOPE, ed. *The International Society of Offshore and Polar Engineers.* October, 2005. Changsha, China: ISOPE.

105. TRAN-CONG, S., GAY, M. AND MICHAELIDES, E.E., 2004. Drag coefficients of irregularly shaped particles. *Powder Technology,* 139, pp. 21-32

106. TURIAN, R. M. AND T. F. YUAN, 1997. Flow of slurries in pipelines. *Journal of American Institute of Chemical Engineers,* 23, pp. 232-243

107. UNIVERSIDADE FERNANDO PESSOA PORTO, PORTUGAL, 2006. *Turbidite system in hydrocarbon exploration.* [online] Available from: http://homepage.ufp.pt/biblioteca/WEBTurdiDepSystems/Pages/Page2.htm

108. VIELMA, M. et al., 2008. Characterization of Oil/Water Flows in Horizontal Pipes. *SPE Projects, Facilities and Construction,*

109. WELL ENGINEERING RESEARCH GROUP, 2007. *Minimum Transport Velocity Models for Multiphase Fluid Flow in Pipes.* Aberdeen, United Kindom: Well Engineering Research Group.

110. WILSON, K.C., CLIFT, R. AND SELLGREN, A., 2002. Operating Points for Pipelines Carrying Concentrated Heterogenous Slurry. *Powder Technology,* 123, pp. 19-24

111. XU, X.X., 2007. Study on oil–water two-phase flow in horizontal pipelines. *Journal of Petroleum Science and Engineering 59 (2007) 43–58,* , pp. 43-58

112. ZASTAWNY, M., MALLOUPPAS, G., ZHAO, F. AND WACHEM, B., 2012. Derivation of drag and lift force and torque coefficients for non-spherical particles in flows. *International Journal of Multiphase Flow,* 39, pp. 227-239

113. ZHOU, L., AHMED, R.M., MISKA, S.Z., TAKACH, N.E., YU, M. AND PICKELL, M.B., 2004. Experimental Study and Modeling of Cuttings Transport with Aerated Mud in Horizontal Wellbore at Simulated Downhole Conditions. In: SPE, ed. *SPE Annual Technical Conference and Exhibition.* September, 2004.

114. ZUBIR, M.A. AND ZAINON, M.Z., 2011. Two-Phase Flow Behaviour and Pattern in Vertical Pipes. *Journal of Applied Sciences,* 11(9), pp. 1491-1500

Appendix A: Published works from the project

SPE 147045

Minimum Transport Velocity Models for Suspended Particles in Multiphase Flow Revisited

K.O. Bello, SPE, M.B. Oyeneyin, SPE, G.F. Oluyemi, SPE, Robert Gordon University, Aberdeen, United Kingdom

This paper was prepared for presentation at the SPE Annual Technical Conference and Exhibition held in Denver, Colorado, USA, 30 October–2 November 2011.

Abstract
Increasing trend in the transportation of unprocessed reservoir fluid from assets located in remote locations and the drive towards maximising existing facilities and optimising production has encouraged many deepwater operators in the use of long subsea tiebacks.

However, the main challenges associated with unprocessed multiphase fluid flow in long subsea pipelines relate to constantly changing patterns and the likelihood of the suspended particles to settle out of flow and deposit in the transfer pipeline causing partial or complete blockage. Flow pattern transition is therefore a critical factor that must be accounted for in any particle transport models. However, current particle transport models do not account for these critical factors; besides the experimental data on which these models were validated are limited. Therefore they are often unreliable when subjected to varying operating conditions.

In this paper preliminary minimum transport velocity (MTV) models developed for rolling and suspended particles under different flow patterns are presented. The concept of particle velocity profile provided the basis on which the models were developed. Further work is planned to acquire large experimental data for the purpose of validating these proposed models.

The problem has been largely attributed to insufficient flow velocity among other parameters required to keep the solids in suspension and prevent them from depositing in the pipe. Additional complexities are introduced because of different flow regimes that occur within the pipe flow depending on the gas and liquid flow rates.

The development of minimum transport velocity models for suspension and rolling based on the concept of particle velocity profiles is a significant breakthrough in particle transport in multiphase flow. This has the potential to solve problems of pipe & equipment sizing, risk of sand deposition & bed formation, elimination of costs of sand unloading, downtime and generally improve sand management strategies.

Introduction
Multiphase oil-gas-water-solid production and transportation is common in the oil and gas industry. Sand is often produced along with oil and gas from different wells tied into production pipelines / tiebacks. The entrained sand particles in multiphase fluids can be separated either at offshore platforms or can be transported some distance away from the well head to a nearby platforms or a processing facility onshore via a long subsea tieback.

The foray into deeper water is expected to continue due to increasing demands for fossil fuel. So will there be the need to evacuate discovered reservoir fluids from deep / ultra deep offshore locations. The use of long subsea tiebacks for transportation of unprocessed multiphase reservoir fluid will continue to gain considerable application. The drive towards optimising production from remote locations which are hitherto considered marginal and maximixing existing facilities has encouraged many more deep offshore operators in the use of multiphase long subsea tiebacks. It is anticipated that advancement in long subsea tiebacks will ultimately fast track offshore/deep offshore field development at relatively low cost.

However, critical issues of concerns are the need to account for the volume of sand that goes into the tieback from various producing wells considering different wells produces different quantity of sand into the tieback. Ability to track continuous changes in the flow patterns is crucial, as the multiphase fluids move through the long subsea tiebacks with different dimensions and torpographies from horizontal through inclined and vertical angles. These will guarantee flow assurance, reduce/eliminate sand deposition in the pipeline which has potential to cause blockage. Solving these challenges could potentially release huge quantities of yet untapped, isolated and commercially uneconomic oil and gas reserves, in addition to extending the viability of many mature and ageing fields.

Flow assurance is one of the major concerns in multiphase sand transport in deepwater production operations. It is therefore critical that accurate estimate of sand minimum transport velocity (MTV) is known. Critical review of existing literatures with regards to oil-water-gas-solids reveals limited information on the solid transport in multiphase fluids especially when viewed in the context of flow patterns. Few authors that have dealt with the subject mainly focused on the measurement of pressure drops and sand transport rate which is independent of flow patterns [1]. In the development of predictive models for solid transport therefore, the objective is to propose models that will apply to all flow patterns at any inclination.
Consequently, accuracy of solid transport models depends on how well the hydrodynamic is described and predicted with sufficient reliability. Therefore to establish accurate predictive model(s) for minimum transport velocity, it is appropriate to understand the mechanism of interaction of fluid flow and sand particles movements. The best way to achieve this is to determine the velocity profile in multiphase flow especially for each of the flow patterns.
The focus of this paper is to establish different velocity profiles for multiphase given the different flow patterns and evaluate the sand production forcast to ascertain the quantity of sand that gets into the tieback from all the wells that produce into it. These will form the basis for the development of minimum transport velocity (MTV) models for suspension and rolling.

Solid Transport Mechanism & Application of Minimum Transport Velocity
The solid transport mechanism is dependent on several parameters of which the most important are the flow velocity and particle size. These two parameters also determine the flow regime which exists when transportation of solid particles takes place. The key objective however is to keep the solid particles in suspension and/or rolling along the bottom of the pipe to prevent sand bed formation.
For flow of solid, liquid and gas mixtures in long tiebacks, the liquid and solid phases may distribute in a number of configurations. A number of authors have classified slurry patterns in pipes [2, 3]. Oudeman's characterised three regimes of sand motion as

- Flow with a stationary bed
- Flow with a moving bed and saltation (with or without suspension)
- Heterogeneous mixture with all solids in suspension

The solid particles will often be deposited at the bottom of the pipe if the velocity of the liquid and/or gas is very low and will form a stationary bed. The bed becomes stationary when the sum of the driving force acting on the bed is lower than the sum of forces opposing the bed motion [4].The sand grains are either rolling or saltating along the bottom of the pipe when there is increased velocity to keep the solid moving.The transition between a heterogeneous suspension and a sliding bed is often dependent on wether the velocity is decreasing or increasing [5-9]. Other authors have classified solid particle transport patterns in a similar way. In a laboratory experiment carried out by Matousek for pipe flow of various sand fractions; he recognised two distinct flow patterns which varied from fully stratified to fully suspended [10].
The particle transport driving forces are further complicated in a transient multiphase flow environment. Multiphase fluid flow is a transient phenomenon. The flow of multiphase production in the long tieback will be accompanied by pressure drop with the multiphase pattern generally changing as a result, from Dispersed Bubble through to Slug, Plug, Annular and Statified flow patterns depending on liquid-liquid-gas void fractions, pipe angle among other factors. Solids entrainement in the different flow patterns as they are transported will therefore be subjected to different driving forces
Of greater importance therefore is the need to know the multiphase pattern change and if, when and where solid will settle in the pipeline / tiebacks? The critical issues with respect to especially tiebacks are:

1. How much sand is produced into the tieback.
2. What are the prevailing multiphase patterns , the transition zones and impact on solid-fluid interaction
3. If solids will settle given the inherent operational conditions, probably yes.
4. When will the solid settle, how much and height of sand in the pipe.
5. Where will solid settle.

These among other critical issues pose serious threat to flow assurance. The desire is to avoid the formation of a stationary deposit while transporting the entrained solids in multiphase fluids which may cause complete / partial blockage of the pipe, thus reducing its efficiency. Thus the prediction of solids settling point will enhance deployment of appropriate pig for pipeline cleanup.
Detailed quantitative risk assessment of solids transport in subsea tiebacks requires the development of accurate models for predicting the key factors listed above. For practical purposes and to simplify the complex phenomena, the concept of Minimum Transport Velocity (MTV) transport mechanism has been adopted. The underlying principle of the MTV concept is that solids in subsea tiebacks will be transported as long as they are upwardly mobile whether by rolling/siliding along the low side wall of a pipeline or in heterogeous suspension. Therefore, there exists a minimum or critical velocity for each of these transport mechanisms to occur. These are referred to as the MTV for Rolling and MTV for Suspension. Thus for average fluid velocity below the MTV for rolling, stationery bed will result. For velocity below the MTV for suspension will result in the solids sliging along the pipe wall which may eventually result in stationary bed as the pressure drops along the pipeline causing further reduction in the particle drag forces.
The unique concept of velocity profile has been used in this study for the development of appropriate minimum transport velocity (MTV) models for solid transport in subsea tiebacks. This concept assumes that the fluid point velocity acting on a

solid particle on the low side wall of the hole needs to be greater than the minimum transport velocity for the solid particle to be upwardly mobile. In the development of velocity profile models, we have used a combination of analytical and numerical methods.

Computational fluid dynamics software was used for numerical computation whilst equation (1) was used as the basis for analytical computation to generate appropriate velocity profile models for different flow patterns.

The actual velocity profile can be computed analytically for laminar and turbulent flows as given by equation (1) [11]

$$V_R = \frac{f}{8} * R_e * V * \left[1 - \left(\frac{r}{R}\right)^2\right] \tag{1}$$

If $f = \dfrac{16}{R_e}$ for laminar flow, then

$$V_R = 2V * \left[1 - \left(\frac{r}{R}\right)^2\right] \tag{2}$$

V_R- Velocity of fluid particle at a particular point in the pipe cross-section,
V – Average velocity of the fluid s in the pipeline,
r – Distance from the pipeline centre to any point in the flow field
R - Radius of the pipeline.
R_e- Fluid Reynolds number which defines the fluid flow regime whether laminar or turbulent flow
f = Fluid flow friction factor which is a function of the pipe roughness, fluid flow regime and type of fluid

Based on the above, velocity profile model is developed for multiphase flow presented in equation (3) below. The model is strongly dependent on Reynolds number and pipe friction factor.

$$V_R = A * f * R_e^B * \left[1 - \left(\frac{r}{R}\right)^2\right]^C \tag{3}$$

Where, f is the friction factor adopted from Blasius correlation, Re is the Reynolds number. The constants A, B & C are as defined in Table 1.

The model has been tested and found to predict the velocity profiles in liquid (oil) see figure 3. A hybrid of this model has been developed for multiphase gas, oil and water.

Multiphase Flow Patterns

Simultaneous passage of gas and liquid in a pipe often results in a variety of flow patterns. Two-phase flow or three-phase flow are simultaneous flow of the discrete phases (gas or multiple liquid). These phases are commonly encountered in the petroleum or allied industry. For subsea deepwater developments, the multiphase production is inevitable especially in the tieback.

In the subsea tieback, the multiphase fluid would generally be made up of gas, oil, condensed water, formation water, chemical inhibitors [hydrate and scale inhibitors] and of course produced solids. The multiphase fluid flow is transient and accompanied by pattern transition which is dependent on flow rates, fluid properties, pipe size, torpography and corresponding pressure drop. The concept of flow patterns in pipes introduces new challenges in the understanding of multiphase fluids principally because of the form in which the fluids exist in pipes. The pipe may be horizontal, near horizontal or vertical or a combination of all depending on the torpography. For gas-oil-water-inhibitor phases, the flow patterns can be grouped into four main classes where each class can be subdivided into sub-classes for detailed description as reported by a number of authors [13, 14, 15].

- Stratified flow (Subclasses: stratified smooth, stratified wavy)
- Intermittent flow (Subclasses: elongated bubble, slug, churn)
- Annular flow (Subclass: wispy annular)
- Bubble flow (Subclasses: bubbly, dispersed bubble)

For the purpose of the research presented in this paper, the patterns have been grouped into:

- Dispersed Bubble
- Annular Flow[for low AGR in gas producers with formation water, condensed water, hydrate inhibitor, etc]
- Slug Flow
- Plug Flow [In vertical pipe sections]
- Stratified Flow[In highly deviated and horizontal pipe sections]

Figures 1a & 1b show general two phase flow patterns for horizontal and vertical pipes [17]

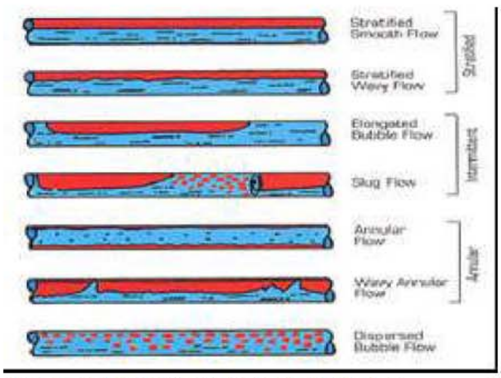

Fig. 1a: Flow patterns in horizontal pipe

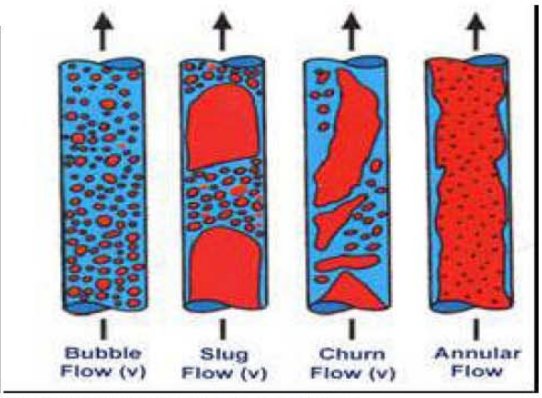

Fig. 1b: Flow patterns in vertical pipe

For oil dominated systems the possible flow patterns are dispersed bubble and intermittent flow. For relatively low gas and liquid rates a stratified configuration occurs with the liquid flowing on the bottom and the gas flowing above it [16]. It is important from the designer's point of view to be able to predict accurately which flow pattern will occur for given input flow rates, pipe size, and fluid properties [17]. Only then can the appropriate flow model be developed. Methods for the prediction of flow pattern are well established in the literatures [18, 19]. However, limited efforts have been directed towards investigating multiphase oil, gas, water [Formation and condensed waters] and inhibitor phenomenon [20, 21].

MTV Models in Multiphase Flow

The significant of velocity profiles in pipe flow as earlier established can be extended to flow of multiphase in pipes. However, the flow of multiphase fluids must be treated differently as it introduces different complexities. There are issues of changing flow patterns as multiphase fluids moves through the pipelines/tiebacks. The importance of predicting different flow patterns in multiphase flows is well established. Knowledge of flow pattern and flow pattern transitions is essential to the development of reliable predictive tools in multiphase solids transport. As the pattern changes so the transport velocity will vary. In order to track the patterns, velocity profile models have been developed for each of the common flow patterns in multiphase hydrocarbon fluid production as part of the research study by the Well Engineering Research Group at Robert Gordon University (RGU).

For example, the flow velocity profiles obtained from CFD for liquid and gas superficial velocities are shown in Figure 2. The observed changing patterns (dispersed bubble flow and stratified flow) at different points along the pipe length from the inlet are an indication of continuous changes in flow patterns as the fluids move through the pipes. What is obvious here is that not one model is adequate for description of multiple patterns encountered in multiphase flow in pipelines.

The above observations therefore informed development of velocity profile models for each of the important flow patterns encountered in multiphase flow in tiebacks / pipelines such as dispersed bubble flow, annular flow and slug flow. The composite equation is as given in equation 4 below. The results of the models compare well with data obtained from CFD simulation. Some of the results from CFD for velocity distribution are shown in Figure 3 to 6.

$$V_R = A * f * R_e^B * V_{\max} * \left[1 - \left(\frac{r}{R}\right)^2\right]^C \tag{4}$$

Where A, B & C are constants defined in the Table 1 below for different flow patterns.

Table 1: Constants of equations for different flow patterns

Flow Pattern	A	B	C
Disp. Bubble	3 – 4	0.2 – 0.5	0.1 – 0.5
Annular Flow	1 - 2	0.2 - 1	0.1 – 0.5
Slug Flow	2.5 – 3.5	0.3 – 0.5	1 – 1.5
Single Phase	0.001-0.003	1 - 2	0.1 – 1

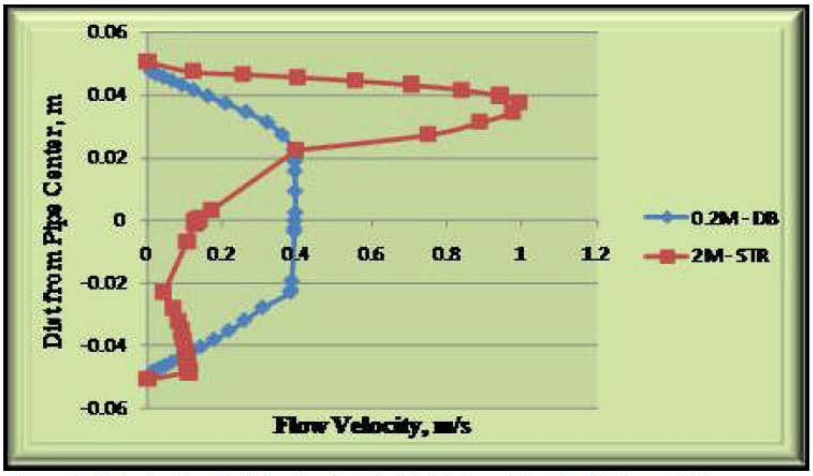

Figure 2: Velocity Profile Distributions in Multiphase Flow in Horizontal Pipe.

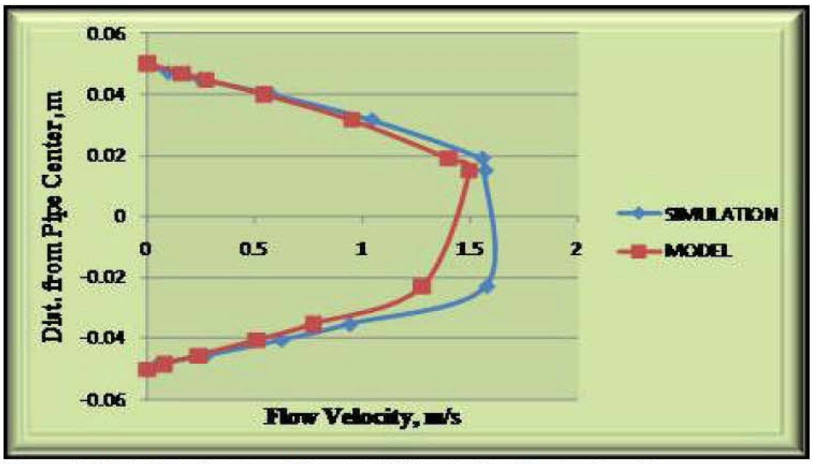

Figure 3: Model Predicted and Simulated Velocity Profiles for Slug Flow.

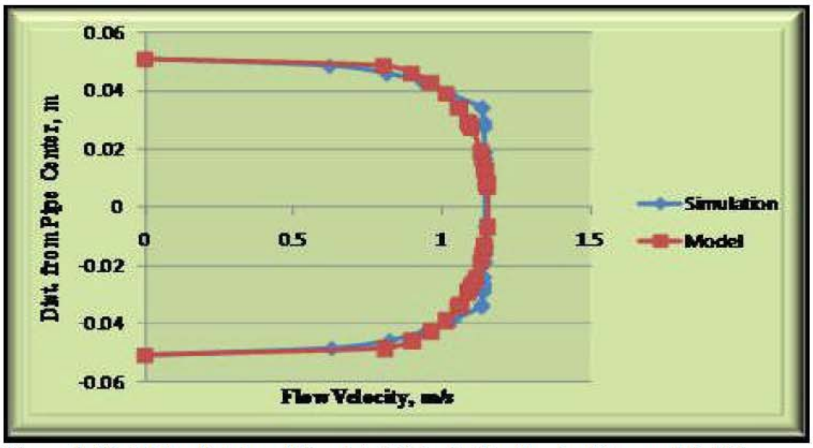

Figure 4: Model Predicted and Simulated Velocity Profiles for Dispersed Bubble.

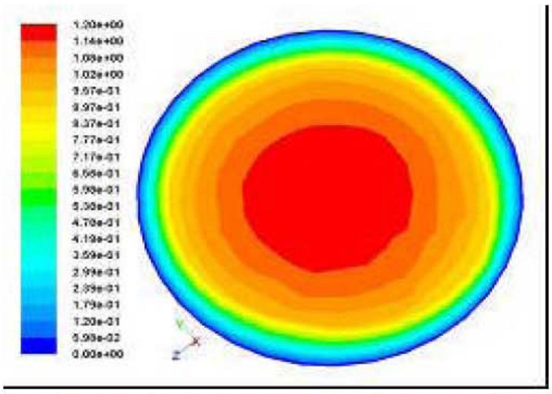

Figure 5: Velocity Profile Distribution for Dispersed bubble in Horizontal Pipe

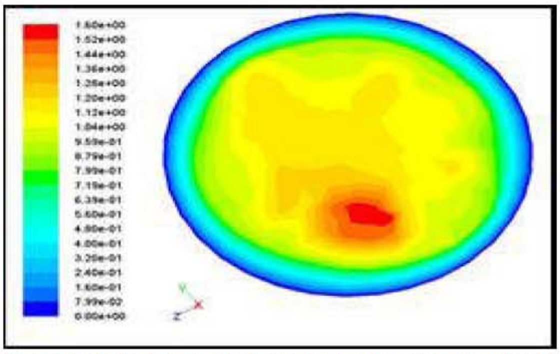

Figure 6: Velocity Profile Distribution for Slug Flow in Horizontal Pipe

The models are strongly dependent on friction factors and Reynolds number. The pseudo-average friction factor and the mixture Reynolds number have been used in this study and are greatly important in order to develop an appropriate correlation for each of the multiphase patterns. A number of two-phase friction factor correlations were considered. The composite friction factor correlations for different flow patterns of Garcia et al (2003) were adopted [12]. This has worked best for this study. The results from the developed models indicated close match when compared with data from CFD.

The concept of MTV specifies definition of the minimum point velocity that should move a solid particle on the low side of a pipe. When the fluid velocity is above minimum to ensure rolling or suspension of the particles, then the particle will be continuously mobile. Settling of solid particles can be avoided with flow velocities above MTV.

Based on this concept, minimum transport velocity models for suspension (eq. 7) and rolling (eq. 8) were developed.

For Suspension: $$V_m = A * \left[\frac{g d_p}{C_L \rho_L} * (\rho_P - \rho_L) \sin\theta \right]^B \left[\frac{D \rho_L}{\mu_L} \right]^C \quad (7)$$

For Rolling: $$V_m = \left[\frac{A * d_p \left[\frac{\rho_P}{\rho_f} - 1 \right] g * [\cos\theta + f_s * \sin\theta]}{[C_D + f_s C_L]} \right]^B \quad (8)$$

For Vertical Pipe

$$V_m = A * \left[\frac{g d_p (\rho_p - \rho_f)}{C_D \rho_f} \right]^B \quad (9)$$

Where C_D & C_L are drag and lift coefficients, ρ_p & ρ_f are particle density and fluid density, d_p is the particle size. A, B & C are constants as defined in the Table 2 below.

$$C_D = \left[\frac{a}{\mathrm{Re}_p^{\,b}}\right] \quad ; \qquad C_L = \left[\frac{c}{\mathrm{Re}_p^{\,d}}\right] \tag{10}$$

$$\mathrm{Re}_p = \left[\frac{\rho_f v_p d_p}{\mu_f}\right] \tag{11}$$

Re_p = Particle Reynolds's Number

a, b and c are empirical constants

Table 2: Constants of equations 7 & 8 for different flow patterns

MTV	A	B	C
Suspension	0.01-0.03	0.5- 1	0.5 - 1
Vertical Pipe	4 – 6	0.1 - 1	-

Analysis of Results

Prametric studies have been carried on different pipe sizes using the developed models. The example results for a 4-in pipe system are presented in Figures 7 to 9.

The current study has shed more light on the interaction of solid particles and fluid movements in the pipeline / tieback given different flow patterns scenerios. It is also clear from the results obtained that a single model cannot be used to predict the MTV for all the flow patterns as highlighted in Figures 7 to 9. There is a huge difference both in terms of MTV for suspension and rolling for dispersed bubble, slug and single phase.

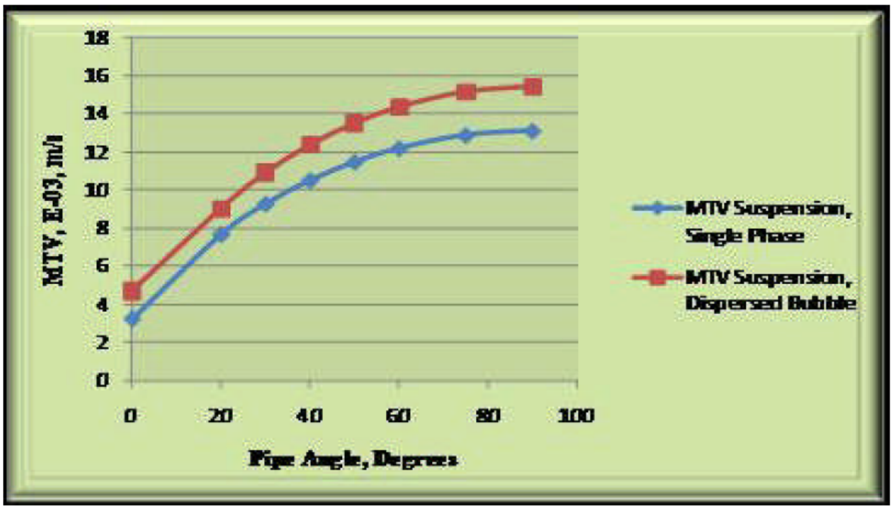

Figure 7: Comparison of MTV Suspension for Single Phase & Dispersed Bubble

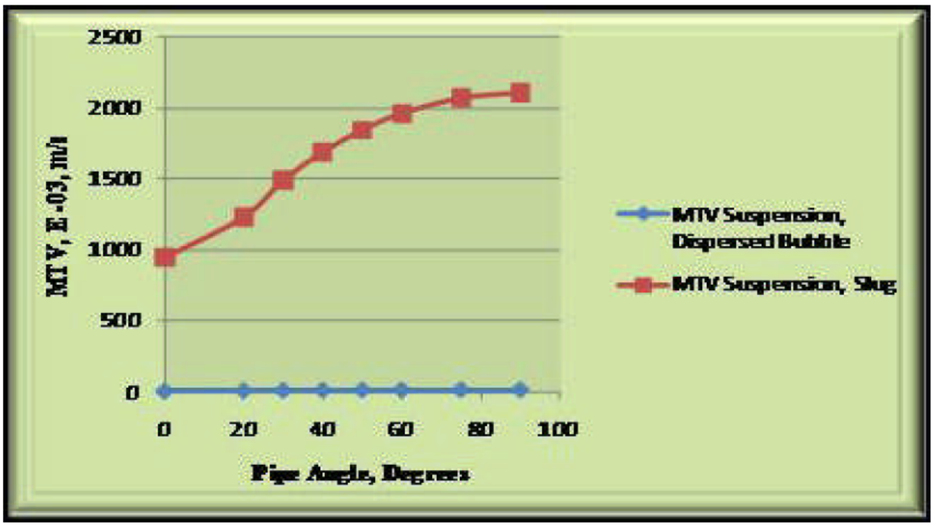

Figure 8: Comparison of MTV Suspension for Slug & Dispersed Bubble

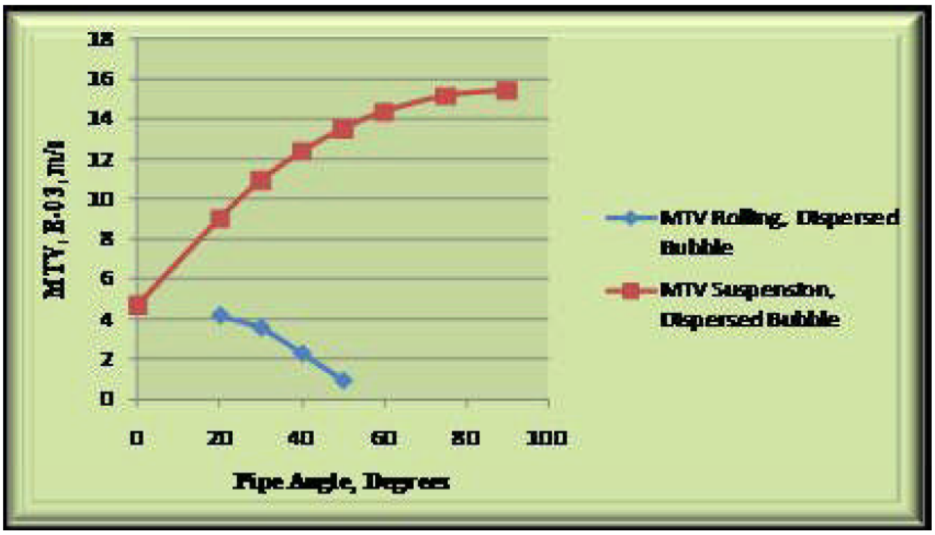

Figure 9: Comparison of MTV Rolling & Suspension for Dispersed Bubble

Conclusions

The studies so far has highlighted the significant gap in the existing solid transport models as applied to multiphase production and multiple fluid flows in subsea tiebacks. This has been largely due to limited understanding of the underlying physics of sand motion in multiphase fluids. The adoption of minimum transport velocity using the velocity profiles concept has thrown more light on solid transport mechanism in multiphase flow.

There is still more to be done. One key issue is the dearth of experimental data in public domain for testing and validation of multiphase flow solids transport models. In order to improve on the transport models, the Well Engineering Research group at The Robert Gordon University has designed and constructed a representative flow loop for comprehensive experimental investigation as part of the set objectives of developing robust MTV models for multiphase sand transport in subsea tiebacks. This will be followed by the development of the prediction model for solids settling point and the volume of solids. The final objective will focus on the development of appropriate management strategy for subsea tiebacks with proactive capability that integrates the in-house sand production prediction model at RGU with the multiphase flow models under development that captures the transient phenomena, and defines the systematic approach to subsea tieback management for effective flow assurance.

Table 3: Numenclature

Numenclature	***Defination***	***Unit***
C_D	*Drag coefficient*	-
C_L	*Lift coefficient*	-
d_p	*Particle size*	*m*
D	*Pipe diameter*	*m*
ρ_f	*Liquid density*	*kg/m*^{3}
ρ_m	*Mixture density*	*kg/m*^{3}
ρ_p	*Particle density*	*kg/m*^{3}
f	*Friction factor*	-
g_c	*Acceleration due to gravity*	*m/s2*
r	*Distance from pipe centre*	*m*
R	*Pipe radius*	*m*
Re	*Reynolds number*	-
[illegible]	*Particle Reynolds number*	-
V_R	*Velocity profile*	*m/s*

References

1. Bello, O.O, Reinicke, K.M and Teodorin, C.: Particle Holdup Profiles in Horizontal Gas-liquid-solid Multiphase Flow Pipeline. Chemical Engineering Technology, Vol. 28 PT 12, PP 1546-1553. 2005
2. Oudeman, P. 'Sand Transport and Deposition in Horizontal Multiphase Trunk lines of Subsea Satellite Developments'. SPE Production & Facilities, November, 1993.
3. Lahiri, S.K. and Ghanta, K.C.: Minimize Power Consumption in Slurry Transport Accurately Predict Critical Velocity. Piping / Fluid Flow, Hydrocarbon Processing, Dec. 2008.
4. Doron, P. and Barnea D: A Three-Layer Model for Solid-Liquid Flow in Horizontal Pipes. International Journal of Multiphase Flow, Volume 19, Pages 1029-1043 1993.
5. Chen, X. and Guo, L.: Flow Patterns and Pressure Drop in Oil-Air-Water Three Phase Flow through Helically Coiled Tubes. International Journal of Multiphase Flow, Volume 25, Pages 1053-1072 1999.
6. Stevenson, P. et al: The Transport of Particles at Low Loading in Near-Horizontal Pipes by Intermittent Flow. Chemical Engineering Science, Volume 56, Pages 2149-2159 2001
7. Akilli, H, Levy, E.K. and Sahin, B: Gas-Solid Flow Behavior in a Horizontal Pipe after 90° Vertical-to-Horizontal Elbow. Powder Technology, Volume 116, Pages 43-52 2001.
8. Liu, H: Pipeline Engineering. Lewis Publisher, A CRC Press Company, 2003.
9. Danielson, T.J: Sand Transport Modeling in Multiphase Pipelines. Offshore Technology Conference, OTC 18691, May 2007.
10. Matousek, V.: Research Development in Pipeline Transport of Settling Slurries. Powder Technology, Volume 156, Pages 43-51 2005.
11. Govier, G.W. and Aziz, K.: The Flow of Complex Mixtures in Pipes. Van Nostrand Reinhold. New York, 1972.
12. Garcia, F.: Power law and composite power law friction factor correlations for laminar and turbulent gas–liquid flow in horizontal pipelines. International Journal of Multiphase Flow, volume 29, pp 1605 – 1624, 2003.

13 Taitel Y.: Flow Pattern Transition in Two Phase Flow. 2nd Annual Meeting of the Institute of Multifluid Science and Technology, March 1999.

14 Hurlburt, E.T. and Hanratty, T.J.: Prediction of the transition from stratified to slug and plug flow for long pipes. International Journal of Multiphase Flow 28 (2002) 707–729.

15 Lin, P.Y. and Hanratty, T.J.: Effect of Pipe Diameter on Flow Patterns for Air-Water Flow in Horizontal Pipes. International Journal of Multiphase Flow Vol. 13, No. 4, pp. 549-563, 1987.

16 Oliemans, R.V.A: Multiphase Science and Technology for Oil/Gas Production and Transport. SPE Paper Number 27958, August 1994.

17 Mandhane, J.M., Gregory, G.A. and AZIZ, K.: A Flow Pattern Map for Gas-Liquid Flow in Horizontal Pipes. Int. Journal of Multiphase Flow, Vol. 1, pp. 537-553.

18 Oddie, G et al: Experimental Study of Two and Three Phase Flows in Large Diameter Inclined Pipes. International Journal of Multiphase Flow, Vol. 29, Pg. 527-558, 2003.

19 Barnea, D: A Unified Model for Predicting Flow Pattern Transitions for the Whole Range of Pipe Inclinations. International Journal of Multiphase Flow, Vol. 13, Pages 1-12 1987.

20 Acikgoz, M. et al: An experimental Study of Three-Phase Flow Regimes. Int. J. Multiphase Flow Vol. 18, No. 3, pp. 327-336, 1992

21 Keskin, C. and Zhang, H.: Identification and Classification of New Three-Phase Gas/Oil/Water Flow Patterns. SPE 110221, 2007.

Advanced Materials Research Vol. 367 (2012) pp 413-420
Online available since 2011/Oct/24 at www.scientific.net
© (2012) Trans Tech Publications, Switzerland
doi:10.4028/www.scientific.net/AMR.367.413

A Novel Approach to Subsea Multiphase Solid Transport

Kelani Bello[1, a], Babs Oyeneyin[2,b] and Gbenga Oluyemi[3,c]

[1,2,3]The Robert Gordon University, Aberdeen, United Kingdom

[a]k.o.bello@rgu.ac.uk; [b]b.oyeneyin@rgu.ac.uk; [c]g.f.oluyemi@rgu.ac.uk

Keywords: Multiphase fluids, Subsea tiebacks, Solid transport, Flow loop, Model development.

Abstract: Transportation of multiphase reservoir fluid through subsea tiebacks has gained considerable attention in recent years especially in the deep offshore and ultra deep offshore environments where there is increasing pressure on the operators to reduce development costs without compromising oil production. However, the main challenge associated with this means of transporting unprocessed reservoir fluids is the need to guarantee flow assurance and optimise production. Solids entrained in the fluid may drop off and settle at the bottom of horizontal pipe thereby reducing the space available to flow and causing erosion and corrosion of the pipeline. The problem has been largely attributed to insufficient flow velocity among other parameters required to keep the solids in suspension and prevent them from depositing in the pipe. The continuous changing flow patterns have introduced additional complexities dependent on gas and liquid flow rates. Acquisition of experimental data for model development and validation in multiphase flow has been largely focused on single and two phase flow. This has impeded our understanding of the behaviour and associated problems of three phase or four phase (oil, water, gas and solid) in pipes. The result is inappropriate solid transport models for three phase and four phase. In order to bridge this gap, the Well Engineering Research group at Robert Gordon University has initiated a project on integrated multiphase flow management system underpinned by comprehensive experimental investigation of multiphase solids transport. The project is aimed at developing precise/accurate sand transport models and an appropriate design and process optimisation simulator for subsea tiebacks. In this paper, the physics of the multiphase transport models being developed is presented. The models will allow for the prediction of key design and operational parameters such as flow patterns, phase velocity, pressure gradient, critical transport velocity, drag & lift forces, flow rate requirements and tiebacks sizing for transient multiphase flow. A new multiphase flow loop is being developed which will be used to generate experimental database for building and validating the theoretical models for use in a proposed integrated simulator for deepwater applications.

Introduction

Multiphase fluids transportation through a pipeline has gained considerable acceptance in the oil and gas production offshore [1]. As a result, there are increasing numbers of deepwater fields which are developed with long distance subsea tiebacks in excess of 200 km length either to a host facility or directly to the beach (Figure 1). It is anticipated that many deep offshore discoveries can be developed as subsea satellite of existing production platforms, particularly marginal fields that are hitherto considered uneconomical. As more and more discoveries are made in deeper water and the world remains hungry for oil and gas, we can expect to see many more tieback developments in the future.

However, the production and transportation of these unprocessed reservoir fluids through a pipeline is prone with many technical challenges, such as solid depositions, especially along the low sides of pipeline causing partial or complete blockage, uncertainties in flow patterns determination, slugging, possible phase separations, among others are common problems in multiphase transport system, [2,3]. All these will continue to be crucial for enhanced production, recovery and flow assurance. The methods and means of intervention in the deepwater environment are limited and often result in higher intervention costs. Therefore understanding the mechanism of sand transport in multiphase flow lines taking into account the continuous changing in flow patterns will have direct impact on estimation, design and detail analysis of subsea tiebacks.

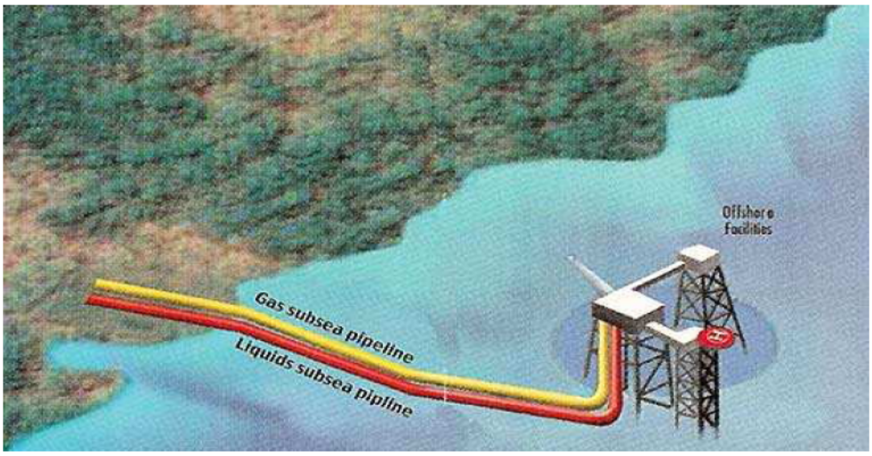

Figure 1 A typical long subsea tieback

Multiphase Flow Patterns

Simultaneous passage of gas and liquid in a pipe results in a variety of patterns. The concept of flow patterns in pipes introduces new challenges in the understanding of multiphase fluids principally because of the form fluids exist in pipes. The pipe may be horizontal, near horizontal or vertical. In the subsea tieback, the multiphase fluid would generally be made up of gas, oil, condensed water, formation water, chemical inhibitors [hydrate and scale inhibitors] and of course produced solids. The multiphase fluid flow is transient and accompanied by pattern transition which is dependent on flow rates, fluid properties, pipe size, torpography and corresponding pressure drop. This may be classified into two different flow modes, fluid flow modes and solid transport modes. Two phase flow patterns and flow pattern transitions are well established in the literatures [4, 5], see Figures [2a & 2b] for flow patterns in two phase, liquid-gas flow.

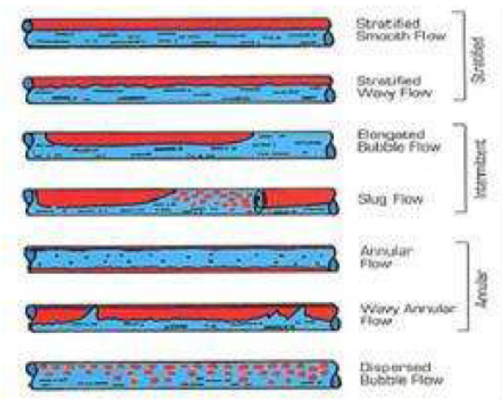

Figure 2a Flow patterns in horizontal pipe

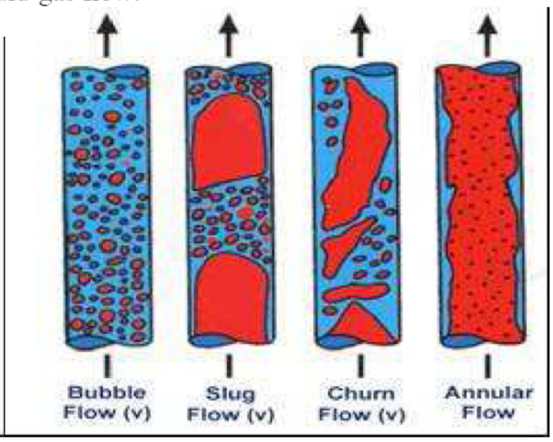

Figure 2b Flow patterns in vertical pipe

The solid transport modes in horizontal pipe can occur as illustrated by [Figure 3]. At low flow rates the entrained sand is deposited at the bottom of the pipe. This will lead to local sand build up. However, above certain critical velocity, the grains start to move, initially as dunes and at higher velocity as a continuous sand bed [6]. With increasing velocity, more particles are suspended in the fluid above the bed until, at some critical velocity, the bed vanishes.

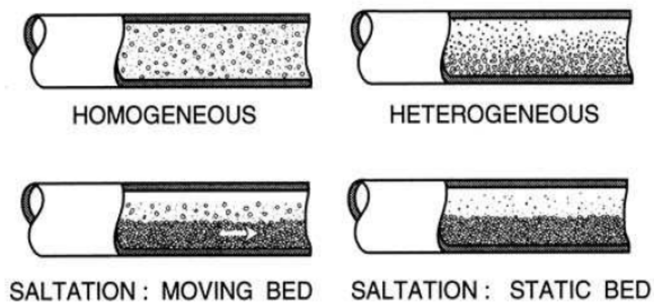

Figure 3 Typical flow patterns in horizontal pipe of solid–liquid (Brennen, 2005)

Flow Pattern Characterisation: The description of flow patterns in pipes is complicated by the existence of an interface between the phases. These interfaces exist in a wide variety of forms depending on the fluid properties, pipe geometry and physical properties of the phases. Predicting flow patterns in multiphase flow in pipes is a rather complex exercise. Experimental data is widely used for the prediction of flow patterns. It involved the collection of experimental data followed by mapping of the data in a two-dimensional plot by locating transition boundaries between the flow patterns. Such a plot is termed flow pattern map, Figure 4. Another approach is the mechanistic modelling. In this approach, the dominant physical phenomena that will cause a specific transition are identified. It is recommended that both approaches are combined. Clearly there exist a number of problems with identifying and defining flow patterns and flow pattern transitions and establishing their range of applicability. For example, the criteria under which waves on stratified liquid flow are expected to grow are given by equation (1). The annular flow is expected to take place under condition of equation (2), [7].

$$\boxed{U_G \geq \left[\frac{4v_L(\rho_L-\rho_G)\rho Cos\beta}{s\rho_G U_L}\right]^{1/2}} \tag{1}$$

$$\boxed{U^2{}_L \geq \frac{gD\left(1-\overline{h}_L\right)Cos\beta}{f_L}} \tag{2}$$

Where $\overline{h}_L = \dfrac{h_L}{D}$, ratio of liquid level to pipe diameter.

Bubble flow is considered the limiting case of slug flow when the liquid slug is free of entrained bubbles. As the liquid flow rate is increased, the bubbles become more evenly distributed over the cross-section of the pipe. Barnea [7] suggested that bubble flow occur when equations (3) is satisfied. The transition from bubble flow to slug flow can be predicted by equation (4)

$$\boxed{D \triangleright 19\left[\frac{(\rho_L-\rho_G)\delta}{g\rho^2{}_L}\right]^{1/2}} \tag{3}$$

$$\boxed{U_{LS}=\frac{1-\alpha}{\alpha}U_{GS}-1.53(1-\alpha)\left[\frac{(\rho_L-\rho_G)g\delta}{\rho_L}\right]^{1/4} Sin\beta} \tag{4}$$

Where α is the void fraction equal 0.25, U_{LS} &U_{GS} are liquid and gas superficial velocities, ρ is the density for liquid and gas, δ is the surface tension.

Accurate description of the flow patterns and flow patterns boundary will continue to generate interest because of lack of complete understanding and subjective definitions by to different authors.

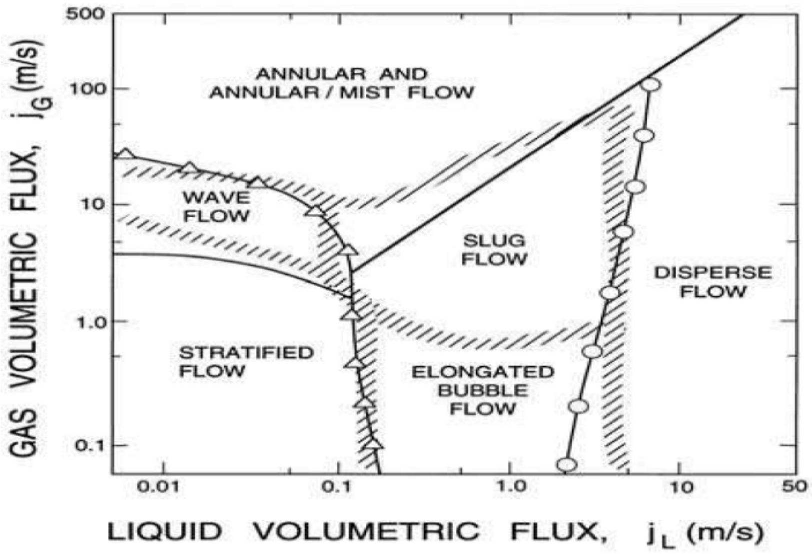

Figure 4 Two phase flow pattern map in a horizontal pipe [6]

Critical Issues of Multiphase Flow – Solid Transport Management

Transportation of unprocessed reservoir fluids through long subsea tiebacks will continue to be crucial for the evacuation of verse oil and gas resource in the deep and ultra deep offshore. The key issues of concerns are related to the fundamental understanding of the flow patterns in multiphase fluids with regards to particle transport models and the need to guaranty flow assurance and optimise production. There is the need to track pattern changes and identify prevailing patterns at any point in the tieback. The two-phase, liquid-solid transport and three phase liquid, gas and solid in horizontal pipes are widely reported [9, 10, 11 & 12]. The prediction of flow patterns in gas-liquid flow in pipes is one of the most important problems in two-phase flow. Traditionally, the approach that has been used to treat this problem was to correlate the data and to plot the results on a flow-pattern map. A wide variety of maps with different coordinate systems have been published [13]. See Figure 5. The pattern classifications are often different from one author to the other. Some have adopted the use of superficial velocity and some others have used pressure drop as means of classifications.

The transition between a heterogeneous suspension and a heterogeneous suspension with a sliding bed is often depended on whether the velocity is decreasing or increasing. Of greater importance however, is the need to know if, when and where solid will settle in the tiebacks?

1. If solid will settle given the inherent operational conditions, probably yes.
2. When will solid settle, how much and height of sand in the pipe.
3. Where will solid settle, this will enhance appropriate deployment of pig.

These among other critical issue pose serious threat to flow assurance. The desired is to avoid the formation of a stationary deposit which may cause complete/partial blockage of the pipe.

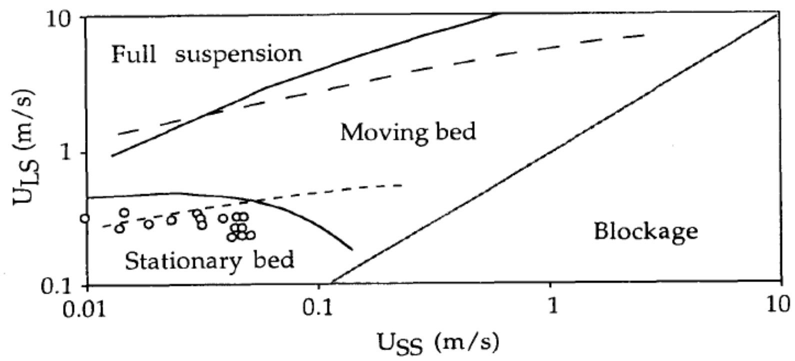

Figure 5 A flow pattern map for solid-liquid flow in pipe

However, there are three ways in which the prediction can be achieved, [14].

1. Experimentally, through laboratory sized models equipped with appropriate instrumentation.
2. Theoretically, using mathematical equations and model for the flow
3. Computationally, using the power and size of modern computers to address the complexity of the flow.

Theory of Solid Movement through a Fluid: Reservoir fluids and entrained solids are commonly transported from the wellhead through long subsea tiebacks to onshore or to processing facility. Sand particle transport can generally be described in terms of the forces acting on the solid of mass m moving in a fluid. The three compelling forces are, gravity force, F_G acting downward, lift force, F_L , acting upward and drag force, F_D , acting perpendicular [15],
Where

$$F_G = mg \tag{5}$$

$$F_L = \frac{m\rho g}{\rho_P} \tag{6}$$

$$F_D = C_D u^2 \frac{A_P \rho}{2} \tag{7}$$

m is the mass of particle, g the acceleration due to gravity, ρ is the fluid density, ρ_P is the particle density, A_P is the projected area of the particle, C_D is the drag coefficient and u is the velocity of the particle relative to the fluid.
The resultant force will equals the force due to acceleration

$$m\frac{du}{dt} = mg - \frac{m\rho g}{\rho_P} - C_D u^2 \frac{A_P \rho}{2} \tag{8}$$

In many practical use of centrifugal force, $\frac{du}{dt}$ is neglected. For a spherical particle of diameter D_P

$$m = \frac{\pi D_P^{\,3} \rho_P}{6} \tag{9}$$

$$A_P = \frac{\pi D_P^{\,2}}{4} \tag{10}$$

Solving equation (8) for velocity, u and substituting m *and* A_P from equation (9) & (10), we can write

$$u = \sqrt{\frac{4gD_P(\rho_P - \rho)}{3C_D \rho}} \tag{11}$$

Equation (11) is the general form of sand transport equation in fluid.
The drag coefficient C_D is a function of particle Reynolds number. The particle Reynolds number can be expressed as

$$N_{\mathrm{Re}\,p} = \frac{u D_p \rho}{\mu} \qquad (12)$$

μ is the viscosity of the fluid.

$$C_D = \frac{a}{N_{\mathrm{Re}\,p}^{\;b}} \qquad (13)$$

a and b are empirical constants.

Drag force is present in all types of flow around solids particles and is mostly superior over other forces during particle transportation, [16]. The proposed experiment will define the empirical constants and establish a generalised drag coefficient equation for different flow patterns and particle Reynolds numbers.

Review of Solid Transport Models: A number of models exist in the literature to estimate particle transport velocity in horizontal pipelines. Probably the most important requirement in the design of any hydraulic transport system is knowledge of the critical deposit velocity, the velocity below which a stationary bed of solids will appear in the bottom of the pipe. In the development of predictive models for solid transport, the objective should be to propose models that will apply to all flow patterns at any inclination. The approach adopted in this paper is to compare the results of selected models from the literature including that developed in house with the same data input. Eight models were compared and the results presented in (Figure 6). It is apparent that there is huge difference in the model results. Engineers are therefore faced with choice of appropriate models for the prediction of particle transport in multiphase. Using the concept of velocity profile will greatly increase the accuracy of the models as this originates from the physics of particle fluids interaction in multiphase flow.

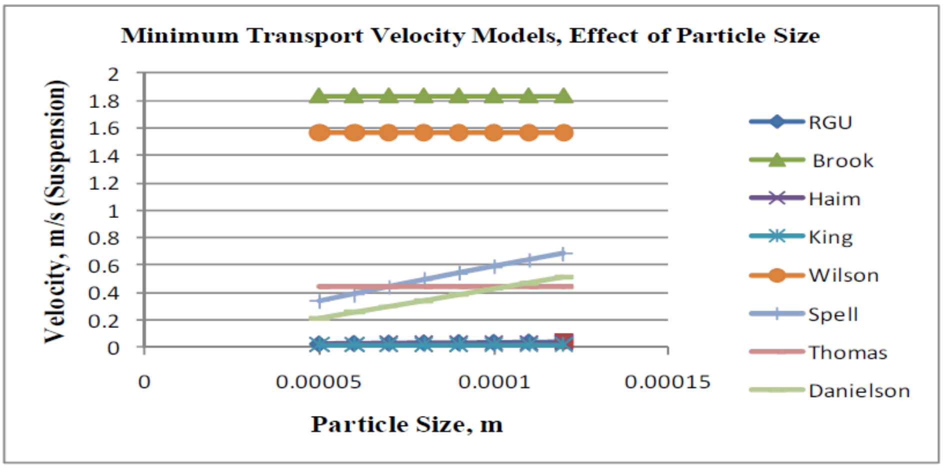

Figure 6 Comparison of Minimum Transport Velocity Models

Conclusion

In this paper an evaluation of some of the existing particle transport velocity models have been carried out to determine their accuracy for prediction purposes. Eight models were evaluated, and results were presented. As can be seen, the models gave different results. This has demonstrated the inadequacy of the existing models to accurately predict the particle transport in pipes. There is huge difference in the prediction for different models. It therefore evident that single phase models upon existing models were developed cannot be used for multiphase flow. These are perhaps reason why the existing models have limited applications. The observed inconsistencies in the results further justified the need for a new model for multiphase that take into account flow patterns transitions. Given the huge investment associated with the operation of subsea tiebacks, it is obvious there is little room for such inaccuracy.

It does appear that the existing models are user specific and cannot be used with confidence for different condition of flow patterns. It is therefore clear that a new approach is required.
The key issue here is the lack of understanding of physics of solid liquid interaction and limited experimental data for testing and validation of models. This is especially important given the current efforts in the deep/ultra deep offshore.

The need to fully understand the phenomena of multiphase solids transport in subsea tiebacks is the key driver behind the new multiphase flow loop being purposely developed for detailed experimental studies.

References

[1] R.V.A Oliemans: Multiphase Science and Technology for Oil/Gas Production and Transport. SPE Paper Number 27958, August 1994.

[2] E.I. Heng, B.F. Ronalds, T.J. Edwards: The Deepwater Subsea Tieback Option for Future Oil and Gas Production in Australia. SPE Asia Pacific Oil and Gas Conference and Exhibition, Brisbane, October, 2000.

[3] I.G. Ball: Challenges of Long Satellite Tiebacks. Offshore Technology Conference, May 2006.

[4] P. Oudeman: Sand Transport and Deposition in Horizontal Multiphase Trunk lines of Subsea Satellite Developments. SPE Production & Facilities, November, 1993.

[5] M. Vielma, S. Atmaca, C. Sarica and H. Zhang: Characterization of Oil/Water Flows in Horizontal Pipes. SPE Projects, Facilities and Construction, December, 2008.

[6] C.E. Brennen: Fundamentals of Multiphase Flows. Cambridge University Press, 2005, ISBN 0521848040.

[7] D. Barnea, O. Shoham, Y. Taitel and A.E. Dukler: Flow Pattern Transition for Gas-Liquid Flow in Horizontal and Inclined Pipes, Comparison of Experimental Data with Theory. International Journal of Multiphase Flow, Volume 6, 1979, 217-225.

[8] D. Barnea: A Unified Model for Predicting Flow Pattern Transitions for the Whole Range of Pipe Inclinations. International Journal of Multiphase Flow, Volume 13, 1987, 1-12.

[9] R.G. Gillies, K.B. Hill, M.J. McKibben and C.A. Shook: Solid Transport by Laminar Newtonian Flows. Powder Technology, Volume 104, 1999, 269-277.

[10] P. Stevenson, R.B. Thorpe, J.E. Kennedy and C. McDermott: The Transport of Particles at Low Loading in Near-Horizontal Pipes by Intermittent Flow. Chemical Engineering Science, Volume 56, 2001, 2149-2159.

[11] T.J. Danielson: Sand Transport Modeling in Multiphase Pipelines. Offshore Technology Conference, OTC 18691, May 2007.

[12] A. Ramadan, P. Skalle and A. Saasen: Application of a Three-Layer Modeling Approach for Solids Transport in Horizontal and Inclined Channels. Chemical Engineering Science, Volume 60, 2005, 2557-2570.

[13] P. Doron and D. Barnea: Flow Patterns Maps for Solid-Liquid Flow in Pipes. International Journal of Multiphase Flow, Volume 22, 1996, 273-283.

[14] V. Matousek: Pressure Drops and Flow Patterns in Sand-Mixture Pipes. Experimental Thermal and Fluid Science, Volume 26, 2001, 693-702.

[15] G.W. Govier and K. Aziz: The Flow of Complex Mixtures in Pipes. Robert E. Krieger Publishing Company, Malabar Florida, 1987.

[16] G. Oddie, H. Shi, L.J. Durlofsky, K. Aziz, B. Pfeffer and J.A. Holmes: Experimental Study of Two and Three Phase Flows in Large Diameter Inclined Pipes. International Journal of Multiphase Flow, Volume 29, , 2003, 527-558.

Appendix B: Output data from simulation

Simulated Output Results for ANSYS Fluent Calibration - single phase			
Water		Gas	
Vr	**r**	**Vr**	**r**
0	0.1524	0	0.1524
0.000416	0.138465	0.000349	0.138465
0.000645	0.128722	0.000573	0.128722
0.000678	0.127288	0.000605	0.127288
0.00074	0.123742	0.000681	0.123742
0.000912	0.113092	0.000899	0.113092
0.000973	0.109461	0.000968	0.109461
0.001352	0.086445	0.001357	0.086445
0.001376	0.084819	0.00138	0.084819
0.001569	0.060914	0.00168	0.060914
0.001571	0.060618	0.001684	0.060618
0.001573	0.060252	0.001687	0.060252
0.00163	0.046695	0.001812	0.046695
0.00168	0.031851	0.001913	0.031851
0.001708	0.023272	0.001953	0.023272
0.001746	0.001129	0.002	0.001129
0.001747	-0.00011	0.002	-0.00011
0.001747	-0.00153	0.002	-0.00153
0.001735	-0.01939	0.001968	-0.01939
0.001722	-0.02741	0.001935	-0.02741
0.001707	-0.03979	0.001864	-0.03979
0.001694	-0.04423	0.001832	-0.04423
0.001644	-0.05702	0.00172	-0.05702
0.001544	-0.06865	0.001594	-0.06865
0.00144	-0.07867	0.001467	-0.07867
0.001232	-0.09536	0.001217	-0.09536
0.001168	-0.09928	0.001151	-0.09928
0.000824	-0.11656	0.00083	-0.11656
0.000747	-0.11981	0.000764	-0.11981
0.000407	-0.13316	0.000473	-0.13316
0.000365	-0.13513	0.000428	-0.13513
0	-0.1524	0	-0.1524

Simulated Output Results for Dispersed Bubble Flow Model Development, Testing & Validations							
20% GOR		30% GOR		40% GOR		50% GOR	
Vr	r	Vr	r	Vr	r	Vr	r
0	-0.1513	0	-0.1513	0	-0.1513	0	-0.1513
0.9615	-0.1266	0.9617	-0.1266	0.9613	-0.1266	0.9630	-0.1266
0.9825	-0.1175	0.9825	-0.1175	0.9807	-0.1175	0.9833	-0.1175
1.0247	-0.0796	1.0240	-0.0796	1.0221	-0.0796	1.0243	-0.0796
1.0289	-0.0747	1.0282	-0.0747	1.0262	-0.0747	1.0285	-0.0747
1.0447	-0.0314	1.0435	-0.0314	1.0433	-0.0314	1.0439	-0.0314
1.0468	-0.0060	1.0456	-0.0060	1.0455	-0.0060	1.0458	-0.0060
1.0467	0.0091	1.0455	0.0091	1.0454	0.0091	1.0456	0.0091
1.0419	0.0462	1.0409	0.0462	1.0409	0.0462	1.0409	0.0462
1.0314	0.0743	1.0302	0.0743	1.0295	0.0743	1.0308	0.0743
1.0268	0.0868	1.0255	0.0868	1.0246	0.0868	1.0263	0.0868
0.9968	0.1144	0.9965	0.1144	0.9960	0.1144	0.9970	0.1144
0	0.1513	0	0.1513	0	0.1513	0	0.1513
0	-0.1513	0	-0.1513	0	-0.1513	0	-0.1513
0.9493	-0.1266	0.9466	-0.1266	0.9477	-0.1266	0.9491	-0.1266
0.9756	-0.1175	0.9729	-0.1175	0.9727	-0.1175	0.9749	-0.1175
1.0318	-0.0796	1.0305	-0.0796	1.0287	-0.0796	1.0311	-0.0796
1.0375	-0.0747	1.0362	-0.0747	1.0343	-0.0747	1.0369	-0.0747
1.0596	-0.0314	1.0596	-0.0314	1.0585	-0.0314	1.0599	-0.0314
1.0625	-0.0060	1.0627	-0.0060	1.0617	-0.0060	1.0626	-0.0060
1.0624	0.0091	1.0625	0.0091	1.0616	0.0091	1.0624	0.0091
1.0564	0.0462	1.0559	0.0462	1.0549	0.0462	1.0559	0.0462
1.0409	0.0743	1.0391	0.0743	1.0390	0.0743	1.0409	0.0743
1.0342	0.0868	1.0317	0.0868	1.0320	0.0868	1.0342	0.0868
0.9944	0.1144	0.9931	0.1144	0.9938	0.1144	0.9947	0.1144
0	0.1513	0	0.1513	0	0.1513	0	0.1513

Simulated Output Results for Annular Flow Model Development, Testing & Validations					
Vr	**r**	**Vr**	**r**	**Vr**	**r**
0	0.147	0	0.147159	0	0.147159
0	0.152	0	0.1524	0	0.1524
0	-0.152	0	-0.1524	0	-0.1524
0	-0.149	0	-0.14937	0	-0.14937
0	-0.149	0	-0.14937	0	-0.14937
0.61	-0.147	0.221872	-0.14678	0.246107	-0.14678
1.401	-0.144	0.549516	-0.14368	0.606626	-0.14368
2.292	-0.14	1.01262	-0.13995	1.10766	-0.13995
3.037	-0.135	1.50206	-0.13549	1.625	-0.13549
3.596	-0.13	1.935	-0.13012	2.07335	-0.13012
4.023	-0.124	2.28567	-0.12368	2.43283	-0.12368
4.361	-0.116	2.56757	-0.11596	2.72093	-0.11596
4.636	-0.107	2.79741	-0.10669	2.95561	-0.10669
4.863	-0.096	2.98695	-0.09557	3.14909	-0.09557
5.05	-0.082	3.14334	-0.08222	3.30865	-0.08222
5.201	-0.066	3.27005	-0.0662	3.43782	-0.0662
5.343	-0.047	3.39249	-0.04699	3.56233	-0.04699
5.344	-0.045	3.39378	-0.04537	3.56363	-0.04537
5.35	-0.038	3.39936	-0.03831	3.56924	-0.03831
5.352	-0.036	3.4014	-0.0356	3.57128	-0.0356
5.352	-0.035	3.40178	-0.0351	3.57166	-0.0351
5.37	-0.011	3.42026	-0.01087	3.59015	-0.01087
5.376	-0.001	3.42683	-0.00103	3.59672	-0.00103
5.379	0.006	3.43024	0.006212	3.60012	0.006212
5.381	0.015	3.43278	0.014664	3.60261	0.014664
5.381	0.033	3.43494	0.033298	3.60455	0.033298
5.38	0.037	3.43484	0.036893	3.60439	0.036893
5.38	0.038	3.43481	0.037857	3.60436	0.037857
5.379	0.046	3.43464	0.046346	3.60405	0.046346
5.276	0.065	3.35603	0.065271	3.52333	0.065271
5.148	0.081	3.2537	0.081042	3.41862	0.081042
4.981	0.094	3.11824	0.094184	3.28014	0.094184

4.771	0.105	2.94755	0.105136	3.1057	0.105136
4.513	0.114	2.73594	0.114262	2.88941	0.114262
4.192	0.122	2.47359	0.121868	2.62087	0.121868
3.784	0.128	2.14775	0.128206	2.28574	0.128206
3.25	0.133	1.75472	0.133487	1.87611	0.133487
2.552	0.138	1.32417	0.137888	1.4189	0.137888
1.739	0.142	0.898233	0.141556	0.96251	0.141556
0.853	0.145	0.447158	0.144612	0.478063	0.144612
0	0.147	0	0.147159	0	0.147159

Simulated Output Results for Slug Flow Model Development, Testing & Validations					
Vr	**r**	**Vr**	**r**	**Vr**	**r**
0	0.147159	0	0.147159	0	0.147159
0	0.1524	0	0.1524	0	0.1524
0	-0.1524	0	-0.1524	0	-0.1524
0	-0.14937	0	-0.14937	0	-0.14937
0	-0.14937	0	-0.14937	0	-0.14937
0.028085	-0.14678	0.130201	-0.14678	0.073545	-0.14678
0.063637	-0.14368	0.287477	-0.14368	0.1621	-0.14368
0.110113	-0.13995	0.4787	-0.13995	0.27043	-0.13995
0.167188	-0.13549	0.700447	-0.13549	0.399654	-0.13549
0.235631	-0.13012	0.940115	-0.13012	0.548283	-0.13012
0.315857	-0.12368	1.1755	-0.12368	0.709454	-0.12368
0.406787	-0.11596	1.38639	-0.11596	0.870661	-0.11596
0.504205	-0.10669	1.5654	-0.10669	1.01911	-0.10669
0.601066	-0.09557	1.71418	-0.09557	1.14795	-0.09557
0.690255	-0.08222	1.83603	-0.08222	1.25578	-0.08222
0.767003	-0.0662	1.93286	-0.0662	1.34282	-0.0662
0.84403	-0.04699	2.02024	-0.04699	1.42333	-0.04699
0.844716	-0.04537	2.02084	-0.04537	1.42392	-0.04537
0.847684	-0.03831	2.02346	-0.03831	1.42647	-0.03831
0.848778	-0.0356	2.02431	-0.0356	1.42732	-0.0356
0.504205	-0.10669	1.5654	-0.10669	1.01911	-0.10669
0.601066	-0.09557	1.71418	-0.09557	1.14795	-0.09557
0.690255	-0.08222	1.83603	-0.08222	1.25578	-0.08222
0.767003	-0.0662	1.93286	-0.0662	1.34282	-0.0662
0.84403	-0.04699	2.02024	-0.04699	1.42333	-0.04699
0.844716	-0.04537	2.02084	-0.04537	1.42392	-0.04537
0.847684	-0.03831	2.02346	-0.03831	1.42647	-0.03831
0.848778	-0.0356	2.02431	-0.0356	1.42732	-0.0356
0.848978	-0.0351	2.02446	-0.0351	1.42748	-0.0351
0.858956	-0.01087	2.03234	-0.01087	1.43542	-0.01087
0.862402	-0.00103	2.03446	-0.00103	1.43774	-0.00103
0.863645	0.006212	2.035	0.006212	1.43832	0.006212

0.86358	0.014664	2.03436	0.014664	1.4378	0.014664
0.861468	0.033298	2.03022	0.033298	1.43433	0.033298
0.860782	0.036893	2.029	0.036893	1.43328	0.036893
0.860604	0.037857	2.02869	0.037857	1.43302	0.037857
0.859049	0.046346	2.02597	0.046346	1.43069	0.046346
0.798009	0.065271	1.94748	0.065271	1.35972	0.065271
0.728936	0.081042	1.85469	0.081042	1.27689	0.081042
0.647011	0.094184	1.73625	0.094184	1.17258	0.094184
0.557809	0.105136	1.59061	0.105136	1.04719	0.105136
0.467969	0.114262	1.41493	0.114262	0.902839	0.114262
0.382941	0.121868	1.20835	0.121868	0.747015	0.121868
0.305386	0.128206	0.97918	0.128206	0.592066	0.128206
0.235534	0.133487	0.747273	0.133487	0.448646	0.133487
0.172318	0.137888	0.532178	0.137888	0.320775	0.137888
0.114319	0.141556	0.340912	0.141556	0.206688	0.141556
0.056149	0.144612	0.162986	0.144612	0.098957	0.144612
0	0.147159	0	0.147159	0	0.147159

Simulated Output Results for Stratified Flow Model Development, Testing & Validations			
Vr	**r**	**Vr**	**r**
0	-0.047632	0	-0.047632
0.109947	-0.047448	0.106554	-0.04661
0.107097	-0.047558	0.105704	-0.045472
0.106554	-0.04661	0.104417	-0.044107
0.105704	-0.045472	0.102493	-0.042469
0.104417	-0.044107	0.0996854	-0.040503
0.102493	-0.042469	0.0956049	-0.038145
0.0996854	-0.040503	0.0895883	-0.035315
0.0956049	-0.038145	0.0806586	-0.03192
0.0895883	-0.035315	0.0672921	-0.027848
0.0806586	-0.03192	0.0426123	-0.022963
0.0672921	-0.027848	0.0426123	-0.022963
0.0426123	-0.022963	0.0426138	-0.022961
0.0426123	-0.022963	0.105626	-0.006673
0.0426138	-0.022961	0.125087	-0.001002
0.105626	-0.006673	0.128105	-0.000386
0.125087	-0.001002	0.128119	-0.000385
0.128105	-0.000386	0.12812	-0.000385
0.128119	-0.000385	0.131679	1.38E-05
0.12812	-0.000385	0.138132	0.0005649
0.131679	0.00E+00	0.17057	0.0034377
0.138132	0.0005649	0.170634	0.0034431
0.17057	0.0034377	0.170646	0.0034441
0.170634	0.0034431	0.395751	0.0226392
0.170646	0.0034441	0.395757	0.0226396
0.395751	0.0226392	0.39577	0.0226407
0.395757	0.0226396	0.749045	0.02745
0.39577	0.0226407	0.887188	0.0314586
0.749045	0.02745	0.974774	0.0348001
0.887188	0.0314586	0.992587	0.0375858
0.974774	0.0348001	0.941424	0.0399078
0.992587	0.0375858	0.838183	0.041843

0.941424	0.0399078	0.703386	0.0434559
0.838183	0.041843	0.553234	0.0448002
0.703386	0.0434559	0.400055	0.0459205
0.553234	0.0448002	0.254454	0.0468541
0.400055	0.0459205	0	0.0476322
0.254454	0.0468541		
0	0.0476322		

Appendix C: Flow patterns experimental results

Flow pattern results for water-gas flow in 0.07m horizontal pipe							
Stratified smooth flow			**Stratified wavy flow**			**Dispersed bubble flow**	
Vsg	**Vsl**		**Vsg**	**Vsl**		**Vsg**	**Vsl**
0.41	0.43		1.09	0.109		15.18	0.001
0.03	0.25		2.19	0.044		15.02	0.002
0.03	0.64		1.8	0.058		15.37	0.005
0.06	0.42		3.2	0.098		15.09	0.01
0.13	0.3		1.6	0.054		15.01	0.015
0.35	0.55		2.9	0.08		15.04	0.02
0.46	0.33		1.01	0.062		15.02	0.025
0.19	0.37		3.6	0.092		15.45	0.03
0.62	0.59		3.2	0.075		15.29	0.035
0.03	0.13		1.9	0.05		15.06	0.04
0.13	0.13		1.8	0.06		14.76	0.045
0.35	0.13		2.7	0.09		15.4	0.049
0.85	0.02		2.03	0.46		1.809	0.52
0.46	0.02		1.28	0.62		3.608	0.45
0.19	0.02		1.3	0.41		3.727	0.32
0.06	0.02		1.12	0.03		3.686	0.14
0.86	1.64		0.99	0.17		8.17	0.42
0.14	2.01		1	0.19		19.144	0.041
0.67	1.28		0.95	0.46		22.01	0.0305
0.13	0.62		0.72	0.62		19.14	0.043
0.11	1.59		0.77	0.13			
0.07	1.75		3.88	1.5			
0.49	1.22		2.46	1.35			
1.14	0.98		3.3	1.28			
0.23	1.59		2.92	2.03			

Flow pattern results for water-oil-gas flow in 0.1m inclined pipe							
Slug flow @ 15^0			**Elongated B flow @ 15^0**			**Elongated B. flow @ 20^0**	
Vsg	**Vsl**		**Vsg**	**Vsl**		**Vsg**	**Vsl**
6.26	0.42		3.162	0.061		10.2	0.121
5.52	0.345		6.084	0.131		6.45	0.112
6.64	0.155		5.706	0.061		4.8	0.121
5.47	0.17		6.379	0.3835		8.2	0.045
4.23	0.22		2.758	0.118		12	0.1
7.89	0.155		6.084	0.148		10	0.179
13.07	0.17		5.635	0.2235		7.2	0.19
13.12	0.22		3.047	0.3135		6	0.092
10.39	0.145		5.411	0.3075		10	0.037
6.26	0.42		3.309	0.4045		9	0.337
5.52	0.345		2.7833	0.046		18	0.395
6.64	0.155		3.15	0.09		19	0.041
5.47	0.17		2.972	0.1415		10	0.391
4.23	0.22		5.333	0.138		18	0.112
7.89	0.155		2.03	0.196		14	0.331
13.07	0.17		4.965	0.2005		13	0.56
13.12	0.22		1.857	0.292		10	0.0305
10.39	0.145		4.572	0.2855		12	0.091
5.507	0.065		3.892	0.4945		12	0.043
14.818	0.0705		2.3	0.2175		10	0.677
15.037	0.13		5.502	0.201		8	0.305
12.881	0.2165		3.903	0.3295		11	0.24
10.43	0.3125						
14.446	0.0385						
17.577	0.0765						

Appendix D: Pressure drop results for multiphase flow experiments

Pressure drop in water-oil-gas multiphase flow, liquid vol. = 0.6166m^3 with 10 % oil			
0.08m horizontal pipe, (0.7 m/s gas vel.)		**0.07m horizontal pipe, (0.6 m/s gas vel.)**	
Vsl	**Pressure, mBar**	**Vsl**	**Pressure, mBar**
0.196201	0.934292	0.191673	1.21027
0.302251	1.10026	0.294028	1.17243
0.403565	1.25417	0.399417	1.14212
0.503182	1.44896	0.4936	1.36113
0.699717	1.65672	0.598022	1.45576
1.00442	1.83138	0.998076	1.71557
0.08m horizontal pipe, (0.6 m/s gas vel.)		**0.07m horizontal pipe, (0.4 m/s gas vel.)**	
0.204039	0.911711	0.199819	0.695855
0.306369	0.967582	0.29903	0.656887
0.403364	0.834103	0.397292	0.771158
0.499919	0.795148	0.495825	0.841646
0.704579	0.906889	0.702844	0.873618
1.01164	1.05996	1.00539	0.961333
0.08m horizontal pipe, (0.4 m/s gas vel.)		**0.07m horizontal pipe, (0.3 m/s gas vel.)**	
0.201369	1.08098	0.200246	0.543487
0.300819	1.18941	0.298849	0.561553
0.39903	1.16758	0.397676	0.543394
0.498496	1.2701	0.499184	0.59055
0.700718	1.42806	0.699296	0.655772
1.00375	1.77742	1.00409	0.753771
0.201426	0.603934		
0.298446	0.499925	**0.07m horizontal pipe, (0.2 m/s gas vel.)**	
0.403753	0.562983	0.199912	0.478097
0.50262	0.661962	0.299035	0.42513
0.704226	0.736919	0.400848	0.423404
1.01137	0.838713	0.502773	0.407086
		0.702471	0.512909
		1.00353	0.675376

Pressure drop in water-oil-gas multiphase flow in 0.1m inclined pipe @ 15^0, liquid vol. = $0.6166m^3$ with 10 % oil	
0.9 m/s gas velocity	
Vsl, m/s	**Pressure, mBar**
0.0975706	1.14787
0.19806	1.66653
0.497631	1.86945
0.700515	2.0069
1.003	2.33354
0.8 m/s gas velocity	
0.198154	1.2849
0.400279	1.49613
0.494872	1.63635
0.697105	1.8184
0.998362	2.2285
0.4 m/s gas velocity	
0.202681	0.88798
0.301982	1.20191
0.403357	1.33291
0.497052	1.36299
0.696764	1.57163
1.00548	2.02991

Pressure drop in water-oil-sand multiphase flow , liquid vol. = 0.6166m^3 with 1.9 % sand							
0.07m horizontal pipe			**0.08m horizontal pipe**			**0.1m inclined pipe @ 15^0**	
Vsl, m/s	**Press, mBar**		**Vsl, m/s**	**Press, mBar**		**Vsl, m/s**	**Press, mBar**
0.8998	1.888322		0.9098	1.847544		0.9201	1.913352
0.8982	1.849034		0.9081	1.799566		0.9188	1.891016
0.8978	1.808171		0.9075	1.738783		0.9172	1.883752
0.8937	1.743688		0.9072	1.691738		0.9168	1.876471
0.8921	1.692794		0.9058	1.663429		0.9151	1.8709755
0.8905	1.615639					0.9138	1.7646064

Appendix E: Sand minimum transport velocity experimental results

MTV (suspension) results for water-sand flow		
	Observed average MTV (liq. vol. = 0.6166m^3)	
Pipe size	**0.94 % sand**	**1.42 % sand**
0.07	0.915	0.9169
0.08	0.92	0.9225
0.1	0.935	0.9371

MTV (rolling) results for water-sand flow		
	Observed average MTV (liq. vol. = 0.6166m^3)	
Pipe size	**1.94 % sand**	**2.50 % sand**
0.07	0.3903	0.3905
0.08	0.4028	0.4143
0.1	0.4265	0.429

MTV (suspension) results for water-oil-sand flow (5 % oil)		
	Observed average MTV (liq. vol. = 0.6166m^3)	
Pipe size	**0.94 % sand**	**1.42 % sand**
0.07	0.8998	0.9123
0.08	0.9098	0.9218
0.1	0.9201	0.9349

MTV (rolling) results for water-oil-sand flow (5 % oil)		
	Observed average MTV (liq. vol. = 0.6166m^3)	
Pipe size	**0.94 % sand**	**1.42 % sand**
0.07	0.3845	0.3852
0.08	0.3933	0.3965
0.1	0.4035	0.4098

MTV (susp) results for water-gas-sand flow (liq. vol. = $0.6166m^3$)		
Pipe size, m	**Gas velocity, m/s**	**MTV, m/s**
0.07	0	0.915
	0.039	0.915
	0.06421	0.919
	0.074	0.923
	0.076	0.929
0.08	0	0.92
	0.039	0.9208
	0.072	0.921
	0.078	0.923
	0.08	0.926
0.1 @ 15^0	0	0.931
	0.039	0.932
	0.056	0.932
	0.079	0.93
	0.09	0.928
0.1 @ 20^0	0	0.931
	0.039	0.93
	0.056	0.93
	0.079	0.929
	0.09	0.927
0.1 @ 25^0	0	0.931
	0.039	0.932
	0.056	0.932
	0.079	0.932
	0.09	0.932

MTV (roll) results for water-gas-sand flow (liq. vol. = 0.6166m^3, 0.94 % sand)		
Pipe size, m	**Gas velocity, m/s**	**MTV, m/s**
0.07	0.014	0.519
	0.015	0.51
	0.065	0.511
	0.08	0.51
0.08	0.014	0.526
	0.045	0.526
	0.065	0.524
	0.08	0.524
0.1 @ 15^0	0.014	0.403
	0.045	0.4
	0.065	0.39
	0.08	0.39
0.1 @ 20^0	0	0.4435
	0.014	0.443
	0.045	0.443
	0.065	0.438
	0.08	0.436
0.1 @ 25^0	0	0.4437
	0.014	0.4437
	0.045	0.444
	0.065	0.444
	0.08	0.444

MTV (susp) results for water-oil- gas-sand flow (liq. vol. = 0.6166m^3) with 5 % oil			
Pipe size, m	**Gas velocity, m/s**	**MTV, m/s (0.94% sand)**	**MTV, m/s (1.42% sand)**
0.07	0	0.8998	0.9123
	0.03	0.8982	0.9112
	0.04	0.8978	0.9098
	0.07	0.8937	0.9072
	0.08	0.8921	0.9069
	0.09	0.8905	0.9063
0.08	0	0.9098	0.9218
	0.05	0.9081	0.9189
	0.06	0.9075	0.9162
	0.07	0.9072	0.9138
	0.08	0.9058	0.9126
0.1 @ 15^0	0	0.9201	0.9349
	0.04	0.9188	0.9345
	0.05	0.9172	0.9287
	0.07	0.9168	0.9271
	0.072	0.9151	0.9265
	0.075	0.9138	0.9271
0.1 @ 20^0	0	0.9208	0.9378
	0.04	0.9205	0.9375
	0.05	0.92	0.9355
	0.07	0.919	0.9345
	0.072	0.9188	0.9345
	0.075	0.9188	0.934
0.1 @ 25^0	0	0.9215	0.9389
	0.04	0.9213	0.9383
	0.05	0.921	0.937
	0.07	0.9211	0.9365
	0.072	0.9211	0.9365
	0.075	0.9212	0.9367

MTV (susp.) results for water-oil- gas-sand flow (liq. vol. = 0.6166m^3) with 10 % oil			
Pipe size, m	**Gas velocity, m/s**	**MTV, m/s (0.94% sand)**	**MTV, m/s (1.42% sand)**
0.07	0	0.8998	0.9123
	0.04	0.8965	0.9101
	0.045	0.8948	0.9093
	0.06	0.8932	0.9093
	0.07	0.893	0.9084
	0.08	0.8919	0.9063
0.08	0	0.9098	0.9218
	0.05	0.9092	0.9184
	0.06	0.9075	0.9143
	0.07	0.9073	0.9137
	0.077	0.9038	0.912
0.1 @ 15^0	0	0.9201	0.9349
	0.04	0.918	0.934
	0.05	0.9171	0.9285
	0.06	0.9158	0.9263
	0.07	0.914	0.9263
	0.074	0.9127	0.9267

Appendix F: Sand deposit experimental results for C_D & C_L models

Experimental Data for Model Testing and Validations				
Single-Phase Oil Flow				
Particle Den	**Particle Size**	**Velocity, m/s**	**Re**	**CD**
1066.67	0.01127	0.186	2.9	14.12926
1034.48	0.01035	0.039	0.42	73.2703
1038.96	0.01302	0.126	1.72	18.22477
1052.63	0.00899	0.034	0.32	96.16358
1090.91	0.01281	0.242	3.24	10.51653
1250.00	0.01152	0.017	0.2	149.7766
1100.00	0.01563	0.057	0.93	33.79908
Two-Phase Oil-Air Flow				
1066.67	0.01127	0.332079	343.28	0.532202
1034.48	0.01035	0.095532	90.65	1.899549
1038.96	0.01302	0.150241	179.35	0.943582
1052.63	0.00899	0.107232	88.37	1.296264
1090.91	0.01281	0.333204	391.35	1.325062
1250.00	0.01152	0.16388	173.09	0.811856
1100.00	0.01563	0.121378	174	1.587986
Two-Phase Oil-Water				
1066.67	0.01127	0.186	2.19	14.12926
1034.48	0.01035	0.039	0.42	73.2703
1038.96	0.01302	0.126	1.72	18.22477
1052.63	0.00899	0.034	0.32	96.16358
1090.91	0.01281	0.242	3.24	10.51653
1250.00	0.01152	0.017	0.2	149.7766
1100.00	0.01563	0.057	0.93	33.79908
Three-Phase Oil-Water-Air				
1066.67	0.01127	0.225128	6.28	5.219091
1034.48	0.01035	0.116084	2.97	11.65592
1038.96	0.01302	0.119877	3.86	8.540476
1052.63	0.00899	0.099228	2.21	14.54396
1090.91	0.01281	0.232556	7.37	5.316265
1250.00	0.01152	0.095857	2.73	11.61268
1100.00	0.01563	0.174339	6.75	5.861403

Appendix G: Schematic of the flow patterns and MTV prediction models

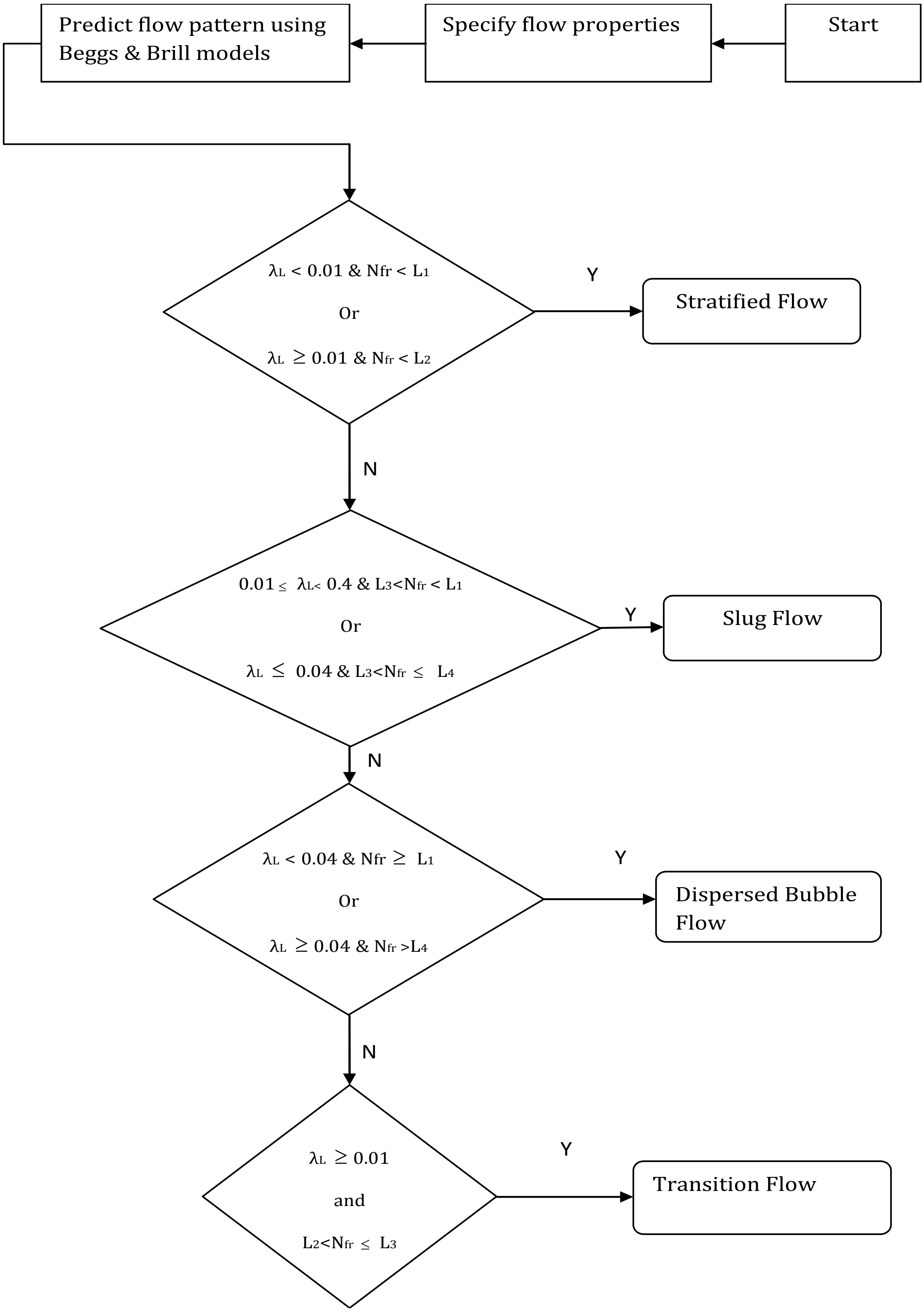

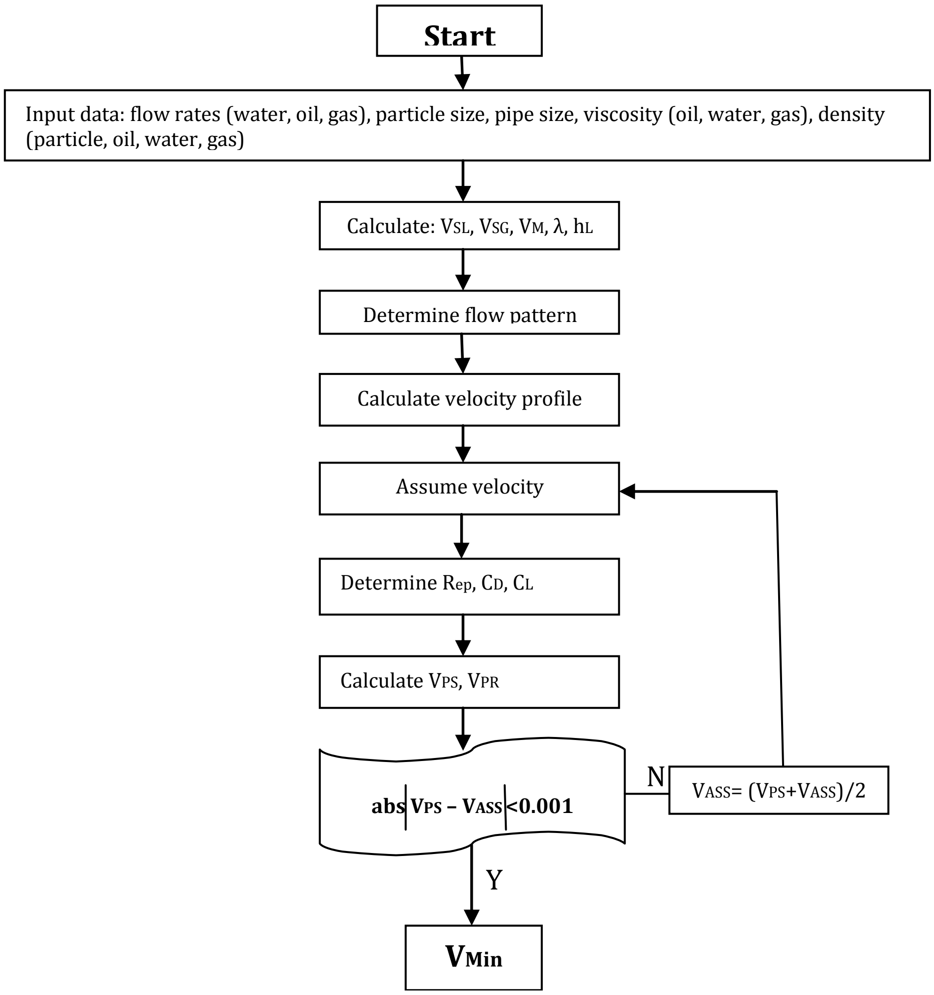

Start
Input data: flow rates (water, oil, gas), particle size, pipe size, viscosity (oil, water, gas), density (particle, oil, water, gas)
Calculate: V_{SL}, V_{SG}, V_M, λ, h_L
Determine flow pattern
Calculate velocity profile
Assume velocity
Determine R_{ep}, C_D, C_L
Calculate V_{PS}, V_{PR}
abs$|V_{PS} - V_{ASS}|$<0.001
N
V_{ASS}= (V_{PS}+V_{ASS})/2
Y
V_{Min}

Appendix H: VB code on Excel for MTV calculations

```
==============================================================
Solid transport velocity optimisation program with VB code in Excel
Kelani Olafinhan Bello, Robert Gordon University
Calculating sand minimum transport velocity in multiphase fluid flow in pipes
===============================================================
```

'Flow type'

```
================================================================
''Define fluids input parameters''
Lambda = (47 + i, 7).Value
Nfr = (47 + i, 6).Value
L1 = (47 + i, 8).Value
L2 = (47 + i, 9).Value
L3 = (47 + i, 10).Value
L4 = (47 + i, 11).Value

If (lambda < 0.01 and Nfr < L1) Or (lambda >= 0.01 and Nfr < L2) Then
Flow = 1(stratified flow)
 (47 + i, 14).Value = Flow
GoTo stratified flow model

Else If (lambda >= 0.01 and lambda < 0.4 and Nfr > L3 and Nfr < L1) Or (lambda <= 0.04 And
Nfr > L3 and Nfr <= L4) Then
Flow = 2 (slug flow)
 (47 + i, 14).Value = Flow
GoTo slug flow model

Else If (lambda < 0.04 and Nfr >= L1) Or (lambda >= 0.04 and Nfr > L4) Then
Flow = 3 (dispersed bubble flow)
 (47 + i, 14).Value = Flow
GoTo dispersed bubble flow

Else If (lambda > 0.01 And Nfr > L2 and Nfr <= L3) Then
Flow = 4 (transition flow)
 (47 + i, 14).Value = Flow
GoTo transition flow model
```

Else

Flow = 5 (annular flow)

(47 + i, 14).Value = Flow

GoTo annular flow model

End If

'MTV Calculations

==

''Define solid particle input parameters''

Logline = 1

Counter = 1

Angnumber = 1

IncTheta = Cells (29, 1).Value

Do ' Slug V_p

R = Pradius - (Partsize / 2)

V_r = 3.3 * f_m * (Re ^ 0.347) * Avgvel * (1 - (R / Pradius) ^ 2) ^ 1.11

R_{ep} = (Avgvel * DenM * Partsize) / Umix

C_D = ((24 / Rep) * (1 + (0.15 * (Rep ^ 0.687))) + ((3.5 / (1 + (42500 * (Rep ^ -1.17))))))

C_L = 2.975 / ((Rep ^ 2) + 1.2) ^ 0.165

Vps = a * (((g * Partsize / (DenM * CL)) * (DenP - DenM) * (Sin(IncTheta))) ^ b) * (Pid * DenM / Umix) ^ c

Assvel = (Vps + Assvel) / 2

V_{min} = Vps + Vr

Loop While Abs (V_{ps} - Assvel) > 0.0001

Cells (47 + i, 15).Value = V_{min}

Avgvel = Range. Value

Assvel = Range. Value

Do ' Slug V_r

R = Pradius - (Partsize / 2)

V_r = 3.3 * fm * (Re ^ 0.347) * Avgvel * (1 - (R / Pradius) ^ 2) ^ 1.11

R_{ep} = (Avgvel * DenM * Partsize) / Umix

C_D = ((24 / Rep) * (1 + (0.15 * (Rep ^ 0.687))) + ((3.5 / (1 + (42500 * (Rep ^ -1.17))))))

```
CL = 2.975 / ((Rep ^ 2) + 1.2) ^ 0.165
Vpr = a2 * (g * Partsize * ((DenP / DenM) - 1) * (Cos(IncTheta) + (fs * Sin(IncTheta))) / ((fs *
CL) + CD)) ^ b2
Assvel = (Vpr + Assvel) / 2
Vmin = Vpr + Vr
 Loop While Abs (Vpr - Assvel) > 0.0001

Cells (47 + i, 16).Value = Vmin
GoTo slug flow
IncTheta = Cells (29, 1).Value
Assvel = Range ("B8").Value
Do ' Dispersed bubble Vsp
R = Pradius - (Partsize / 2)
Vr = 3.7 * fm * (Re ^ 0.366) * Avgvel * (1 - (R / Pradius) ^ 2) ^ 1.37
Rep = (Avgvel * DenM * Partsize) / Umix
CD = ((24 / Rep) * (1 + (0.15 * (Rep ^ 0.687))) + ((3.5 / (1 + (42500 * (Rep ^ -1.17))))))
CL = 2.975 / ((Rep ^ 2) + 1.2) ^ 0.165
Vps = a * (((g * Partsize / (DenM * CL)) * (DenP - DenM) * (Sin (IncTheta))) ^ b) * (Pid * DenM
/ Umix) ^ c
Assvel = (Vps + Assvel) / 2
Vmin = Vps + Vr
Loop While Abs (Vps - Assvel) > 0.0001
Cells (47 + i, 15).Value = Vmin
Avgvel = Range. Value
Assvel = Range. Value
Do ' dispersed Bubble Vr
R = Pradius - (Partsize / 2)
Vr = 3.7 * fm * (Re ^ 0.366) * Avgvel * (1 - (R / Pradius) ^ 2) ^ 1.37
Rep = (Avgvel * DenM * Partsize) / Umix
CD = ((24 / Rep) * (1 + (0.15 * (Rep ^ 0.687))) + ((3.5 / (1 + (42500 * (Rep ^ -1.17))))))
CL = 2.975 / ((Rep ^ 2) + 1.2) ^ 0.165
Vpr = a2 * (g * Partsize * ((DenP / DenM) - 1) * (Cos(IncTheta) + (fs * Sin(IncTheta))) / ((fs *
CL) + CD)) ^ b2
Assvel = (Vpr + Assvel) / 2
Vmin = Vpr + Vr
Loop While Abs (Vpr - Assvel) > 0.0001
```

```
Cells (47 + i, 16).Value = Vmin
GoTo dispersed bubble
IncTheta = Cells (29, 1).Value
Assvel = Range. Value
Do ' Annular Flow
R = Pradius - (Partsize / 2)
Vr = 1.863 * fm * (Re ^ 0.4) * Avgvel * (1 - (R / Pradius) ^ 2) ^ 1.11
Rep = (Avgvel * DenM * Partsize) / Umix
CD = ((24 / Rep) * (1 + (0.15 * (Rep ^ 0.687))) + ((3.5 / (1 + (42500 * (Rep ^ -1.17))))))
CL = 2.975 / ((Rep ^ 2) + 1.2) ^ 0.165
Vps = a * (((g * Partsize / (DenM * CL)) * (DenP - DenM) * (Sin (IncTheta))) ^ b) * (Pid * DenM
/ Umix) ^ c
Assvel = (Vps + Assvel) / 2
Vmin = Vps + Vpr
Loop While Abs (Vps - Assvel) > 0.0001
Cells (47 + i, 15).Value = Vmin
Avgvel = Range. Value
Assvel = Range. Value
Do ' Annular Flow
R = Pradius - (Partsize / 2)
Vr = 1.863 * fm * (Re ^ 0.4) * Avgvel * (1 - (R / Pradius) ^ 2) ^ 1.11
Rep = (Avgvel * DenM * Partsize) / Umix
CD = ((24 / Rep) * (1 + (0.15 * (Rep ^ 0.687))) + ((3.5 / (1 + (42500 * (Rep ^ -1.17))))))
CL = 2.975 / ((Rep ^ 2) + 1.2) ^ 0.165
Vpr = a2 * (g * Partsize * ((DenP / DenM) - 1) * (Cos (IncTheta) + (fs * Sin (IncTheta))) / ((fs *
CL) + CD)) ^ b2
Assvel = (Vpr + Assvel) / 2
Vmin = Vpr + Vr
Loop While Abs (Vpr - Assvel) > 0.0001
Cells (47 + i, 16).Value = Vmin
GoTo annular flow
i = i + 1
Loop
End Sub
```